Late Weichselian to Holocene sedimentation in the inner Kara Sea: Qualification and Quantification of Processes

Sedimentationsprozesse in der inneren Kara See (spät Weichsel bis Holozän)

Klaus Hauke Dittmers
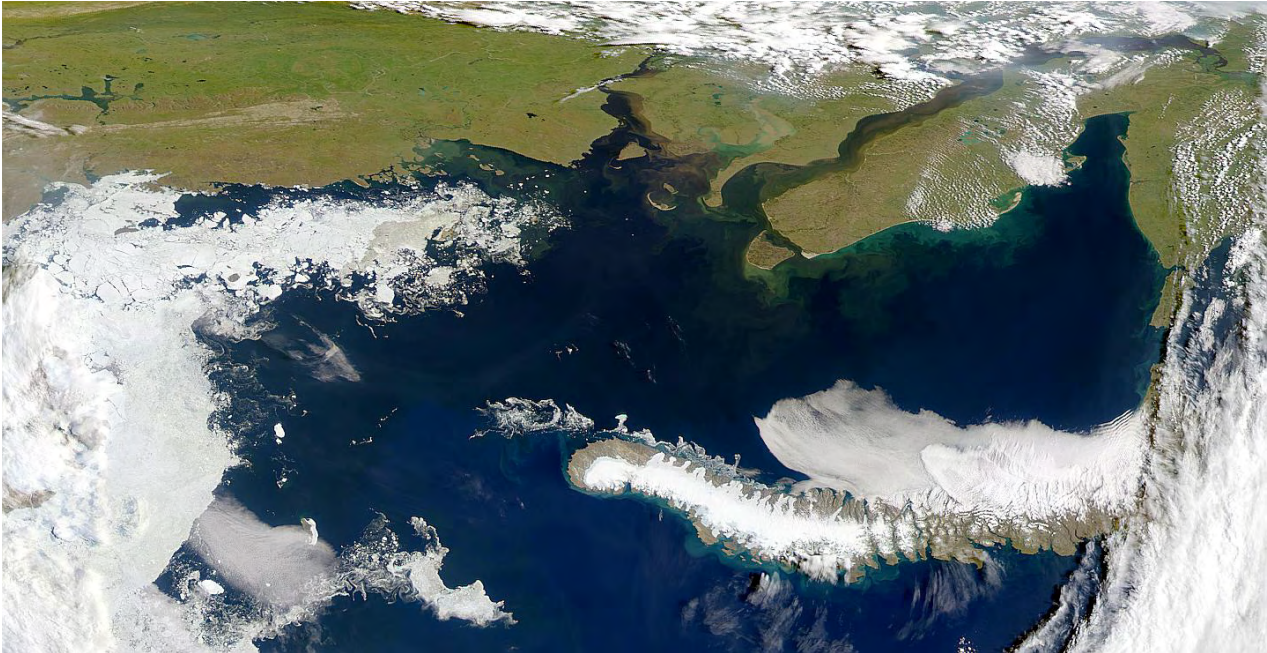
Late Weichselian to Holocene sedimentation in the inner Kara Sea: Qualification and Quantification of Processes

Sedimentationsprozesse in der inneren Kara See (spät Weichsel bis Holozän)

Klaus Hauke Dittmers

Picture taken from http://visibleearth.nasa.gov

dedicated to my parents

Klaus Hauke Dittmers

Alfred Wegener Institute for Polar and Marine Research
Columbusstraße
Haus D
D-27515 Bremerhaven
Germany
kdittmer@awi-bremerhaven.de

Content

Part C

Key results

Part D

Summary

Recent sediment pathways (Chapter 3.2)

Surface sediments of the Kara Sea display a strong bimodal distribution in the mud fraction. The peaks cluster at 8 ɸ (4 µm), the dominant mode, and at a secondary peak of 5 ɸ (25-40 µm). The widespread occurrence of bimodal grain-size distribution mode in the sortable silt fraction leads us to the interpretation that two main processes are responsible for the material transport, strongly suggesting a twofold peak in current intensity. On the basis of our data it is impossible to relate a distinct grain-size fraction with a certain transport mechanism and there is some bias to identify the "exact" processes. We favour a "summer" mode dominated by extensive, suspended sediment-laden freshwater influx, and a "winter" mode characterised by material redistribution and resuspension enhanced by sea-ice and polynia formation and various processes related to them.

Furthermore, Magnetic susceptibility of surface sediments was investigated to reconstruct recent transport pathways of magnetic minerals (terrestrial sediments). The MS signal clearly originates in the Putoran Mountains in the drainage area of the Yenisei branch and values decrease with increasing water depth. We see this as evidence that the channels distribute the MS signal on the shelf. It is evident that sediment pathways follow the morphology of the sea-floor, indicating density-driven bottom layer transport. After the particles have made their way through the water column they settle and accumulate in density-induced flow following the Pleistocene bottom relief. This process is active mainly during summer. During winter resuspension, enhanced particle reorganisation occurs.

Sedimentation in the Ob and Yenisei estuaries: evolution and budget (Chapter 3.3)

Soft sediments in the Ob and Yenisei estuaries can be divided into two major acoustic and lithological Units I and II. Unit II forms the pre-Holocene basement with little acoustic penetration. During the last sea level lowstand, the erosional surface was formed on top of this unit including several incised river channels. The younger Unit I can be divided into three subunits, Ia to Ic. The lowermost subunits Ic and Ib show fluvial to shallow-marine character comparable to typical channel-levee-complexes representing a fine-grained meandering river depositional environment overlain by a transgressive system tract and finally high-stand system tract after about 5 Calender ka BP.

During the Holocene an estimated total of 50 % and 75 % of the amount of modern river-supplied material extrapolated for the Holocene, accumulated. A progressive

southward migration of the position of the marginal filter in response to the elevating sea level is favoured to account for the "missing" material.

The existence of filled paleo-river channels suggests a pre-Holocene history of the southern Kara Sea Shelf similar to that in the Laptev Sea (Kleiber and Niessen, 1999). These channels must have been eroded during the sea level lowstand and were filled with sediments during the Holocene transgression. River erosion of the exposed shelf of the southern Kara Sea during the Last Glacial Maximum (LGM) implies continuous river transport across the shelf and absence of an ice sheet in the area of channel erosion.

Acoustic facies on the inner Kara Sea Shelf: implications for late Weichselian to Holocene sediment dynamics (Chapter 3.4)

Late Pleistocene to Holocene seismic units on the inner Kara Sea Shelf are composed of sedimentary units the deposition of which was strongly controlled by sea level fluctuations. We studied the impact of sea level fluctuations on sediment "dynamics" in the inner Kara Sea by using high-resolution acoustic sub-bottom profiling. The acoustic lines were ground-truthed with dated sediment cores. The first model data on LGM isostatic rebound for this region led us to the first confined interpretation of acoustic units in terms of sequence stratigraphy. We identified and mapped three characteristic sedimentary and depositional surface environments and established sediment masses for each facies type for the Holocene. Furthermore we refined the location of the eastern LGM ice margin, by new sub bottom profiles.

Sea level fluctuations resulted in periods of sub-aerial exposure of huge shallow shelf areas especially in the circum Arctic realm. The Kara Sea Shelf is characterised by a major incised dendritic paleo-river network, that is variably infilled with late Pleistocene to Holocene estuarine sediments topped by marine facies, showing draping geometries.

The Kara Sea can be subdivided into three facies areas A to C: estuaries, the shelf and deeper (> 120 m water depth) lying areas that accumulated a total of 114×10^{10} t of Holocene sediments.

The shelf channel system was formed during the Weichselian sea level cycle having its lowstand in the LGM. Deposition occurred constantly in Facies C, with higher sedimentation rates during sea level lowstand when all material by-passed Facies A and B. Sediment accumulation progressively shifted towards the modern coastline and the recent estuary of Ob and Yenisei, making up Facies A. There is a significant component of reworked material in Facies B making up at least 50 % of the sediment mass.

Fluvial evolution of the Kara Sea Shelf (Chapter 3.5)

The analysis of numerous channels on the Kara Sea shelf led to the conclusion that they were formed during the last global sea level regression phase, having its peak during the LGM. There is a distinct difference between the Ob and Yenisei branch resulting from the different slope gradients of their paleo-drainage paths and possibly different catchment characteristics. Both systems display filled channels, preferable found in shallow water depths, and open or partly filled channels.

Morphometric analysis of channel dimensions showed that they predominantly belong to the meandering river regime. These findings argue for a time interval of subaerial exposure and channel formation sufficient long enough for rivers to incise into the dry fallen shelf area and to adjust under equilibrium conditions.

The paleo-channels` dimensions are larger than the modern dimensions of recent gauge stations of Ob and Yenisei rivers on land, probably caused by colder climate conditions during LGM resulting in a distinct peakedness of river run-off.

Most of the channels under investigation plot in the meandering river field, they are quite mature in terms of fluvial development. Although an absolute chronology is missing, the more than 700 km northward extent of fluvial features on the shelf, the good conservation of incised channels and their maturity argue for a fluvial-dominated history of the Kara Sea shelf.

It could be feasable that the larger Yenisei paleo-channels evolved from a rapid melt down of the LGM Putoran ice cap enhancing the fluvial discharge of the paleo-Yenisei effectively for several hundred years. It is remarkable that a sudden decay of a relative thin (300 to 400 m) ice cap, could account for the additional water volume necessary to form the larger dimension of the paleo-Yenisei channels.

Zusammenfassung

Rezenter Sediment Transport (Kapitel 3.2)

Oberflächensedimente der Karasee zeigen eine stark bimodale Verteilung in der Schlickfraktion. Die Maxima finden sich zum einen um 8 φ (4 μm), der dominanten Fraktion, und des weiteren bei 5 φ (25-40 μm). Der Großteil aller Proben weist diese bimodale Verteilung in unterschiedlicher Ausprägung auf. Das weit verbreitete Vorkommen der bimodalen Korngrößenverteilung in der Siltfraktion weist auf zwei Hauptprozesse für den Materialtransport hin.

Auf der Basis unserer Daten ist es jedoch nicht möglich, eine bestimmte Korngrößenfraktion mit einem Transportmechanismus zu verknüpfen, und es ist schwer, den „genauen" Prozess zu identifizieren. Wir favorisieren ein Szenario mit einem Sommer-Modus, der von extensivem, sedimentgesättigtem Süßwassereintrag dominiert wird, und einem Winter-Modus, welcher durch Materialumverteilung und Resuspension hervorgerufen durch Meereis- und Polyniabildung, charakterisiert ist.

Weiterhin haben wir die Magnetische Suszeptibilität (MS) an Oberflächenproben untersucht. Das MS Signal stammt eindeutig aus dem Putoran Gebirge im Einzugsgebiet des Yeniseis, und die Werte der MS nehmen mit zunehmender Wassertiefe ab. Dies deutet darauf hin, dass unverfüllte Flussrinnen, die den tiefsten Punkt in der Morphologie bilden, das MS-Signal entlang des Schelfs „verteilen". Die Partikel sinken durch die Wassersäule ab und akkumulieren am Meeresboden. Dichte-induzierte Strömungen folgen dem pleistozänen Relief. Dieser Prozess läuft in erster Linie im Sommer ab. Im Winter treten Resuspension und vermehrte Partikelumverteilung auf.

Sedimentation in den Ästuaren von Ob und Yenisei: Entwicklung und Sedimentbilanzierung (Kapitel 3.3)

Weichsedimente der Ästuare von Ob und Yenisei können in zwei akustische lithologische Sedimenteinheiten I und II (Unit I and II) unterteilt werden. Einheit II formt die prä-Holozäne Basis mit sehr geringer bis keiner akustischen Eindringung. Während des letzten Meeresspiegel Niedrigstandes stellte diese Basis eine Erosionsoberfläche mit zahlreichen eingeschnittenen Flussrinnen dar. Die jüngere Einheit kann in drei Untereinheiten Ia - Ic, unterteilt werden. Die untersten Einheiten Ic und Ib zeigen einen fluviatilen bis flach-marinen Charakter, und werden von einem „transgressiven System Trakt" und schließlich von einem „Hochstand System Trakt" (seit ca. 5000 Jahren vor heute) überlagert werden.

Berechnet auf der Basis heutiger Suspensionsdaten, akkumulierten während des

Holozäns zwischen 50 % und 75 % der fluviatilen Suspensionsfracht in den Ob und Yenisei Ästuaren. Eine stetige, südwärts über den heutigen Schelf gerichtete Migration des „Marginal Filters" (Lisitzin, 1995), dem Übergangsbereich zwischen Fluss und Ozean, als Folge des steigenden Meeresspiegels wird favorisiert, um die „fehlenden" Anteile zu erklären.

Die Existenz verfüllter Flussrinnen auf dem heutigen Schelf deutet darauf hin, dass die prä-Holozäne Geschichte der Kara See mit jener der Laptevsee vergleichbar ist (Kleiber und Niessen, 1999). Diese Rinnen müssen während des Meeresspiegel Niedrigstandes ausgeräumt worden sein und wurden während der Holozänen Transgression mit Sediment verfüllt. Flusserosion auf dem exponierten Schelf der südlichen Karasee während des Letzten Glazialen Maximums (LGM) impliziert kontinuierlichen fluviatilen Transport über den Schelf, sowie kein größeres Eisschild im Gebiet der Flusserosion, d.h. dem heutigen Kara See Schelf.

Akustische Fazies des inneren Karasee Schelfes: Implikationen für die Sediment-dynamik während des Spät Weichsel- bis zum Holozän (Kapitel 3.4)

Spät Pleistozäne bis Holozäne akustische Einheiten auf dem inneren Karasee Schelf bestehen aus Sedimenteinheiten, deren Ablagerung stark von Meeresspiegelschwankungen beeinflusst war. Wir haben die Auswirkung dieser Schwankungen auf die Sedimentdynamik in der inneren Karasee mittels hochauflösender akustischer Profile untersucht, die anhand von AMS-C^{14} datierten Sedimentkernen zeitlich eingehängt wurden. Des weiteren haben wir die Position des östlichen LGM Randes präzisiert. Modellrechnungen von isostatischen Bewegungen der Erdkruste während des LGMs bis zum Holozän führten zur ersten regional kalibrierten Meeresspiegelkurve und erlauben eine sichere sequenzstratigraphische Interpretation der akustischen Profile.

Wir haben drei charakteristische Sedimentablagerungsprovinzen identifiziert und auskartiert, sowie die Sedimentmenge für jeden Facies-Typ ermittelt. Fazies A nimmt den Bereich der heutigen Ästuare ein, Fazies B macht den Schelf bis zu einer Wassertiefe von 120 m aus und Fazies C die tieferliegenden Gebiete.

Die gesamte Holozäne Sedimentmenge aller drei Fazies Gebiete summiert sich auf 114×10^{10} t, von dem sich ein Drittel in den Ästuaren angereichert hat. Ablagerung trat in Facies C fortwährend auf, mit höheren Sedimentationsraten während des Meeresspiegeltiefstandes. Zu dieser Zeit passierte das gesamte Material Fazies A und B und es fand keine Ablagerung statt. Die Sedimentakkumulation verschob sich allmählich zur rezenten Küstenlinie und hin zu den rezenten Ästuaren von Ob und Yenisei (Fazies A). Fazies B enthält Anteile von umgelagertem Material, welche mindestens 50% der Sediment-Masse ausmachten.

Meeresspiegelschwankungen führten in weiten Teilen des flachen Schelfs zu Phasen von subaerischer Exposition. Der Karasee Schelf zeichnet sich durch ein großes eingeschnittenes, dendritisches Paläo-Flussrinnen System aus, welches unterschiedlich stark mit Pleistozänen bis Holozänen Ästuar-Sedimenten verfüllt ist, die von mariner Fazies überlagert werden.

Fluviale Entwicklung des Karasee Schelfes (Kapitel 3.5)

Zahlreiche Flussrinnen auf dem Karasee Schelf wurden während der letzten globalen, regressiven Meeresspiegelphase, die ihr Maximum während des LGM hatte, angelegt. Es gibt einen deutlichen Unterschied zwischen dem Ob und dem Yenisei System, der u.a. auf unterschiedliche Gradienten ihrer Paläo-Abflusspfade zurückzuführen ist. Beide Systeme zeigen vollständig verfüllte, vorzugsweise in Wassertiefen unter 30 m anzutreffende sowie offene oder teilweise verfüllte Rinnen.

Die morphometrische Analyse der Rinnen zeigte, daß diese in erster Linie dem mäandrierenden Flussregime angehören. Diese Ergebnisse deuten auf ein ausreichend langes Zeitintervall der subaerischen Exposition hin, in dem sich die Flüsse in das trocken gefallene Schelfgebiet einschneiden und sich unter Gleichgewichtsbedingungen dem mäandrierenden Flussregime anpassen konnten. Sie sind relativ reif in Bezug auf ihre fluviatile Entwicklung. Obwohl eine exakte, absolute Chronologie nicht existiert, lassen die mehr als 700 km nach Norden auf den Schelf reichenden fluviatilen Rinnen und deren gute Erhaltung auf eine fluviatil dominierte Geschichte der Karasee schließen.

Die Dimensionen der Paläo-Rinnen sind größer als die rezenter Flussläufe an Pegelstationen des Ob und Yenisei im Hinterland der heutigen Mündung, was auf kältere Klimabedingungen während des LGM zurückzuführen ist, die in ausgeprägten Abfluss-Maxima resultierten.

Die Dimensionen der Paläo-Yensiei Rinnen sind größer als die Paläo-Ob Rinnen. Es scheint plausibel, dass die größeren Yenisei-Rinnen sich während eines raschen Abschmelzens der LGM Putoran-Gebirgs-Eiskappe entwickelten, was den Flusseintrag des Paläo-Yenisei während einiger hundert Jahre deutlich verstärkte. Es ist bemerkenswert, dass solch ein rasches Schmelzen der relativ dünnen Eiskappe (300-400 m Mächtigkeit) für das enorme zusätzliche Wasservolumen verantwortlich sein könnte, das zur Erklärung der großen Dimensionen der Paläo-Yenisei Flussläufe nötig ist.

Part A

Introduction

1.Introduction

1.1. Aims of this thesis

1.1.1 The Project

This thesis is part of the joint German-Russian project "Siberian River Run-off" (SIRRO) and includes four manuscripts, generally focussing on the interpretation of acoustic sub bottom profiles, measurements of physical properties of sediment cores and on their sedimentological investigations, as well as investigations of the recent sedimentary processes on the shelf. The project SIRRO was initiated to investigate the nature of continental run-off from Siberian rivers, especially Ob and Yenisei rivers (Stein et al., 2003a and further references therein). The study of its behaviour in the Kara Sea and the adjacent Arctic Basin is the main objective of multidisciplinary research of the SIRRO project. Within SIRRO, six expeditions with RV "Akademik Boris Petrov" were carried out in 1997, 1999, 2000, 2001, 2002 and 2003 (Matthiessen and Stepanets, 1999; Stein and Stepanets, 2000, 2001, 2002; Schoster and Levitan, 2003, 2004). Geological investigations concentrated on characterisation and quantification of terrigeneous matter. For multidisciplinary geological studies a large number of surface sediment samples as well as long sediment cores were obtained. The first results of geological, geochemical, biological, hydrological and modelling studies were summarised by Stein et al. (2003a). The present study is closely related to the topics of SIRRO subproject E: "Terrigeneous sediment and particulate organic carbon flux: Sources, pathways, sinks, and variability", and mainly covers the subjects of sediment characterisation, flux and sediment volume calculations as well as paleo-environmental reconstructions.

1.1.2 Overview

Passive continental margins are an ideal area to study depositional and or erosional processes controlled by eustatic sea level fluctuations. In contrast, active continental margins are strongly subjected to hinterland variations in fluvial sediment delivery (Milliman and Syvitzky, 1992). Sea level change has a profound impact on the behavior of a fluvial system leading to total reorganization of the drainage system (Schumm, 1993). Rivers stretch across the shelf, discharging at the shelf edge, depositing drapes and submarine fans (Piper and Nourmark, 2001).

On the Kara Sea Shelf the following factors acted during the late Quaternary

- Sea level rise (changes)
- Glaciations
- Variable fluvial input
- Variable erosion, subaerial exposure of the shelf

In our working area, the sea level change is further complicated by the existence of ice sheets, which may have physically blocked the free fluvial development. During sea level lowstand rivers emerge over the dry fallen shelf. Dynamic sea level changes, especially during transgression, control the shape of sedimentary units, changing the accommodation space available: sedimentary units aggregate and prograde at a pace dictated by the sea level rise (Posamentier and Vail, 1988), diminishing the amount of material supplied to the lowstand deposits. Phases of deceleration resulted in infilling of coastal plains, promoting formation of deltas (Knox et al., 1993).

The thesis addresses recent and ancient sedimentation processes. The late Weichselian history in the Kara Sea has been reconstructed focussing on shelf shaping processes prior to the Holocene during the sea level lowstand of the last glaciation cycle.

High-resolution acoustic profile surveys with a length of more than 20,000 kilometres in total (obtained by several different sounding systems) offer detailed information about the seafloor topography and the thickness and structure of the upper Quaternary sediment cover of the southern Kara Sea. In combination with dated sediment cores we classified the sedimentary packages in terms of sequence stratigraphy. Furthermore, these data offer a substantial basis to calculate a post-glacial sediment mass balance and provide the basis for other studies, especially geochemical investigations (e.g. Stein et al., 2002a, 2003, 2004; Gebhardt et al., 2004). It also delivers topo-physiographic information for further geochemical (e.g. Kodina et al., 2003), paleontological (e.g. Simstich et al., 2003, 2004), and biological (e.g. Fetzer et al., 2003) studies.

Major objectives addressed in the frame of this thesis are:
- to study the dispersal of the fluvially-derived material on the (recent) shelf: what are the pathways of sediment? (CHAPTER 3.2, partly CHAPTER 3.3)
- to establish a Holocene sediment budget (CHAPTER 3.3 and CHAPTER 3.4)
- to interpretate the Holocene evolution of the inner Kara Sea Shelf and late Weichselian (last glacial) to Holocene change in sedimentary processes, sediment flux (CHAPTER 3.3 and CHAPTER 3.4) in relationship to paleoriver discharge (CHAPTER 3.5) and glaciation in the Kara Sea area (CHAPTER 3.4 and 3.5)
- to reconstruct the pathways ot the large west Siberian rivers Ob and Yenisei during last glacial maximum sea level lowstand, and their extended onto the shelf (CHAPTER 3.4 and 3.5)

1.1.3 Outline and Structure of the Thesis

Detailed information on special topics are given in each individual chapter. The background information (Chapter 2) concentrates on the physiography, further detailed in Chapter 3.1 by our own mapping, and the hydrography. Chapter 3.1 and 3.2 can be regrded as an extended introduction, representing the first results of our investigations.

Chapter 3.2: Dittmers, K., Niessen, F. and Stein, R. (submitted to GeoMarine Letters). Recent sediment distribution pattern and pathways on the inner Kara Sea Shelf.

Chapter 3.2 deals with physical processes impacting the modern sedimentation on the Kara Sea Shelf, conducted on surface sediment samples. We studied physical sediment parameters characterised by the silt fraction. Secondly magnetic susceptibility was studied to enlighten sediment distribution and pathways on the shelf as a good provenance indicator. Terrestrially derived sediments can be traced by the magnetic susceptibility, while the study of silt properties yield information about the transport mechanisms.

Chapter 3.3: Dittmers, K., Niessen, F. and Stein, R. (2003). Holocene sediment budget and Sedimentary History for the Ob and Yenisei Estuaries. *In: Stein, R., Fahl, K., Fütterer, D.K. and Galimov, E. M. (Eds.), Siberian River Run-off in the Kara Sea: Characterisation, Quantification, Variability, and Environmental Significance, Proceedings in Marine Sciences, Elsevier, Amsterdam, 457-484.*

High-resolution echosounding data and several sediment gravity cores taken in the Ob and Yenisei estuaries allow us to calculate the Holocene sediment budget of both rivers and to reconstruct their sedimentary history. Cores were radiocarbon-dated and linked to acoustic profiles using whole-core physical properties obtained by a multi-sensor-core-logger. The entire sediment fill of the present estuaries reflects a deepening-upward sediment growth structure suggesting that sea level rise exceeded sediment accumulation.

Chapter 3.4: Dittmers, K., Lambeck, K., Niessen, F. and Stein, R. (to be subm. Marine Geology). Acoustic facies on the inner Kara Sea Shelf: implications for late Weichselian to Holocene sediment dynamics.

In Chapter 3.4 we utilise the chronostratigraphic framework established for the Yenisei estuary and correlate it with profiles of the whole Kara Sea Shelf. We subdivide the shelf into sedimentary-physiographic domains and differentiate their evolution.The paleo-reconstruction reveals important information about the interaction of the LGM ice sheet and the Ob and Yenisei rivers. An important contribution is made by the first

model results that neglect what field data suggest: no isostatic movements exceeding the order of 15 metres.

Chapter 3.5: Dittmers, K., Niessen, F. and Stein, R. (subm. Global and Planetary Change). Late Weichselian Fluvial Evolution on the Southern Kara Sea Shelf, North Siberia.

Chapter 3.5 deals with morphological analysis of widespread channels on the basis of their geometry to deduce the paleo-hydrological conditions. Fluvial dimensions were identified on acoustic profiles. The channels bear valuable information about the riverine extensions onto the Kara Sea Shelf and their interaction with the LGM ice sheet.

The division into different publications focusing on the relevant topic of this cumulative thesis results in some thematic overlaps and repetitions between the chapters of topics, especially in the general introduction/background, which cannot be avoided. Data will be available at the Pangaea database (www.pangaea.de).

In the text numbers of chapters are cross references in this thesis to ease the reader its handling, In the puplications they are substituted by the correct citation.

All ages are given in calibrated calender years before present and are abrreviated ka BP (=thousand years before present).

Contributions to other publications

Stein, R., Dittmers, K., Fahl, K., Kraus, M., Matthiessen, J., Niessen, F., Pirrung, M., Polyakova, Ye., Schoster, F., Steinke, T., Fütterer, D., (2004). Arctic (paleo) river discharge and environmental change: evidence from the Holocene Kara Sea sedimentary record., Quaternary Science Reviews, 23, 1485-1511.

Stein, R., Fahl, K., Dittmers, K., Niessen, F., Stepanets, O., (2003). Holocene siliciclastic and organic carbon fluxes in the Ob and Yenisei estuaries and the adjacent inner Kara Sea: Quantification, variability, and paleoenvironmental implications, Proceedings in Marine Sciences, Vol. 6, Elsevier Amsterdam, 401-434.

Stein, R., Niessen, F., Dittmers, D., Levitan, M., Schoster, F., Simstich, J., Steinke, T., Stepanets, O.V. (2002). Siberian River Run-Off and Late Quaternary Glaciation in the Southern Kara Sea, Arctic Ocean: Preliminary Results, Polar Research, 21, 315-322.

2. Background

2.1 Physiographic Settings of the Study Area

   The entire Arctic Ocean (Fig. 2.1) makes up 4.3 % of the world's ocean area but only 1.4 % of the volume, representing the shallowest (mean depth 1,200 m) of all the major ocean basins of the world (Jakobsson, 2002). Continental shelves occupy more than 52 % of the area of the Arctic Ocean – while average shelves of the worlds oceans only constitute between 9.1 and 17.7 % of the respective areas (Menard and Smith, 1966).
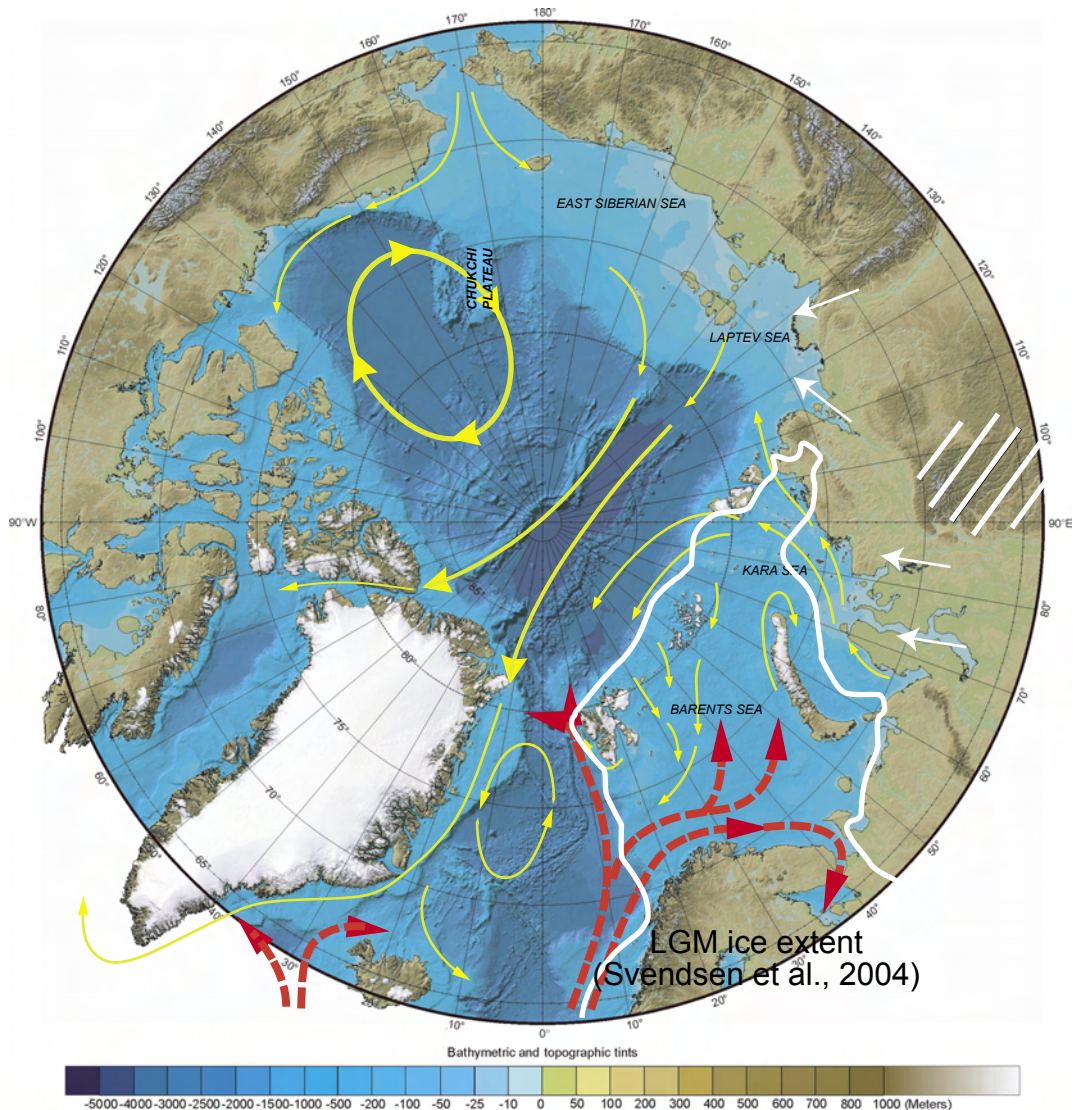
Figure 2.1. Arctic Ocean. Hatched arrows indicate warm Atlantic surface waters, yellow arrows Arctic waters and their circulation pattern (Aagaard and Carmack, 1989). The white line denotes the Last Glacial maximum most proximal ice extent with some uncertainties for the Putoran Mountains (hatched). Major riverine freshwater sources indicated by white arrows. Modified after (Knies and Vogt, 2003) based on IBCAO bathymetry (Jakobsson et al., 2000).

The Kara Sea Shelf alone (Fig. 2.2) makes up almost 10 % of the whole Arctic area (Jakobsson, 2002), measuring 873 x 10^3 km^2. Our working area in the inner Kara Sea covers 299 x 10^3 km^2. The expeditions carried out within the SIRRO Project were limited to sampling stations and acoustic profiles south of 78° N. Being very shallow with an average water depth of only about 130 and 50 m for the whole Kara Sea and inner Kara Sea, respectively (Jakobsson, 2002), this shelf area is very sensitive to eustatic sea level changes between glacial and interglacial time periods. More than 50 % of the Kara Sea area are occupied by water depths of less than 50 m (Table 2.1). Among the Arctic marginal seas the Kara Sea is the third largest in area and the second largest in recent water volume (Jakobsson, 2002; Table 2.1).
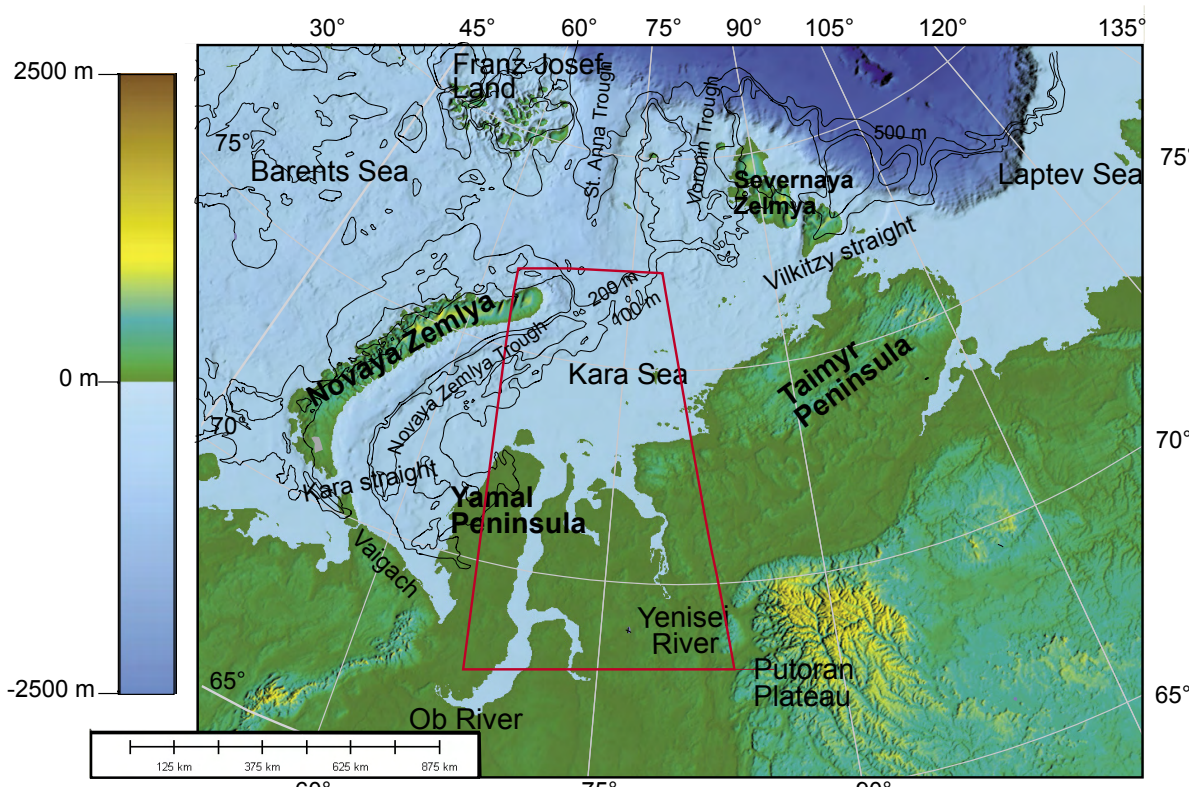
Figure 2.2 Kara Sea: overview and physiography

In general, the bottom topography of the northern Kara Sea, north of 76° N, is characterised by water depths of more than 50 m (Fig. 2.2) while the South is dominated by shallow waters (with mean depths of 25-30 m) of the "Ob-Yenisei Delta" (Johnson and Milligan, 1968). Two major depressions are found in the northern Kara Sea: the roughly north-south aligned St. Anna Trough (up to 610 m deep) and the Voronin Trough (up to 450 m deep). These troughs with depths greater than 300 m are thought to represent glacial outlet fjords of former glaciations (prior to LGM: Polyak et al., 1997). The Novaya Zemlya Trough is aligned along the east coast of Novaya Zemlya with water depths of up to 350 m and probably represents a sediment starved

Table 2.1. Kara Sea hypsometric characteristics after Volkov (2002)

	Water Depth			
	0-50 (m)	50-100 (m)	100-200 (m)	200-500 (m)
Area (x10^3 km^2)	373	170.7	189.7	146.9
Volume (km^3)	9,3	12.8	28.5	51.4

basin (Lastochkin, 1978).

The name "Kara" may origin from the Tartian/Kasachian term for "black" possibly due to the Kara Sea's waters being enriched in humic acids and thus exhibiting a much darker colour than the neighbouring Barents Sea's clear waters. The Kara Sea ("Karskoye More") is a semi-enclosed ocean basin bounded by Novaya Zemlya in the North-West, the Siberian Coast in the South and Severnaya Zemlya in the East, while to the North it opens to Central Arctic Ocean waters. In the South-West the Kara Sea is connected to the Barents Sea via the Kara Strait which is 45 km wide, 33 km long and up to 119 m deep. Pavlov and Pfirman (1995) estimate a through-flow of 1,640 km^3/y – the same magnitude as the total river run-off into the Kara Sea, while a water volume of 5,000-10,000 km^3/y flows from the Barents Sea into the Kara Sea north of Novaya Zemlya (Pavlov and Pfirman, 1995). The Vilkitsky Strait between the Siberian mainland and Severnaya Zemlya connecting Kara Sea and Laptev Sea in the East is characterised by a minimum width of 56 km and depths reaching 210 m. The water flow from Kara to Laptev Sea is estimated to be 4,900 to 11,000 km^3/y (Pavlov and Pfirman, 1995).

2.2 Hydrography

The whole circumarctic drainage area measures 1.5 times the area occupied by the Arctic Ocean, and is consequently the world`s most land-dominated drainage area (Petersen et al., 2002). The catchment area of the Russian Arctic measuring 12.6 x 10^6 km^2 makes up 56 % of the area of the former Soviet Union. Run-off totals 2,808 km^3/y of which 85% are supplied by Siberian rivers (Romankevich and Artemyev, 1985; Holmes et al., 2002, Romankevich et al., 2003).

River run-off largely contributes to the Arctic Ocean freshwater budget and presently accounts for 50 to 60 % of all freshwater influx into the Arctic Ocean, with saline water import through the Bering Strait between the Asian and American continents, and precipitation in the Arctic Ocean being lower than evaporation accounting for most of the remainder.

The largest river falling into the Arctic based on discharge is the Yenisei river, while

the Ob river is characterised by the largest catchment area. Medianly directed rivers have a characteristic spring-summer flood wave surge moving northwards breaking up ice causing ice dams and high water levels (Aagaard and Carmack, 1989; Carmack, 2000).

Table 2.2. World's largest rivers' characteristics (from Degens et al., 1991 and Telang et al., 1991)

Rank	Based on drainage area (x1000 km^2)		river length (km)		total anuanl Run-off (km^3/y)		Suspended sediment (km^3/y)
1	Amazon	6915	Nile	6670	Amazon	6923	1150
2	Congo	3680	Mississippi	6420	Ganges	1386	970
3	Murry	3520	Amazon	6280	Congo	1320	???
4	La Plata	3100	Yangtze	5520	Orinoco	1007	150
5	Ob	2990	Mackenzie	5472	Yangtze	1006	480
6	Mississippi	2980	La Plata	4700	La Plata	811	???
7	Nile	2870	Hiwang Ho	4670	Yenisei	618	5
8	Yenisei	2580	Mekong	4500	Lena	539	11
9	Lena	2490	Lena	4400	Mississippi	510	210
10	Niger	2090	Congo	4370	Mekong	505	160
11	Amur	1885	Niger	4160	Chutsyan	430	???
12	Yangtze	1800	Ob	3650	Ob	404	16
13	Mackenzie	1790	Yenisei	3490	Amur	360	???
14	Ganges	1730	Murray	3490	Mackenzie	325	100

Table 2.2 gives an overview of the world`s 14 largest rivers, by several criteria. The Ob and Yenisei rivers are characterised by large dimensions and drainage areas, but with moderate discharge and little sediment load. The Ob and Yensiei rivers discharge 404 km^3/y and 618 km^3/y freshwater on the average, respectively (see Table 2.2 and Figure 2.3 for details). Significant portions of the drainage area of both rivers are dominated by permanent and seasonal permafrost. The recent discharge of total suspended matter by the Ob and Yenisei rivers averages to 15.5 x 10^6 t/y and 4.7 x 10^6 t/y, respectively. For the Yenisei, a total suspended matter supply of 14.4 x 10^6 t/y which is about three times higher than the modern value, has been measured for times preceding the dam constructed near Krasnoyarsk in 1967 (Telang et al., 1991; Holmes et al., 2002, see Table 2.2). In Figure 2.3 the average discharge is compared to data obtained during the SIRRO expedition 2001 (Gebhardt et al., 2004).

The enormous water release into the Kara Sea leads to the establishment of a halocline below a relatively thick low salinity surface layer extending up to approximately 80° N. The total annual run-off would accumulate to a 1.5 m thick layer of freshwater for the Kara Sea area (Gebhardt et al., 2004). Thus, the whole system can be seen as

an estuary. The existence of the giant freshwater layer with its associated halocline has profound impact on the sediment distribution on the shelf, but also enhances sea-ice formation and influences primary production.
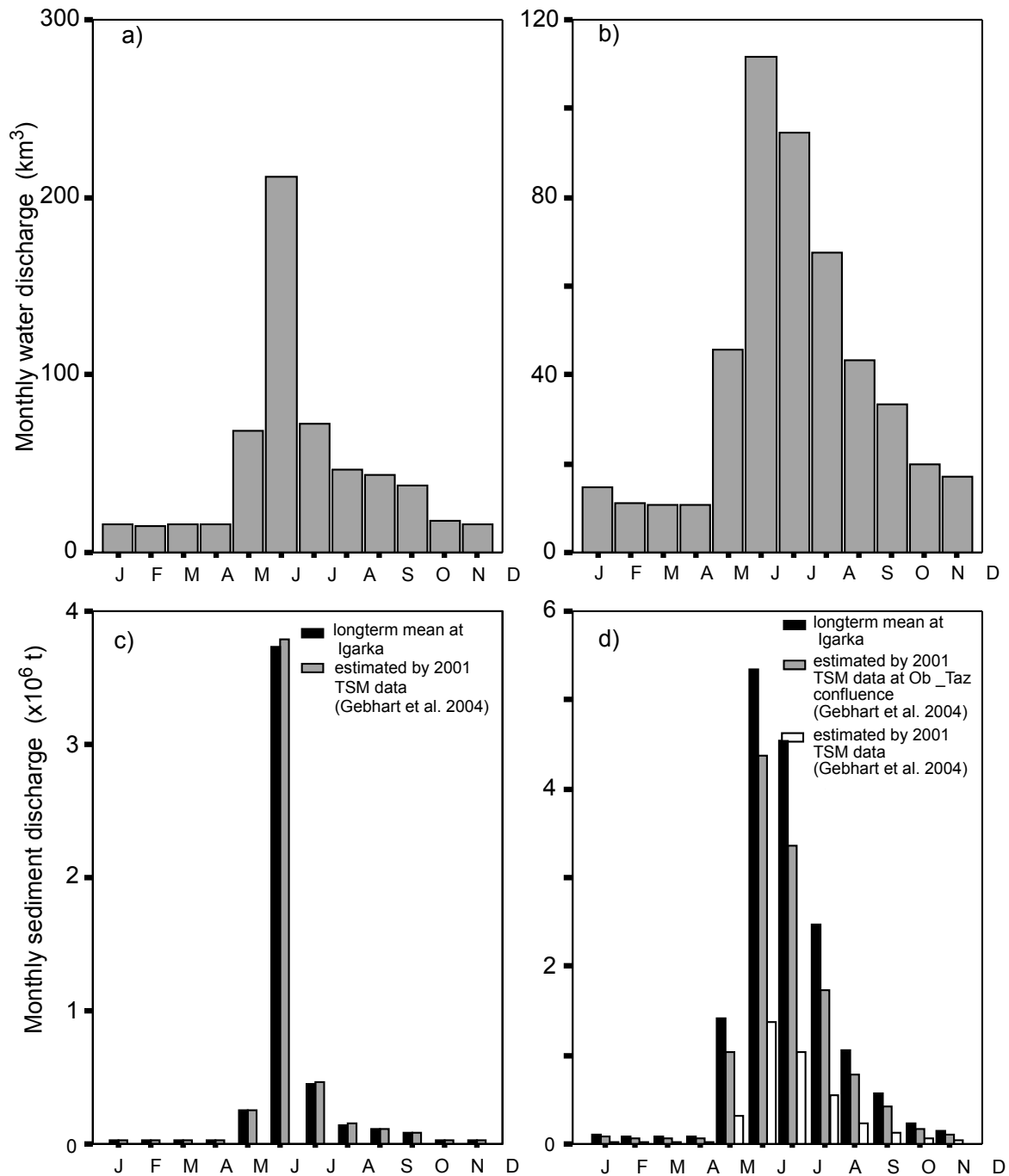
Figure 2.3. Water and sediment discharge of Ob and Yenisei rivers after Gebhardt et al. (2004). Long term mean water discharge are given in a) Yenisei and b) Ob and sediment discharge for Yenisei in c) and Ob in d).

2.3 Research History

Seibold (2001) gives an overview on the exploration and map development along the Arctic coast of Siberia and an example of an early map drawn in 1721 of our working area (Fig. 2.4). The coasts west of the Ob estuary have been fairly well known from about 1600 B.C. on, mainly by merchants, sailors and fishermen and finally by British and Dutch as well as some land-based expeditions. In the beginning of the 16th century first fortified towns along the major rivers evolved (Tobolsk on the Irtish: 1587, Tomsk on the Ob: 1604, Yeniseyesk on the Yenisei: 1619). These towns became

Figure 2.4. Historical map of Seuter from 1721 of the working area taken from Seibold (2001)

exploration centres from where investigations started down river and along the coasts. First scientific data on the Kara Sea were collected by the Swedish expeditions of Nordenskjöld in 1875 (on the Pröven), in 1876 (on the Ymer) and in 1878 (on the Vega). In 1893, the Kara Sea was surveyed by Nansen's famous Fram, followed by several smaller pushes of several expeditions. Since the early 1920's, the Russians intensified their investigations strictly keeping other countries from entering the area. Thus the Kara Sea became "Terra Incognita" again for other nations during Soviet times for two reasons: 1. nuclear weapon testing on Novaya Zemlya and dumping of nuclear waste in the Novaya Zemlya trough, 2. the discovery of gigantic gas resources in the South Kara Sea basin situated in the southern Ob estuary, a gas-prone province at least for the Cretaceous and Upper Jurassic section. Russian scientific investigations have been undertaken since the 1950's but with only little output in western literature (Kulikov and Martynov, 1961). The „Atlas of ground of the Arctic Ocean" (Treshnikov, 1985) summarises this knowledge, consisting of a large suite of maps including generalised maps and contour plots. However, the data source is uncertain. In 1965, the first „western" ship entered the Kara Sea again conducting the Northwind expeditions (Johnson and Milligan, 1968). The first multidisiplinary, modern investigation was carried out by RV "Dimitry Mendeleev" in 1993 (Lisitzin et al., 1995).

Part B

3.Results
3.1 Bathymetry

3.Results

3.1 Bathymetry

A detailed high-resolution elevation model was not available for our working area, thus we modelled the Kara Sea on the basis of sea-bottom depth soundings of the ELAC sub bottom profiler, calibrated to mean sea level, conducted during RV "Akademik Boris Petrov" expeditions in 1999, 2000 and 2001 (Stein and Stepanets, 2000, 2001, 2002) (Figs 3.1 and 3.2). Combined with soundings of nautical charts great areas have been completely remapped. The influence of tides is neglectable with a ranging from 0.3 m to 0.5 m (Pavlov and Pfirman, 1995). In order to combine available data of the Arctic Ocean and our data we merged our data set with the IBCAO data set (Fig. 3.2, Jakobsson et al., 2001). For both datasets, (Latitude, Longitude, and water depth) data points were simply merged and a gridfile created with the Generic Mapping Tool (GMT,
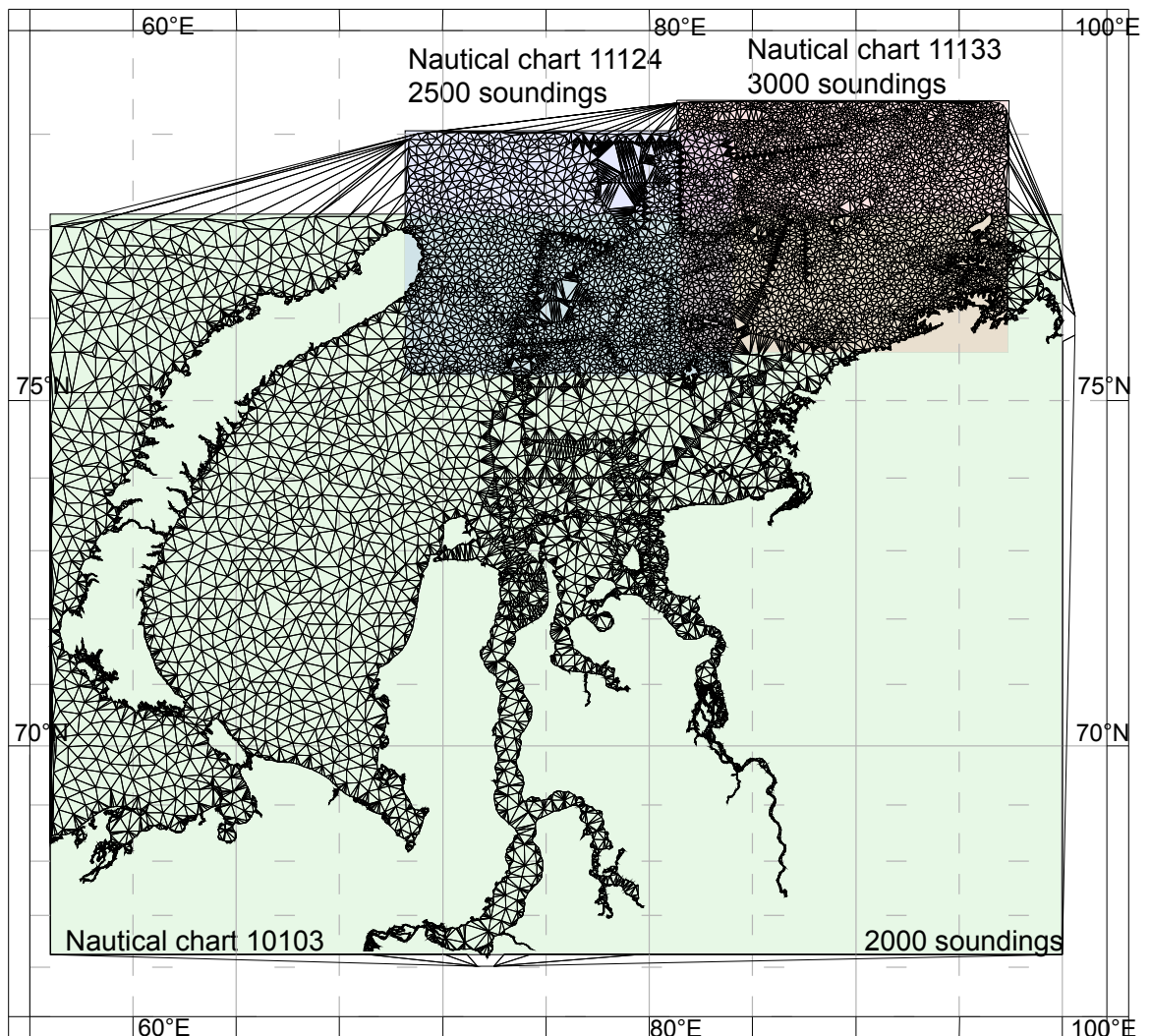
Figure 3.1. Triangulated digital elevation model with the relevant data points. Nautical charts are shaded.

Wessel and Smith, 1991) .

The resulting elevation model (Figs 3.2 and 3.4) was carefully cross-checked with our soundings and a clear improvement in vertical resolution was achieved (Fig. 3.3). In combination with GIS tools, e.g. Global Mapper, was useful for area calculations and estimates of water volume as well as for the cons truction of morphological sections of the shelf.
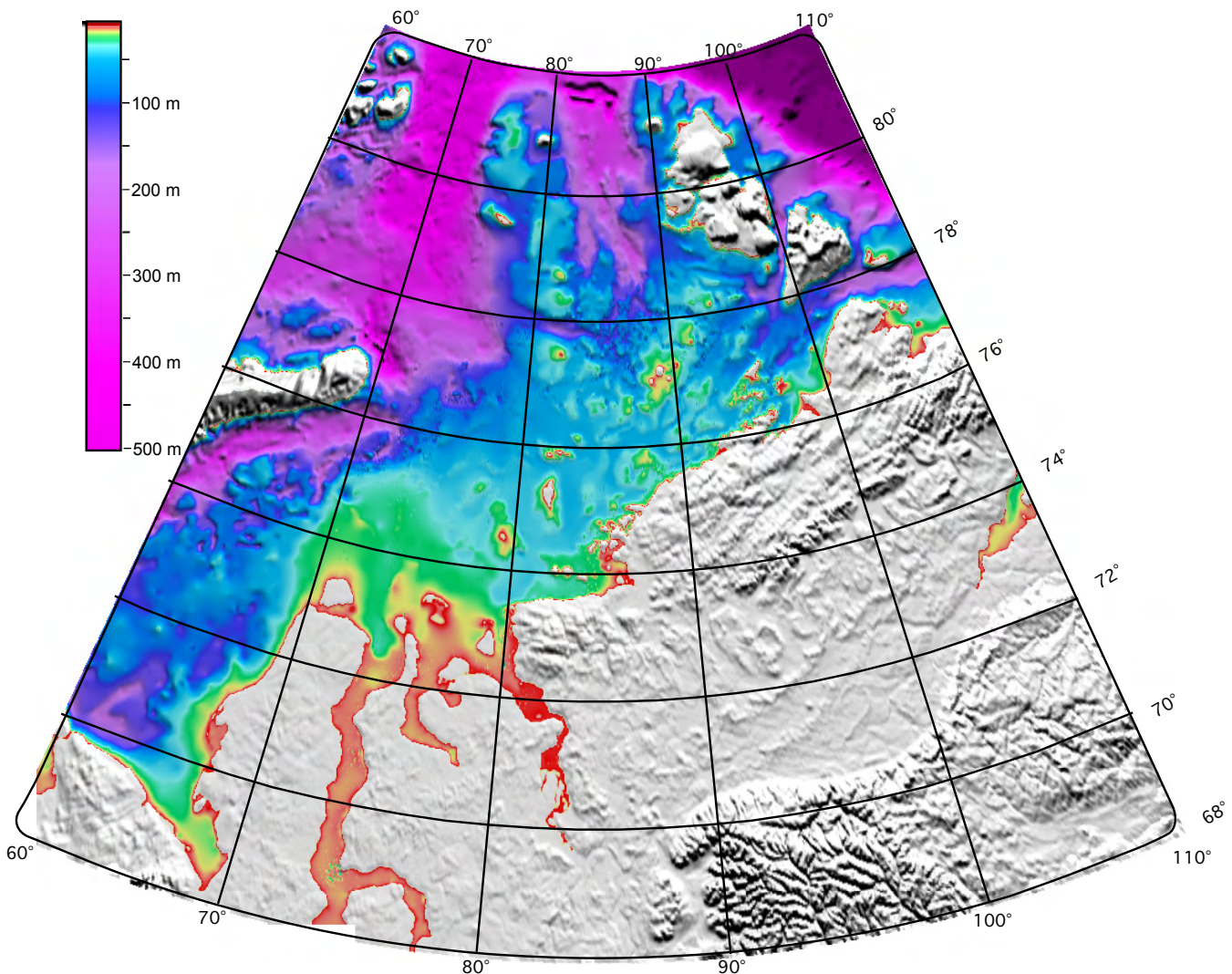
Figure 3.2. Isobath map of the new elevation model. Note the hummocky relief at the shelf break and in the NE area of the working area. Equidistance until the 150 m isobath: 10 m. The data presented here are available at www.pangaea.de.

Data Basis

A total of 10,000 ship's soundings and some additional 8,000 soundings obtained from the nautical charts were digitised and used to compute the elevation grid (Figs 3.2 and 3.4). Geo-referenced soundings were gathered generally every 5 minutes

(ship`s time), with a higher frequency at diversified terrains. The nautical charts were geo-referenced, transformed, rectified, and digitised subsequently by KK+W (Kiel, Germany). Isolines were created using the "tin contour" function of ARC Info. Conflicts arising from the different data sources were addressed as follows: the first problem encountered was the different scale, resolution, and cut-outs from the nautical charts, which is especially problematic in combination with our echo-soundings. Thus, a priority of data sets was established: the primary category used are the echosoundings of our expeditions with RV "Akademik Boris Petrov". Then, according to their resolution, maps 11133 and 11124, and sheet 10103 at last, displaying the lowest resolution and lowest density of soundings, were used.

Additionally, in order to emphasise our soundings, where we have the best confidence in data quality, a buffer of 1.5 km width was established around the ship's track lines beyond which all other soundings were excluded.
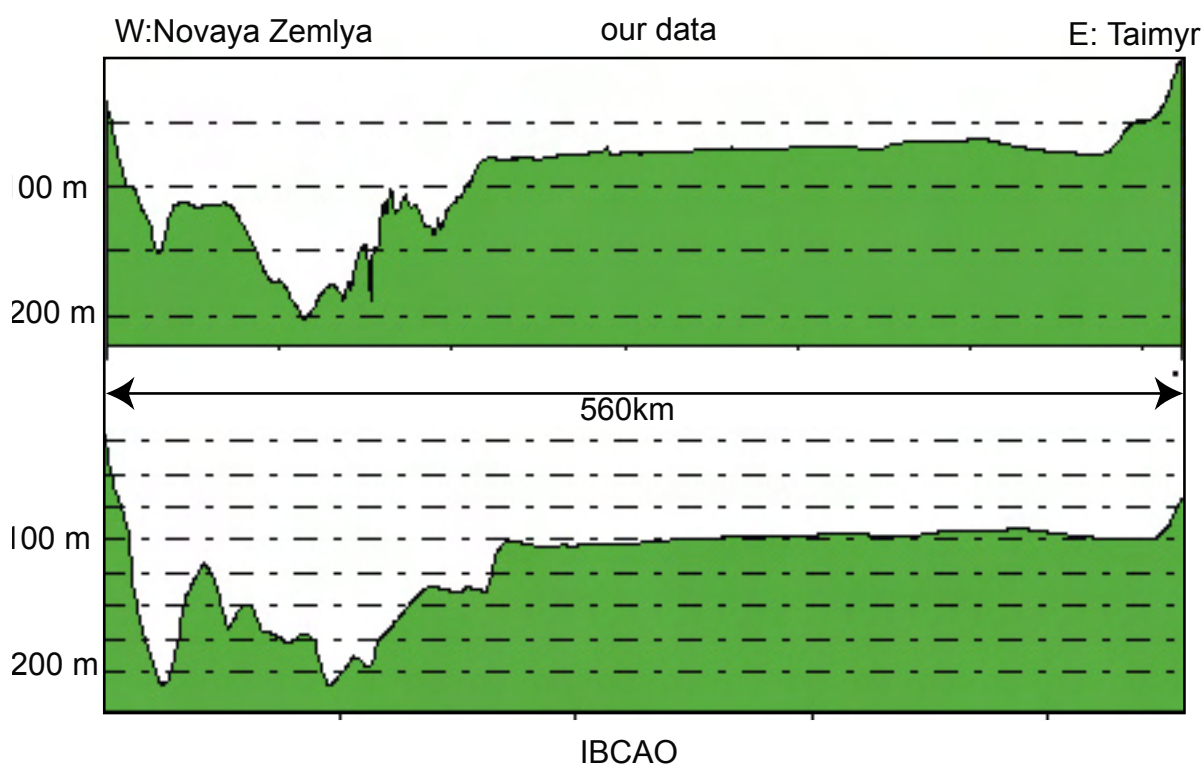
Figure 3.3. Selected sections of IBCAO model and our data.

First Implications from new elevation data

Figure 3.2 displays the dendritc pattern of the paleo-Yenisei branch: This pattern evolved during times of sea level lowstand when the Yenisei ancestor incised into the seabed of the Kara Sea. This process is described and interpreted in detail in Chapter 3.4 and Chapter 3.5.

The seabed roughness shown in Figure 3.4 gives a first impression of the shape of the
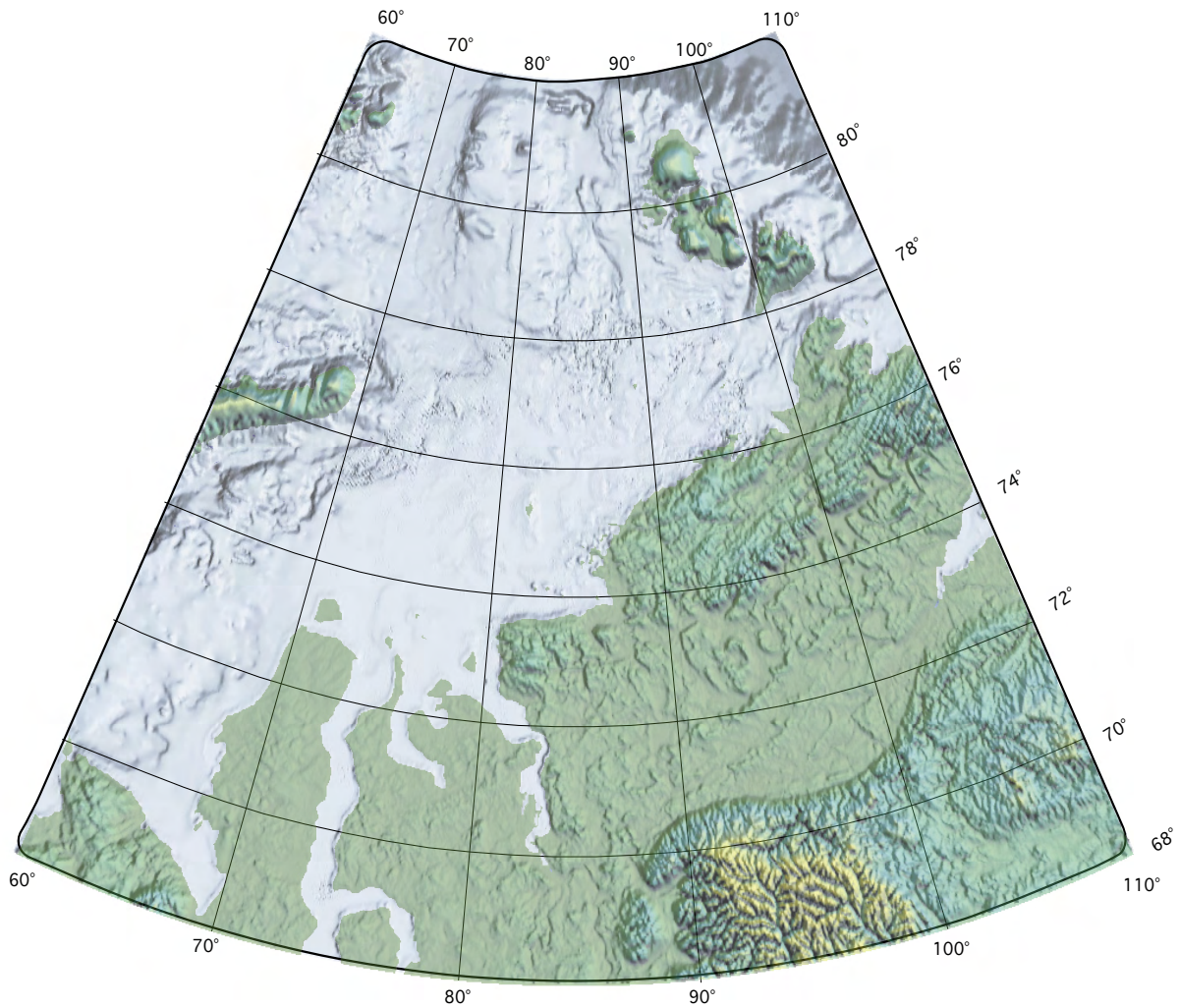
Figure 3.4. Elevation model of our data, visualised with Global Mapper (VERSION 5.10). In this illustration the sea-floor, area that lies underneath 0 m, elevation gradient is shown as shading. Note that large areas of the shelf are rather planar. Formerly glaciated terrain is identifiable by irregular shadings in the NE of the working area north of 76° N and in the west around 70° E.

Kara Sea sea bottom. It is remarkable that the Kara Sea can be subdivided visually into different provinces. In Chapter 3.4 these provinces are related to paleoenviron-mental processes that shaped them. Hummocky relief is for example produced by the action of glaciers and ice sheets that constantly advanced and retreated and defor-med the surface. This formerly glaciated terrain is in evidence by irregular shadings in the NE of the working area north of 76° N and in the west around 70° E. Whereas the shelf and the modern estuaries are rather planar over large distances.

Data are available at www. Pangaea.de.

3.2 Recent sediment distribution patterns and pathways on the inner Kara Sea Shelf (Siberia)

3.2 Recent sediment distribution patterns and pathways on the inner Kara Sea Shelf (Siberia)

Dittmers, K., Niessen, F. & Stein, R.

Alfred Wegener Institute for Polar and Marine Research, Columbusstrasse 2, 27568 Bremerhaven,Germany

Abstract

We studied the silt fraction on the shallow (20-30 m) continental shelf of the Kara Sea, Siberia, with the Sedigraph 5100 in order to enlighten sedimentary processes. Magnetic susceptibility of surface sediments was investigated to reconstruct recent transport pathways of magnetic minerals indicative of terrestrial sediments. From the distribution of magnetic susceptibility, we reconstructed a gravity driven sediment, guided by incised channels on the shelf, representing topographic lows.

Surface sediment samples exhibit a prominent twofold grain-size distribution. The peaks cluster around 8 φ (4 μm), the dominant mode, and at a secondary peak at 5 φ (25-40 μm). The majority of all samples display both peaks unequally strong pronounced. The twofold grain-size peaks strongly suggest two peaks in current intensity, probably related to at least two different processes.

It is evident that sediment pathways follow the morphology of the sea-floor, indicating density-driven bottom layer transport: magnetic susceptibility values abate away from distributary channels. The distribution pattern of magnetic susceptibility in dependence on water depth can be seen as a dilution indicator for the river-derived material. The susceptibility signal clearly originates in the Putoran Mountains in the drainage area of the Yenisei branch. The susceptibility values decrease with increasing water depth to the North. Basically there are two atmospheric regimes driving the water circulation and thus the sediment distribution in the Kara Sea. this results in enhanced particle input by rivers during the summer and prevailing erosion during winter.

Keywords: surface sediments, silt fraction, terrigeneous fraction, Kara Sea, river run-off

1. Introduction

Continental shelves play an important role for the distribution and "digestion" of fluvially-derived fines, by advection and particle settling (Windom and Gross, 1989). It is estimated that less than 10 % of river-supplied particles are transported across the shelf and reach the deep sea (Drake, 1976; Eisma, 1982; Postma, 1990). Therefore they act as an interface between land, river and ocean (Rudels et al., 2000).

In the Arctic realm terrigeneous sediment supply is controlled by river discharge, sea-ice transport and coastal erosion (e.g. Darby et al., 1989; Stein and Korolev, 1994; Rachold et al., 2003). Particularly the shallow waters of the shelf are subject to reworking by press ice ridges and enhanced water circulation due to ice formation (Reimnitz et al., 1992, 1993, 1994; Dethleff, 1994; Eicken et al., 1997, 2000). On the other hand shallow coastal and estuarine areas are effectively sheltered by fast-ice

from vigour wave-induced currents from autumn to spring (Divine et al., 2003, 2004). Biological productivity in the water column is relatively low compared to other oceans due to the nearly permanent sea-ice cover and low temperatures (Subba Rao and Platt, 1984; Grebmeier, 1995; Stein, 1996). Therefore, the mineralogy parameters of sediments can be used to study the imprint of processes on the sedimentary record without significant distortion (Wahsner et al., 1999; Schoster et al., 2000). So far granulometric investigations of the major components have focused on bulk sand-silt-clay fractions (Steinke, 2002; Stein et al., 2004). In the inner Kara Sea recent fresh water and terrigeneous sediment fluxes are quite well-studied (Telang et al., 1991; Gordeev et al., 1996; Gordeev, 2000; Holmes et al., 2002). The incoming suspended sediment masses are also investigated by Lisitzin et al. (1995) and recently by Beeskow et al. (2003) and Gebhardt et al. (2004). We intend to study and characterise transport ways and mechanisms of fine-grained, riverborne particulate matter. The main focus of this paper is the investigation of suspended sediment dispersal in the inner Kara Sea (up to 78° N).

First of all we studied physical sediment parameters characterised by the silt fraction best suited to study suspended material processes and the physical factors controlling sedimentation. The silt fraction resembles the grain-size fraction that currents are capable to mobilize (McCave et al., 1995). Magnetic susceptibility was studied to highlight sediment distribution and pathways on the shelf, as tracer and important indicator for sediment flux. In this study we expand our existing surface data (Dittmers et al., 2003; Stein et al., 2004) by stations especially north of 75° N. Magnetite, titanomagnetite or maghemite (Thompson and Oldfield, 1986) are the main carriers of magnetic susceptibility. Variations in magnetic susceptibility mainly reflect compositional variations in the terrigeneous source material: the Putoran Mountains-originated fraction of the Yenisei River (Dittmers et al., 2003; Stein et al., 2004) (Fig. 1). The upper Permian to lower Triassic basalts lavas and tuffs of the Putoran mountains are made up of up to 2 km thick basalts covering an area of 1,800 km striking NE to SW and of about 1,000 km width (Sharkov, 1980).

According to Ceasium isotopic studies all surface samples are recent (Stepanets et al., 2000 in Stein and Stepanets, 2000) and exhibit no significant older ages.

Background: Environmental settings

In the summer sediment transport processes are dominated by a northwest, clockwise directed surface flow consisting of a top flow fed by the strong fluvial freshwater and sediment supply (Fig. 1) and a highly saline, denser and colder "counter-current" intruding into the shallow shelf through depressions formed by channels (Chapter 3.5)
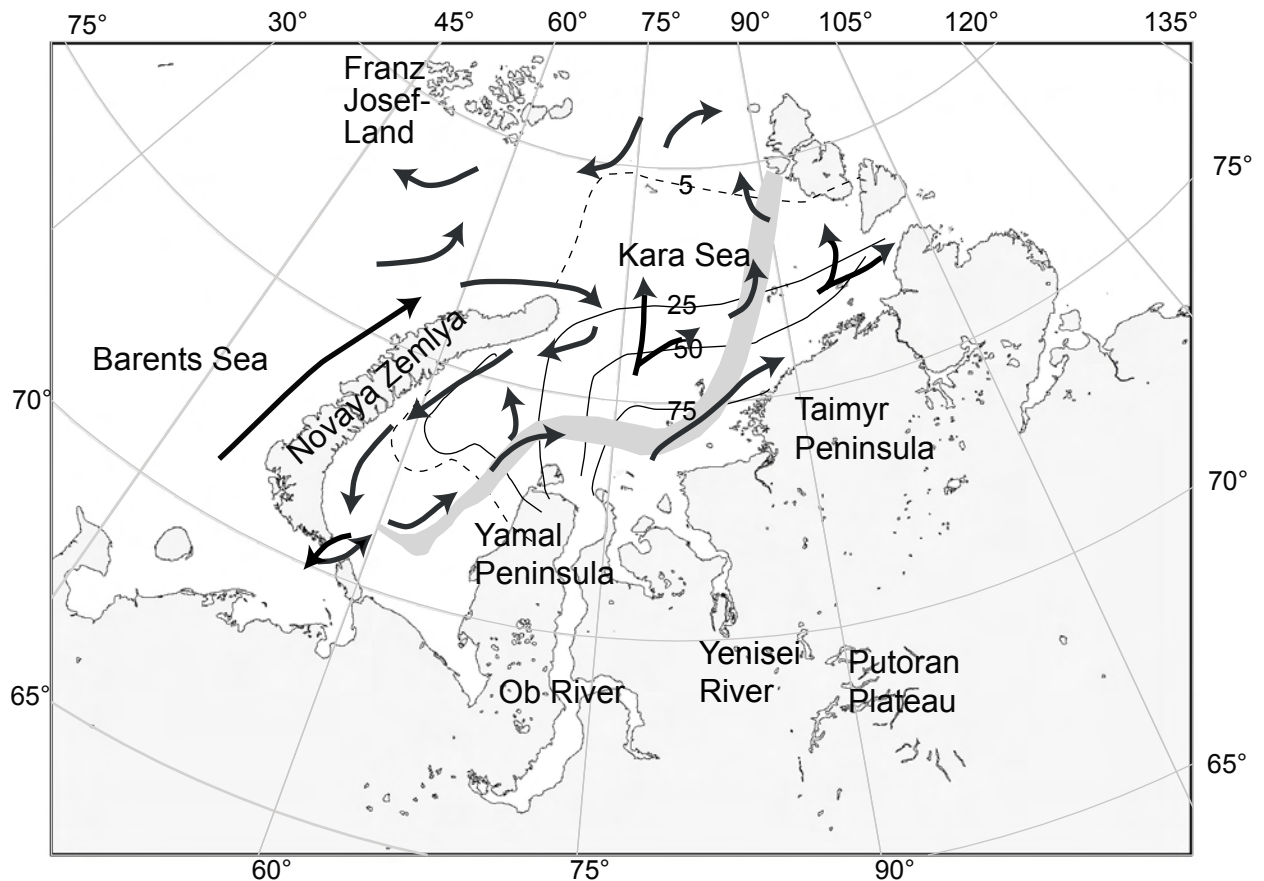
Figure 1. Working area with position of annual polynia, surface circulation and salinity after Pavlov and Pfirman (1995). Position of Polynia after Polyakov and Johnson (2000) and Divine et al. (2003, 2004) indicated by grey shaded area; arrows indicate prevailing summer surface currents; summer surface salinity isolines indicate relative dilution of fluvial freshwater.

into the estuaries as visible in the bottom salinities (Fig. 2a) (McClimans et al., 2000; Simstich et al., 2003). Winter surface circulation is the opposite with anti-cyclonal flow (McClimans et al., 2000), and reverses the bottom currents to a net outflow (Harms et al., 1999, 2000). The total winter discharge accounts for only 5-10 % of the total river run-off (Antonov, 1970; Holmes et al., 2002). Harms et al. (2000, 2002, 2003) developed an atmospheric driven circulation model for the Kara Sea and also computed bottom current speeds (Fig. 2b). The highest current speed is observed in the shallow waters of Ob and Yenisei, as well as in near-coast regions.

Besides their water loads the Arctic rivers also transport large amounts of dissolved and suspended material towards the ocean (Gordeev et al., 1996; Holmes et al., 2002; Rachold et al., 2003). The modern annual discharge of total suspended matter by the Ob and Yenisei rivers is 15.5×10^6 t y^{-1} and 4.7×10^6 t y^{-1}, respectively (Holmes et al., 2002; Telang et al., 1991). Based on filtration studies of the 2001 expedition, Gebhardt et al. (2004) estimate that the Yenisei annually delivers 5.0×10^6 tons of sediment to the Kara Sea, while in contrast the Ob river estuary "absorbs" 75 % of the fluvial
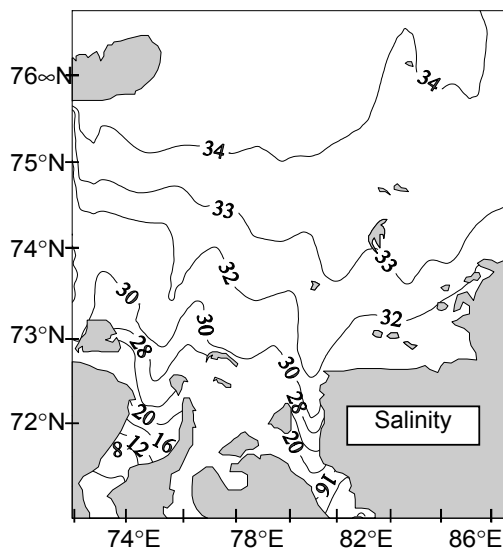
Figure 2 a). Bottom salinity gradients of Simstich et al. (2003)

supplied material and releases 3.76 x 10^6 tons of sediment into the Kara Sea.

Basically the suspended matter is trapped in the estuaries where a freshwater wedge overlays the sea water. Mixing with salt water promotes rapid precipitation of fine-grained suspension due to coagulation processes, resulting in high sediment accumulation rates (Dittmers et al., 2003). Approximately more than 90 % of the suspended matter and about 30 % of the dissolved matter accumulate within this "marginal filter" (Lisitzin, 1995). Accumulation rates rapidly decrease north of about 73° 30´N (Stein et al., 2003b, 2004), as visible on acoustic records (Dittmers et al., 2003). From the Mississippi mouth, for example, it is also well known that concentrations in the river plume are reduced by 90 % within 5–10 km of the river mouth (Hill et al., 2000). Recent research showed that estuaries not only act as chemical boundaries, but also influence the settling behaviour of suspended matter due to a rapid change of hydrological/physical settings (Dyer et al., 2004).
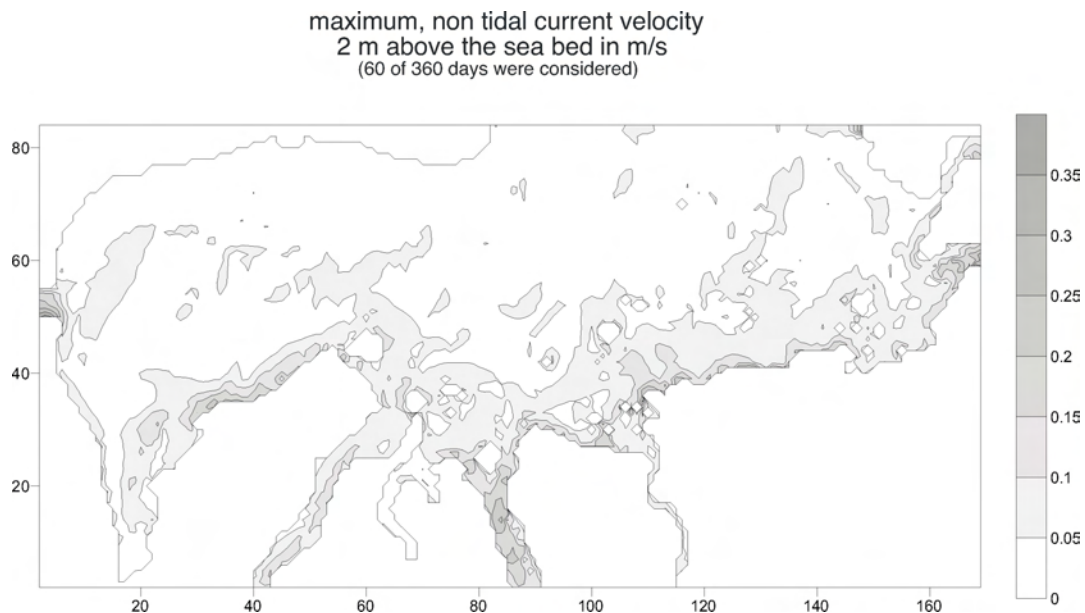
Figure 2 b). Modelled bottom velocity of atmospheric forced shelf model after Harms et al. (2000,2003)

2. Methods

Surface sediment samples were obtained during three expeditions with RV "Akademik Boris Petrov" carried out in 1999, 2000 and 2001 (Stein and Stepanets 2000, 2001, 2002). Wet surface sediments were obtained with the multicorer, giant box corer and an oceangrab (Stein and Stepanets, 2000, 2001, 2002). Priority of station selection was to sample high Holocene thickness sites.

The bulk organic carbon contents of surface sediments of the Kara Sea Shelf are moderate ranging from 1 % with to values around 2 % in the estuaries, along depression and in the vincinity of the coast (Stein and Fahl 2003, Stein et al., 2004). Towards the North the shelf values lie below 1 % in the working area. This fact eases silt-size sample analysis and preparation (Stein, 1985) and minimizes difficulties due to coagulation effects. Biogeneic opal content in Kara Sea sediment is < 2 % (Stein and Nürnberg, 1995) and can be neglected.

Silt-size analysis

The sand fraction (> 63 µm) was separated by wet sieving, while the remainder fraction (< 63 µm) was collected in 50 ml plastic bottles. From the fine fraction calcium carbonate was removed by 3 % acetic acid and organic content was oxidised by 10 % hydrogen peroxide (standard AWI procedure, for details see Hass, 2002). The carbonate-free samples are regarded as the terrigeneous fraction hereafter. For ideal dispersal after this treatment sediment was put 24 h on a shaker and spiked with sodium polyphosphate. The grain-size distributions was determined using a Micromeritics Sedigraph 5100 over the 1.5 to 63 µm range measuring the grain-size distribution of silt in 1/10 φ steps. Analytical details and errors are described by Stein (1985), McCave et al. (1995) and Bianchi et al. (1999).

After grain-size analysis samples were dried and weighed for calculation of weight percentages of the sand, silt and clay fraction. For the silt fraction (McCave et al., 1995) cumulative curves of the sedimentological parameters were plotted and various statistics characterising the grain-size distribution were computed (Pettijohn, 1975). Statistical parameters such as arithmetical mean, modal size (peak occurence), sorting (= standard deviation) and skewness were determined after the method of moments (Krummbein, 1936).

Magnetic Susceptibility (MS)

Magnetic susceptibility is defined as the dimensionless proportional factor of an applied magnetic field in relation to the magnetisation in the sample of a known volume (expressed in SI units; Thompson and Oldfield, 1986; Pirrung et al., 2002). The volume

magnetic susceptibility of the freeze-dried bulk samples (10 cm^3) were measured after the method of Niessen and Weiel (1996) at high (4.6 kHz, hf) and low (0.46 kHz, lf) frequencies in SI units using a susceptibility control unit (MS2B Bartington Ltd, UK), before samples were proceeded for the silt-size analysis.

On the basis of frequency-dependent magnetic susceptibility measurements in situ formation of ultra fine (<0.03 mm) super-paramagnetic and ferromagnetic minerals produced by bacteria and chemical processes (Thompson and Oldfield, 1986; Chang and Kirschvink, 1989; Dearing, 1994) can be neglected. Aeolian input in our working area can be disregarded (Niessen and Weiel, 1996; Shevchenko et al., 2003).
In this study we use the porosity-corrected susceptibility, calculated according to Niessen and Jarrard (1998) in order to account for the pure grain signal. MS of the interstitial pore water is negligible (Thompson and Oldfield, 1986, Dearing, 1994).

3. Results

All stations were classified on the basis of high-resolution echo-sounding surveys (Chapter 3.3-3.5) and sub-divided into three sea-floor morphology environments: estuaries, shelf and channels on the shelf (Fig. 3a). This differentiation was made in order to account for different environmental influences on the sedimentary regime. The estuaries are restricted to the Ob and Yenisei river mouths up to 74° N. The shelf occupies the rest, cut occasionally by channels with variable Channel depth (Chapter 3.5).

Grain-size

Particles are fine-grained and silt-size particles are the dominant fraction (Figs 3a and 3b), with contents varying between 38% and 100%. From the total of 74 samples silt is the dominant grain-size
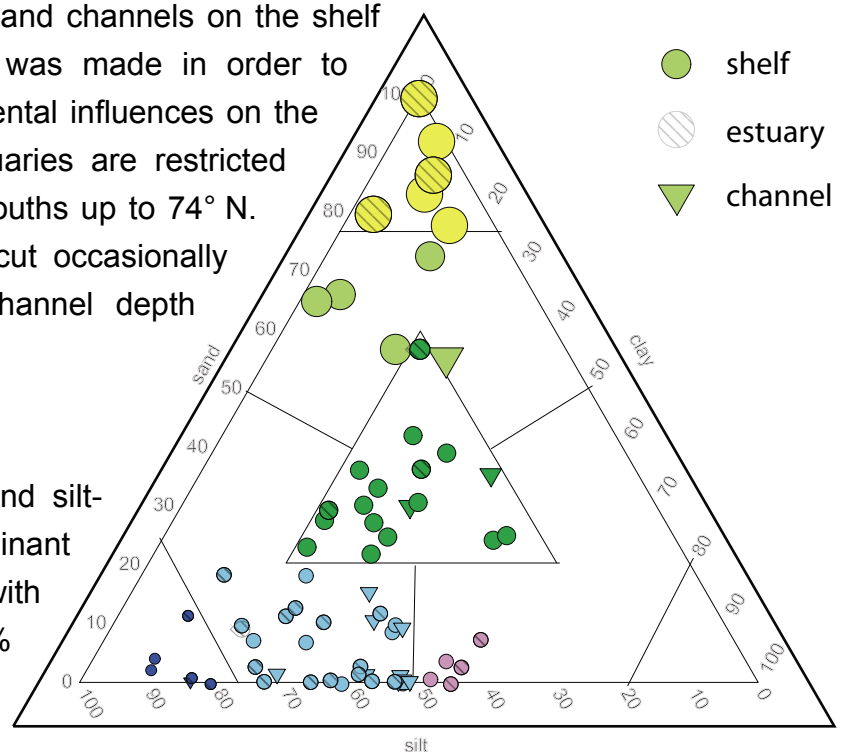
Figure 3a. Total sand-silt-clay size characterisation (Shepard, 1954) of surface sediments; note difference in symbols of shelf (circles) and estuaries (hatched circles), while channels are represented by triangles; Samples were obtained during year 1999, 2000 and 2001 expeditions (Stein and Stepanets, 2000, 2001 and 2002, respectively) channels on the shelf shown as triangles and samples from the estuaries are hatched, differnt colors and size of symbols represent grain size classes
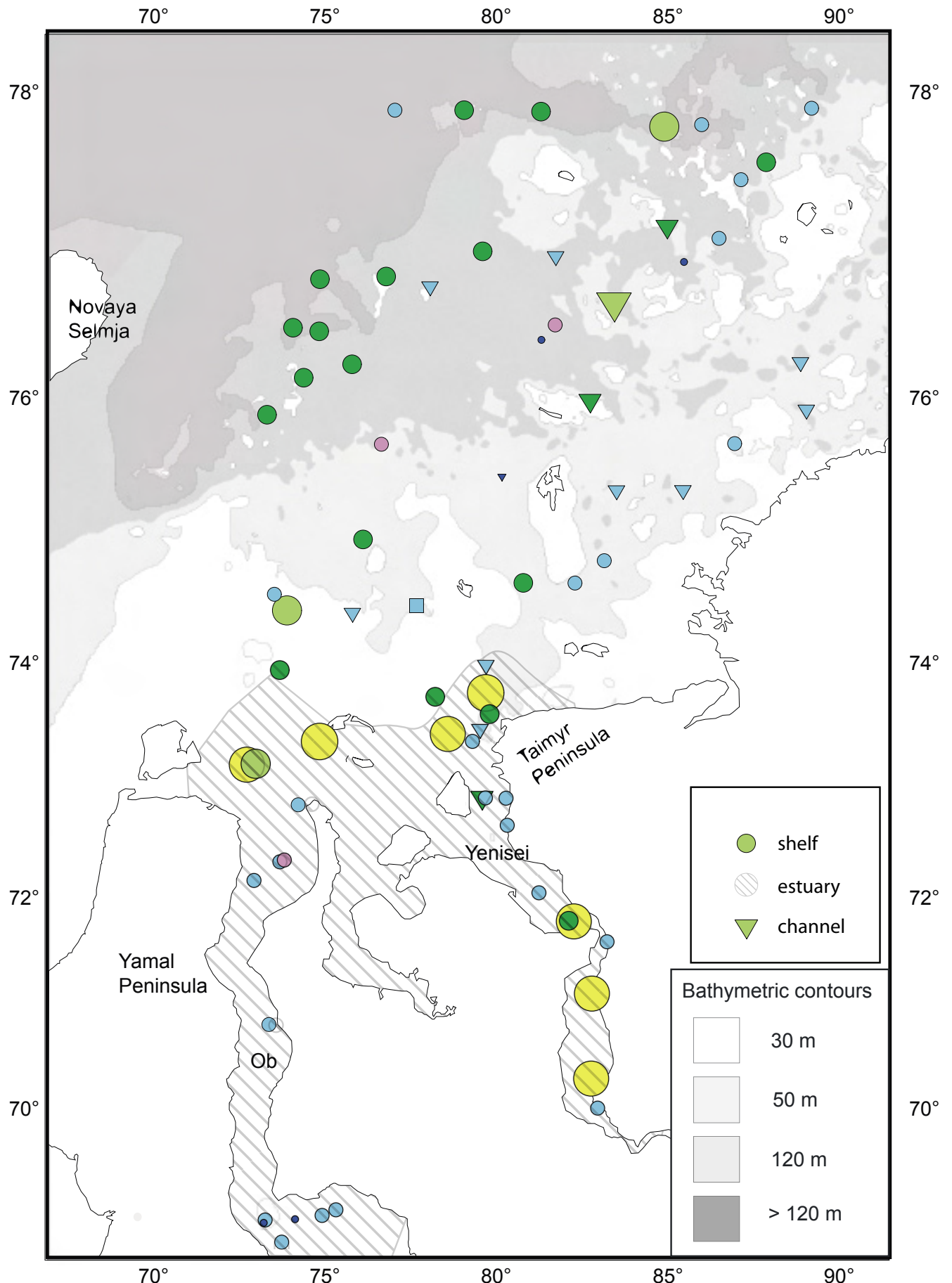
Figure 3b. Overview of stations and total grain size characterisation (Shepard, 1954) of surface sediments; classification after Figure 3a, note that there is no difference in symbols of shelf and estuaries; channels are shwon as triangle and estuaries are hatched.
Samples were obtained during year 1999 , 2000 and 2001 expeditions (Stein and Stepanets, 2000, 2001 and 2002, respectively)
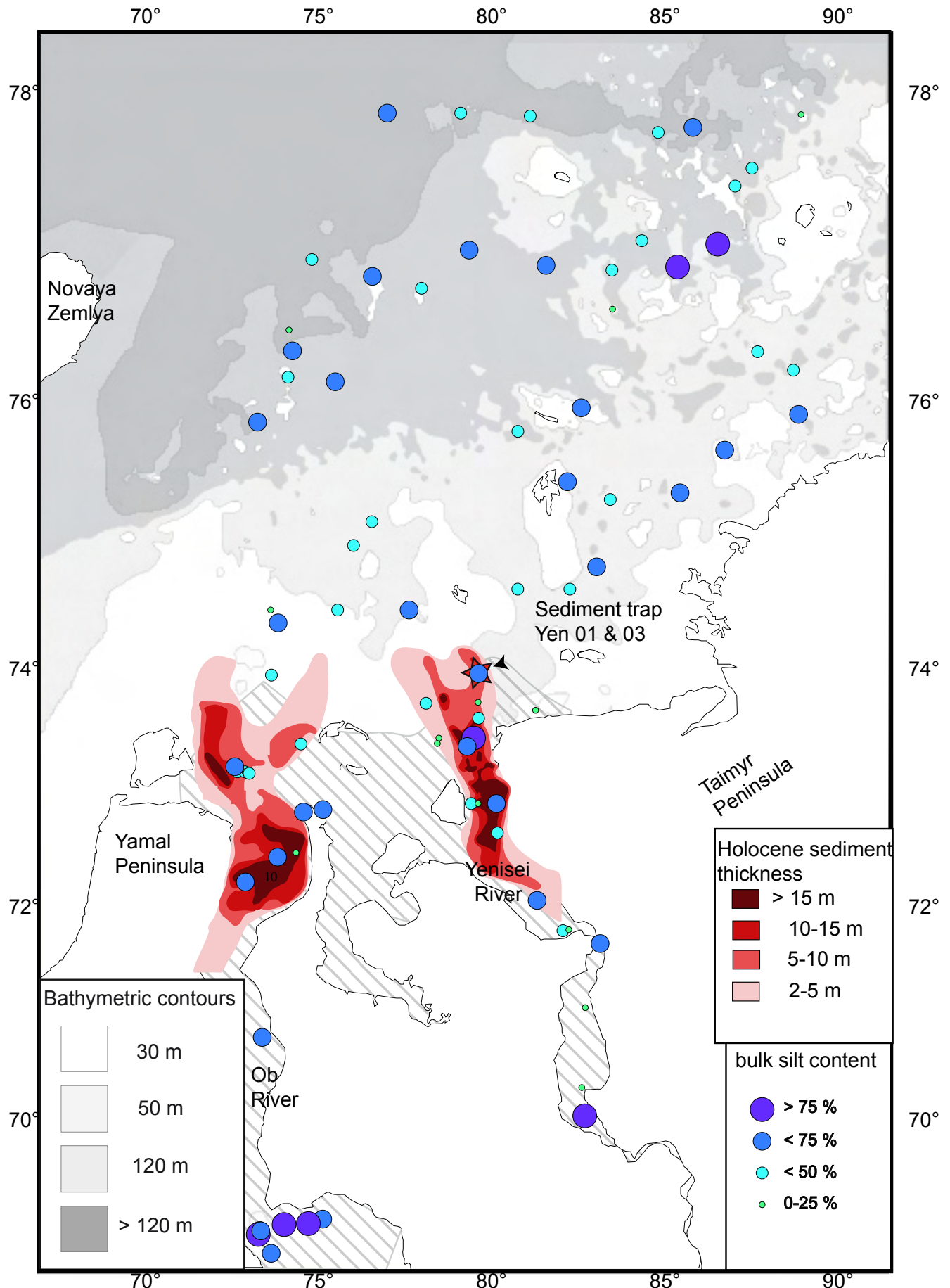
Figure 4. Mass percentage of silt content; Holocene sediment thickness after Dittmers et al. (2003). Position of sediment trap Yen 01 (1999) and Yen 03 (2000) denoted by star, for further informations see Gaye-Haake et al. (2003)
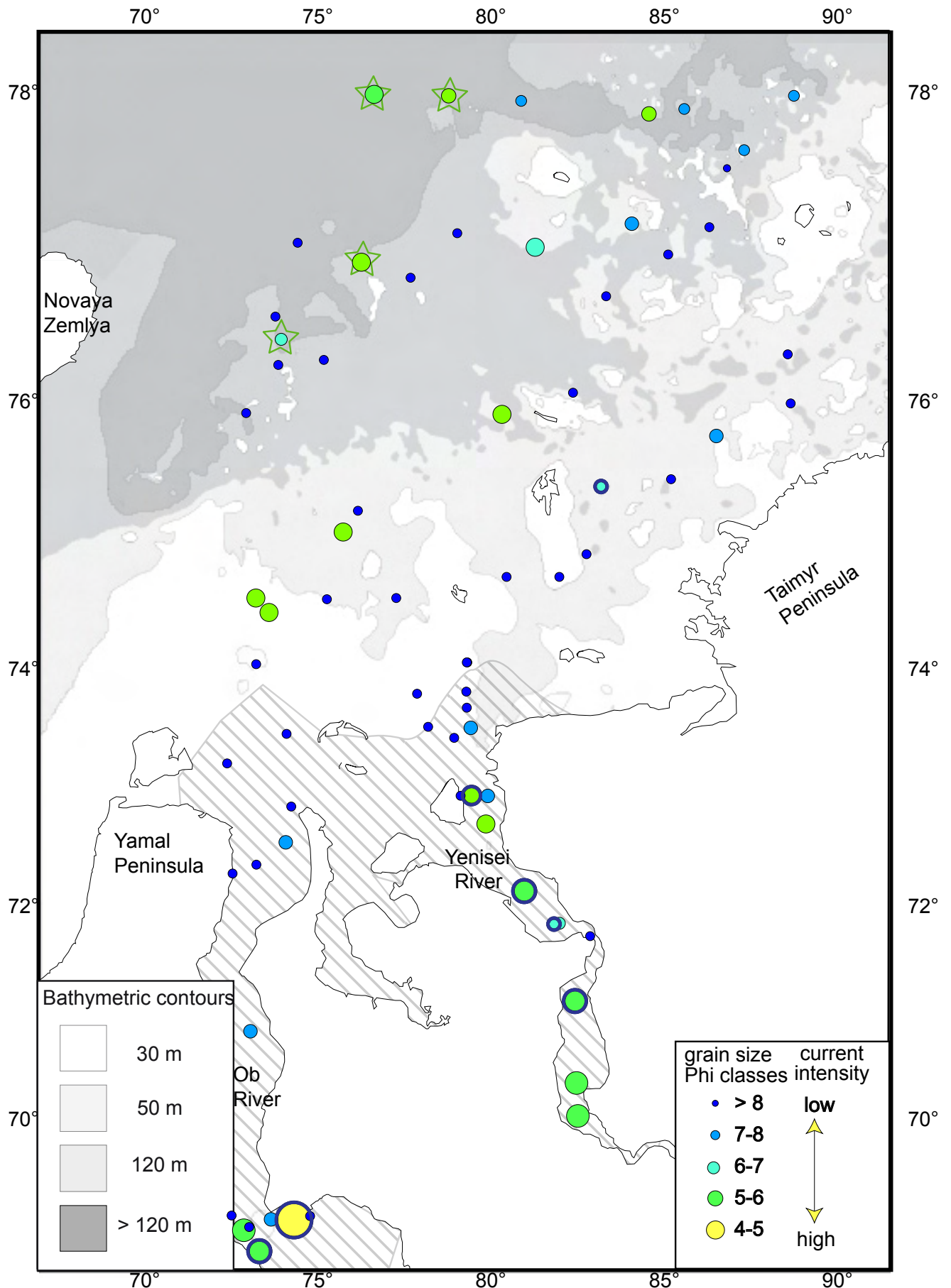
Figure 5. Modal silt-size of surface samples. Stars denote symetrically distributed samples and thick edges coarse skewed samples. For detailed silt size distribution see Figure 6.

fraction (> 50 %) in 61 samples (Figs 3a, 3b and 4). North of the coastline in the NE working area, a band trending from the SW to NE coast parallel is characterised by relatively low values, while towards the north and west values increase slightly (Fig. 4).

Figure 3a exhibits the grain-size classification and distribution after Shepard (1954). Sand-rich sediments are concentrated in the recent estuaries and on the shelf of Ob and Yenisei rivers displaying the shallowest waters and highest current velocity. The shelf is more mud-dominated. Lowest sand content is found in channels on the shelf. The distribution of the coarse fraction shows the same tendency as the model results of Harms and Karcher (1999) and Harms et al. (2000), where shallow water depths are related to high current speed (Fig. 2b).

Modal silt-size

We characterise the silt-size fraction mainly by the modal (dominant) grain-size, i.e. the grain-size making up the main peak. The modal silt-size, as well as the bulk silt content show much variability throughout the working area (Fig. 5). In the estuaries, high values are observed in the southern Ob Estuary south of 70° N and in the Yenisei Estuary up to 73° N. To the North, facing the open shelf, modal grain-size decreases markedly in the estuaries. The area along the southern and north-easterly coast and around the islands is characterised by uniform low modal grain-size > 4 µm. Coarser modal grain sizes are found north of the Ob mouth at 75° N with three samples of 35 µm size, and in the north-western area north of 76° N.

Statistical parameters

The mean silt values of all samples range from 14 to 35 µm, which is medium to coarse silt. Again highest values with the highest variation occur in the estuaries, while low values are observed north of the estuaries and in the nearshore NE eastern area. On the shelf medium silt is predominant with values average between 20-30 µm, and shows a very equal distribution. Sorting displays very similar values of 0.2-0.5 (ɸ classes), i.e. very well to well sorted; this is an index of dispersion/scatter of the population. Skewness, an index of symmetry of the grain-size distribution, is symmetrically for the estuaries. North of the Ob, samples are coarse-skewed (negatively), while to the East samples becomes more fine-skewed, i.e. symmetrically to positively skewed.

Frequency Curve of silt-size sediments

The frequency curve of silt-size material is shown in Figure 6, ranging from 4 ɸ (finer than sand) to 9 ɸ (clay). In most silt populations there is the tendency to show

a peak in the fines at 8 ɸ. Additionally, there is another sub-population at 4-5 ɸ (62-31 µm), variably pronounced.

Figure 6a shows examples of the estuaries displaying a distinct bimodality, and a pronounced maximum on the coarse fraction at 4-5 ɸ. In comparison the examples from the shelf are much more fine-tailed with a suppressed secondary mode at 4-5 ɸ (Fig. 6b). The green-coloured curves are examples from the NW corner of the working area, characterised by high water depths. The curves display rather uniform distribution with minor "current shapening". Examples from channels on the shelf show
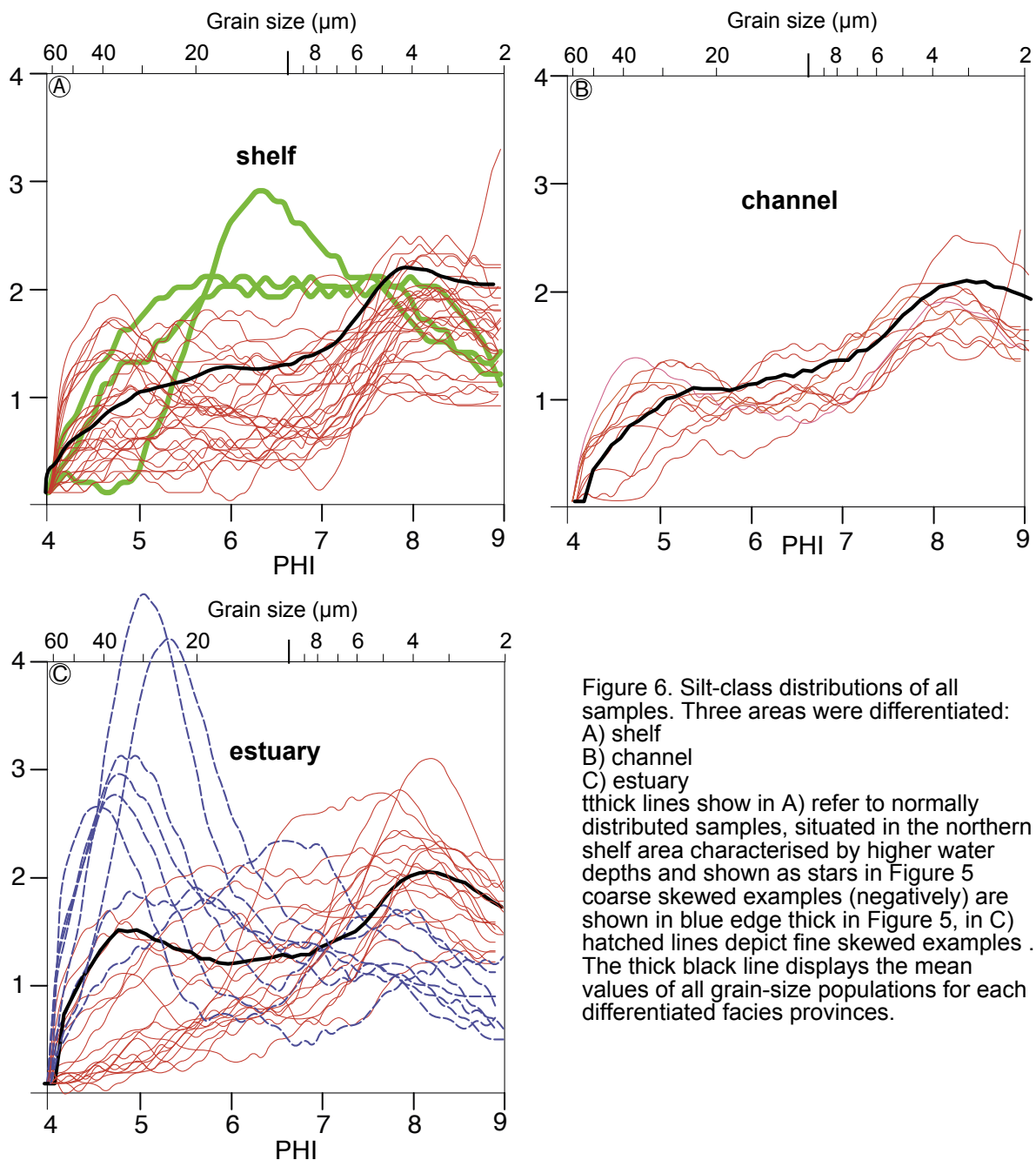
Figure 6. Silt-class distributions of all samples. Three areas were differentiated:
A) shelf
B) channel
C) estuary
tthick lines show in A) refer to normally distributed samples, situated in the northern shelf area characterised by higher water depths and shown as stars in Figure 5 coarse skewed examples (negatively) are shown in blue edge thick in Figure 5, in C) hatched lines depict fine skewed examples . The thick black line displays the mean values of all grain-size populations for each differentiated facies provinces.
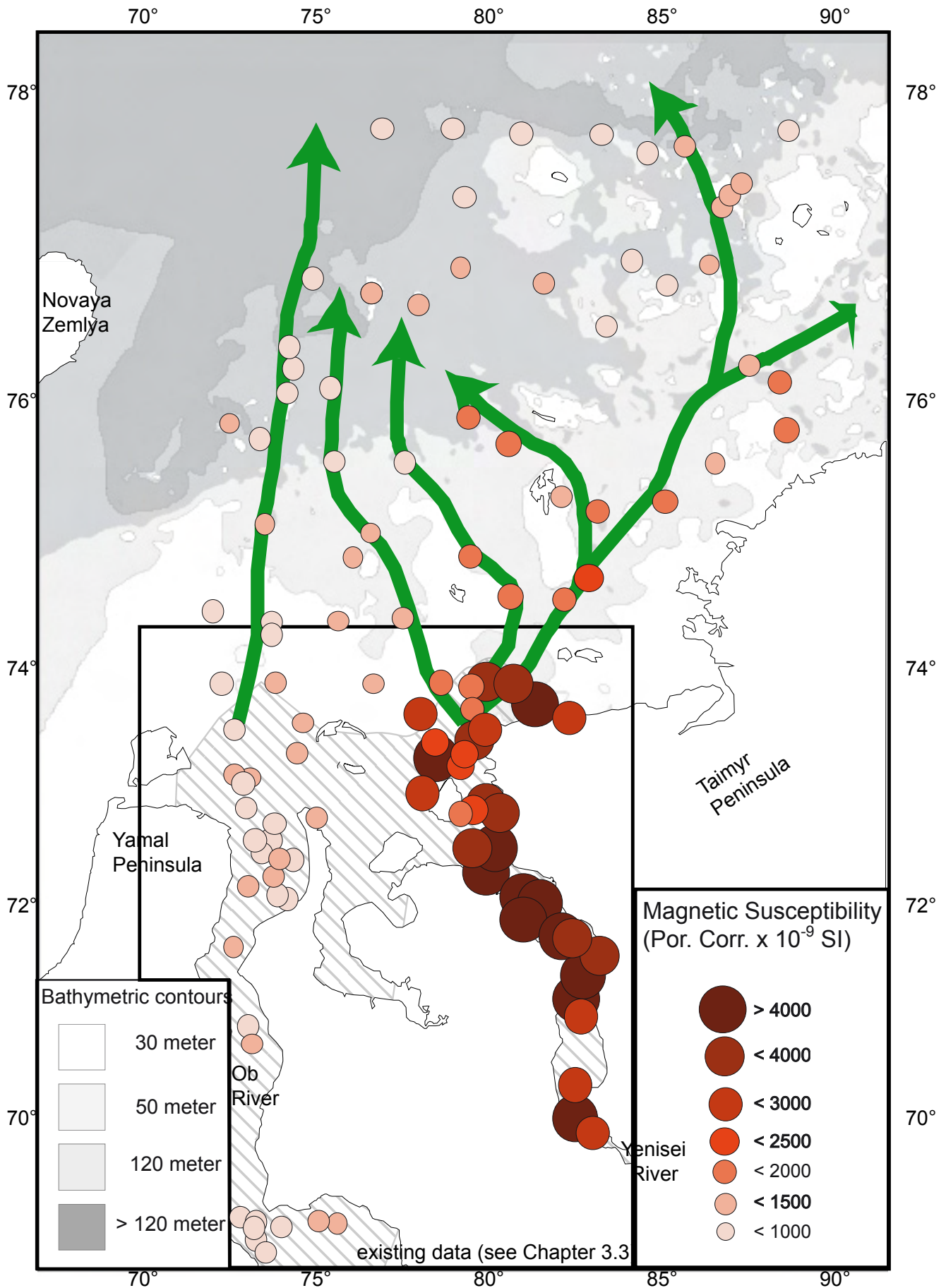
Figure 7. Distribution pattern of porosity corrected susceptibility

a trend similar to those in Figure 6b for the shelf, with the exception that the scatter between individual samples is much lower and that there is only a faint coarse mode detectable.

Magnetic susceptibility

The porosity-corrected magnetic susceptibility of surface sediments shows two major trends (Fig. 7). The first is that values from the Yenisei river are significantly higher than in the Ob area with averages at 3,000 to 4,000 x 10^{-9} SI and <1, 000 x 10^{-9} SI, respectively. The other important observation is a distinct decrease in values occurring north of 74° N. Despite the distinct decrease off the Yenisei estuary some samples north of 74° N show slightly increased susceptibility compared to other areas of the southern Kara Sea. Values are higher east of 76° E indicating the Yenisei water`s influence. North of 76° N another decrease in the values of magnetic susceptibility is obvious but not as pronounced as for the estuary-ocean transition.

4. Discussion

Currents capable of moving/dispersing sediments normally affect the clay and silt fraction in the marine environment. This is clearly underlined by the fact that surface sediments of the Kara Sea are dominated by the fines with generally minor sand components (Figs 3).

In the following section processes effecting the grain-size distribution are reviewed.

Sedimentation by grain coagulation

Particles below 10 µm tend to behave cohesively, because clay minerals with their charge imbalances are small enough to be effected by van de Waals forces (McCave, 1985; Weaver, 1989). Therefore, only a measurement of (disaggregated) individual medium to coarse silt particles are a reliable reflection of sediment sorting processes in marine environments (Bianchi et al., 2001). The silt fraction is traditionally used as a paleocurrent indicator (McCave et al., 1995; Bianchi et al., 1999, 2000), concentrating on deep sea environments so far (Hall et al., 1989; Hass, 1996, 2002; McCave and Carter, 1997).

In general the peaks are thought to result from distinct flow speeds responsible for deposition, but nevertheless it is possible that grains aggregate to large flocs resulting in a "virtual" grain-size, with hydraulic behaviour of a larger size. It is known that „marine snow" is formed by large aggregates of relatively fine, smaller than 10 µm material. The flocculation process is reviewed by McCave (1984) and Eisma (1986). In

estuarine to shelf marine environments at least parts of the suspension is flocculated (Kranck, 1984; Eisma, 1986; Wells and Shanks, 1987). Flocculation should produce an unsorted signal, because particles, regardless of their size coagulate and fall out of the suspension randomly. Fines could be effectively concentrated in "fluid muds", a process recently observed on river fed shelves (Wright et al., 1990; Kineke et al.,1995). This is a phenomenon of salt induced particle settlement due to coagulation, formerly relegated to estuaries only, as demonstrated in the "marginal filter" (Lisitzin, 1995) of the Ob and Yenisei estuaries.

However, our samples show distinct peaks at defined intervals and contradict a pure flocculation settlement. The abundant fine peak could be the result of preferential agglomeration of the fine fraction.

Environmental factors shaping silt populations
Summer mode: River Run-Off

River-flush events are important to "inject" the suspended material into the system with subsequent particle settlement out of the sediment-plume. Widening of estuaries reduces current speed/flow and results in sedimentation. Reaching the ocean the buoyant river plume is subjected to less friction at its bottom boundary and particle settlement is physically enhanced (Hill et al., 2000; 2001). In addition flocculation accelerates particle settlement. However, although the flocs behave hydrometrically as sand or coarse silt, once deposited they behave like muds, i.e. they show higher resistivity towards eroding currents (Zanke, 1982). River-induced surface currents are too weak for the resuspension of agglomerated bottom sediments. The only possible source of resuspension are the induced bottom counter-currents (Harms et al., 2000). With a maximum speed of 12.5 cm/s they are rather capable of holding the suspension (Harms et al., 2000). However, we think that the discharge peak observed during 3 months, when the Ob and Yenisei rivers release 70-80 % of their annual discharge (Holmes et al., 2002), has profound impact on sediments in the estuaries, because stream power is increased markedly. These events could explain the coarse peak (Fig. 6a) for the estuarine environment. Furthermore, during spring melt ice floes can create ice jams resulting in river damming with subsequent dynamic break-ups as especially known from the Yenisei river (AMAP assessment report 2002). However, these events additionally boost up the stream power at the peak discharge.

During the rest of the year, especially north of the estuaries, suspended particle settling and distribution prevails. The frequency curve of silt-size distribution curves for the shelf and channels (Figs 6b and 6c) show very similar patterns. A marked difference is that the scatter for the shelf is much broader (Fig. 6a) as for examples

from the channels that show very uniform behaviour (Fig. 6b).

Winter mode: Sea-ice-related Processes

Shore fast-ice is formed from October to December bound to shallow water depths of 20-30 m (Polyakov and Timokhov, 1994; Divine et al., 2003). The surface water beneath flaw leads is turbulent with convective cells and Langmuir-type circulation (Dethleff, 1994; Dethleff et al., 2000). Current speed may reach 10-15 cm/s strong enough to hold suspension and possibly capable to erode or resuspend deposited material. It is not surprising however, that the highest current speed is observed in late October from current meters attached to sediment traps (Fig. 8). The fine signal at 8 φ (Fig. 6) could either reflect a direct transport signal or an "opportunistic" sedimentary
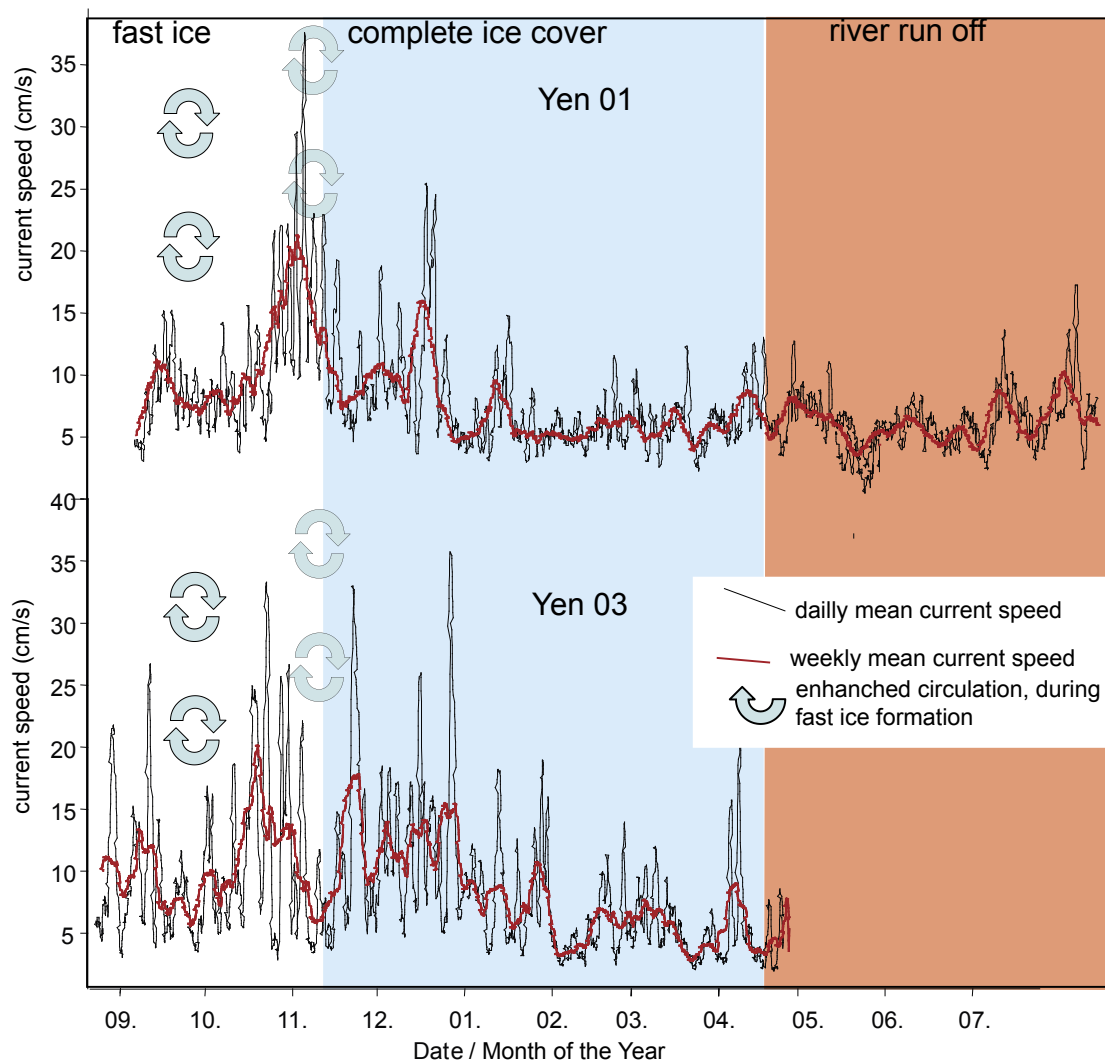
Figure 8. Current speed measured at the Yenisei mooring station; the current meter was employed 15 m above the sea-floor; for positions see Figure 4. It must be kept in mind that the current meters were deployed 15 m above the sea-floor and that the vigour of indicated currents is diminishing to the sea-floor, because of boundary frictional of the flow (Zanke, 1982); Note that traps were deployed during slightly different times of the year but that the major trends are similar. Data by the courtesy of B. Gaye and N. Lahajnar, IFBM Hamburg, Germany; Schoster and Levitan, 2004

signal from particle settling out of the water column. The estuaries and NE nearshore area are ice covered during most of the year. These conditions result in high mud and bulk silt content in the surface sediments as well as a fine skewed modal size spectrum. These areas are probably effectively sheltered from storm wave action and from large-scale water circulation (Divine et al., 2003, 2004). In contrast north of the Ob River, another facies is established related to more open water conditions during most of the year. Here the modal grain-size values are coarser. This could be related to the fact that the sheltering fast-ice is missing.

Sea-ice can be excluded as transport agent for coarse material (Fig. 6a), because it is freshly formed each year and not of glacial origin with incorporated debris. Evidence from the Laptev Sea (Dethleff, 1994; Dethleff et al., 2000) indicates that preferentially fine material is frozen in during suspension freezing.

Samples north of 76° N are characterised by higher water depths (Fig. 5) and are not as susceptible to surface currents and show a unimodal distribution (green curves in Figure 6). The bimodal grain-size distribution curve strongly suggests twofold peaks in current intensity, probably related to at least two different processes. On the basis of our data it is impossible to relate a distinct grain-size fraction to a single transport process. There is some bias to identify the "exact" processes.

Sediment pathways

The pathways of terrestrial sediment signal and dispersion, mapped by magnetic susceptibility, strikingly resembling the established palaeoriver drainage net indicated by arrows in Figure 7 described in more detail in Chapter 3.5. This is probably related to density-driven sediment flux by a bottom nepheloid layer (McCave, 1972; Nittrouer and Wright, 1994, Pak et al., 1980), predetermined by ancient incised channels. It is proven that grain-size distributions in turbidity currents show the same composition as bottom nepheloid layers on the adjacent shelf (McCave; 1972; Pak et al., 1980). A residual, lag deposits, origin of the relatively high magnetite values along palaeo-river pathways in channels thalwegs, can be excluded, mainly because of the high sediment thickness of the well documented Holocene marine infill as visible in acoustic profiles (Stein et al., 2002, Dittmers et al., 2003, Chapter 3.4 and 3.5).

The overall average values for the estuaries, the channels and the shelf are 1, 915 x 10^{-9} SI, 1, 398 x 10^{-9} SI and 1, 159 x 10^{-9} SI, respectively. We see this as evidence that the channels distribute the MS signal on the shelf. After the particles have made their way through the water column they settle and accumulate in density-induced flow following the bottom Pleistocene relief. This process is active mainly during summer. During winter resuspension, enhanced particle reorganisation occurs. The

resuspended material could settle again and flow downward the bottom topography. Sea-ice formation accelerates circulation, especially at its marginal polynia, while in contrast the coast-near waters appear to be quite well sheltered by fast ice, despite their shallow water depth.

Channels

The fact that the highest fine-silt content is found inside the channels means that the flow speed in the channel axis is sufficiently strong to keep the fines in suspension temporarily. It is very likely that these currents decrease very gradually. Each slowing step in the current flow results in deposition of finer material. If the flow turns on again the compaction and bounding forces of the fines are strong enough to counteract/ resist the erosional force (Bagnold, 1968; Gibbs et al., 1971; Zanke, 1982). The shelf examples show similar silt distribution, but with a more pronounced coarse mode (Fig. 6b). It is likely that channels are more sheltered from the vigour of currents and additional fines are "collected" .

5.Conclusion

In most silt populations of the investigated inner Kara Sea Shelf sediments, there is the tendency to show a peak in the fines at 8 ф (4 µm). In some samples another sub-population at 5 ф (25-40 µm) may be variably pronounced. Samples from the estuaries display a distinct bimodality, and a pronounced maximum in the coarse fraction at 30 µm. In comparison, the examples from the shelf are much more fine-tailed with a suppressed secondary mode at 5-6 ф (30 µm). Examples from channels on the shelf show a trend similar to that for the shelf, but the scatter between individual samples is much lower and there is only a faint coarse mode detectable. The two-fold grain-size peaks strongly suggest two peaks in current intensity, probably related to at least two different processes.

The Ob and Yenisei estuarine grain-size peaks are either transport signals displaying a river run-off shadowing a background sedimentation producing a secondary mode in the fines, or could be related to enhanced flocculation in the mixing zone, producing a peak in the coarse fraction. Samples from the shelf are all dominated by a fine mode at 8 ф with a minor peak at 5 ф.

The distribution pattern of terrestrial-derived sediment can be demonstrated by the magnetic susceptibility, while the study of silt properties yields information about the transport mechanisms. We strongly promote the existence of a „summer" and a „winter mode" of ocean circulation on the shelf, reflecting the bimodal grain-size distribution. In the summer the whole system is controlled/ influenced by strong riverine water and sediment influx. The sediment plume is controlled by the prevailing surface currents,

mainly induced by winds, before the fines settle and sediment on the sea-floor. The winter situation is characterised by little direct sediment and freshwater input but due to the high current energy, ice transport and ice erosion the winter rather marks a period of intense sediment redistribution, erosion and resuspension. Coastal, nearshore and estuarine areas are effectively sheltered by the fast-ice from vigour wave-induced currents and finer grain-size populations are dominant.

The denser (re)suspended material follows the deepest points in the bottom topography, especially in the NE. These features are former fluvial channels formed during sea level lowstand, forming a nepheloid layer that is more sediment-saturated than the surrounding water masses. This process may be enhanced during sea-ice freeze-up with the residual ocean water being more dense thus sinking to the sea-floor ("brine formation"). One major task for the future is to examine factors enhancing bottom shear stress and associated sediment resuspension using in-situ measurements covering several seasons and current regimes during the year to characterise the hydrodynamic and sedimentation conditions. A proposal in order to further enlighten sedimentation processes in cooperation with the University of Cambridge (I.McCave) has been submitted (DAAD grant No D/05/10823).

More sophisticated analysis of the polymodal distributions in order to distinguish between different responsible processes will also be useful. The numerical-statistical analysis introduced by Weltje (1997) has proven is an ideal tool for "unmixing" grain-size populations (Frenz, 2003; Holz, 2005). However, this is beyond the main subjects of this thesis, but remains a valuable topic for future research

3.3 Holocene sediment budget and sedimentary history of the Ob and Yenisei estuaries

3.3 Holocene sediment budget and sedimentary history of the Ob and Yenisei estuaries

K. Dittmers, F. Niessen, R. Stein

Alfred Wegener Institute for Polar and Marine Research, Columbusstrasse 2, 27568 Bremerhaven,Germany

Abstract

High-resolution acoustic data and several sediment gravity cores taken in the Ob and Yenisei estuaries allow us to balance the Holocene sediment budget of both rivers and to reconstruct their sedimentary history. Cores were radiocarbon dated and linked to acoustic profiles using whole-core physical properties.

The Ob and Yenisei estuaries, with their sea water fresh water mixing zone, act as major sediment sinks for fluvially-derived terrigeneous material in Holocene times. Most of the suspended and large amounts of dissolved matter precipitate in this zone termed "marginal filter". High thickness of Holocene sediments occurs between 72° N and 73°30`N where a distinct decrease in thickness is observed to the north. Two major acoustic units could be differentiated, separated by a prominent reflector interpreted as the base of the Holocene. High-resolution echosound data suggest a fluvial-dominated depositional environment for the early Holocene displaying lateral accretion as point bars and vertical accreted overbank deposits in a fluvial channel-levee-complex. During the early Holocene sea level rise the marginal filter migrated progressively southward (upstream) to its present position forming a typical high-stand system tract in acoustic images. Estuarine sedimentation in a sedimentary environment similar to today started at approximately 5 ka BP. An estimated total of

14.3 * 10^{10} t and 9.2 * 10^{10} t of fine-grained brackish-marine sediments, in the Ob and Yenisei estuaries, respectively, were accumulated during Holocene times. This is only about 75% and about 50% of Ob and Yenisei estuarine sediment budgets, respectively, estimated by extrapolation of recent river run-off data over the last 7500 years. Filled paleoriver channels indicate active river incision in the southern part of the Kara Sea Shelf prior to the Holocene.

1 Introduction

Sedimentation in the Arctic Ocean is dominated by terrigeneous input which leads to high siliciclastic contents in marine sediments (Stein and Korolev, 1994; Stein, 2000). Biological productivity plays a minor role in sediment supply because the availability of nutrients is limited (Grebmeier, 1995). There are two major sources of terrigeneous input: (i) riverine discharge which is prevailing in the western Arctic (MacDonald et al., 1998), and (ii) coastal erosion which is typical for the Laptev Sea (Rachold et al., 2000). At present, total annual run-off sums up to 3330 km³ for the whole Arctic. Approximately 30% of the Arctic Ocean fresh water input is supplied by the rivers Ob (429 km³y⁻¹) and Yenisei (620 km³y⁻¹) through their estuaries into the Kara Sea (Fig. 1;

Aagaard and Carmack,1994).

In the Ob and Yenisei estuaries there are generally two factors controlling sediment accumulation and thus the sediment budget. One is sediment input and the other is erosion and/or resuspension.

Sediment input into the system mainly depends on river run-off which varies strongly both seasonally and interannually (Pavlov and Pfirman, 1995). The annual maximum discharge rate is observed in June. During this peak, 45 to 65% of the annual freshwater run-off and 80% of the annual sediment masses are released (Gordeev et al., 1996; Shiklomanov and Skakalsky, 1994).
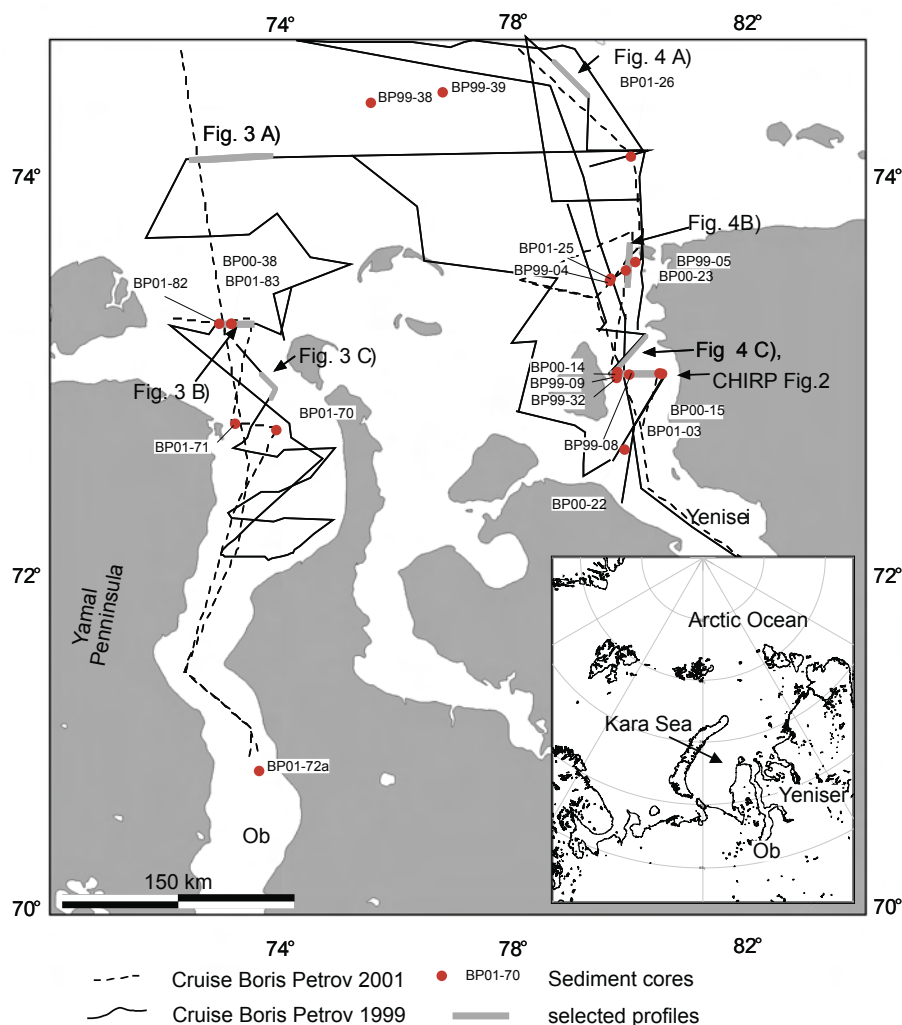
Figure 1. Location map of working area showing track lines of ELAC profiles and core positions. Heavy lines denote position of profiles shown in Figs 4 and 5; for CHIRP-profile see Figure 8.

In Arctic coastal waters, resuspension and lateral transport of sediments can be enhanced by several factors and processes. These include brine-induced currents associated with sea-ice formation (Blanchet et al., 1995; Lisitzin, 1995), wave-induced currents during storm events (Løset et al., 1999; Are, 1996; Stein, 2000), sediment erosion by grounding sea-ice (Løset et al., 1999; Barnes and Lien, 1987)

and incorporation of particles into sea-ice during „suspension freezing" (Reimnitz et al., 1993; Dethleff, 1994). These processes are important on the open shelf with large areas exposed to strong winds and significant sea-ice-formation. They are not expected to play a major role in sheltered estuaries, such as those of Ob and Yenisei.

Estimations of sediment fluxes on arctic continental margins are rare. Stein (2000) quantified the carbon fluxes into the Laptev Sea and Bauch et al. (2000) estimated sediment input in the eastern Laptev Sea shelf. There are some rough flux estimates including the Ob and Yenisei estuaries by Russian authors (e.g. Lisitzin, 1995). Very recently, a synthesis about sediment and organic carbon fluxes in the Arctic Ocean and surrounding marginal seas has been compiled by Stein and Macdonald (2003).

The major aim of this paper is the calculation of a Holocene sediment budget for the estuaries of Ob and Yenisei as a basis for assessment of material fluxes into the Kara Sea and further into the Arctic Ocean. These estuaries may function as major sediment sinks.

In this study, we interpret high-resolution acoustic reflection profiles (2-12 kHz) to map the thickness and lateral extent of fine-grained Holocene sediments between 70° N and 74°30' N (Fig. 1). High-frequency single channel systems are particularly capable to penetrate these muddy sediments. This, in combination with AMS ^{14}C dating and the physical properties of the retrieved gravity cores, enables us to evaluate the Holocene sediment budget of the area. We further discuss the evolution and depositional history of the Ob and Yenisei estuaries particularly with regard to the post-glacial sea level rise and migration of deposition centers. The data was collected during the expeditions of the RV "Akademik Boris Petrov" in 1999, 2000 and 2001 (Stein and Stepanets, 2000; 2001; 2002; Fig. 1).

In the area of interest extensive surveys have been carried out by Russian authorities and many shallow acoustic lines have been recorded. Unfortunately, this data is not accessible because the region is strategically relevant for military and commercial reasons.

2 Materials and Methods

During three expeditions (1999, 2000 and 2001) more than 5000 kilometers of high-resolution subbottom profiles in the estuaries of Ob and Yenisei were recorded (Fig. 1) using the hull-mounted ELAC system of RV "Akademik Boris Petrov" (ELAC echograph LAZ 72, Honeywell-Nautik, Kiel, Germany) which operates at 12 kHz. In 2001 we amplified and plotted the ELAC signal using a GeoAccoustics receiver and Ultra printer 120, respectively (Stein and Stephanets, 2002). In addition, for higher acoustic resolution and penetration a towed CHIRP system was used (Geochirp,

GeoAcoustics, Great Yarmouth, UK). The CHIRP sweep was set to 2-8 kHz (high-penetration mode). Digitising of acoustic data was achieved with a digital receiver (Octopus 360, Deddington, UK). Analogue data including GPS positions and time were stored on a four-channel DAT recorder. A detailed description of the whole system is given by Stein and Stepanets (2002). Time-to-depth conversion was done using a sound velocity of 1500 m s^{-1} for water (Hamilton, 1972). Digital processing was carried out using PC–based software REFLEX (HarbourDom GmbH, Köln, Germany).

Sediment cores of up to eight meters in length were retrieved with a gravity corer. Wholecore physical properties were measured in 1 cm depth intervals using a Geotek Multi Sensor Core Logger. The system provides data of density, P-wave velocity and magnetic susceptibility (e.g., Schultheiss et al., 1987; Schultheiss and McPhail, 1989; Weaver and Schultheiss, 1990). Changes in these parameters reflect changes in porosity and/or sediment composition (Thompson and Oldfield, 1986; Weber et al., 1997). The technical setup of the logging system, as used during "Akademik Boris Petrov" expedition in 2001, is described in Stein and Stephanets (2002). After splitting the cores were described (Matthiessen and Stepanets, 1999; Stein and Stepanets, 2000; 2001; 2002) and sampled for determination of sedimentological parameters.

For the determination of magnetic susceptibility of surface samples, freeze-dried samples were densely packed in 12.5 cm^3 plastic vials and measured using a MS2B sensor, Bartington Ltd, UK (for further information see Niessen and Weiel, 1996). Mass-specific susceptibility was calculated by normalising volume-specific susceptibility to 10 cm^3 and dividing by the sample weight (Dearing, 1994).

Linear sedimentation rates were calculated between AMS ^{14}C-dated fix points. All AMS ^{14}C ages presented in this paper are in Calendar kilo years B.P. (ka BP, see Stein et al., 2003b). The acoustic subunits were differentiated after the sequence stratigraphy concept of Vail et al. (1977). Mass accumulation rates (MAR) were calculated according to Stein (1991):

$$MAR \; (g \; cm^2 \; ky^{-1}) = LSR * (WBD - 1.026 \; GRP/100)$$

Sediment porosity was determined by gamma-ray absorption and calculated using the following equation (Weber et al., 1997):

$$GRP = \frac{Dgp - GRD}{Dgp - Dw}$$

Where: GRP = Gamma-ray Porosity
GRD = Gamma-ray Density
Dgp = Grain Density: 2.65 g cm^{-3}
Dw = density of (salt) water: 1,024 g cm^{-3}

LSR = linear sedimentation rate
WBD = wet bulk density (all values and abbreviations after Weber et al., 1997).

3. Results

3.1 Subbottom profiling and seismic stratigraphy

In general, two major acoustic units (Unit I and Unit II, top to bottom) (Figs 2 to 4) and three subunits (Ia to Ic; Figure 2) were distinguished in the echograph profiles. Major units are separated by a distinct reflector (Figs 2 to 4).

In the CHIRP profile (Fig. 2), located in the central area of the Yenisei estuary (Fig. 1), subparallel reflections of Unit I indicate well-stratified sediments. At its base Unit I drapes concordantly the variable topography of the underlying Unit II (Fig. 2). Subbottom topography is gradually more levelled towards the top of the sediment fill. In both the western and eastern end of the section, two nearly 10 m deep channels characterise the present sediment surface (Fig. 2).

The CHIRP profile (Fig. 2) and two enlarged profile sections (Figs 5 and 6) exhibit important detail information about the seismic stratigraphy of Unit I. This record suggests the definition of three subunits Ia to Ic based on their geometries. In general, all subunits of Unit I are resembling the same back scatter behaviour which is typical of mud (Damuth, 1975; 1978).

Subunit Ia exhibits almost constant total thickness along the whole profile and very little lateral fluctuations of sediment thickness between individual reflectors including the eastern channel. Only in the western channel some thinning of infill strata can be observed. The sediment surface exhibits some incision marks typical of ice gouging, especially in the central section of the profile where water depth is 20 m or less (Fig. 2A).

Subunit Ib has an asymmetrical geometry with higher thickness in the western end of the profile. Between the two channels, the top of this unit forms a nearly horizontal plane at 25 m below present sea level and contains sediment fills of about 5 to 10 m thickness in the eastern channel. In the western area of the CHIRP profile, the asymmetry of Subunit Ib is defined by reflector downlaps onto the surface of Unit II (Figs 2, 5 and 6). Subunit Ib sediments in the eastern channel are characterised by a complex reflector geometry related to channel migration associated with filling (Fig. 6). Subunit Ic shows an asymmetrical, prismatic geometry decreasing in thickness to the west with increasing distance from the eastern channel (Fig. 2C). Subunit Ic sediments are missing in both channel locations and towards the outer edges of the profile so that Subunit Ic is only present in the central area of the cross section (Fig. 2C). Near the eastern channel, Subunit I sediments exhibit inclined reflector downlaps

W
72°56,1 N
79°41,8 E

E
72°55.9 N
80°45,7 E

A   ice gouges

Figure 5

Figure 6

— 20 m

— 30 m

— 40 m

B

— 20 m

Ia

Ib

— 30 m

Ic

— 40 m

II

C

BP 00-14   BP 99-32   BP 99-08   BP 01-03

— 20 m

Ia

Ib

— 30 m

Ic

— 40 m

II

32 km
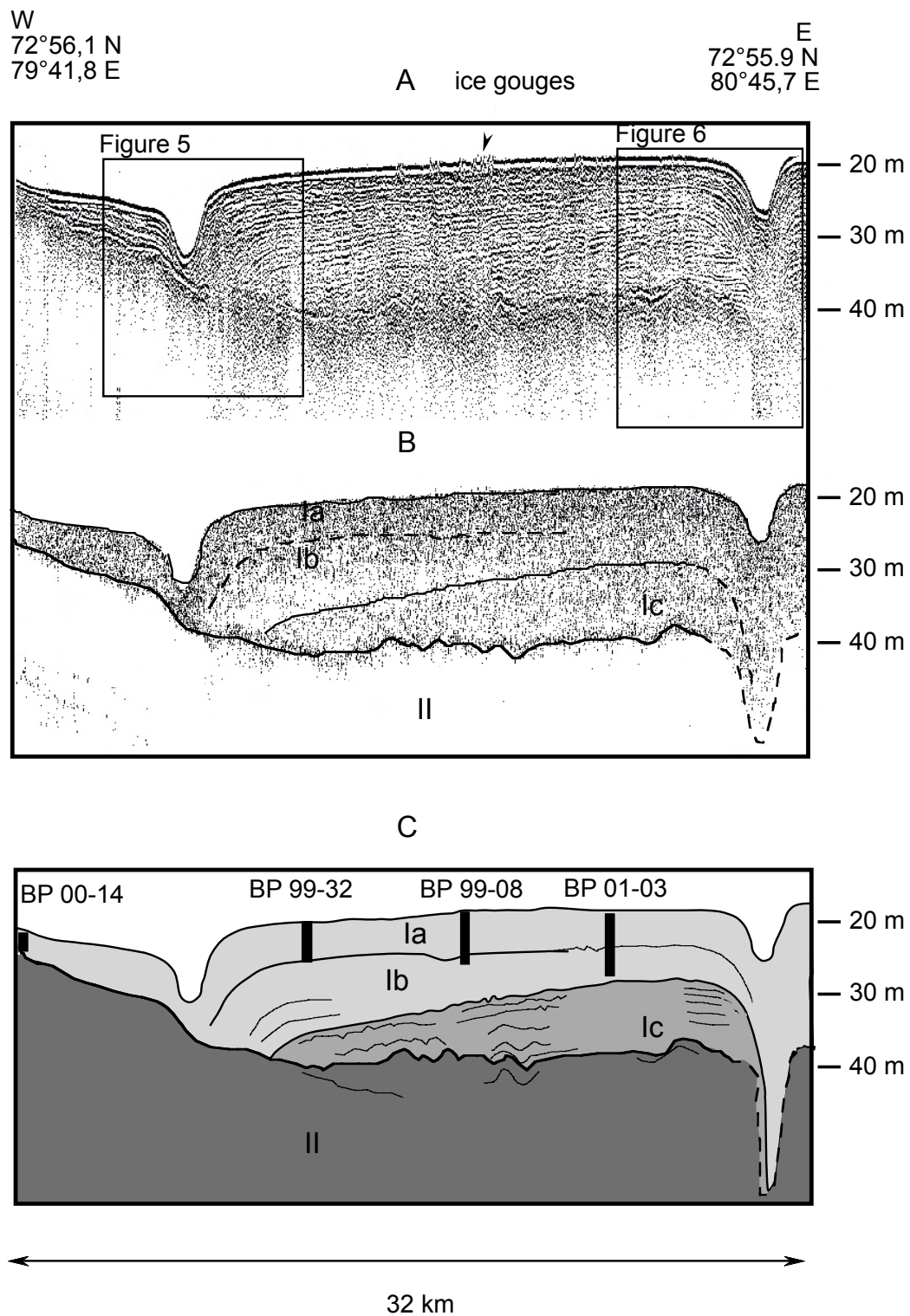
Figure 2. High-resolution profiles from the central Yenisei Estuary (see Figure 1 for location). CHIRP (A) and ELAC (B) profiles were recorded simultaneously along the same line. C: acoustic Units and sediment core locations.
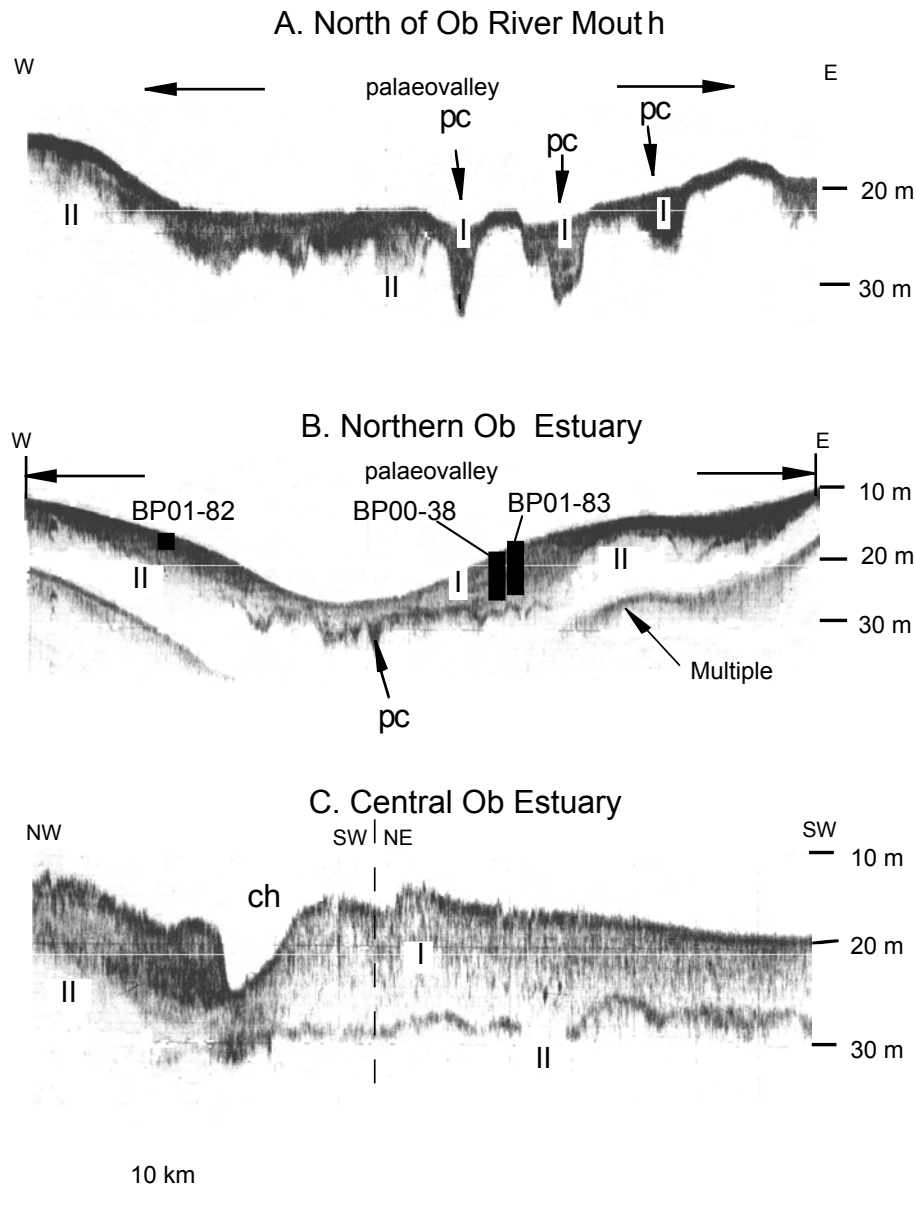
Figure 3. A to C ELAC sound profiles from the Ob area exhibiting thickness of Unit I on top Unit II and sediment core positions. Seismic Units indicated by bold numbers. Water depth given in meters on the right hand side. For location of profiles see Figure 1. Note course change in C. Palaeochannels (pc) and present channels (ch) are indicated.

onto the upper flank of the channel (Fig. 6). In general, Unit I exhibits the character of a sequence representing a depositional cycle from more asymmetric, channel-levee type of deposits near the base (Ic) to more symmetric type of reflectors (Ia) indicative for sediments draping the cross section at the top. The boundaries between subunits Ia/Ib and Ib/Ic appear to be conformable with the exception of some erosional truncation that is visible near the flank of the eastern channel (Figs 2 and 6). In places, Unit I is affected by diffractions (Fig. 5) typical of „gas blanking" (Fader, 1997) which mask the

NW   A. North of Yenisei River Mouth   SE

S   B. Northern Yenisei Estuary   N

SW   C. Yenisei Estuary   NE

10 km
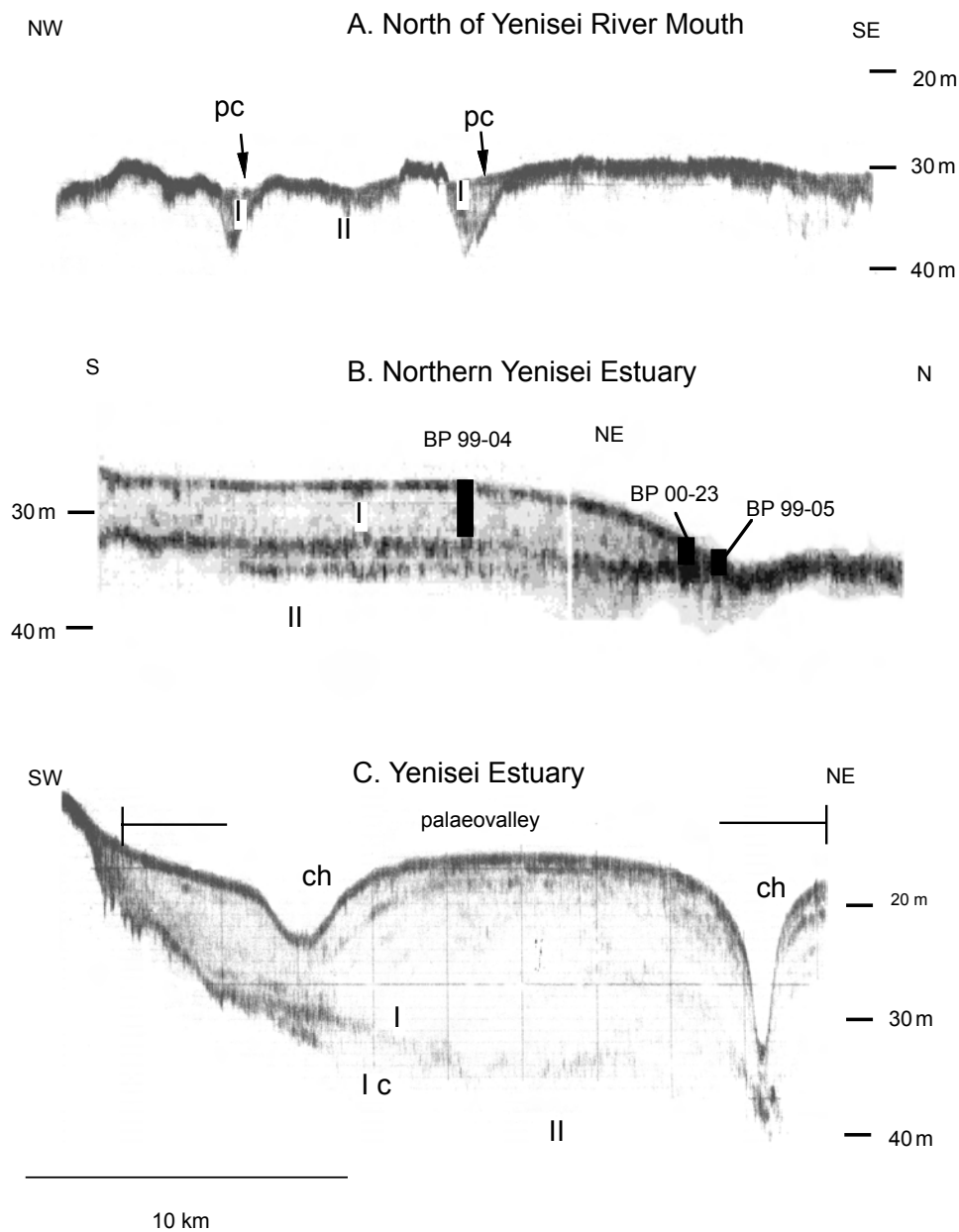
Fig 4 A to C: ELAC echosound profiles from the Yenisei area exhibiting thickness of Unit I overlying Unit II. Black bars: sediment core positions. Vertical scale is water depth below present sea level. For location of profiles see Figure 1. Note course change in C. Paleo-channels (pc) and present channels (ch) are marked.

underlying sediments. This may indicate some content of sediment gas possibly related to decomposition of organic matter.

The top of Unit II forms a prominent reflector which is present in the whole working area both in CHIRP and ELAC profiles (Figs 2 to 4). The acoustic impedance contrast between Unit I and Unit II appears to be large because there is almost no penetration
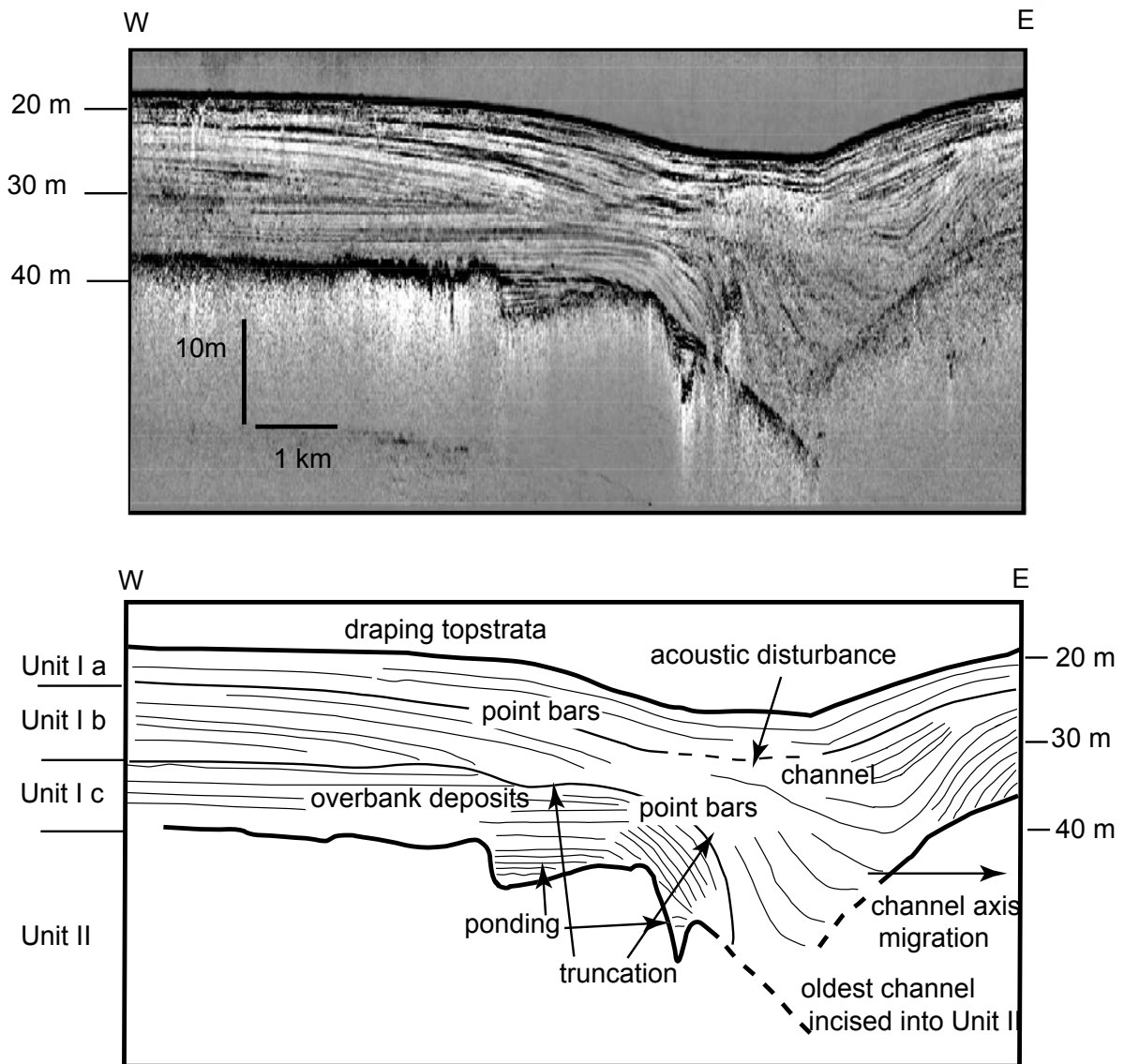
Figure 5. Processed CHIRP section of Figure 2 displaying the western channel and adjacent flanks.

below. The surface of Unit II shows an irregular, rough morphology indicative of an erosional surface. Paleo-channels incised into Unit II including the eastern channel of the CHIRP profile (Figs 2A and 6) and several channels recorded in ELAC profiles (Figs 3C and 4C) which are partly filled with Unit I sediments. In other profiles (Figs 3A and 4A), channels are completely filled and are not, or hardly visible in the present surface morphology. In high exaggerated echosounding profiles, channels appear as typical v-shaped incisions of 5 to 10 m depth. They occur more frequently on the shelf north of 73° N in front of the recent river estuaries (Figs 3A and 4A). Some incisions

W   E

W   E
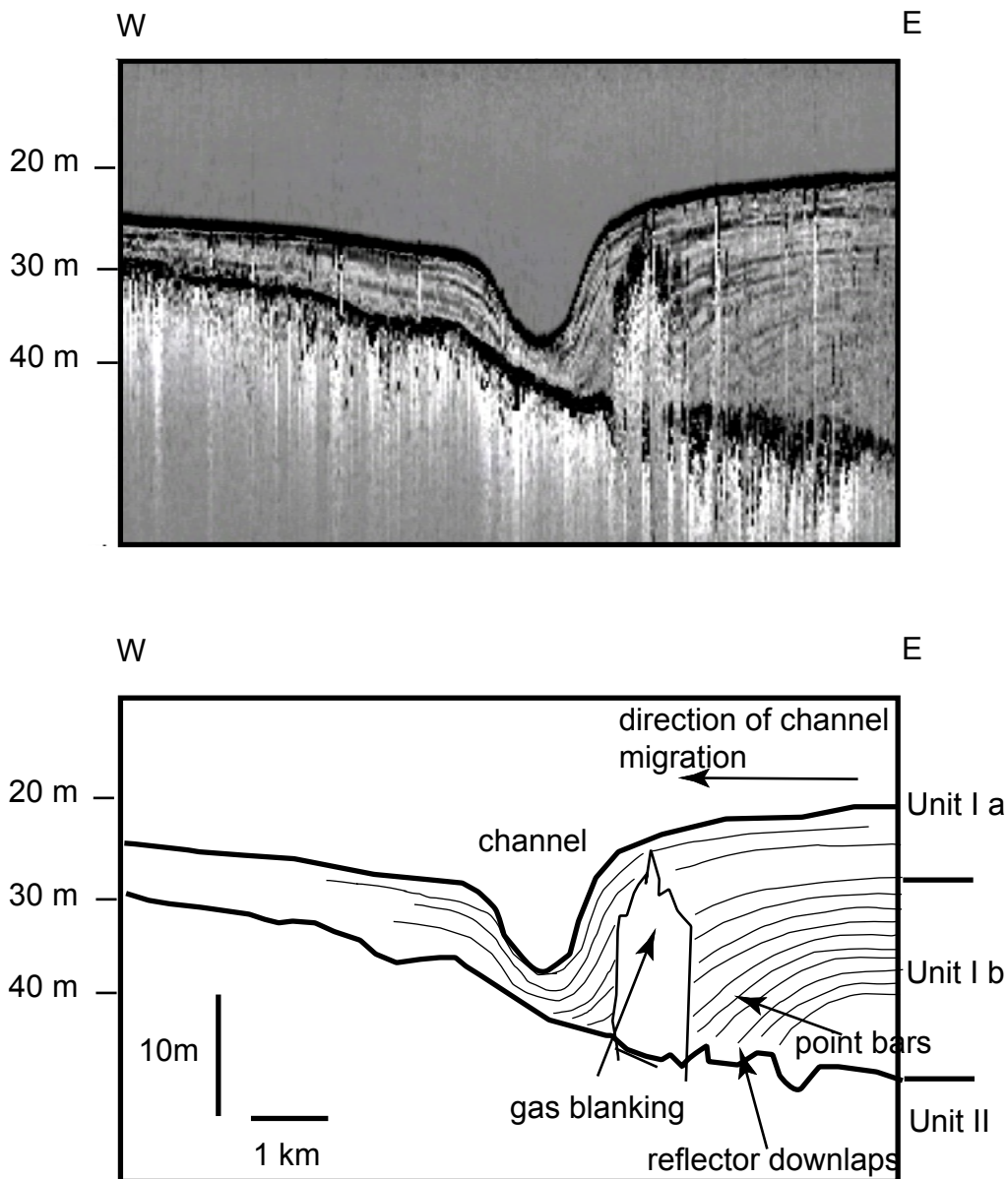
Figure 6. Processed CHIRP section of Figure 2 displaying the eastern channel and adjacent flanks.

appear to be considerably wider than distinct channels and are better described as paleovalleys (Figs 3A, 3B and 4C).

Across the Yenisei estuary (Figs 2A and 2B), the ELAC and CHIRP systems were in operation at the same time which provides a direct comparison between data of both echosounders. The CHIRP system (2-8 kHz) enables higher resolution suitable for subdivision of Unit I although penetration of both systems is about the same (Fig. 2). Both have in common that they can pick up prominent reflectors below the soft sediment such as the top of Unit II (Figs 3 and 4). Therefore, the ELAC system is also capable to identify Unit I including its thickness (Fig. 2).

3.2 Distribution and thickness of Unit I sediments

Acoustic travel times, as recorded in echosounding profiles during "Akademik Boris Petrov" expeditions, are used to determine and map the thickness of Unit I in the area under investigation (Fig. 7). Between profile lines, unit thicknesses were interpolated (Fig. 8). The highest sediment thicknesses occur in the estuaries between 72° and 73°30` N (Fig. 8). Further north, Unit I is virtually absent on the shallow shelf and deposition is concentrated in morphological depressions and sediment sinks such as channels and paleovalleys (Figs 3A and 4A).

In the narrower Yenisei Estuary, the sediment cover appears more canalised and extends further to the north than in the Ob Estuary (Fig. 8). Maximum sediment thickness of 20 m is found at 73° N in the Yenisei Estuary (Figs 2A and 8). From there northward, an approximately 15 m thick sediment blanket extends to 73°30` N (Fig. 8). North of this position, sediment thickness decreases distinctly, although in two elongated areas, thicknesses of up to 10 m continue further north up to 74° N (Fig. 8).

In the Ob Estuary, areas with higher sediment thicknesses are wider but do not extend as far north as in the Yenisei Estuary (Fig. 8). Here, the maximum sediment thickness is reached at 72°20` N. North of 72°50` N increased sediment thickness occurs along a south to north directing axis following 73° E. There is a second area with lower sediment thickness of up to 10 m extending in a SW-NE direction near 74° E.

3.3 Sediment-core lithology, physical properties and chronology

According to the lithological descriptions of the cores from the area under investigation (Stein and Stepanets, 2000; Stein et al., 2003b), major changes in lithology correspond with both boundaries between acoustic units (Fig. 9) and distinct changes in physical property records (Figs 10 to 12).

Lithological descriptions of sediment units

The predominant lithology of Unit I is a clayey silt to silty clay (Stein et al., 2003b) with quartz and clay minerals as major components (e.g. Stein and Stepanets, 2000). Bivalve shells associated with bioturbation are very common which can grade into horizontal, non-bioturbated bedding with fewer shells in the lower sections of Unit I (e.g. Stein and Stepanets, 2000). After calculating porosity from density data of all cores (Figs 10 to 12), an average porosity of Unit I sediments of 66% was quantified for all stations (Fig. 1). This porosity is used to determine the bulk net sediment mass from the sediment volume of Unit I (Figs 7 and 8; Table 1) determined by sediment
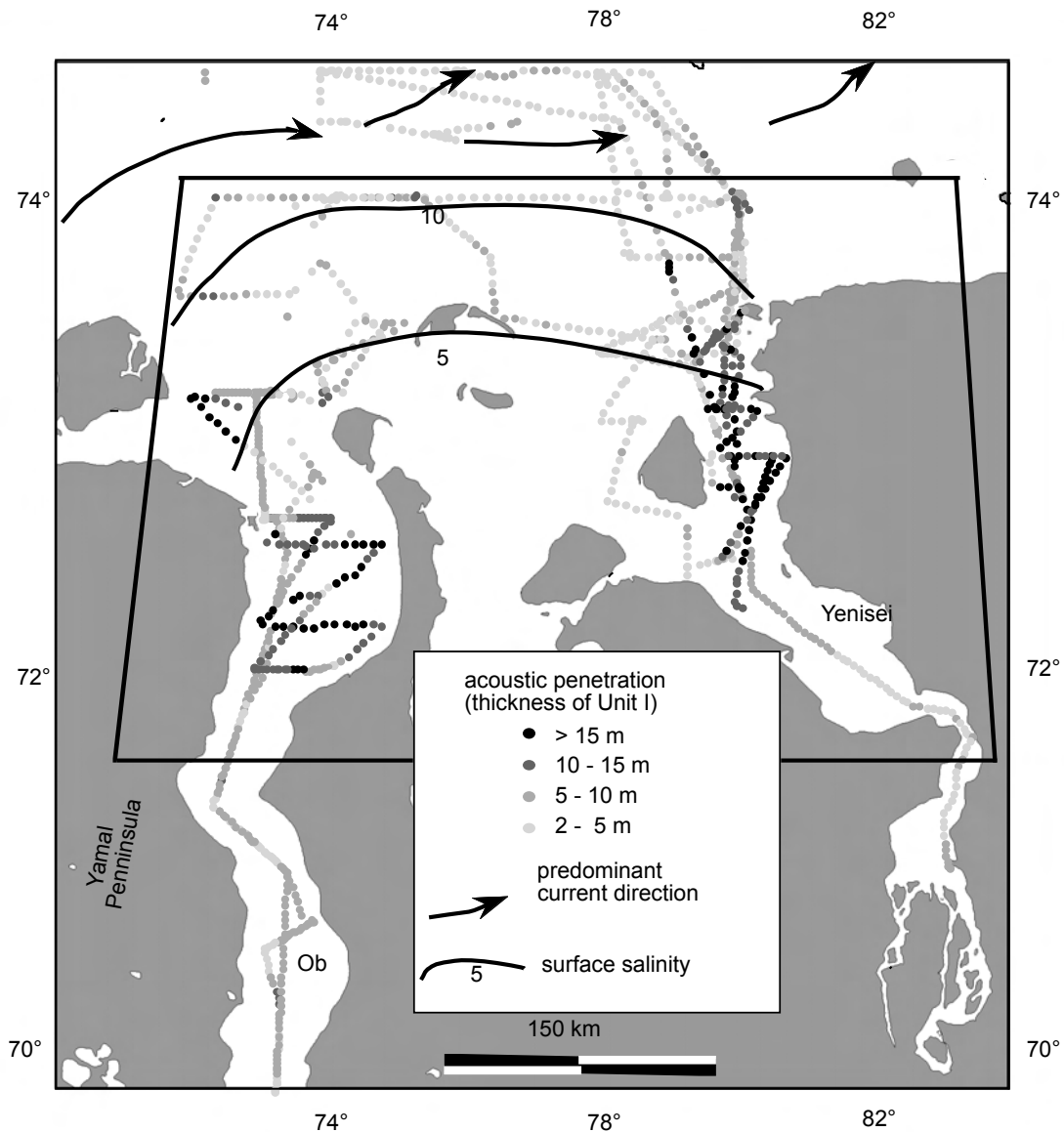
Figure 7. Thickness of Unit I in meters determined by sediment echosounding. Hydrographical conditions after Pavlov and Pfirmann (1995). The trapeze indicates position of Figure 8.

from the sediment volume of Unit I (Figs 7 and 8; Table 1) determined by sediment echosounding (see 3.4). Magnetic Susceptibility:

In general, the upper part of Unit I displays the lowest susceptibilities gradually increasing down-core (Figs 10 to 12). Similar to the density records, the transition from Unit I into Unit II is often characterised by a steep gradient with peak susceptibility at the boundary between Unit I and Unit II (Figs 10 to 11) cores BP99-04, BP99-09, BP00-23 from the Yenisei and BP00-38, BP01-83 from the Ob estuaries (Fig. 12). In some cores higher susceptibility values are associated with increased density as,
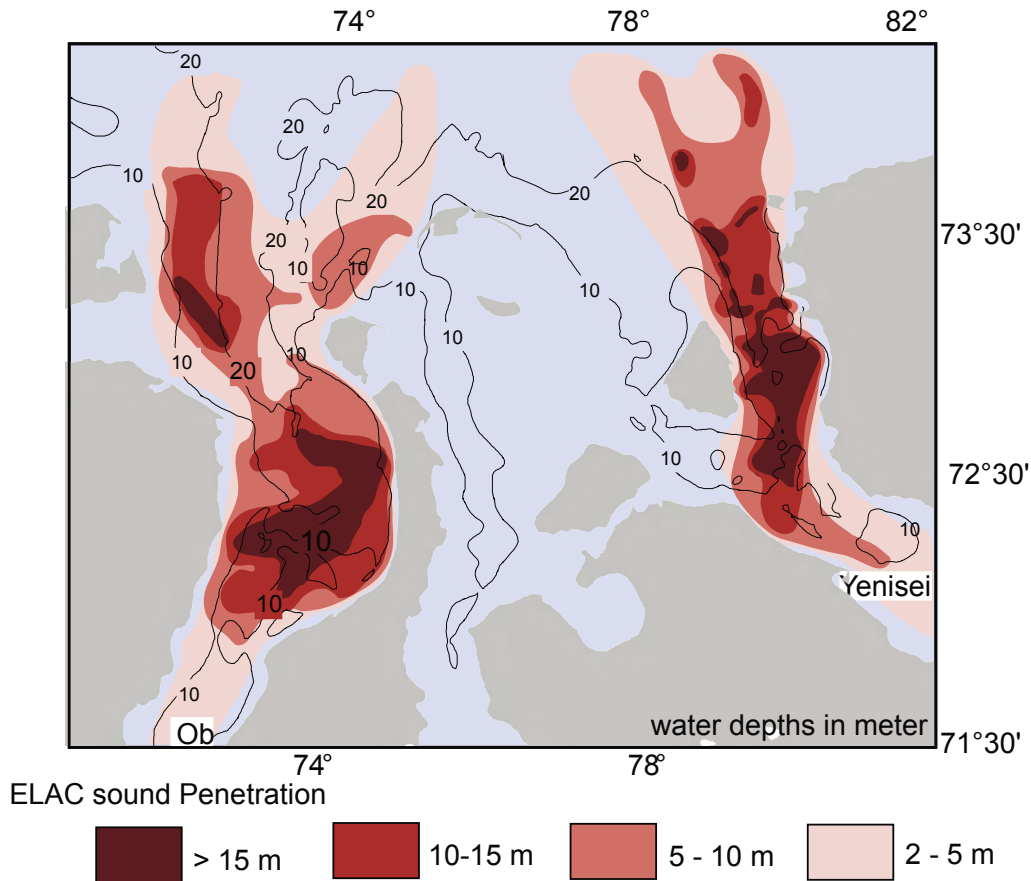
Figure 8. Isopach map showing the total thickness and extend of acoustic Unit I in Ob and Yenisei estuaries based on ELAC sound profiles.

for example, in cores BP99-32, BP01-03 (Fig. 11), BP01-83 and BP00-38 (Fig. 12). These values can probably be accounted to decreased sediment porosity and thus more susceptibility bearing material in the core rather than a change in dry sediment composition. Other cores show susceptibility fluctuations independent of the density record as, for example, in cores BP99-39, BP99-04, BP00-23, BP00-14 (Fig. 10) and BP00-22 (Fig. 11) indicative for variations in content and/or composition of magnetic grains.

In the Yenisei Estuary, susceptibility is $100 * 10^{-5}$ (SI) on average with peak values of $250 * 10^{-5}$ (SI) and $550 * 10^{-5}$ (SI) in core BP00-22 and BP00-23, respectively (Figs 10 and 11). Both cores penetrate Unit II and in both cores peak susceptibility values are in Unit II (Figs 9 to 11). In sediment cores from the Ob Estuary, values are significantly lower, averaging about $30 * 10^{-5}$ (SI). Here, the highest values reach $70 * 10^{-5}$ (SI)

(Core BP00-38; Figure 12). The mass-specific magnetic susceptibility of recent surface sediments (Fig. 13) shows two major trends. The first is, as observed in sediment cores, that values for the Yenisei river are significantly higher than in the Ob area with averages at 3,000 to 4,000 * 10–9 m^3 kg^{-1} and 1,000 to 1,500 * 10^{-9} m^3 kg^{-1}, respectively. The other important observation is a distinct decrease in values north of 74° N which is most pronounced in the Yenisei area. Despite the distinct decrease off the Yenisei Estuary some samples north of 74° N show slightly increased susceptibility compared to other areas of the southern Kara Sea. Core correlation: Core-to-core correlation using physical properties is not possible for the entire area under investigation. Only in case where core locations are in relatively close distances to each other, lateral correlation by density and susceptibility is obvious such as for cores BP99-04 to BP01-25, BP99-39 to BP99-38 (Fig. 10), BP99-32 to BP99-08 to BP01-03 (Fig. 11) and BP00-38 to BP01-83 (Fig. 12).

Chronology

All datings of sediment cores penetrating into Unit I reveal Holocene ages (Fig. 9, Stein et al. 2003). The oldest Unit I age of 9 ka BP is determined at the base of Core BP99-04 located in the norther Yenisei Estuary. The distinct down-core increase of both density and susceptibility at the bottom of core BP99-04 (Fig. 10) suggests that the transition into the underlying Unit II is exposed and dated and the gravity corer got stuck at or shortly above the UnitI/II boundary.

The only dateable core penetrating into Unit II is BP99-05. An age of 15.5 ka BP was determined at a core depth of 3.15 m (Fig. 9). The dated material is a relatively fresh shrub wood suggesting a nearly contemporaneous sedimentation. Though it is driftwood, the good preservation can be used as first evidence for a pre-Holocene age of Unit II.

3.4 Correlation of acoustic units with sediment cores

The coring locations BP00-14, BP99-32, BP99-08 and BP01-03 are on the track of the CHIRP profile (Fig. 2C). BP00-14 cored both Unit I and II. Lithology and physical properties demonstrate that the increase in sand content correlates with higher density. The density gradient defines the major acoustic impedance contrast causing the strong seismic reflector at the boundary between Units I and II. The same is true for a correlation of Unit I/II boundaries cored by BP00-23 and BP99-05 (Fig. 9) with the ELAC profile from the northern Yenisei Estuary (Fig. 4B). This suggests that the transition from Unit I to II observed in cores and acoustic profiles are identical in the entire area.
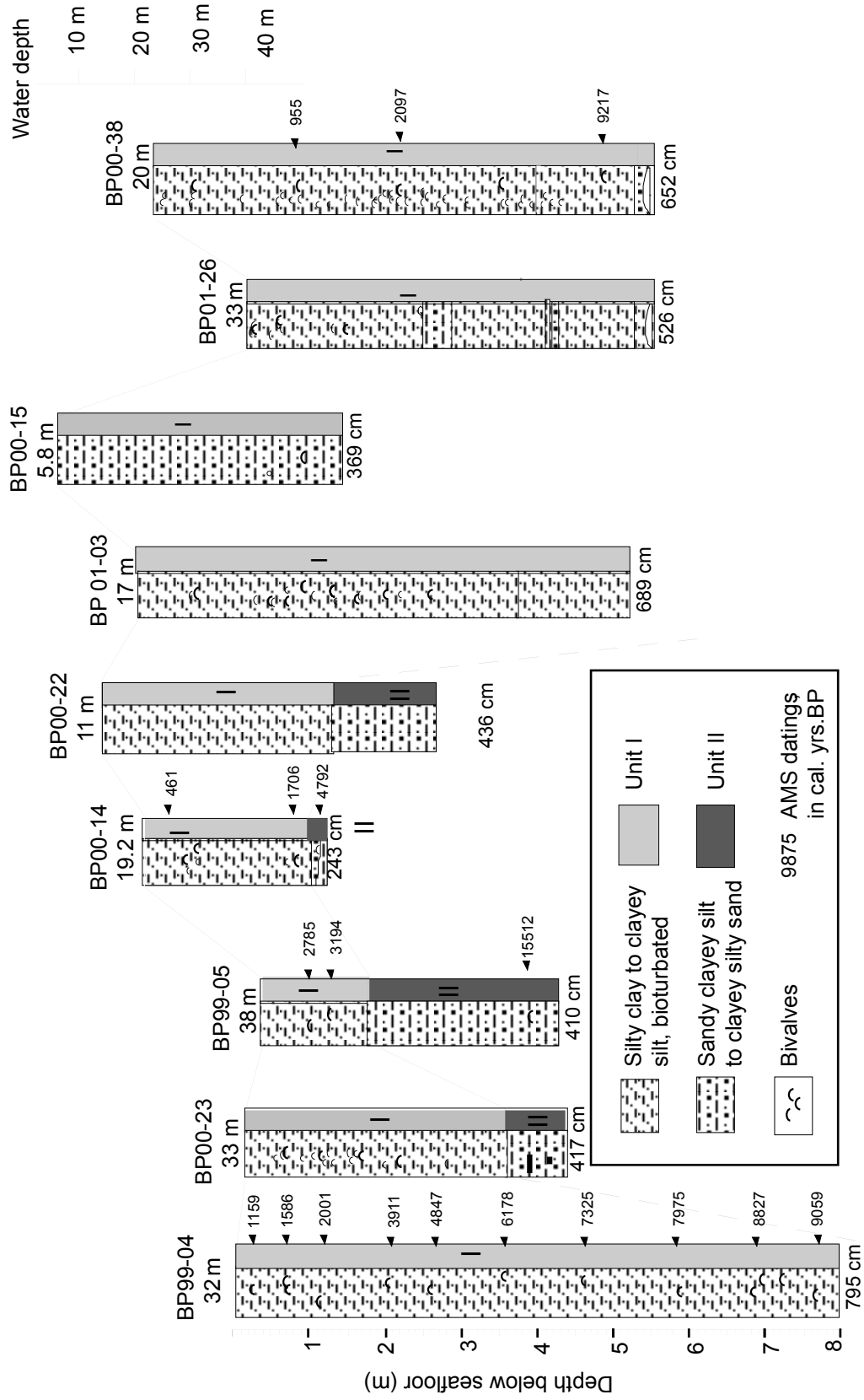
Figure 9. Stratigraphic correlation of selected cores based upon core description, datings and echo-sounding. Cores are arranged according to their water depth (right hand scale) see Figure 1 for location.

Figure 10. Density and magnetic susceptibility records of Unit I and II sediments from the northern Yenisei Estuary.
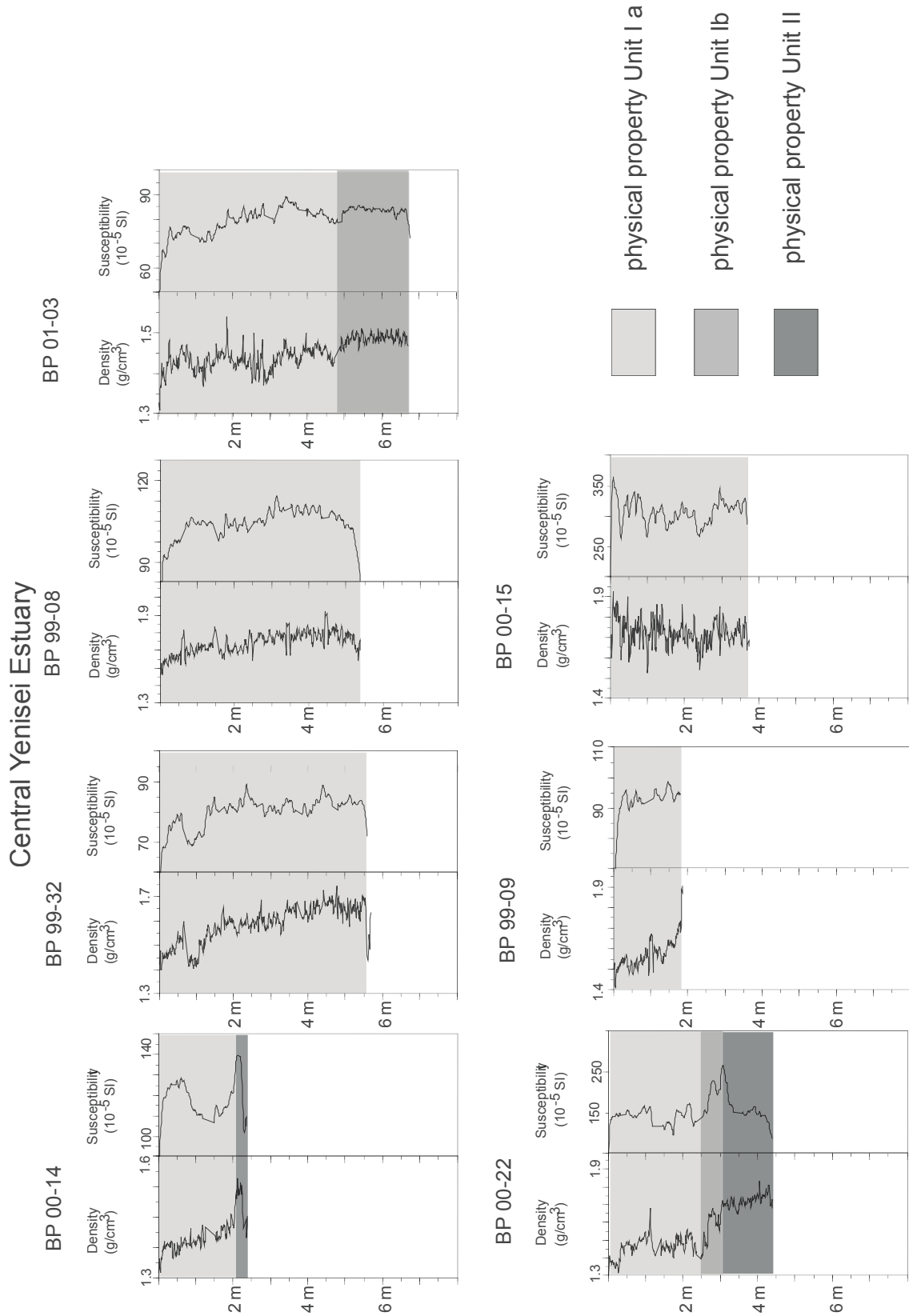
Figure 11. Density and magnetic susceptibility records of Unit I and II sediments from the inner Yenisei Estuary.
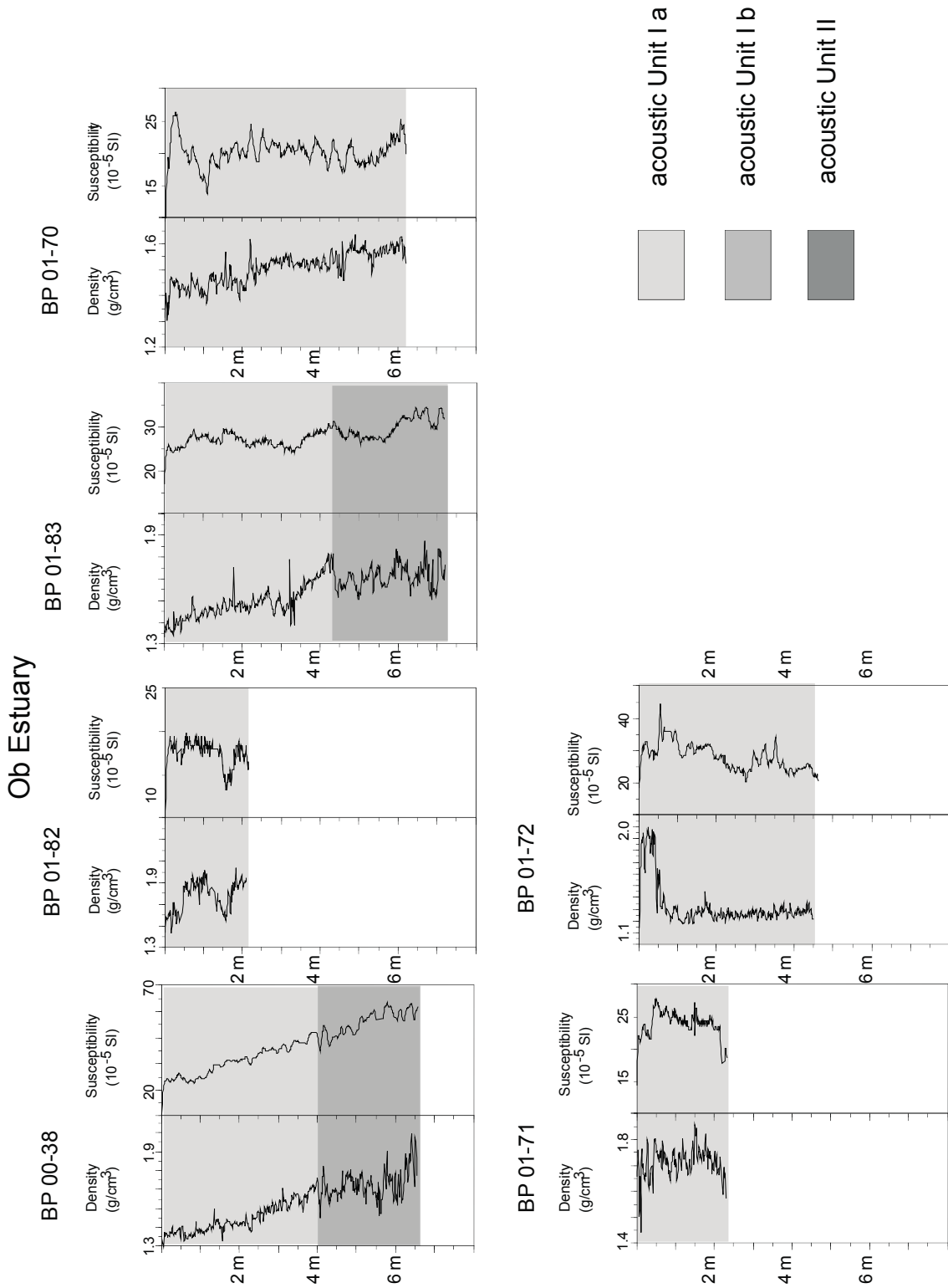
Figure 12. Density and magnetic susceptibility records of Unit I and II sediments from the Ob Estuary.

The only core, which clearly penetrated the acoustic boundary between subunits Ia and Ib of the CHIRP profile, is BP01-03 whereas BP99-32 and BP99-08 probably only comprise Subunit Ia sediments (Fig. 2C). The boundary between Subunit Ia and Ib is insignificant in physical property records of both density and susceptibility (Figs 10 to
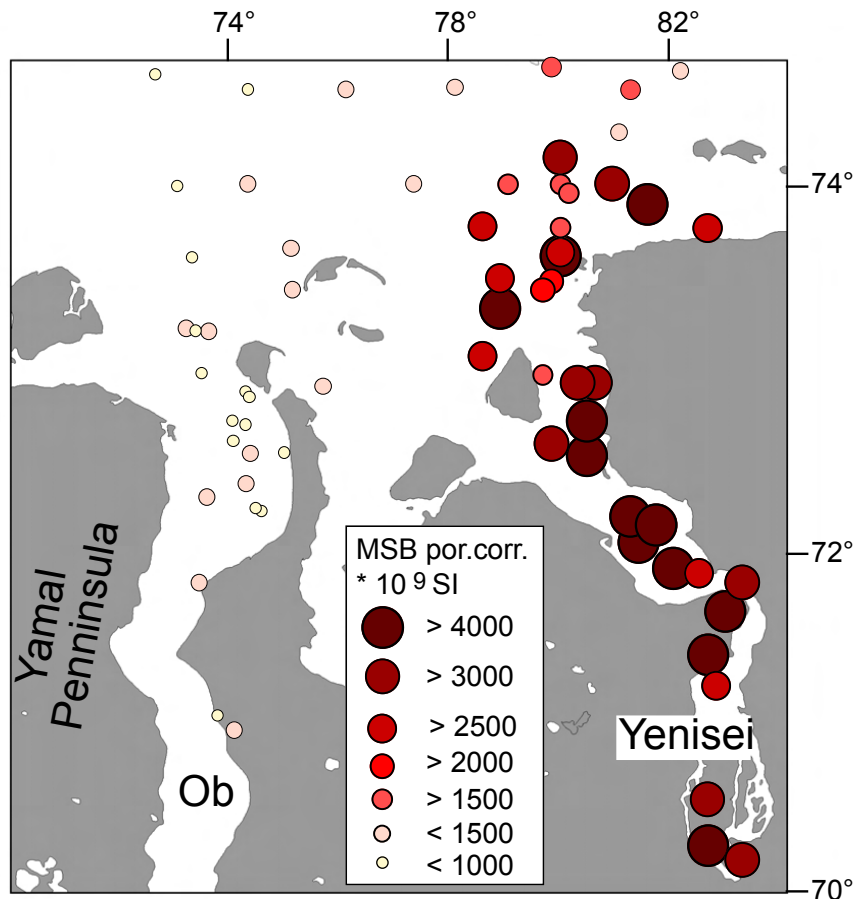
Figure 13. Mass-specific magnetic susceptibility of surface sediments in the Ob and Yenisei estuaries and the adjacent inner Kara Sea.

12) and not visible in the lithology (Fig. 9).

Along the CHIRP profile, Subunit Ic was not cored because it is below the maximum gravity-corer sediment-penetration limit of about eight metres (Fig. 2C). Along ELAC profiles, where cores recovered both Unit I and Unit II sediments, Subunit Ic could not be identified due to limited echosounding resolution or may not be present.

3.5 Sediment mass

The total sediment volume was calculated from the areal extent of Unit I sediments, compiled by echosounding, multiplied by its thickness (Figs 7 and 8; Table 1). The amount of dry sediment was quantified by subtracting the average volume of pore water (66% porosity) from the total wet sediment volume. The net sediment mass was

then quantified by multiplying the porosity corrected value of dry sediment volume with the average grain density of 2.65 g cm^{-3} (e.g. Weber et al., 1997). The total estimated sediment yields of the estuaries of Ob and Yenisei differ significantly but are in the same order of magnitude (Table 1). Acoustic Unit I yields 14.3 * 10^{10} t and 9.2 * 10^{10} t of dry sediment (Table 1) in the Ob and Yenisei estuaries, respectively.

Table 1. Quantified sediment area and volume based on isopach map (Fig.8). The net sediment mass was determined by the sediment volume and the average porosity of sediment cores and the average dry grain density.

Sediment Thickness (m)	Area (km^2)	Volume (km^3)	Netto Sediment Mass (*10^{10}t)
Yenisei			
>15	1815.1	31.8	
<15	2022.1	25.3	
<10	3789.4	28.4	
<5	6512.1	19.5	
total		105.0	9.2
Ob			
>15	2452.0	42.9	
<15	3805.4	47.6	
<10	5938.9	44.5	
<5	8709.4	26.1	
total		161.1	14.3

4 Discussion
4.1 Late Quaternary sedimentary environments
Age model

The radiocarbon datings of Unit I and II suggest that the boundary may represent the pre-Holocene transition or unconformity. The susceptibility spike observed near the top of Unit II in cores BP99-05, BP99-09, BP99-38, BP00-23 and BP00-22 (Figs 9 and 10) is similar to a comparatively high spike of susceptibility described in cores from the eastern Kara Sea and Laptev Sea by Kleiber and Niessen (2000).

The susceptibility peak revealed a pre-Holocene age of 10 to 13 ka BP and is interpreted as a result of enhanced input of magnetic minerals during Termination I which have their source in the basaltic Putoran Plateau (Kleiber and Niessen, 2000). The spike is thought to originate from a melt-water run-off peak related to deglaciation of the Putoran Plateau which results in increased delivery of high susceptibility bearing material. If this interpretation is correct, the susceptibility peaks of Unit II observed

in our cores from the Kara Sea are probably related to the same origin (Stein et al., 2003) because the Yenisei is draining part of the Putoran Plateau. The interpretation of magnetic susceptibility peaks near the top of Unit II, together with the radiocarbon age of 15.5 ka BP of Core BP99-05, suggest that Unit II is of late Pleistocene age including Termination I.

Because radiocarbon dating of Unit I confirmed Holocene ages (Fig. 9; Stein et al., 2003), it is likely that the distinct reflector separating Units I and II (Figs 2 to 4) is the base of Holocene deposition. This reflector appears as pre-transgressive, erosional boundary in most locations. Thus, Unit I thicknesses (Figs 7 and 8) are interpreted to represent total Holocene sediment accumulation.

Sedimentary history

Unit II was probably subaerially exposed and partly eroded during sea level low stand. For example, a relatively deep river channel (at least 55 m below present sea level) was incised into the strata of Unit II (Figs 2 and 15: Phase I) during the last sea level lowstand at the location of the present Yenisei Estuary. According to the modern shelf morphology, the paleoshoreline and related estuaries were situated further to the north along the present day outer shelf. Thus, the pre-Holocene paleoenvironment between 72° and 74° N was fluvial or subaerially with erosion as predominant process.

The geometry of Subunit Ic is dominated by typical fluvial architecture elements such as point bars (lateral accretion) and overbank deposits described by e.g. Allen (1965) and Miall (1996 and references therein) in modern fluvial sedimentary environments. In Subunit Ic downlaps onto the upper channel flank are interpreted as accretion of inclined point bars (Fig. 6). This suggests channel migration towards the east (Fig. 6). There are no Subunit Ic sediments preserved inside the channel which indicates high current velocities near the channel axis. Outside the channel, strata grade laterally into sediments with parallel reflectors. This indicates decreased influence of currents resembling typical overbank sediments (Allen, 1965), accumulated in a wedge-shaped structure on a floodplain (Fig. 15: Phase II), typical of a natural levee (Brierly et al., 1997; Bown and Kraus, 1987). According to Galloway and Hobday (1996) horizontal aggradation on a floodplain occurs when sediment-laden water overflows and releases its suspension load due to flow stripping.

In the CHIRP profile, the bottom of Subunit Ic (Fig. 2) is located approximately 40 m below present sea level which is the same depth as the base of core BP99-04 (Figs 2 and 4B) situated some 80 kilometers further downstream of the profile (Fig. 1). AMS 14C dating of the base of the core reveals an age of 9 ka BP (Fig. 9). Sedimentology (Stein et al. 2003) and palynological investigations (Kraus et al. 2003) indicate fluvial influences for the lowermost part of core BP99-04 and changes to a marine environment

in the upper part.

Bauch et al. (2001) used age and eustatic sea level data by Fairbanks (1989) for the reconstruction of the Holocene transgression in the Laptev Sea. The sea level curve serves as a rough indication for paleosea levels at a given age, if the area is not affected by isostatic rebound after deglaciation. According to Fairbanks (1989) the eustatic sea level trend was about 30 m below present at 9 ka BP (Fig. 14). Assuming no (or negligible) isostatic rebound of the Yenisei Estuary area during the Holocene, the onset of sedimentation in core BP99-04 took place near the sea level in very shallow water (Fig. 14). If true both locations BP99-04 and the CHIRP profile (Fig. 1) must have been strongly influenced by the paleoriver Yenisei at 9 ka BP. This is consistent with the fluvial character of the lowermost sediments of Core BP99-04 and the interpretation of the seismic pattern above. This suggests a terrestrial, fluvial-dominated depositional environment for Subunit Ic in the CHIRP profile (Fig. 2). The paleoenvironment of Subunit Ic is best explained by a fine-grained meandering river system as proposed e.g. by Miall (1996). Probably, pronounced seasonal flood events similar to those observed in Siberian rivers today during late spring/early summer (Gordeev et al., 1996; Shiklomanov and Skakalsky, 1994) caused the accumulation of overbank deposits on the floodplain.

The age of the boundary between subunits Ib and Ic is difficult to assess because the core, which penetrated this boundary, is not dated yet (Fig. 9). However, the truncations at the top of Subunit Ic in Figure 5 could originate from an erosional transgressional ravinement surface (Thorne and Swift, 1991). This surface possibly formed in response to the landward migration of the shoreline associated with erosion during transgression, for example, as a result of wave action. If the entire Subunit Ic is a relict fluvial floodplain deposit, the marine transgression reached the top of this unit (30 m below present sea level, Figure 2) at about 8.5 to 8 ka BP (Fig. 14) and formed the onset of marine/ estuarine Subunit Ib.

Subunit Ib is characterised by sediment accumulation in the entire channel with highest bed thickness at the channel axis that thins towards the flanks resulting in a divergent fill geometry (Fig. 6; Mitchum et al., 1977). This suggests a gradual decrease in current velocity possibly related to increasing water depth during an early Holocene transgression associated with higher settling rates of particles in a shallow and widening estuarine environment.

As a result of rapid sedimentation in the eastern channel, the upper portion of Subunit Ib reached a higher bathymetric level than the channel base at the western end of the profile where no Subunit Ic and Ib sediments accumulated (Fig. 2). Subsequently, near the western deepest point of the profile, a new channel system was established,

where point bar deposits migrated westward forming Subunit Ib downlaps onto Unit II (Fig. 5). Formation of the western channel (Fig. 5) started in the same range of water depth (downlaps on Unit II at approx. 35 to 40 m below sea level; Figure 2) as the termination of current controlled sedimentation in the eastern channel (Fig. 6). The western channel displays sediment layers that are thinner at the channel base than at the adjacent flanks (Fig. 5) which is typical of an aggradating channel-levee-complex (Allen, 1965). The western channel probably represents the recent thalweg because, at present, its channel bottom has the maximum water depth of the entire cross section (Fig. 2C). In addition, the slightly thinner channel-fill suggests that recent sedimentation is affected by currents.

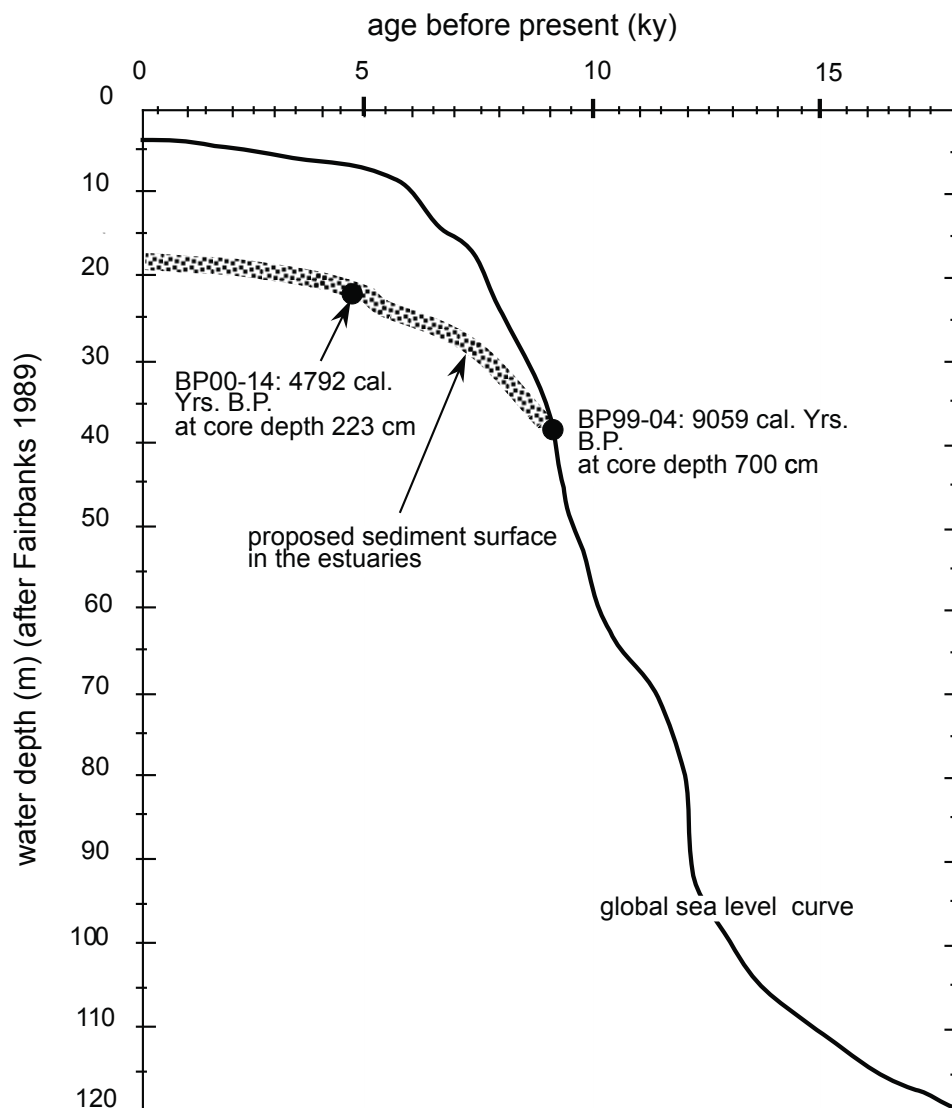Figure 14. Eustatic sea level trend for the last 15000 years (after Barbados sea level curve by Fairbanks 1989) and reconstruced sediment surface in the Yenisei Estuary after chronological data from cores P99-04 and BP00-14 (Fig.9). Note that channel erosion was before and onset of sedimentation after 10 ka BP. During the Holocene transgression sea level rise exceeded sediment accumulation in the area of the cores.

The entire Subunit Ib is typical for a shallow marine/estuarine channel-levee-complex characterised by high sedimentation rates in both channel and levee areas. The change in the depositional environment compared to Subunit Ic is interpreted as the result of sea level rise, decrease in current velocity and southward migration of marginal filter-type deposition centers. It is interesting to note that the well defined chronology of Core BP99-04, located 80 km to the north of the CHIRP profile also revealed high sedimentation rates for the early Holocene until about 7.5 ka BP which gradually decrease to lower rates until about 5 ka BP (Fig. 9). Consistently high sediment accumulation rates of 650, 250, and 240 (g cm^2 ky^{-1}) are quantified between 9.5 to 7.5 ka BP in cores BP00-36, BP00-26, and BP00-07 located 390 km, 250 km, and 130 km north of the Yenisei Estuary, respectively (Stein et al., 2003). It is suggested that these early Holocene deposition centers north of the present estuaries are lateral counterparts of the rapidly filling shallow-marine channel-levee-systems of Subunit Ib indicative of a southward migration of the marginal filter during the transgression. Draping subbottom topography and nearly constant thickness of Subunit Ia implies precipitation-type of particle settling out of the water column across the entire estuary, possibly overprinted by more active bottom currents in the western channel. This pattern is typical for the marginal filter setting of today with a relatively stable high sea level where salinity induced processes are important such as particle coagulation followed by rapid settling. Retrieved near the western end of the CHIRP profile from 19.2 m water depth, core BP00-14 reveals a minimum age of 4.8 ka BP for the base of Subunit Ia (Fig. 9). This suggests a major hiatus at the core location with Subunit Ia unconformably overlying Unit II. This is consistent with the seismic stratigraphy (Fig. 2) indicating that subunits Ib and Ic are missing at the coring location. The hiatus was possibly caused by subaerial exposure during the early Holocene until the transgression reached the location.

It seems to be reasonable that the onset of the drape geometry of Subunit Ia is related to the end of the transgression which reached the present sea level by about 5 ka BP. Therefore, we assume that the marginal filter reached its recent position between 7.5 and 5 ka BP.

The distribution pattern of magnetic susceptibility of recent surface sediments (Fig. 13) documents the recent spatial extent of the deposition center in the Yenisei Estuary because magnetic grains derived from the Putoran Plateau trace terrestrial input into the Kara Sea. The susceptibility pattern is consistent with the distribution of Holocene sediment thickness (Fig. 8) demonstrating that a large amount of riverine material is trapped in the estuaries indicative for the marginal filter effect (Lisitzin, 1995). Because there is no similar source of magnetic grains in the Ob catchment, magnetic susceptibility in surface sediments of the Ob Estuary remains low (Fig. 13) despite

increased sediment accumulation (Fig. 8). Therefore susceptibility cannot be used to trace the marginal filter effect in the Ob Estuary.

The proportions of sediment thicknesses of subunits Ia to Ic a were estimated from the transect section in Figure 2 to assess the time-dependent sediment accumulation in the present Yenisei Estuary. Each Subunit represents approximately 1/3 of the Holocene sediments in this particulate section. Subunit Ic covers a time interval ranging from 11.5 to about 8 ka BP. By comparison with the global sea level curve (Fig. 14), it seems likely that significant deposition in Subunit Ic started after 10 ka BP with high sedimentation rates of about 0.33 cm y^{-1}. Subunit Ib comprises some 3000 years from about 8 to 5 kys. BP and Subunit Ia the last 5000 years, resulting in sedimentation rates of 0.2 cm y^{-1} and 0.14 cm y^{-1}, respectively.

This assumption clearly demonstrates that those units comprising acoustic evidence for enhanced current activities (active channel-levee-complexes as subunits Ia and Ib), and thus higher rates of sediment by-pass, are also characterised by higher sedimentation rates than the marginal filter of the younger Holocene (Subunit Ia). We suggest that the location of channel-levee-complexes are strongly controlled by the location of the paleoshoreline and sea level, therefore of small spatial extent and steadily migrating southward during the early Holocene transgression. In contrast, the marginal filter setting after 5 ka BP remains in relatively stable steady state. Sediment accumulation took place in deeper water and thus over a relatively large area (Figs 2 and 8) resulting in overall lower sedimentation rates.

4. 2 Sediment budget

The Holocene sediment budget from seismic data and sediment cores as presented in this paper is difficult to test because a number of uncertainties remain which affect the sediment accumulation. This includes additional input from coastal erosion long-term variations in the riverine discharge, and transfer rates from the estuaries to the shelf. The effect of these processes are hard to quantify with an appropriate spatial and temporal resolution.

For example, Rachold et al. (2003) conclude for the Laptev Sea that the amount of coastal erosion ($44 * 10^6$ t y^{-1}) is almost twice as high as the riverine input ($25 * 10^6$ t y^{-1}). However, this estimate was made for the open shelf. In the sheltered estuaries of Ob and Yenisei, we expect lower rates of coastal erosion because erosional energy by waves is minor and thus the coastline is more stable. Furthermore, there is a different type of permafrost along the Kara Sea coast (International Permafrost Association, Data and Information Working Group, comp. 1998) because no ice complexes are found as described from the Laptev Sea (Schirrmeister et al., 2002). Such ice

Fairbanks Sea Level Curve   Phase I: Pre Holocene

erosion of Unit II

— 10 m

— 30 m

II

— 50 m

S.L.

Phase II: early Holocene

deposition of Unit I c

— 10 m

? S.L

— 30 m

I c

II

— 50 m

Phase III: Holocene to recent

S.L.

— 10 m

I a

I b

— 30 m

I c

II

— 50 m

active formation of Unit I a & Unit I b

▪ ▪ ▪ ▪ ▪ ▪ approximated sea level
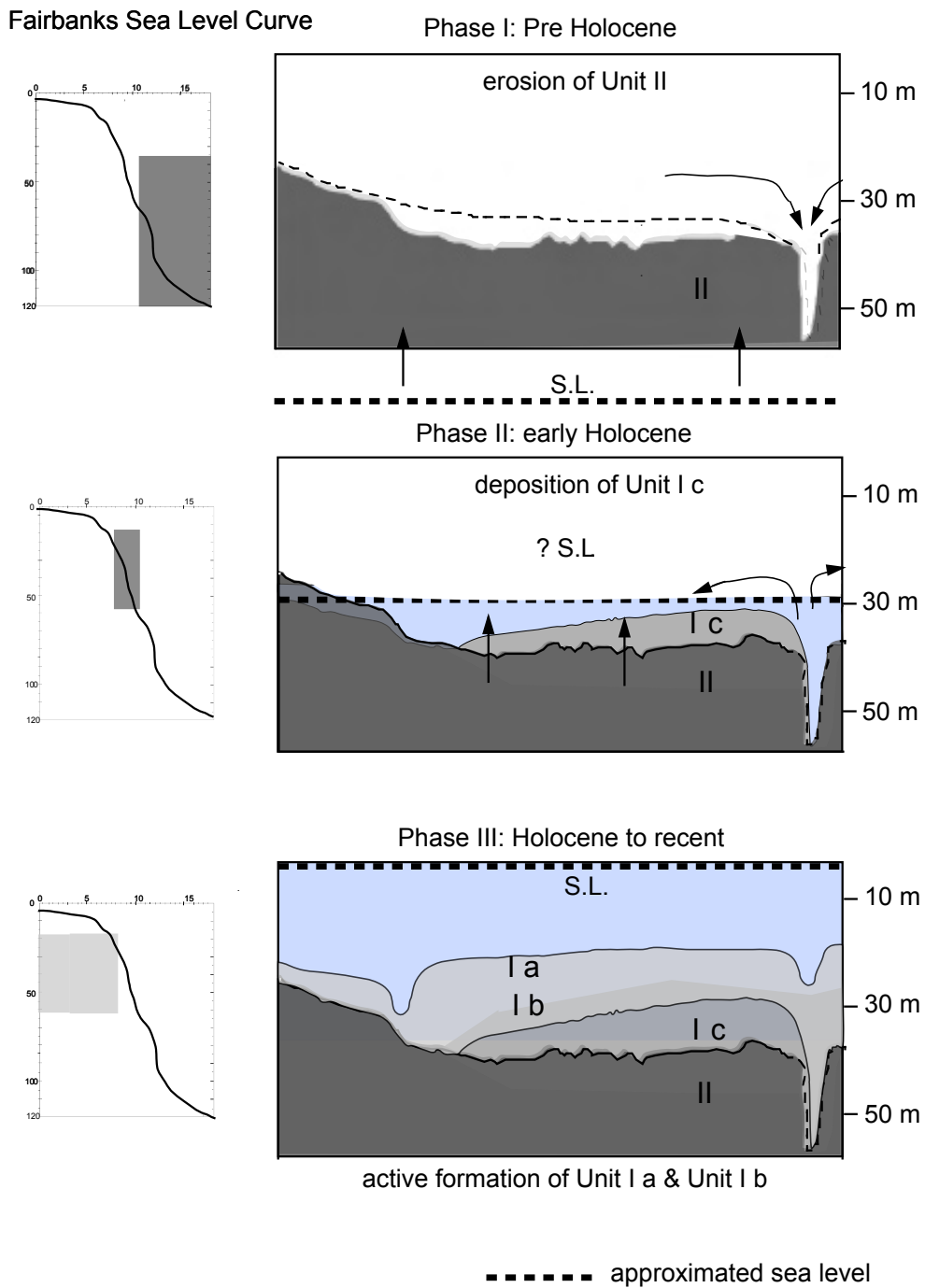
Figure 15. Late Quaternary evolutionary model for the high-resolution CHIRP profile (Fig. 2).

complexes commonly contain up to 80% of water which melts during the summer thereby forming unstable sediment cliffs susceptible to coastal erosion. Missing ice complexes in association with a low relief (Gordeev et al., 1996; Milliman and Syvitzky, 1992) suggest that significant coastal erosion is unlikely in the sheltered Ob and Yenisei estuaries.

If coastal erosion is not important, one simple way of testing our budget is to compare the total net sediment masses estimated from this study with the modern average discharge of suspended and dissolved matter (Gordeev et al., 1996; Telang et al., 1991) extrapolated back over the last 7500 years (Table 2), the time period during which we believe the establishment of the modern marginal filter system has occurred. In order to be closer to Holocene conditions not affected by anthropogenic change, we include data from before A.D. 1950 (Table 2; Telang et al., 1991; Holmes et al., in press) for the Yenisei River. This takes into account dam building (e.g., the Krasnoyarsk Dam) duringthe last 50 years in the catchment area of the Yenisei Estuary.

Table 2. Recent sediment discharge for the Ob and Yenisiei rivers. II: Discharge amount of suspended and dissolved matter during the last 7500 years quantified by linear extrapolation of I. III: Total amount of material expected as accumulated sediments present in the marginal filter according to Lisitzin (1995);

I.	suspended matter (10^6 t a^{-1})	dissolved matter (10^6 t a^{-1})	
Ob	16.5(2) 13.4(1) **15,5**	**34(1)**	(1) Telang et al. (1991)
Yenisei	5.9(2) 14.4(1) **14,4**	**43.2(1)**	(2) Gordeev et al. (1996)

II.	total discharge in 7500 years (10^{10} t 7500 a^{-1})	total discharge in 8000 years (10^{10} t 7500 a^{-1})	
Ob	11,6	25,5	
Yenisei	10,8	32,4	

III.	90 % of II (10^{10} t 7500 a^{-1})	30 % of II (10^{10} t 7500 a^{-1})	Total (10^{10} t 7500 a^{-1})
Ob	11,0	7,7	**18,7**
Yenisei	10,3	9,7	**20,0**

The extrapolation suggests that the Ob River released 11.6 * 10^{10} t of suspended matter and 25.5 * 10^{10} t of dissolved matter during the last 7500 years (Table 2). The Yenisei River discharged 10.8 * 10^{10} t of suspended matter and 32.4 * 10^{10} t of dissolved matter (Table 2). According to Lisitzin (1995), 90% of the total suspended matter and 30% of the dissolved matter precipitate and accumulate in the marginal filter at the river-sea interface. If true, this would result in a total sediment accumulation of 18.7 * 10^{10} t for the Ob River and 20 * 10^{10} t for the Yenisei River (Table 2). These numbers are significantly higher than the Holocene sediment masses estimated from mapping of Unit I sediment thickness in the Ob and Yenisei estuaries which results in 14.3* 10^{10} t (about 75% of the modern-based calculated value), and 9.2 * 10^{10} t (about 50% of the modern-based calculated value), respectively (Table 1). It may suggest that the study of Lisitzin (1995) describing the marginal filter as efficient sediment trap for fluvially-derived material underestimates sediment by-pass and/or export into the Kara Sea. The discrepancy between our and Lisitzin's approximation is highly relevant for both assessment of material exported from the Ob and Yenisei catchments into the Kara Sea and the sediment budget of the entire Arctic Ocean. Thus, the possible reasons, which can account for the discrepancy, need to be discussed in further detail.

One reason may be that the ELAC system used for our quantification does not penetrate Unit I down to the top of Unit II in all locations thereby underestimating Unit I thickness and mass. This is not very likely because the strong reflector marking the top of Unit II is visible in most profiles (Figs 4 and 5). Moreover, comparison along lines, where both CHIRP and ELAC data were recorded during the expedition BP01, demonstrate that both systems revealed the same thickness for Unit I (Stein and Stepanets, 2001; Figure 2).

Another reason may be that the extrapolation of recent run-off data as summarised in Table 2 may not be correct and/or not valid for the last 7500 years because climate change could have caused variation in run-off during the Holocene (Stein et al., 2003b). Here it is interesting to note that our assessment of sediment accumulation for Subunit Ia for the last 5000 years matches almost exactly recent sedimentation rates in the marginal filter using Cs 137 records (Stepanets et al., 1999). Combining the average porosity (66%) with the mean Subunit Ia sedimentation rate (0.2 cm y $^{-1}$) and the average sediment surface porosity (74%) with near-surface sedimentation rates of 0.3 cm y $^{-1}$ (Stepanets et al., 1999), respectively, results very similar in mass accumulation rates (MAR) of 0.21 g cm^{-2} ka^{-1} in surface sediments and 0.2 g cm^{-2} ka^{-1} in the entire Subunit Ia.

Thus, the most reasonable explanation for this discrepancy is that our study does not quantify early Holocene accumulation correctly until ca. 5 to 6 ka BP, the time

when sea level reached the present level. The southward migrating position of the marginal filter during the transgression is difficult to compile from the data available. Possibly, there are additional depositional centers further north, which are outside the area of data acquisition and thus not yet mapped (Stein et al., 2003b). The character of a deepening upward sedimentary sequence in the estuaries in association with acoustic pattern indicative for currents in the early Holocene (Figs 2, 5 and 6) suggest that current-induced by-passing of sediments onto the open Kara Shelf has decreased during the Holocene. In turn, this implies higher sediment export out of the area mapped in this study before 5 ka BP This export must have been significant because Subunit Ic sediments, interpreted as fluvial deposits possibly older than 8 ka BP, are included in the budget based on mapping. Therefore, our approach using the total thickness of Unit I sediments should overestimate the actual budget for the last 7500 years thereby increasing the discrepancy between the different ways of quantification.

Although early Holocene by-pass probably accounts for most of the budget discrepancy discussed above, sediment export out of the estuaries may also play some role today and during the last 5000 years. Is there evidence for sediment erosion and lateral transport?

Ice gouges visible in the acoustic images are evidence for grounded ice floes (Fig. 2) which can disperse sediment at the bottom (Barnes and Lien, 1987; Reimnitz et al., 1972; 1978) when drifting sea-ice ridges plough through the sediment. Ice thickness can reach up to 20 m in pressure ridges (Løset et al., 1999; Barnes and Lien, 1987). However, at least for the area of Ob and Yenisei estuaries sediments appear mostly undisturbed in acoustic images and ice gouges only occur locally (Fig. 2). Therefore, ice gouging is expected to play only a minor role in the sediment budget of the Ob and Yenisei marginal filter systems.

Sediment by-pass may be enhanced by bottom currents which can be provoked by tidal activity, changes in the river discharge (especially at the spring discharge peak), and brine formation by freezing of seawater (Reimnitz et al., 1993; Dethleff, 1994; Løset et al., 1999; Barnes and Lien, 1987; Lisitzin, 1995; Pfirman et al., 1995; Are, 1996). Evidence from this and other studies suggest that, at least for the Yenisei Estuary, considerable by-pass has to be considered for the present situation of the marginal filter. Material export along certain pathways out of the Yenisei Estuary is documented by relatively high values of magnetic susceptibility in surface sediments on the open Kara shelf, mainly concentrated in morphological depressions and/or channels (Fig. 13; Stein et al., 2003b).This is consistent with the fact that in cores from the area north of the Yenisei marginal filter (BP0036, BP00-26, and BP00-07) there is still accumulation today, but with smaller rates of 7, 17 and 40 (g cm^2 ka^{-1}),

respectively, compared to the early Holocene. Moreover, according to our estimates, there is a smaller Holocene sediment mass in the Yenisei Estuary (Table 1) than in the Ob Estuary although they receive nearly the same influx (Table 2). Thus, accumulation rates, magnetic susceptibility in surface sediments and the sediment budget indicates some unquantified sediment export from the Yenisei Estuary to the shelf probably active during the entire last 5000 years.

Higher export rates of particulate matter out of the Yenisei Estuary could be related to different estuarine morphologies and hydrological regimes. It is interesting to note that inflow of sea water into the Yenisei Estuary is enhanced by its deeper bathymetry compared to that of the Ob. Harms et al. (2003) describe a strong sea water underflow in the Yenisei as a result of channelled river-water inflow into the Kara Sea which is of the same direction as the main summer winds thereby enforcing Ekman transport. Thus, through the Yenisei Estuary surface waters are transported relatively far to the north. In contrast, the mouth of the Ob Estuary is characterised by a tide-wave interference zone with relatively high kinetic energies which may influence sediment transport, mixing, and deposition in relatively unstratified waters (Harms et al., 2003). These different characteristics may result in a larger sediment export to the open shelf out of the Yenisei Estuary as compared to the Ob.

5 Conclusions

The sediments in the Ob and Yenisei estuaries can be divided into two major acoustic and lithological Units (I and II). Unit II forms the pre-Holocene basement with little acoustic penetration. During the last sea level lowstand, the erosional surface was formed on top of this unit including several incised river channels. The younger Unit I can be divided into three subunits, Ia to Ic. Their formation is related to post-glacial sea level rise after about 12 ka BP and the southward migration of the river-sea marginal filters to their recent position in the estuaries between 72° to 73° N. The lowermost subunits Ic and Ib show fluvial to shallow-marine seismic features comparable to typical channel-levee-complexes representing a fine-grained meandering river depositional environment overlain by a transgressive system tract and finally high stand system tract after about 5 ka BP.

The entire sediment fill of the present estuaries reflects a deepening-upward sediment growth structure suggesting that sea level rise exceeded sediment accumulation although migration of the marginal filter during the Holocene shifted depositional centers south.

The present estuaries of the Ob and Yenisei rivers are the major Holocene sediment sinks of terrigeneous material supplied by rivers. An estimated total of 14.3 * 10^{10} t and

$9.2 * 10^{10}$ t of dry sediment have accumulated during the Holocene, which is about 75% and 50% of the material expected from extrapolation of modern run-off data, respectively.

Sediment deposition in early Holocene times outside the recent position of the marginal filter is proposed to be the reason for the differences in the sediment budgets. A progressive southward migration of the position of the marginal filter in response to the elevating sea level is favoured to account for the "missing" material. This would mean that a significant amount of material was deposited on the present shelf and not in the position of the recent marginal filter. Extensive sediment reworking is not observed but significant sediment by-pass through the marginal filter system cannot be excluded. Further studies are necessary to improve the temporal and spatial resolution of Holocene sediments for a better assessment of the early Holocene budget particularly in the central and northern areas of the Kara Sea.

The existence of filled paleoriver channels suggests a pre-Holocene history of the southern Kara Sea Shelf similar to that in the Laptev Sea (Kleiber and Niessen 1999). These channels must have been eroded during the sea level lowstand and were filled with sediments during the Holocene transgression. River erosion of the exposed shelf of the southern Kara Sea during implies continuous river transport across the shelf and absence of an ice sheet in the area of channel erosion.

Acknowledgements

3.4 Acoustic facies on the inner Kara Sea Shelf: implications for late Weichselian to Holocene sediment dynamics

3.4 Acoustic facies on the inner Kara Sea Shelf: implications for late Weichselian to Holocene sediment dynamics

Dittmers, K.*, Lambeck, K.+, Niessen, F. *, Stein, R.*

*Alfred Wegener Institute for Polar and Marine Research, Bremerhaven, Germany
+ The Australian National University, Canberra, Australia

Corresponding Author kdittmers@awi-bremerhaven.de

Abstract

We studied the impact of sea level fluctuations on sediment dynamics in the inner Kara Sea by using high resolution acoustic sub-bottom profiling, combined with the physical properties of AMS ^{14}C-dated sediment cores.

The first model data on LGM isostatic rebound for this region led us to confined interpretation of acoustic units in terms of sequence stratigraphy. The acoustic lines were ground-truthed with dated sediment cores. We identified and mapped three characteristic sedimentary/depositional environments and established sediment masses for each facies type. Furthermore we refined the location of the eastern LGM ice margin.

Sea level fluctuations resulted in periods of sub-aerial exposure of huge shallow shelf areas. The Kara Sea Shelf is characterised by a major incised dendritic paleo-river network that is variably infilled with late Pleistocene to Holocene estuarine facies topped by marine sediments, having draping geometries.

During sea level lowstand sediments by-passed the shelf, accumulating in water depths exceeding 120 m, while Holocene sedimentation concentrated on the recent estuaries. The shelf channel system was formed during phases/episodes of sea level lowstand during the Last Glacial Maximum and subsequent marine post-glacial sea level rise across the Kara Sea Shelf. During transgression the shallow shelf was subjected to intensive reworking and erosion.

The Kara sea can be subdivided into three Facies areas: estuaries, the shelf and deeper (> 120 m water depth) lying areas that accumulated a total of 114 x 10^{10} t of Holocene sediments.

Continuous (sub)marine channel-levee complexes located at the LGM ice margin and are most probable of late glacial to early Holocene age.

Keywords: high resolution seismic, sequence stratigraphy, sea level, shelf deposits, isostasy, Kara Sea

1.Introduction

Glaciations played a major role in the sedimentary history of northern Siberia and in particular the Kara Sea (e.g. Mangerud et al., 2003; Svendsen et al., 2004) (Fig. 1). Ice sheets covered Scandinavia and parts of northern Eurasia and its adjacent shelf areas. In particular, the Barents and Kara Seas were covered by thick grounded ice sheets during the Early and Middle Weichselian but this cover was less extensive during the Last Glacial Maximum (LGM), being largely restricted to the Barents Sea (Lambeck et al., 1995; Svendsen et al., 2004). The Barents-Kara Sea ice sheet was grounded, and may therefore have been susceptible to rapid changes due to a sea level rise (Lindstrom and MacAyeal, 1993), possibly triggered by deglaciation in the southern or the western hemisphere. After the LGM there were well-dated brief intervals of accelerated sea level rise (originating in rapid deglaciation phases) at 14.2-13.7 ka BP and 12.6-11.4 ka BP, named melt water peak 1A (MWP1A) and 1B (MWP1B), respectively (Fairbanks, 1989).

After 14 ka BP there is evidence for increased Arctic melting documented by ice-

Figure 1. Working area, general overview and glaciation limits

ice sheet limits
(according to Svendsen et al. 2004)

——— ice margin ca. 90-80 kyrs BP
∙∙∙∙∙∙∙ ice margin ca. 60-50 kyrs BP
——— LGM ice margin ca. 20 kyrs BP
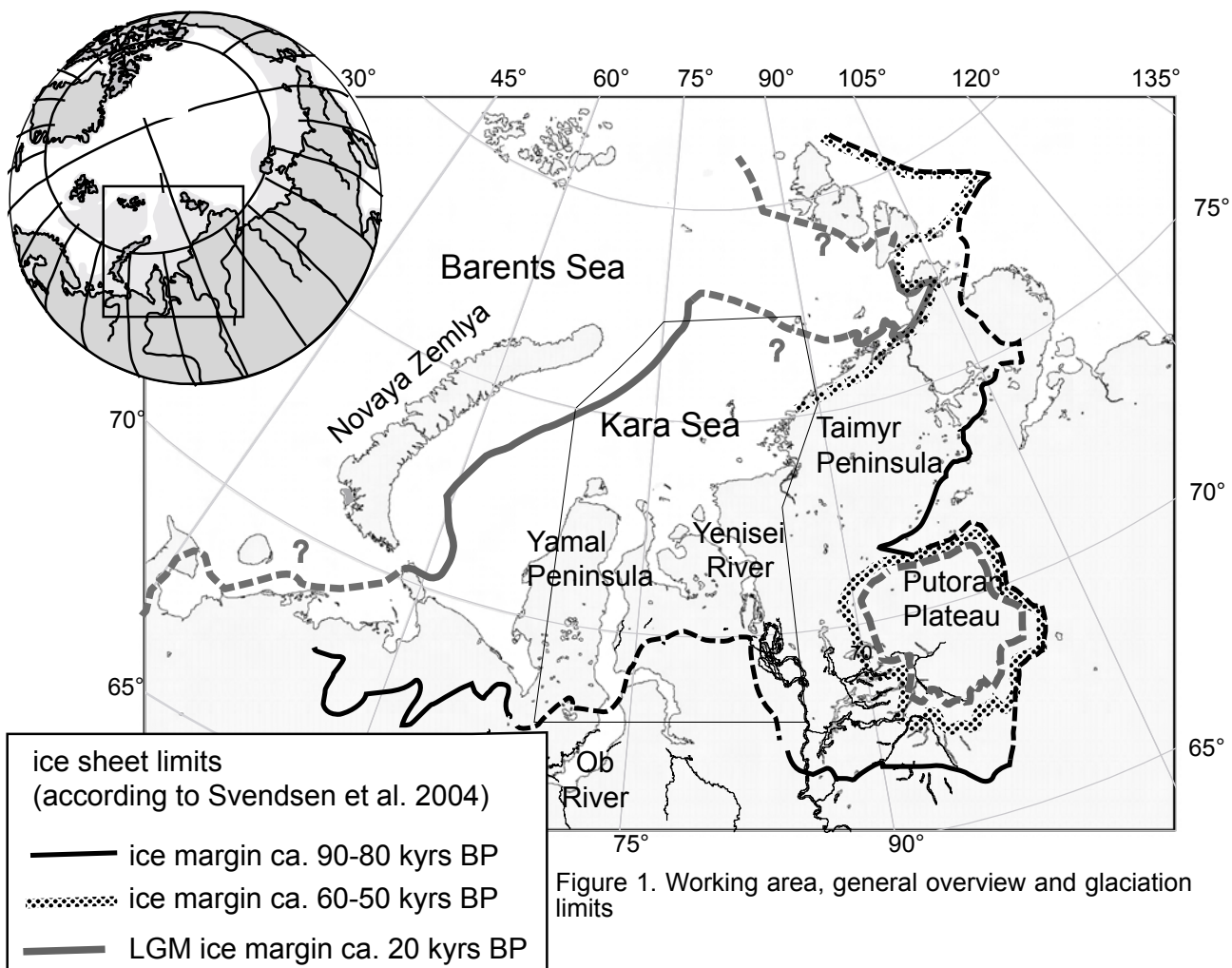
rafted debris (IRD) events (Clark et al., 1996; Norgaard-Pedersen et al., 1998, 2003).

The sea level curve for Weichselian times is characterised by an asymmetric shape with relatively slow regression preferentially preserving lowstand features in the sedimentary record and higher rates of transgression (Posamentier et al., 1992; Lambeck and Chappell, 2001; Coe et al., 2003). As examples of other well studied shelf areas show, sea/base level fall results in fluvial incision phase(s) during lowstand often followed by amalgamated channel infill during subsequent transgressions (Suter and Berryhill, 1985; Miall, 1993; Shanley and McCabe, 1993; Ashley and Sheridan, 1994).

In the Siberian realm of the Arctic investigations of sea level change during the Late glacial and Holocene period have been sparse, except for regional sea level reconstructions for the Laptev Sea by Bauch et al. (2001) and Stein and Fahl (2004) who describe the sedimentary evolution of the shelf with a diachronous reduction in accumulation rates from north to south related to the Holocene transgression at the Eurasian continental margin. Kleiber and Niessen (1999) identified major riverine extensions on the shelf, while Kleiber et al. (2000) reconstructed the LGM glaciation history. On the Kara Sea Shelf, Stein et al. (2003b, 2004) reconstructed sedimentary records and interpreted their formation as a consequence of the time transgressive southward shift of the depocentre during the post-LGM sea level rise. The studies were based on dated sediment cores and no acoustic data were included.

Using sequence stratigraphic methods (Mitchum et al., 1977; Vail et al., 1977) Dittmers et al. (2003) distinguished three Subunits in the Holocene succession of the Yenisei area. At its base Unit I fills the underlying topography and shows signs of a fluvial environment grading into a deeper water draping facies at the recent sea-floor. They form a classical deepening upward sequence, reflecting a change in depositional environment in response to post-glacial sea level rise. The chronostratigraphic frame has been previously established for the restricted area of the Ob and Yenisei estuaries south of 74° N (Dittmers et al., 2003) and in the present paper we extend this onto the shelf, using the original results of Stein et al. (2002) and Dittmers et al. (2003) and incorporating more than 8,000 km of echosounding surveys of the 2001 (Stein and Stepanets, 2002) and 2003`s PARASOUND survey (Dittmers and Schoster, 2004) as well as the results for the physical properties of 14 sediment cores from the shelf, 12 of which are AMS ^{14}C-dated.

This present investigation is mainly based upon the interpretation of widespread acoustic profiles with dense spatial coverage of the Kara Sea Shelf. In particular the focus of the seismic analysis is on:

(1) mapping the spatial distribution of acoustic surface facies provinces,

(2) identification and characterisation of key surfaces responsible for reflector ter-

minations of depositional packages and

(3) determination of the internal configuration and geometry of sedimentary units within the acoustic surface facies provinces.

In addition we investigated several AMS ^{14}C-dated sediment cores to establish a local sea level curve that can be compared with predicted sea level changes based on modelling of isostatic crustal rebound of Lambeck et al. (2001, 2002) (Fig. 2), included AMS ^{14}C-dated cores BP99-04 and BP00-38 and the exact depth of the terrestrial-marine transition into recent models, also coming out with no major isostatic movements.

Figure 2. Sea level calculations after Lambeck`s et al. (2002) earth model for the Ob (BP00-38) and Yenisei (BP99-04) in comparison to Fairbanks (1989) sea level curve. note that for the Ob a stronger rebound is estimated in comparison with the Yenisei
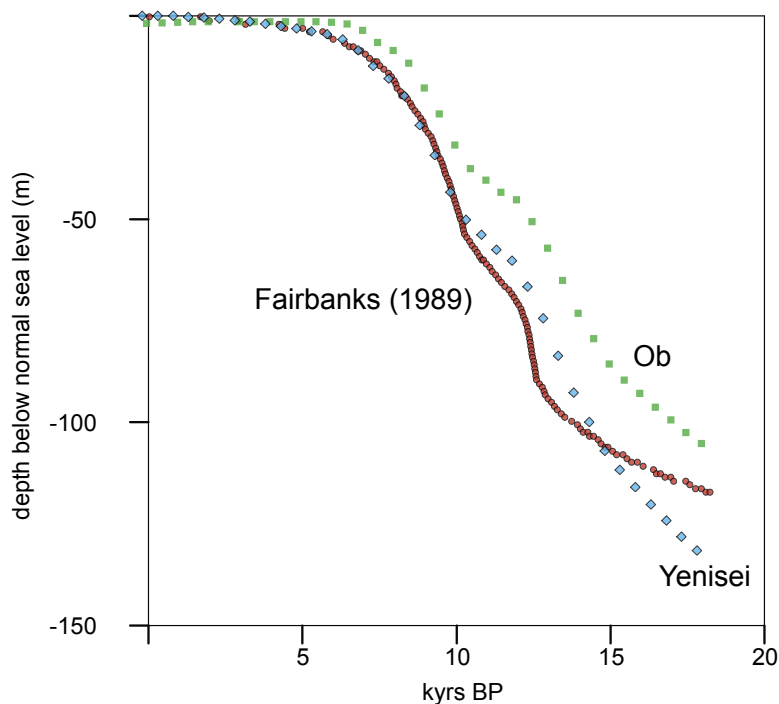
Regional setting

The Kara Sea is a typical marginal Arctic shelf sea which is ice-covered during nearly nine months of the year (Blanchet et al., 1995; Pfirman et al., 1995). It is characterised by high rates of fluvial run-off, i.e. 404 and 620 km^3/y from the Ob and Yenisei rivers, and suspended matter discharge of 15.5 x 10^6 t/y and 4.8 x 10^6 t/y, respectively (measured after dam construction in the upper reaches Telang et al., 1991; Holmes et al., 2002; Rachold et al., 2003). The recent relief of the sea-floor is shaped by fluvial activity intermingling with the complex Weichselian glaciation history (e.g. Svendsen et al., 2004). A more detailed description of the physical environment is given in Dittmers et al. (2003, Chapter 3.2) and Stein et al. (2003b, 2004).

Glaciation history

The recently published outcomes of the QUEEN project (Quaternary environments of the Eurasian North (e.g. Mangerud et al., 2004; Svendsen et al., 2004) exclude a massive glaciation of the Kara Sea Shelf as proposed by Grosswald and Hughes(1999)

and limit ice thickness to 300 m for the working area.

The eastern boundary of the LGM Barents-Kara Sea ice sheet extent is now well studied with the exception of some small uncertainties in the North-East of the Kara Sea Shelf (Fig. 1). However, these areas are of major importance, because the sea-floor of the western side of the LGM ice sheet limit is characterised by an uneven glacially imprinted morphology (Dittmers et al., subm., Chapter 3.5; Stein et al., 2002), whereas the inner Kara Sea to the east and south of the mapped ice extent is charac-terised by relatively flat relief and shallow water depth, associated with several fluvial truncations (Dittmers et al., subm., Chapter 3.5).

The interaction of different forcing factors on the Kara Sea Shelf resulted in a fairly complicated sedimentation history. These factors are a) variable sediment supply due to natural variations in both fluvial discharge and coastal erosion, b) the heterogeneous relief of the Kara Sea, c) a non-uniform sea level rise and d) the direct neighbourhood of the LGM ice sheet.

Sea level history

For the inner Kara Sea there is no field evidence of a late or post-glacial coast-line emergence (Mangerud et al., 2004). Studies of raised beaches concentrating on Novaya Zemlya (Forman et al., 1995, 2004; Zeeberg et al., 2001) reported only moder-ate uplift of maximally 20 m during the Holocene. This implies that isostatic rebound of the Kara Sea coast is less than eustatic rise. Thus, the maximum thickness of any ice on the shelf and adjacent coastal plain is unlikely to have exceeded about 400 m (Lam-beck et al., 1996; Svendsen et al., 2004). We included AMS ^{14}C-dated cores BP99-04 (73°24.9 N; 79°40.4 E) and BP00-38 (73°11.8 N; 73°14.3 E) and the exact depth of the terrestrial-marine transition based on pollen studies of Kraus et al. (2003) into elastic earth rebound models, defined in Lambeck et al. (2002) (Fig. 2). Sea level predictions for the two Kara Sea sites indicate a maximum rebound of 20 m before the Holocene and allow us to neglect major isostatic effects.

2. Methods

2.1 Acoustic Data Collection/Acquisition

This multidisciplinary study was carried out in the southern and inner Kara Sea (Fig. 3a) within the frame of the German-Russian research project SIRRO ("Siberian River Run-off", Stein et al., 2003a and references therein). Data were collected dur-ing the expeditions of the RV "Akademik Boris Petrov" in 1999, 2000, 2001 and 2003 (Fig. 3a) (Stein and Stepanets, 2000, 2001, 2002; Dittmers and Schoster, 2004). Dif-

ferent echosounding systems were used. During the 2000 and 2001 echosounding surveys we employed the hull-mounted ELAC echograph of the ship (ELAC echograph LAZ 72, Honeywell-Nautik, Kiel, Germany) operating at a frequency of 12 kHz. Since 2003 RV "Akademik Boris Petrov" is equipped with a parametric ATLAS PARASOUND system (Dittmers and Schoster, 2004) and profiles presented in this study are examples from the Parasound survey of 2003 (Schoster and Levitan, 2004). This narrow-beam system utilizes the parametric effect for signal generation which is a non-linear interaction of sinusoidal waves or wavelets (Westervelt, 1963). Grant and Schreiber (1990), Rostek et al. (1991) and Spieß (1993) describe the predecessor models and the functioning in more detail. For the data presented here, a 3.5 kHz frequency was chosen as source signal (Dittmers and Schoster, 2004).

Surveys were archived as paper scrolls printed online at the time of acquisition and in digital format on CD-ROM (Niessen and Dittmers, 2002; Dittmers and Schoster, 2004). PARASOUND profiles were reproduced using SENT Version 1.0. Details are given by Dittmers and Schoster (2004). Time-to-depth conversion was done using a standard sound velocity of 1500 m/s for water (Hamilton, 1972).

2.2 Groundtruthing by gravity coring

The Gravity Corer (core diameter: 12 cm) used for our studies has a penetration weight of 1.5 t and is used with up to 8 m long core barrels. Physical properties of sediment cores were logged using a Geotek Multi Sensor Core Logger (MSCL 25). P-wave travel time, attenuated gamma counts, magnetic susceptibility and core temperature were measured. Using Geotek software the raw data were processed for determination of wet bulk density, porosity and p-wave velocity. For technical details of the Multi Sensor Core Logger set-up see Dittmers and Niessen (2002). Magnetic susceptibility is defined as the dimensionless proportionality factor of an applied magnetic field in relation to the magnetisation in the sample and has been measured with a BARTINGTON MS2C coil sensor. Calibration was carried out according to the method of Weber et al. (1997) and Best and Gunn (1999). After splitting the cores into work and archive halves, X-ray radiographs of the intermediate 5-10 mm slabs were conducted to reveal sedimentary structures (Grobe, 1987). The chronostratigraphic framework of sediment cores is based on several AMS ^{14}C radiocarbon dates (Stein et al., 2001, 2002, 2003b; Table 1). The base of Unit I is determined on the basis of linear sedimentation rates of dated cores (Fig. 3b). The sedimentary record and physical property data were used to correlate sediment cores as well as for sequence stratigraphic interpretation. The magnetic susceptibility data reflecting the changing source signal proved to be especially helpful in this interpretation (Dittmers et al., 2003; Stein et al., 2004).
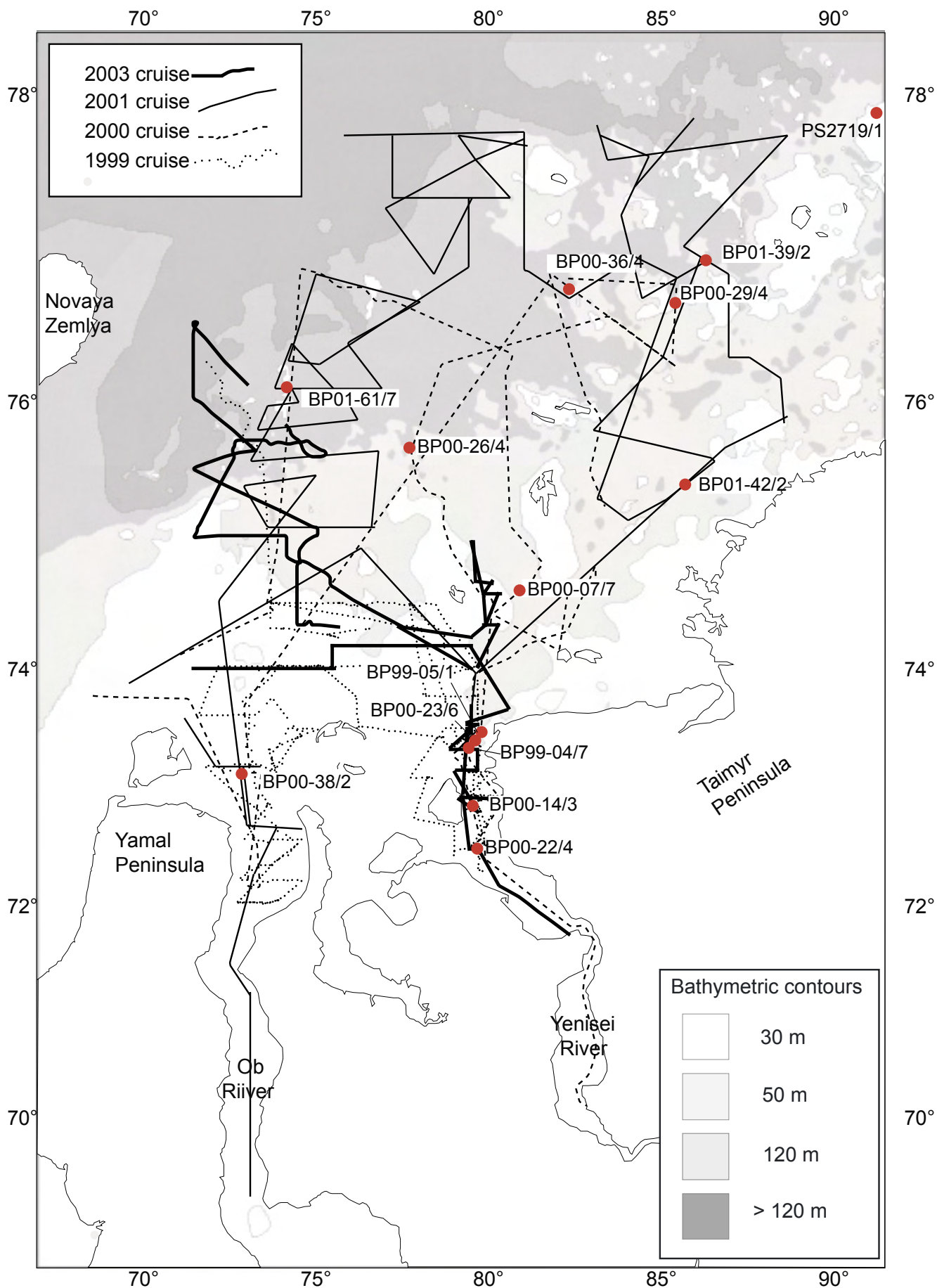
Figure 3a. Overview of cruises of RV "Akademik Boris Petrov" during several years, and position of sediment cores under investigation.

2.3 Data analysis

Sedimentary sequences have been analysed with respect to the geometry of their internal reflection patterns, their external morphology and their physiographic positions in terms of system tracts according to Posamentier and Vail (1988) and Vail et al. (1991). GPS positioning provided accurate location and orientation of the profiles and sediment stations/cores. The GIS programme Global Mapper (version 5.10) was used for visualisation of our elevation model based on our soundings in combination with nautical charts (Dittmers, 2001; www.pangaea.de) and for determination of the spatial extent of the different identified acoustic facies.

Sediment mass calculations were also based on those area measurements in combination with GRAPE (Gamma Ray Attenuated Porosity Evaluation) data of Dittmers

Table 1. Core location and water depth of AMS ^{14}C dated sediment cores and depth of sedimentary Unit see Figure 3b for linear sedimentation rates

Station	Lat (° N)	Long (° E)	Water depth (m)	Recovery (m)	Unit I (m) base	HST (m) base	TST (m) base	date of base of Unit I	AMS date source
BP99-04/7	73° 24.9	79° 40.4	32.0	7.95		5.40		9,500 [2]	Stein et al. 2002
BP99-05/1	73° 30.1	80° 00.7	38.0	4.1	1.10	0.65	1.20	av. 10,000	Stein et al. 2002
BP00-07/7	74°39.5	81°08.5	38.0	7.23		5.60			Stein et al. 2002
BP00-14/3	72°55.8	79°47.4	19.0	2.43	1.80	1.60	1.95	>6,000 [1]	Stein et al. 2002
BP00-22/4	72°33.9	79°54.9	11.0	4.36	2.40	1.90	2.50	no data	
BP00-23/6	73°28.5	79°51.3	33.0	4.17	2.75	2.40	3.30	no data	
BP00-26/4	75°42.5	77°57.6	68.0	3.96	2.10	1.80	3.30	8,545 [1]	Stein et al. 2002
BP00-29/4	76°56.2	85°45.8	68.0	3.29	2.50	2.30	2.80	11,400 [1]	Stein et al. 2002
BP00-36/4	76°57.7	81°57.8	66.0	5.63		2.50			Stein et al. 2002
BP00-38/2	73°11.8	73°14.3	20.0	6.52		6.00		10,000 [2]	Stein et al. 2002
BP01-39/2	77°06.7	86°44.9	106.0	5.38		4.30			Stein et al. 2002
BP01-42/2	75°26.2	86°03.7	49.0	5.72		4.40			Stein et al. 2003
BP01-61/7	76°12.9	75°53.2	111.0	5.66		3.20			Stein et al. 2003
PS2719/1	77°360	97°32.0	135.0	5.18	3.42	2.21	4.30	9,640 [1]	Stein et al. 2001

[1] inferred from linear sedimentation rates; Fig. 3c

[2] inferred by Pollan sudies of Kraus et al., 2003)

et al. (2003) obtained by whole-core logging during the BP 2000 and 2001 expeditions (Dittmers and Niessen, 2002; Dittmers et al., 2003). Thickness of the hanging wall sediments of a prominent pre-Holocene unconformity (sub sea-floor thickness) was determined on sub-bottom profiles (see below). This average thickness value in con-
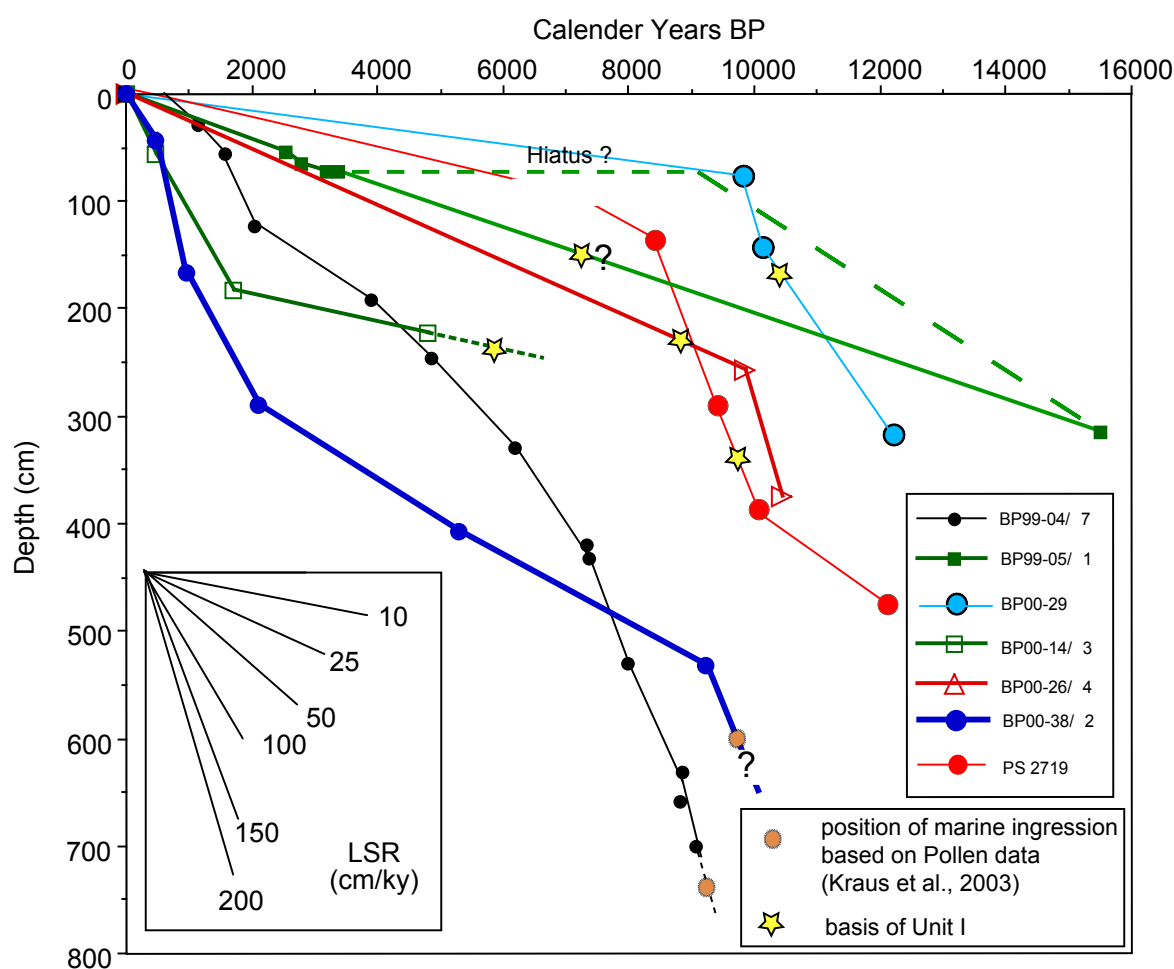
Figure 3b. Linear sedimentation rates of AMS ^{14}C-dated sediment cores (Stein et al., 2001, 2003b supplemented); base of Unit I is shown based on sediment core description (Stein and Stepanets 2000, 2002) and pollen investigations of (Kraus et al., 2003) in the lower parts without confined dates the position has been inferred.

junction with the areal extent/coverage of each facies type, provides an estimate of the sediment volume of each differentiated facies area. In order to calculate the sediment mass (grain density) from the estimated volumes we use the average porosity of 66%, determined by Dittmers et al. (2003), based on GRAPE estimates from a total of 95 sediment cores (Dittmers and Niessen, 2002; Dittmers et al., 2003).

3. Results and Interpretation

3.1 Recent sedimentary acoustic facies types (surface) and their spatial distribution

Based on the interpretation of acoustic profiles we divided the working area into three distinct (surface) provinces (Facies A to C) characterised by: (1) sediment penetration above the pre-Holocene unconformity, (2) sea-bottom roughness and (3) geometry of seismostratigraphic units. These are:

Facies province A: a high mud accumulation, fluvial to marine succession with laterally consistent reflectors. It is restricted to the modern estuaries up to 74° N.

Facies province B: covers the shallow and flat central shelf to water depths up to 120 m. Sediment thickness is variable and highest in depressions. Outside the depressions sediment penetration is minor. It is restricted to the shelf.

Facies province C: This shows the highest relief energy associated with little sediment accumulation and high sediment thickness with draping reflectors in channel-levees complexes. It occurs north and westward of Facies B and generally below the 120 m isobath.

Facies province A

The recent estuaries of the Ob and Yenisei rivers (Fig. 4a) are characterised by shallow water depths between 20 m and 30 m. Further to the North the facies rapidly grade into Facies province B with a pronounced decrease in sediment thickness above the basal (unconformity) reflector in the central estuary. Sediment penetration above the unconformity is high, up to 20 m in places, indicating relative rapid sediment accumulation. Sea-floor and depositional packages have smooth surfaces and a prolonged continuously stratified, layered internal assembly with draping character in the upper part of the succession. Internally, there are several discontinuities accomplished as downlapping surfaces. Acoustic profiles strikingly display the threefold division of Holocene sediments above the unconformity (Dittmers et al., 2003, Chapter 3.3). Their vertical succession represents a deepening upward sequence with fluvial character at its base (Fig. 4b).

Facies province B

Facies B covers the inner Kara Sea Shelf areas extending to the 120 m depth isobath. It is characterised by impermanent Holocene sediment penetration above the regional unconformity, due to variable accumulation of sediment. Incised fluvial channels, with different sedimentary infill-stages (Fig. 4c) are characteristic features (Dittmers et al., in press, Chapter 3.5). Underneath the prominent basal reflector, probably

due to energy attenuation by reflection, there is little penetration and only some weak local stratification, interpreted as bedrock or basal tills (see below), can be seen. The relief of the Facies B surface is smooth and almost plain, characterised by a low slope gradient of 1:6,000 on average. Several channels have been incised into the shelf and were subsequently filled such that sediment thickness increases drastically measuring up to 20 m in the channel axis (Fig. 4c). In places, well-stratified older strata show deformation and intense folding (Figs 4d, 5). The dislocations could be related to glaciotectonic ground moraine deformation during mid-Weichselian ice sheet advance (Svendsen et al., 2003) when an ice sheet advanced from the Kara Sea onto the mainland, forming a prominent chain of end-mo-
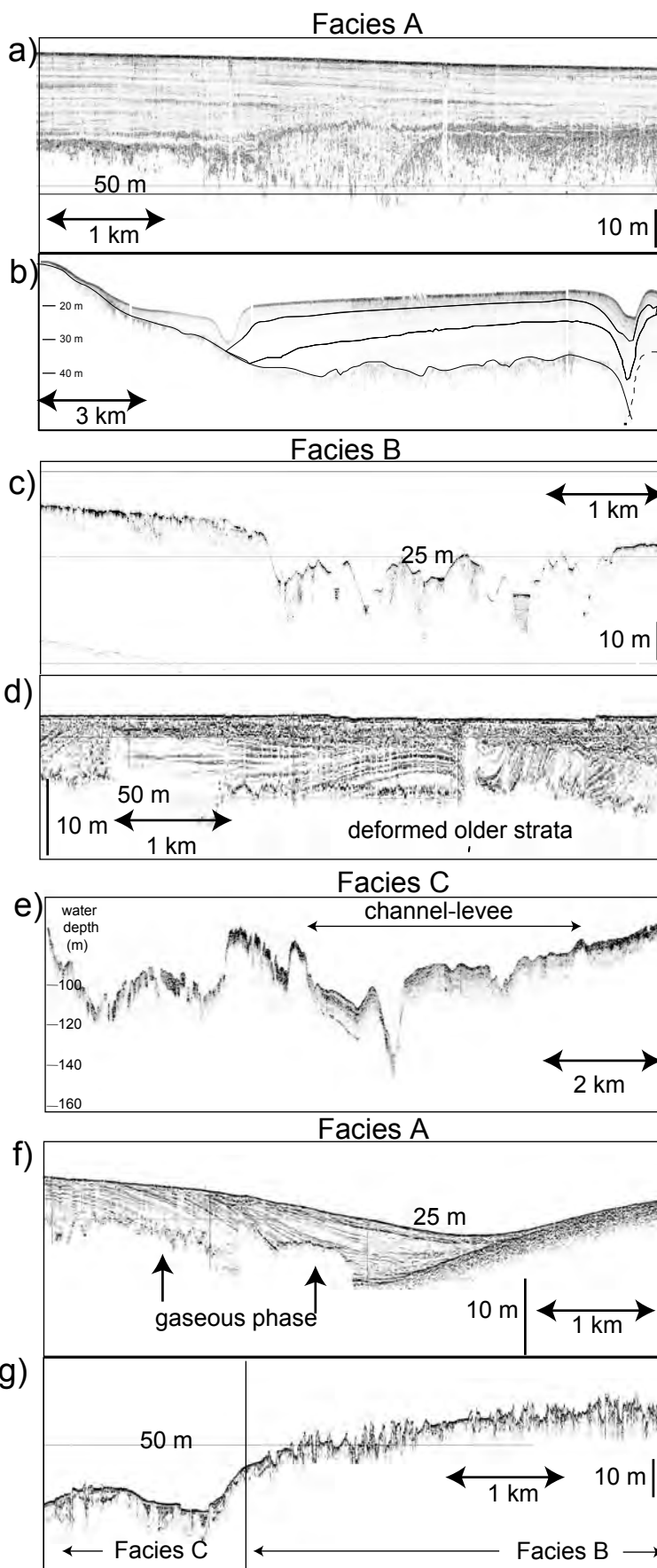
Figure 4. Major Facies types and characterising features.
a) Facies A; Yenisei Estuary
b) cross section of Yenisei Estuary
c) Facies B; shelf with incised channels with higher sediment accumulation in channel axis
d) Glacial deformation of sub bottom Facies B sediments.
e) Facies C displaying glacial morphology neighbouring channel-levee system
f) Gas blanketing in Facies A; gaseous phase "intrudes" into well-stratified sediments, the front is characterised by high acoustic attenuation
g) Intensive ice gouging, here depicted in Facies B
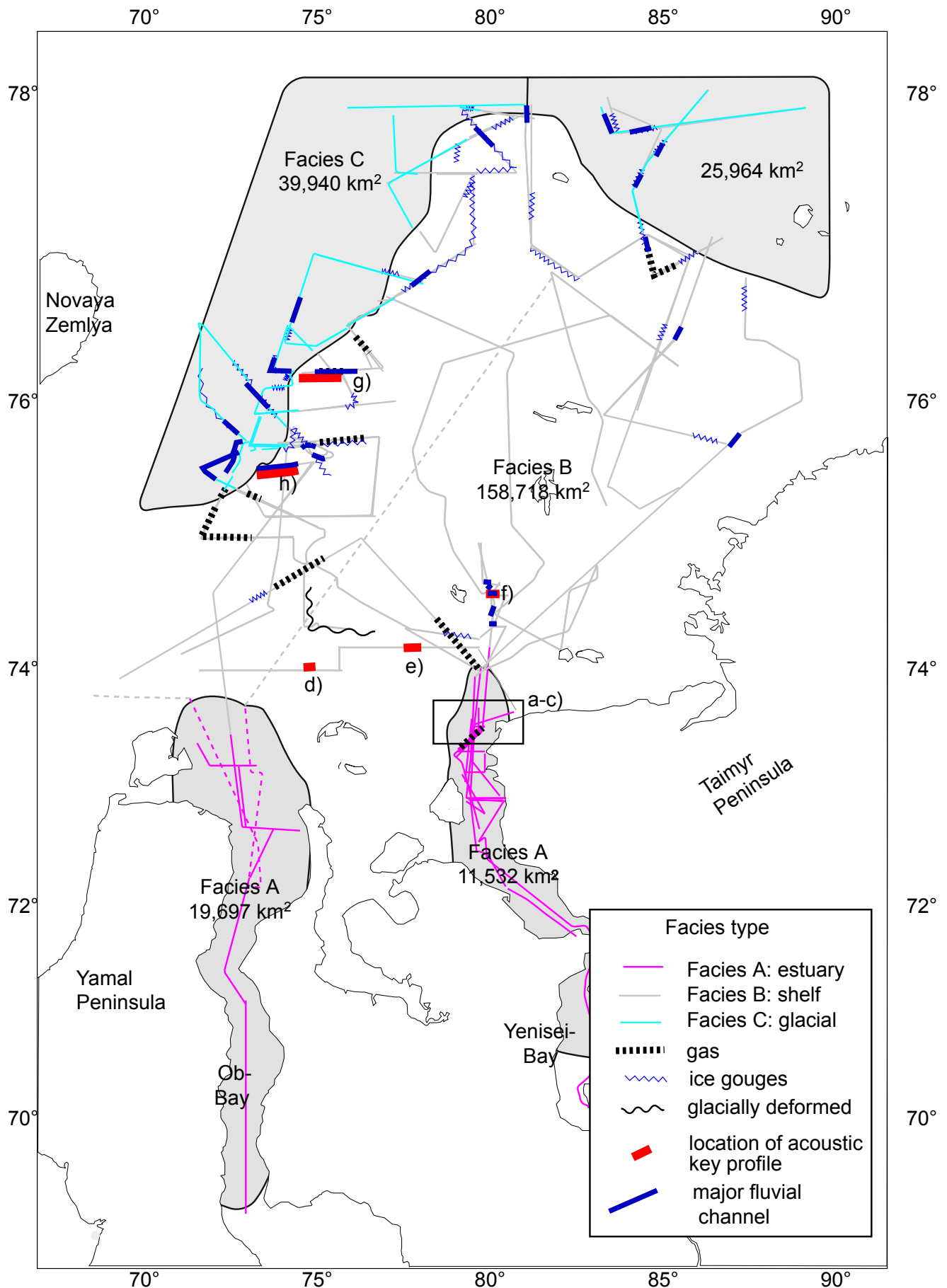
Figure 5. Spatial distribution of Facies types differentiated in Figure 4; and division into major Facies areas. Area measurements were conducted with the GIS tool Global Mapper: a-g refer to sections in Figure 8.

raines known as the "Markhida line" (Mangerud et al., 1999).

Facies province C

Facies C covers the area deeper than the 120 m depth contour and is characterised by an irregular morphology (Fig. 4e). There is a distinct difference in the facies between the western region with high sediment thickness in the levee/overbank area, and the north-eastern region (Fig. 5) which is acoustically well-stratified along profiles and which is also of greater lateral extent (Niessen and Dittmers, 2002; Stein et al., 2002). The overall slope gradient is steeper than 1:1,000. Associated with channels there is a well-stratified, layered levee overbank facies along the channel margins. These levees are characterised by their typical external wedge shape and drape-like character, with internal sub-parallel reflectors, thinning away from the channel axis (Fig. 4f). They are often fringed by moraines. Laterally the channels grade into overbank facies deposits, which in turn are often bordered by morainic ridges accompanied by a rapid decrease in thickness of the sediment cover (Fig. 4e). They appear in water depths between 79 and 120 m (Dittmers et al., in press, Chapter 3.5). Besides glaciated, hummocky (ground) morainic terrain, channel, levee complexes are the most prominent sedimentary features in Facies C.

Channel-levee complexes often overlie formally glaciated terrain, of probably mid Weichselian age, but their dating proves difficult. Their genesis is discussed in Dittmers et al. (subm., Chapter 3.5). in more detail.

Features commonly observed in all facies provinces

A few acoustic features are observed in all facies described above. These include acoustic voids ice gouges and fluvial channels. A widespread phenomenon is the occurrence of an acoustic transparent zone in the lower part of acoustic images. Apparently, the acoustic voids, are post-sedimentary in origin cutting across layering and bedding or other structures, with no penetration below (Fig. 4f). The strong backscatter at this front implies a major difference in acoustic impedance and suggests a transition to material with major difference in density. We interpret this feature as gas-saturated sediment. In the sediment cores these acoustic voids coincide with an occurrence of meta-stable mineral Ikaite ($CaCO_3 \cdot H_2O$) which is formed by meteoric methane (Kodina et al., 2003). This effect is encountered in all facies types at different grades (Fig. 5).

Approaching the shelf/slope break and greater water depths, intense but locally restricted ice-gouging is visible possibly originating from drifting icebergs and/or press ice ridges that plough through the sediment (Fig. 4g) (Reimnitz et al., 1972, 1978; Barnes and Lien, 1987; Løset et al., 1999).

Unit II cross lamiation including erosive surfaces
BP99-05 185 -210 cm

Unit Ib non-bioturbated lamination
BP99-04 670-695 cm

Unit Ia partly laminated/ bioturbated
BP99-04 245-280 cm

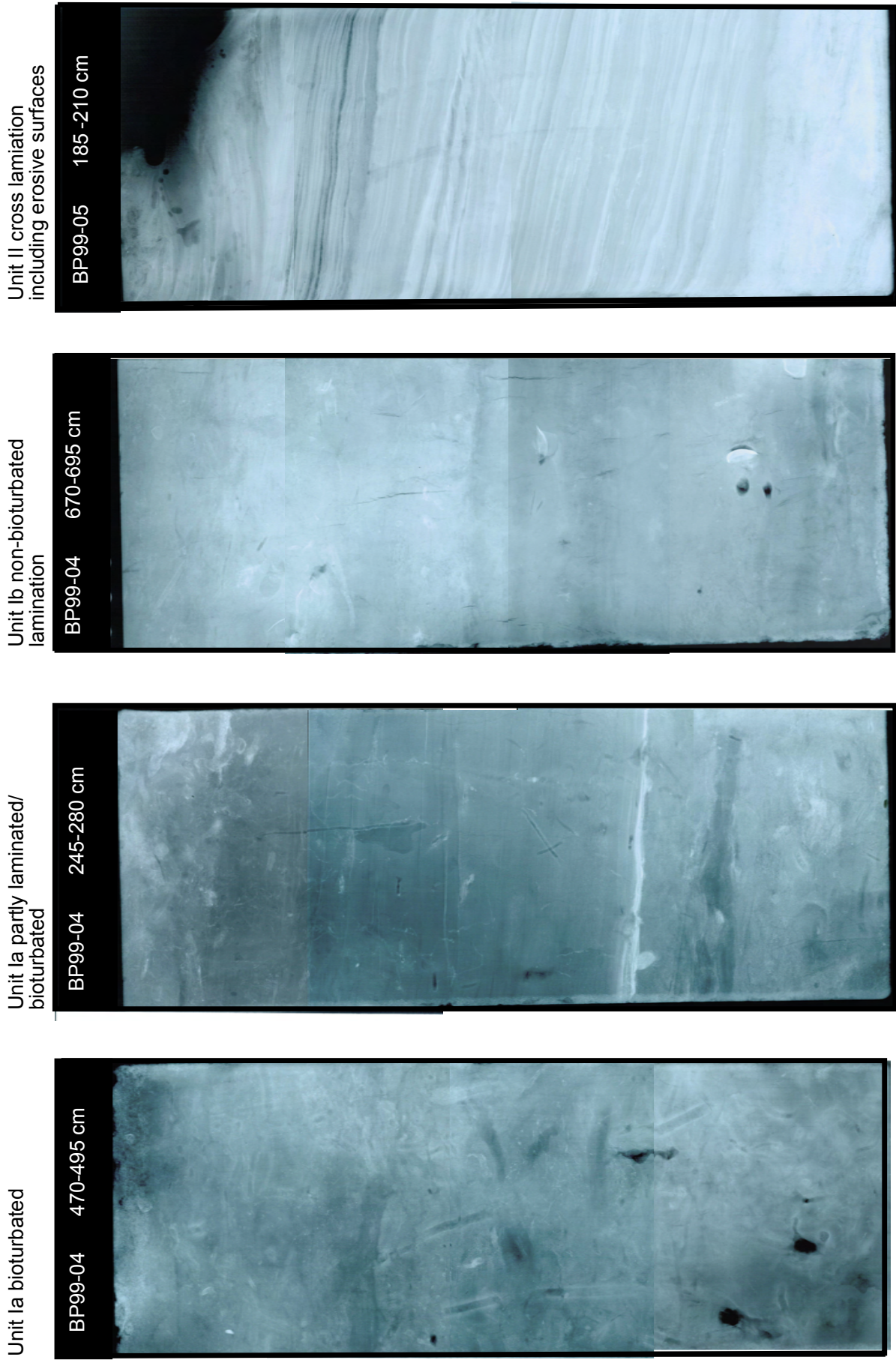Unit Ia bioturbated
BP99-04 470-495 cm

Figure 6. Radiographs of main sedimentary units; each slab measures 25 cm in length; Sediment cores of ther Yensiei estuary; for location see Figure 3.

Outstanding features are the channels in all facies regimes; Dittmers et al. (subm., Chapter 3.5) examine these features and their evolution/development in more detail. Within Facies A, the channels are buried at the base of the sequence (Figs 4f and 4b), or on top of the succession, indicative of recent current activity (Dittmers et al., 2003). In Facies B fluvial channels are abundant and show different levels of infill. Facies C is characterised by channel-levee complexes, indicative for underwater formation, in contrast to the subaerial formation of the channels in Facies A and B.

3.2 Lithofacies

Two major siliciclastic lithofacies, Units I and II have been previously identified in the cores, expressed by a distinct change in sediment composition (Stein et al., 2002, 2003b; Dittmers et al., 2003) as dividing the sediments that accumulated before and after the Holocene transgression. This boundary between Unit I and II correlates with the strong reflector seen in the acoustic profiles.

In Unit I, the amounts of clay, silt and sand are in the range of 50-80%, 25-50%, and < 10%, respectively (Steinke, 2002; Stein et al. 2004). In some cores at the base of Unit I a subunit is distinguished that is visually characterised by a distinct lamination that has not been disrupted by bioturbation (Fig. 6). In Unit II, the sand fraction values may reach up to 75% of the grain size spectrum. Unit I is mostly unfossiliferous and bioturbation is very rare (Stein and Stepanets, 2000). It has only been cored at stations BP99-05, BP00-29, BP00-26, BP00-23, BP00-22 and in PS-2719 (Fig. 3) (Kleiber and Niessen, 2000; Stein et al., 2001). In this Unit cross-stratification is visible and individual beds are erosively capped by overlying laminated strata (Fig. 6).

3.3 Lithostratigraphy and age control

Cores penetrating Unit I are of Holocene age (Fig. 7a), except for cores BP01-39 and BP00-26. In these latter cores there is no visible distinct facies shift during sea level rise, probably related to the relatively great water depths of 109 and 66 m, respectively. However, the susceptibility signal (Fig. 7b) shows higher values at the base of both cores, indicating a transition to Unit II. The transition from Unit I and Unit II is marked by a distinct change in magnetic susceptibility with markedly higher values in Unit II (Fig. 7b). The boundary has been AMS ^{14}C -dated to approximately 10 ka BP (Dittmers et al., 2003; Stein et al., 2002). Unit II could be dated in cores PS-2719 (11.2 ka BP, Kleiber and Niessen, 2000, Stein et al., 2001), BP00-29 (12.2 ka BP, Stein et al, 2004) and BP00-26 (10.0 ka BP, Stein et al., 2004) with confidence and in core BP99-05 (15.5 ka BP) was determined from a piece of well-preserved driftwood (Dittmers et al., 2003; Stein et al., 2003b).
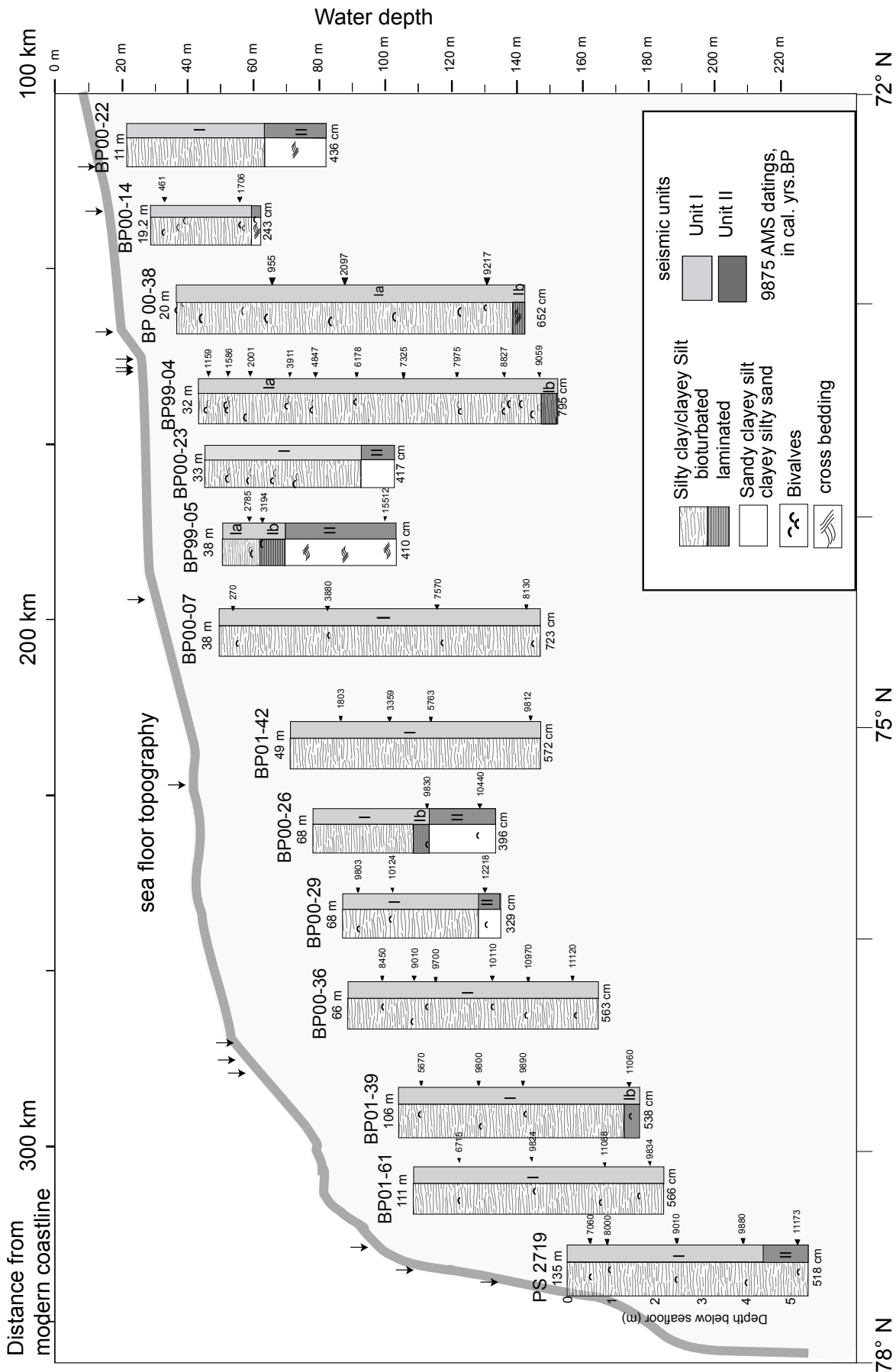
Figure 7a. Sediment key cores aligned according to water depth and distance from the recent coastline, lithological logs indicated. AMS ^{14}C dates indicated by arrows; major facies divisions according to Stein et al. (2004), division into acoustic units according to Dittmers et al. (2003)
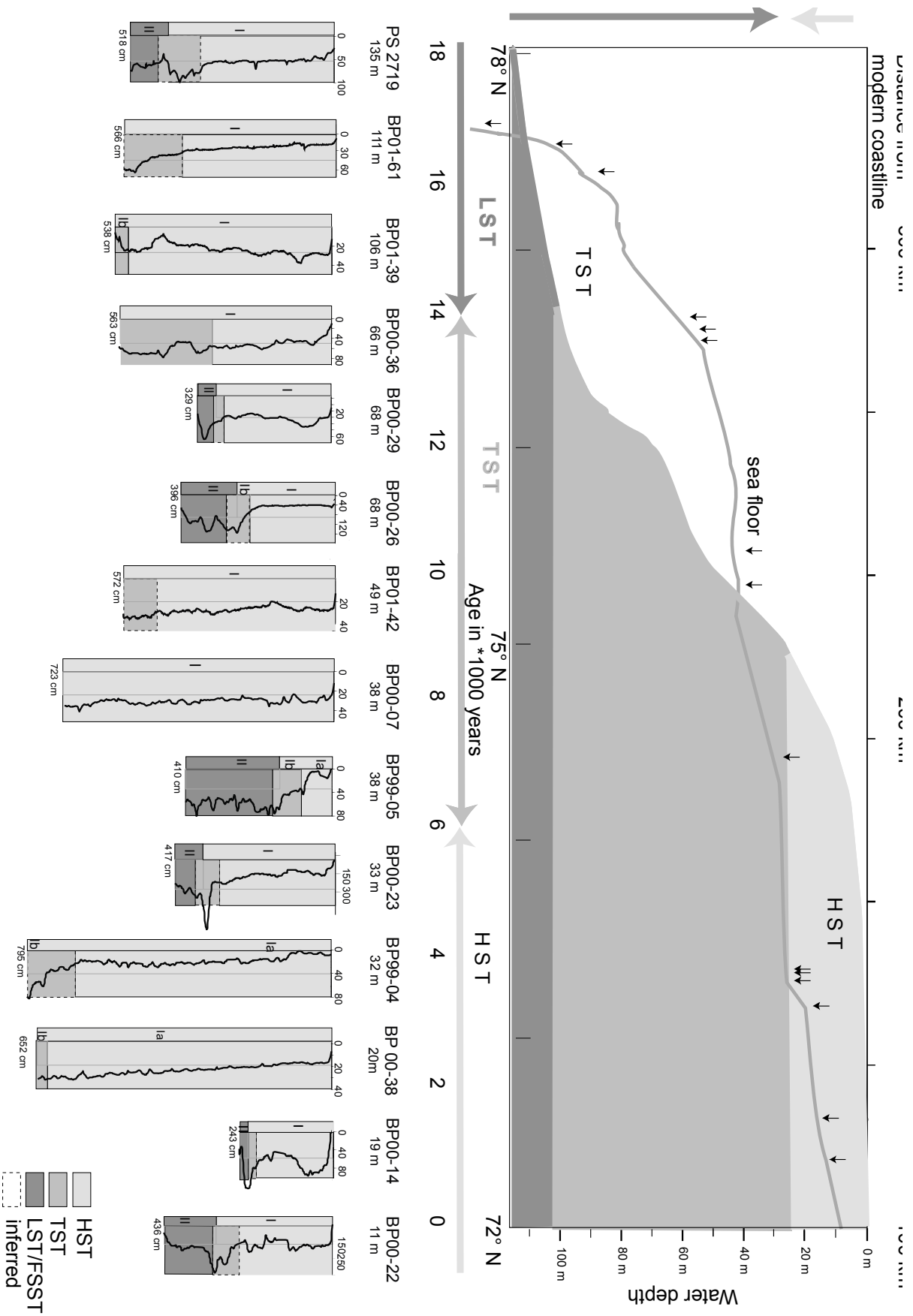
Figure 7b. The sequence of cores shown in Figure 5a); magnetic susceptibility curves shown in 10^{-5} SI sensor units, on the basis of which subdivision into sequence stratigraphic units has been conducted. Depositional units shown in dependence of water depth and age.

4. Discussion

Seismic Sequence Stratigraphy

Sea level changes can be used for regional correlation of stratigraphic units (Vail et al., 1977; Posamentier and Vail, 1988; Posamentier et al., 1988) and act as a good link between geomorphology, sedimentology and stratigraphy (Schumm, 1993). A prominent feature visible in profiles across the region is a strong irregular uniform reflector, separating two major acoustic units (Unit I and Unit II) (Figs 4) (Stein et al., 2002, Dittmers et al., 2003). Dittmers et al. (2003) interpreted this feature as an erosional surface representing an unconformity similar to the "upper regional unconformity" (URU) described by Solheim and Kristoffersen (1984) for the Barents Sea. A similar feature was reported by Polyak et al. (2000) from the Pechora and western Kara Sea and by Kleiber et al. (2001) for the Laptev Sea.

After Mitchum and Van Wagoner (1991) seismic sequences are defined as genetically related successions of strata without internal unconformities, arranged in system tracts and bounded by unconformities and thus representing depositional sequences/environments. Ideally a sequence consists of four system tracts: low stand system tract (LST); transgressive system tract (TST); highstand system tract (HST), succeeding a regressive system tract (RST) or forced RST (FRST), if it is related to a global sea level fall (Coe et al., 2003). The major difference between the RST and LST units is that the LST sediments belong to the new sequence and lie above the sequence boundary. These latter comprise subaerially exposed areas during the onset of sea level rise whereas the RST is associated with falling sea level which, in our study area, is the time interval before the LGM.

The FRST is represented by the regional unconformity on the shelf and its deposits can only be found in deeper areas that have not been subaerially exposed. Polyak et al. (2002) report a high sediment accumulation beyond the 120 m depth contour for the Kara Sea that could represent a lowstand wedge in the sense of Wetzel and Allia (2000).

Figures 8 a-c give examples of the transition of the estuarine Facies A towards Facies B. The TST is characterised by moderate sea level rise manifested in a phase of non deposition/sediment by-pass (Vail 1987; Van Wagoner et al., 1987). The subsequent HST is equally well developed, with constant sediment thickness that indicates a relatively deeper water environment at time of deposition.

Facies B (Fig. 8d-f) is best preserved in depressions, created by channels cut into the Kara Sea Shelf during sea level lowstand, in the older sediments (Chapter 3.5). Infilling started earliest with the LST fluvial and possibly estuarine facies as in the lower

reaches of Facies A. In Figure 8d an example of a filled channel is shown with parallel reflectors and traces for lateral channel migration in the RST (dark grey). In Figure 8e the same evolution is visible for the upper part of the succession, but in the lower part, making up the LST strata, beds are much more inclined as compared to Figure 8d. This can be explained by relatively strong currents. We interpret those formations as depositional current controlled cross bedding. Figure 8e shows a filled channel with evidence for weak current activity during LST sedimentation since there has been no levelling of the old relief. The TST and HST grade into draping deposits almost leaving no relief differences to the surrounding sea-floor indicative of deeper water. Figure 8f shows an example of an unfilled channel with lateral accretion, indicative of paleo-fluvial activity that formed a meander bend with the undercut slope side to the east and typically inclined point bar sedimentation to the west. Only a thin cover of HST draping
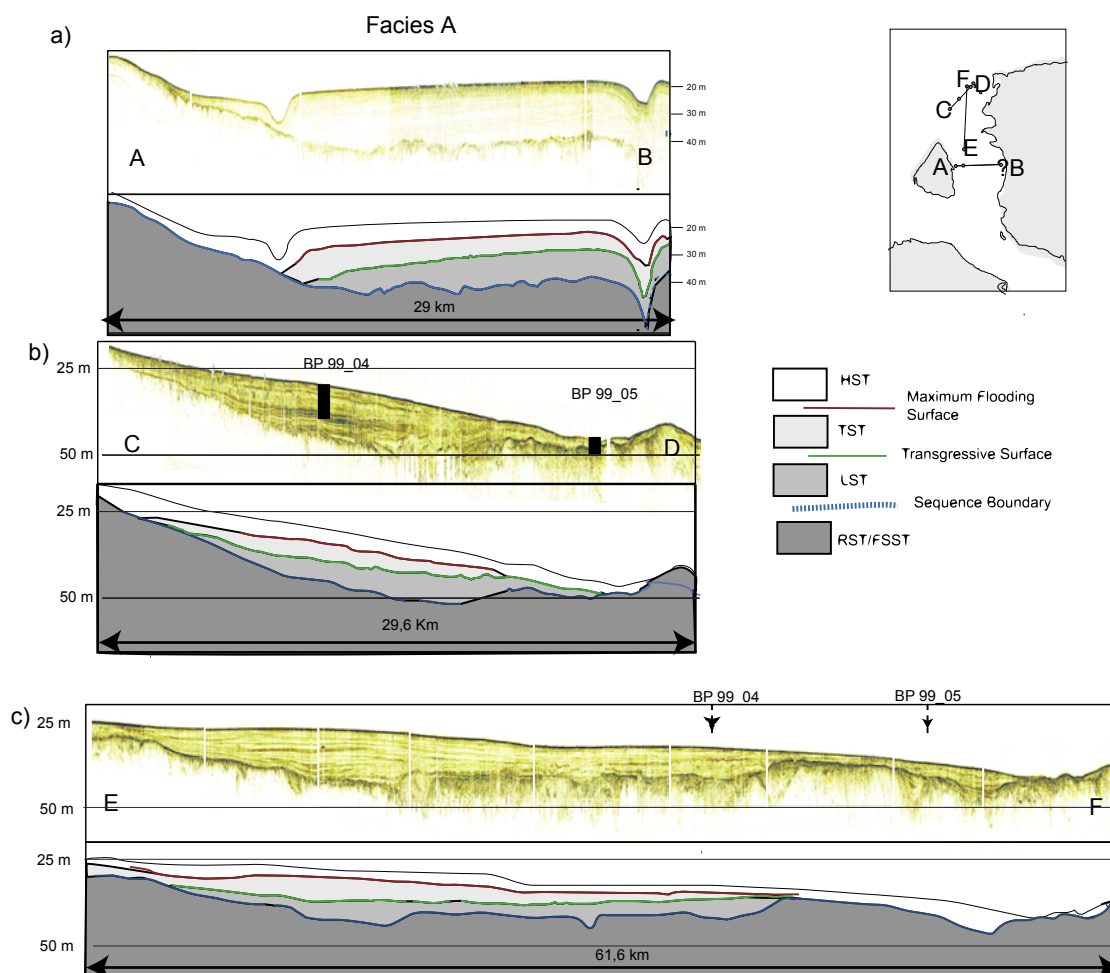

Figure 8. Interpreted sections of differentiated key Facies A and their sequences stratigraphically interpretation showing depositional units; system tracts have been developed in the response to changing sea level

sediments overlies the channel, indicating relative sediment starvation. All successions display deepening upward conditions.

A channel-levee complex typical for Facies C is shown in Figure 8g. Boundaries can only be inferred in Unit I and between Unit I and Unit II, because as discussed above, it is possible that they contain FRST sediments and there is no unconformity visible. Furthermore the exact dating remains unclear, because they overlie formerly glaciated terrain of probably early to mid Weichselian age and on the other hand they are often bordered by LGM moraines, which could imply co-existence of the channel-levees and the ice sheet. However, Dittmers et al. (subm.) in Chapter 3.5 deal with the fluvial evolution of the Kara Sea and their underwater prolongations (channel-levee complexes) in more detail.

Ground truthing of acoustic units by sediment core data

In the inner Kara Sea it is difficult to dirrectly link recovered gravity cores to seismostratigraphic key horizons because the majority of the cores consists of homogeneous marine to estuarine muds with only little variation in the grain size composition and uncharacteristic changes in sediment colour. Furthermore the limited penetration depth of the gravity corer does not always cover the complete sedimentary interval of interest, with the additional problem that areas of non-soft sediment deposition cannot be cored. AMS ^{14}C datable material, especially in formerly glaciated terrain is very rare.

With respect to this sedimentary homogeneity the investigation of physical properties, in particular the analysis of magnetic susceptibility, sheds new light on the sedimentary record, including important information about the sediment source. As outlined by several workers, magnetic susceptibility is a useful tool for the determination of terrestrial influx component, especially from the Yenisei branch (Dittmers et al., 2003; Stein et al., 2002, 2003b). High concentrations of ferromagnetic materials, especially magnetite, lead to high values of low-field magnetic susceptibility (Robinson, 1993). Magnetic susceptibility is commonly used as an indicator for the magnetic mineralogical composition of sediments and prooved to be valuable for lateral core correlation (e.g. Kleiber and Niessen, 2000). High values of magnetic susceptibility characterise the Kara Sea, because magnetite minerals are supplied via the Yenisei River from the basaltic Putoran Mountains (Stein et al., 2002, 2003b, 2004; Dittmers et al., 2003).

The main stages of the flooding and the sequence stratigraphic division of sedimentary units are characterised as follows:

Unit II is characterised by the highest values of magnetic susceptibility, often co-inciding with an increased sand content. These sediments belong to the FRST and LST. They are characterised by high-energy transport mechanisms and relative prox-
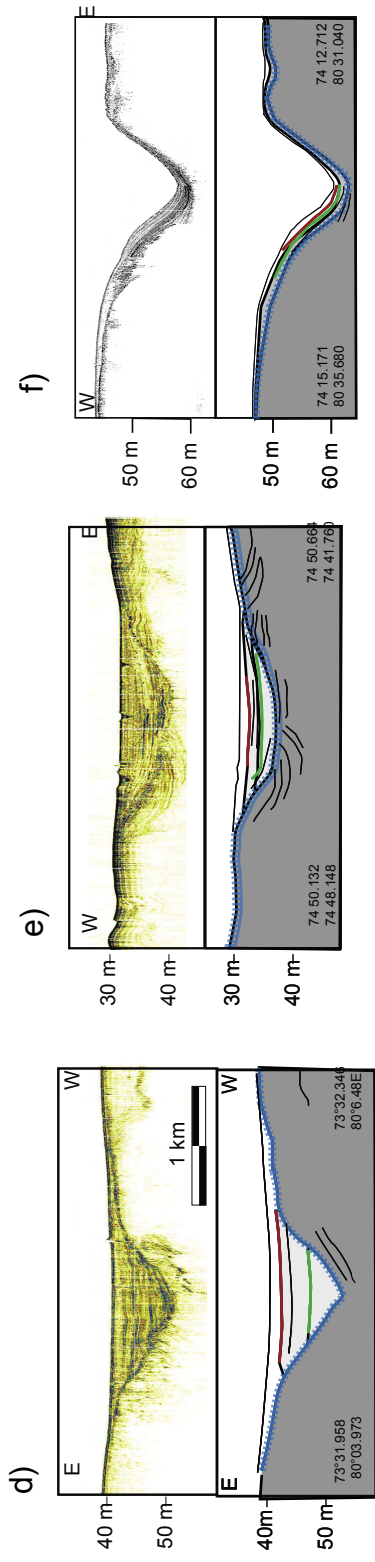
Figure 8. Interpreted sections of differentiated key Facies B and C and their sequences stratigraphically interpretation. showing depositional units; system tracts have been developed in the response to changing sea level
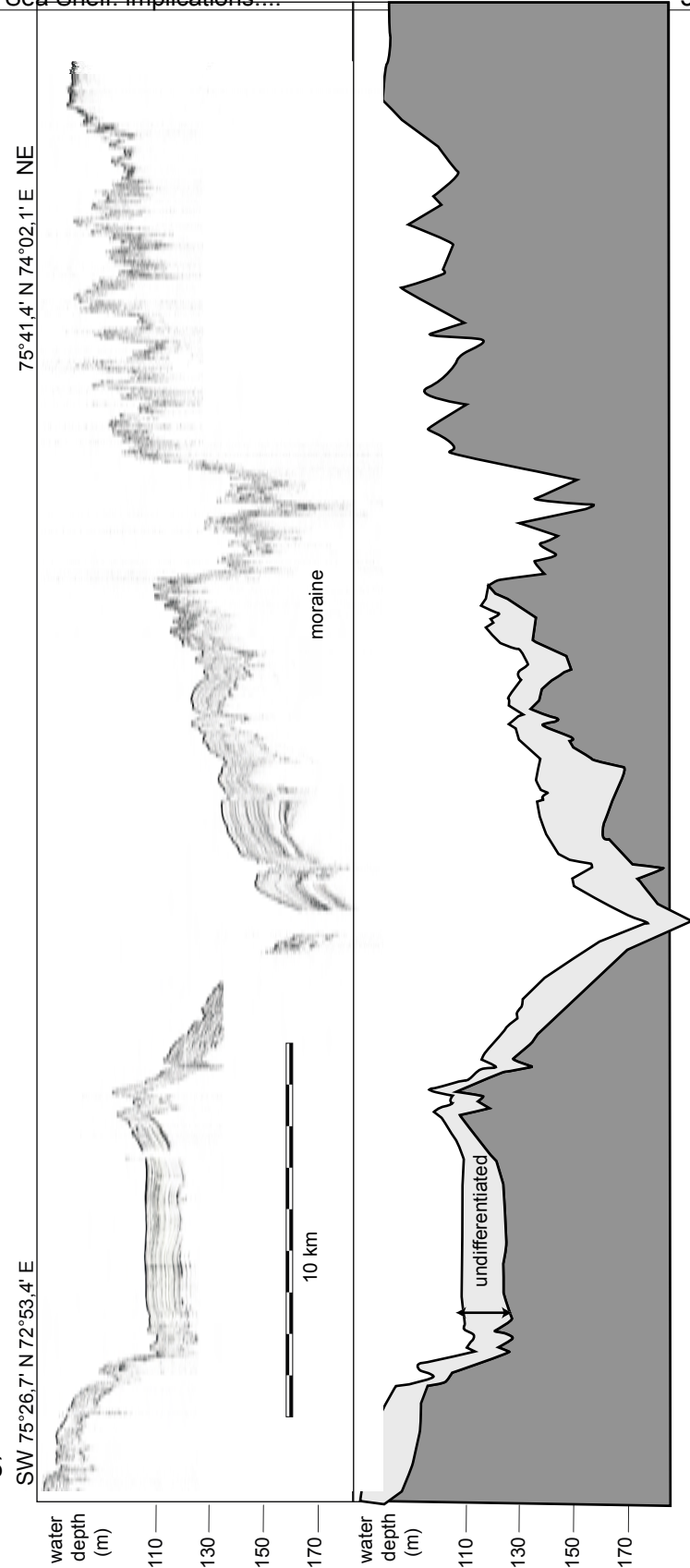
imity to the source inferred from the high magnetic susceptibility values. To the top
the transition to Unit I is characterised by higher values of magnetic susceptibility.
Frequently a spike occurs at the base of Unit I, as visible in cores PS-2719, BP99-05,
BP00-22 and BP00-23 (Fig. 7b), and described by Kleiber and Niessen (2000) for the
Laptev Sea. This spike is generally dated between 10-13 ka BP and reflects a deposi-
tional peak. The peak is explained by the enhanced decay of a continental (Putoran)
ice sheets and increased fluvial discharge rates due to climatic warming (Kleiber and
Niessen, 2000; Dittmers et al., 2003), coinciding with accelerated sea level rise (Fair-
banks, 1989). During the deposition of Unit Ia water depth is greatest in relation to the
preceding units. The absolute distance to the high susceptibility bearing material is
greater. Transport energies are generally lower resulting in finer particles. The upper
part of Unit I displays the lowest susceptibility values and is related to the HST. The
maturity of sediments progressively indicating, reflected in finer particles manifested in
an elevated clay content.

Sequences stratigraphic evolution and sea level cycle

The interaction of the global transgression and the smooth slope gradient of the
Kara Sea Shelf resulted in very high lateral transgression rates, exposing huge areas
to intense reworking and subaerial erosion, particularly during times of large meltwa-
ter release such as MWP1 and MWP2 (Fairbanks, 1989), averaging to 100 m/y for
the Holocene. This physical process resulted in a superimpositioning of system tracts
rather than in a migrating depositional equilibrium surface as suggested by Swift and
Thorne (1991) leading to a facies succession in the sense of Walther`s Law (Middle-
ton, 1973). It is very likely, for example, that during the LGM sea level lowstand an
estuarine environment similar to that of the Facies A in the present Ob and Yenisei
estuaries prevailed at the present 120 m isobath in the Facies C sediments.

An interpretation of the entire seismic unit configuration in dependence of the rela-
tive/eustatic sea level is given in Figure 8 and Table 2. The whole flooding history of
the shelf is reconstructed in Figure 9. All terms used in the following discussion are
used in the sense of Vail et al. (1987) and Posamentier and Vail (1988).

Regressional and lowstand system tracts (RST) 15 ka BP (Fig. 9 a)

We interpret the top of Unit II as a sequence bounding unconformity eroded dur-
ing the regression, representing a Type 1 sequence boundary in the sense of Van
Wagoner et al. (1988). The top of this Unit is irregular (Fig. 8). During the sea level
lowstand the present shelf areas were transformed into alluvial plains acting mostly as
non-deposition or sediment by-passing zones with sediment accumulation beyond the

a) Late Weichselian Regressional/Lowstand system tracts (RST and LST) before 15 ka BP
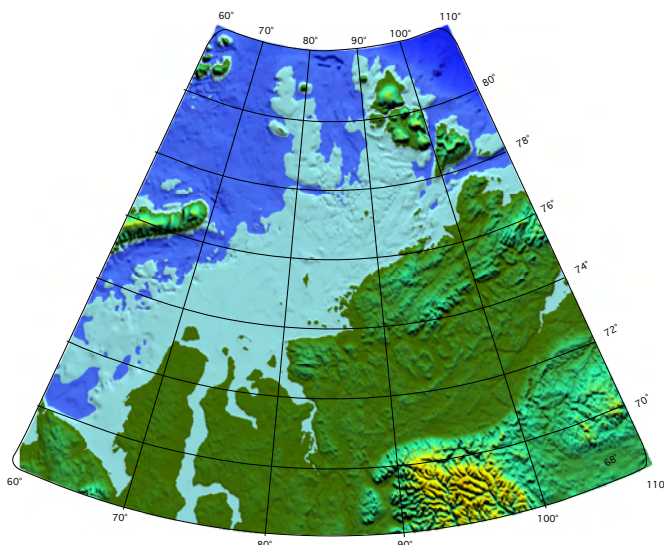
b) Transgressive system tract (TST) 15 ka BP- 8 ka BP
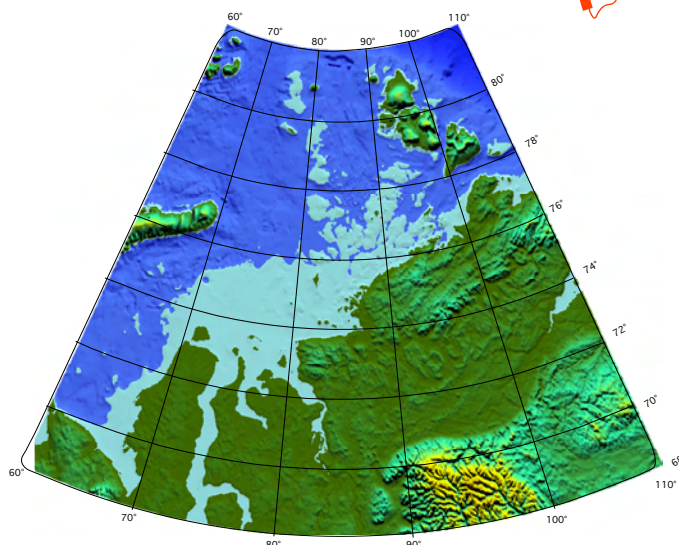
c) Transgressive/Highstand system tract (TST/HST) 8 ka BP-5 ka BP
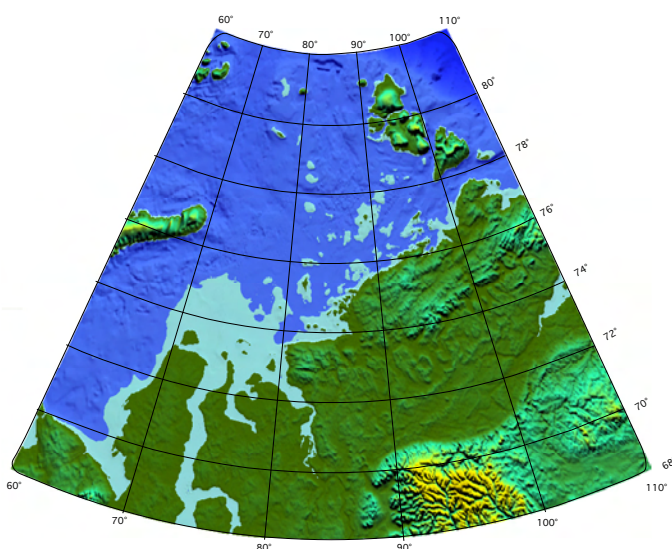
d) Highstand system tract (HST) since 5 ka BP
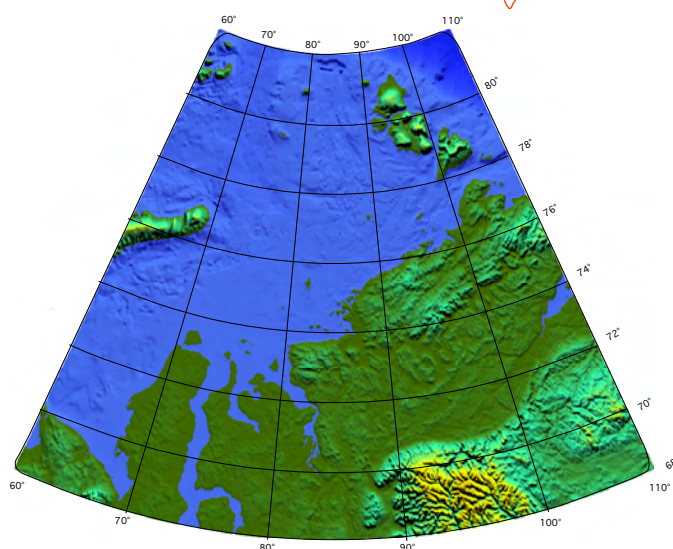
Figure 9. Major steps of sea level states and distribution of land and sea during flooding/transgression history of the Kara Sea. Major steps in conjunction with stratigraphic units.
The portion of the global eustatic sea level display in each illustrator is marked by the red bold line
a) depicts period when shoreline moved seaward during last regression
b) LGM shelf subaerially exposed, major phase of channel incision
c) onset of the transgression shoreline progressively moves southward towards the Siberian mainland; channels and incisions start to get filled
d) modern situation
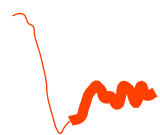
Table 2. Summary of seismic stratigraphy/depositional window of differentiated units, the age estimates refer to the area of the Ob and Yenissei estuaries (Dittmers et al., 2003) and represent a rough framework; note that for deeper water depths major surfaces (RS & MFS) yield older ages.

characteristic features	Sequences stratigraphic interpretation		rel. sea level/ vertical location	depositional time window
- whole unit has draping character - well stratified, downlaps at the base - acoustic masking due to gas in the sediment ==> deposition in estuarian setting with low current influence	HST	Unit Ia		
maximum flooding surface (MFS)				5 ka BP
- well stratified downlapping reflectors at the base - on the shelf often assymetric channel infills - sediment thickness increases away from channel axis ==> deposition in alternating marine-fluvial environment with moderate current influence	TST	Unit Ib		
transgressive surface (TS)/ ravinemet surface (RS)				8-8.5 ka BP
- draping irregular top of Unit II - assymetric depositional bodies; indicative for current influences on sedimentation - occurence at the topographic lowest part of incised channels	LST	Unit Ic		
sequence boundary				15 ka BP
- top characterised erosional surface - irregular highly reflective toplayer - seldom internal stratitfication ==> older sediments incised during sea level lowstand	RST	Unit II		

shelf edge. Channels were formed on the shelf erosively in Facies A and B while channel-levee complexes developed in Facies C`s deeper water environment.

In sediment cores this is manifested by high transport energies indicated by high sand content (Fig. 7a), cross lamination (Fig. 6), high susceptibility values (Fig. 7b), and erosional surfaces.

The sequences boundary is a discontinuity on the shelf and grades conformably into a non-distinguishable correlative conformity in Facies C (Coe et al., 2003).

Transgressive system tract (TST) 15 ka BP- 5 ka BP (Figs 9 b and c)

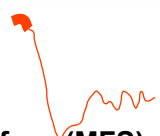During late lowstand relative sea level began to rise, forming first onlapping strata onto Unit II in a transgressive surface as well as the base of Unit Ic, the transgressive system tract (Fig. 8).

Sediments on the shelf (< 120 m water depth) comprising this time interval are of fluvial origin. Shortly after the LGM, shoreline transgressed over the shelf area involving a sea level rise of more than 80 m. Submarine accommodation space was rapidly increased so that sedimentation could keep pace with sea level rise, resulting in a deepening upward sequence. In facies A-C this is manifested by high accumulation rates

expressed by high relative thickness of this Unit (Fig. 8). The transgression formed the transgressive surface due to the action of waves, a shore face ravinement in the sense of Swift (1968), eroding underlying strata. This surface defines the boundary between subunit Ic to subunit Ib, dated to 8.5 ka BP in the Yenisei area (Table 2). Sediments exhibit a distinct susceptibility spike at the base of the TST grading into elevated values (Fig. 7b), and are commonly finely laminated without bioturbation (Figs 6 and 7a).

To the top the TST is bound by the maximum flooding surface at ca. 6 ka BP marking the highest rate of available accommodation space between sea and sediment surface and relatively deepest water conditions during sea level rise, manifested in high accumulation rates.

Highstand system tract (HST) since 5 ka BP (Fig. 9 d)

Since approximately 6 ka BP sea level approached a relatively stable position. The deposition of draping HST (Fig. 8) started at least 5 ka BP. The topmost sediments in all facies areas have draping character, implying weak currents in relatively deep water. During this depositional episode sediments prograde-agrade above the maximum flooding surface and marine shelf sediments associated with low relative sea level form the "condensed section" as a result of slow rate of sediment accumulation of (hemi-) pelagic sediments as introduced by Mitchum (1977). Sediment cores show low magnetic susceptibility values (Fig. 7b), parallel bedding often obscured by bioturbation and are often rich in bivalves (Figs 6 and 7a).

Evolutionary scenario and paleo-environmental reconstruction

Especially for Facies C, as noted earlier, there is no existing confined age model. Channel-levee complexes often overly formally glaciated terrain, of probably mid Weichselian age, but their dating proves difficult. A key to answer this question is the interrelation of channel-levee complexes with the bordering LGM morphology (Fig. 10). The channel levee complexes overly glaciated ground (Fig. 10) and therefore postdate the LGM. A striking feature is the fact that the levees often terminate abruptly towards the contact to LGM morainic terrain with the typical hummocky relief of LGM origin (Polyak et al., 2002; Stein et al., 2002). In these key sections sedimentation on the overbank facies takes place on higher ground than the ice sheet occupied area.

On the otherhand it is possible that the terminal moraines acted as barriers. However, it is not exactly clear when the marine ice sheets decayed, but they could have existed until 15 ka and even have survived a major part of the marine transgression, which would give an early Holocene age.

The widespread association of channel levee complexes with the LGM margin (Fig.
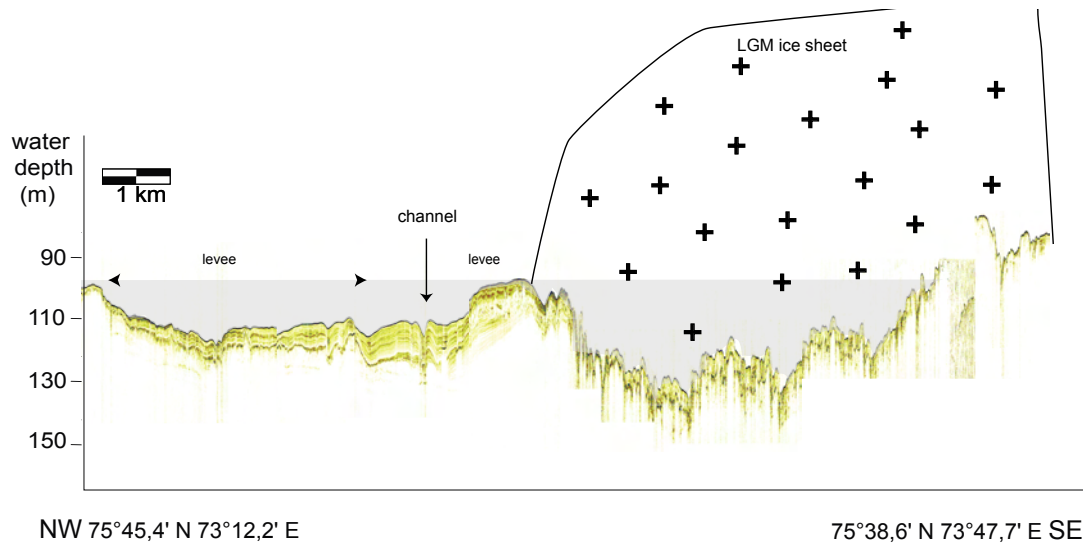
Figure 10. Acoustic section of channel-levees bordering glacially overprinted terrain. Note the abrupt change in sediment thickness in the transition from channel-levee facies to LGM ice overlain area. Note that channel deposition (shaded area) did not occur in the left side of the section although it lies topographically lower.

11) displays a complex interrelationship. The general geometry of the channels and their morphology hold clear evidence for the sedimentation under current influenced conditions (e.g. Flood and Damuth, 1987). This evidence neglects a genesis in an ice dammed lake setting. This in turn, if our interpretation of the relative chronological succession is correct, implies that there was a steady (suspension) flow through the channels axis during levee/overbank formation. Our interpretation of the channels in Figure 11 seems to give evidence of a submarine flow direction somewhere to the north. This implies that the ice sheet could not have been closed the passage to the north, also
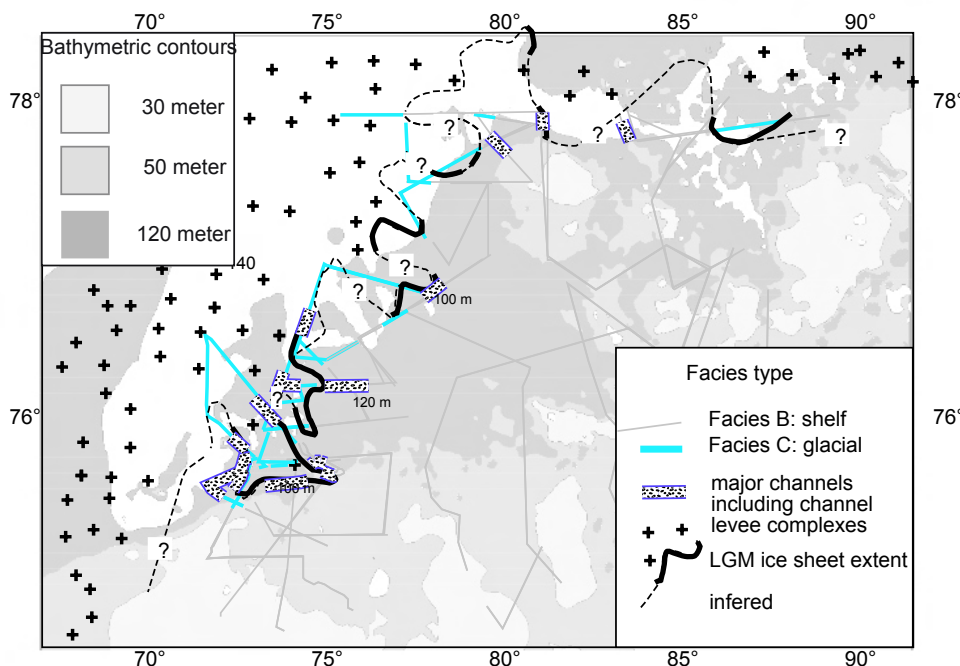
Figure 11. Enlargement of Last Glacial Maximum ice margin. We refined our former results and conclude a much more lobate form of the ice border.

indicating a post LGM date for the channel levee complexes. Moreover the fact that some channels are situated westward of the maximal ice extent (Fig. 11) implies a formation after the LGM.

However, their genesis is discussed in Chapter 3.5 in more detail. It is not possible to establish absolute dates but interpretation of acoustic profiles reveals important information about the relative chronology.

Figure 12 summarises the evolution of the Kara Sea Shelf schematically in a Wheeler- type diagram (Wheeler, 1958). The widespread occurrence of fluvial channels on the whole shelf, up to 700 km north of the recent coast line (Chapter 3.5), speaks in favour of a long lasting subaerial erosional period. These channels are partly unfilled and well preserved. They are quite mature in terms of auto-cyclic fluvial development. The majority belongs to the meandering river regime (Chapter 3.5). complexes.

Sediment volume

Sediment accumulation on the Kara Sea Shelf can be estimated from acoustic data assuming that the widely observed near sub bottom unconformity represents the Holocene transgressional surface. Occasionally, difficulties were faced when mapping the unconformity due to the presence of gas (Figs 4 and 5).

The lateral resolution of our sounding data proved not to be suitable for the calculation of contour plots. Although having a huge data set, the individual expeditions did
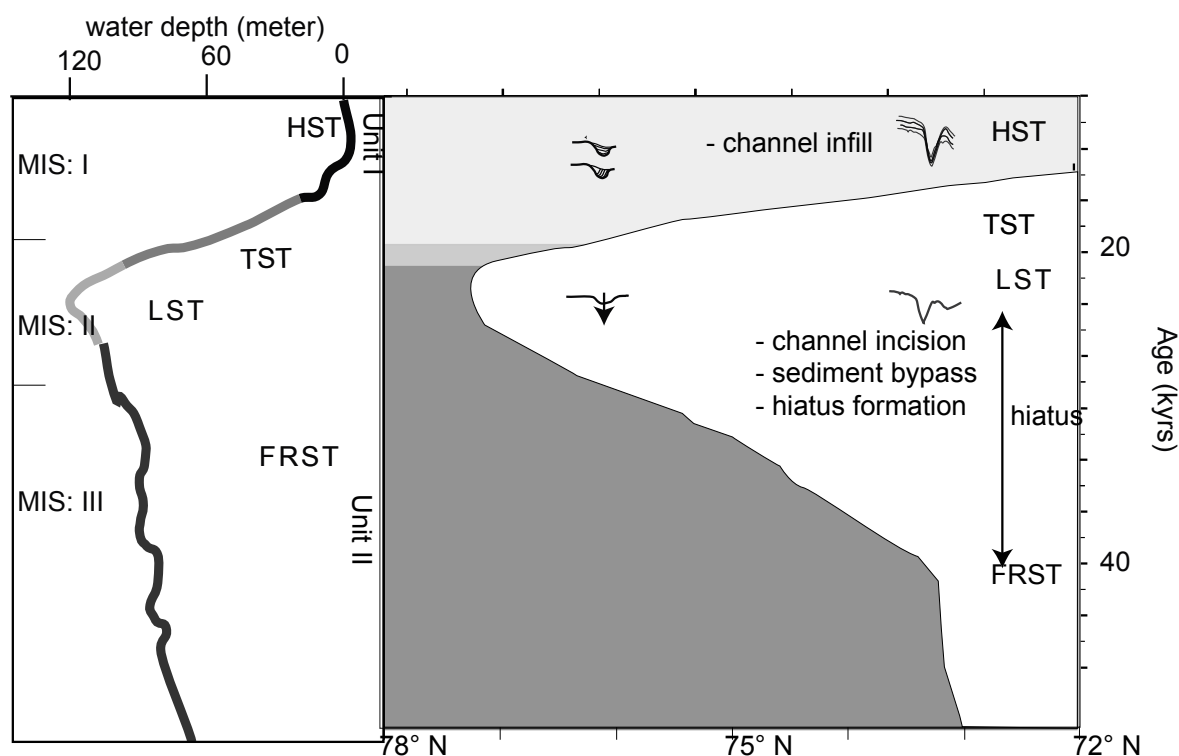
Figure 12. Wheeler (1958) type chronostratigraphic chart of working area in dependence to sea level stand; horizontal axis represents distance along the proximal to distal profile; the vertical axis represents time.

not cover the Kara Sea in an equivalent pattern producing areas, as for example the Yenisei Estuary with very high sounding density, while coverage of the shelf holds some gaps across which makes it difficult for automatic procedures to interpolate. Attempts to evaluate the sediment thickness by software utilising kringing algorithms (for e.g. Surfer and Ocean Data View) failed, because cruise tracks have a preferred and irregular spatial distribution.

Therefore, we used a different, simplified approach. Having defined the surface facies types A-C (Figs 4 and 5) we chose areas for each individual type where the spatial coverage of soundings is high, and estimated an average value of sediment thickness (Fig. 13, Table 3).

We refined our estimates for the Yenisei Estuary by a total of 800 line kilometres of new PARASOUND profiles (Dittmers and Schoster, 2004). Our calculations for Facies A, the Yenisei and Ob estuaries, 8.0×10^{10} t and 14.1×10^{10} t, respectively (Table 3), lie in the same range as described by Dittmers et al. (2003) with slightly lower values for the Yenisei Estuary.

For Facies B, covering the largest area with the least sediment thickness, the outcome sums up to 468 km^3 sediment volume and a mass of 42.2×10^{10} t (Table 3). The

Table 3. sediment mass estimates for differentiated Facies A-C (Figs 3 and 4). For the calculation of the sediment mass an average porosity of 66 % has been used (Dittmers et al., 2003).

Holocene sediment thickness (m)	A ESTUARY		B: SHELF	C GLACIAL	
	OB	Yenisei		west	north-east
soundings in sample area	534	157	554	880	245
Min:	2	2	0	1	2
Max:	21	23	15	31	26
Mean:	8	8	3	7	11
	7	7	2	6	11
spatial extend of FACIES type (km²)	19,697	11,532	15,8718	39940	25,964
sediment Volume (km³)	**157**	**89**	**468**	**266**	**286**
Netto sediment mass(10 ¹⁰ t)	**14**	**8**	**42**	**24**	**26**
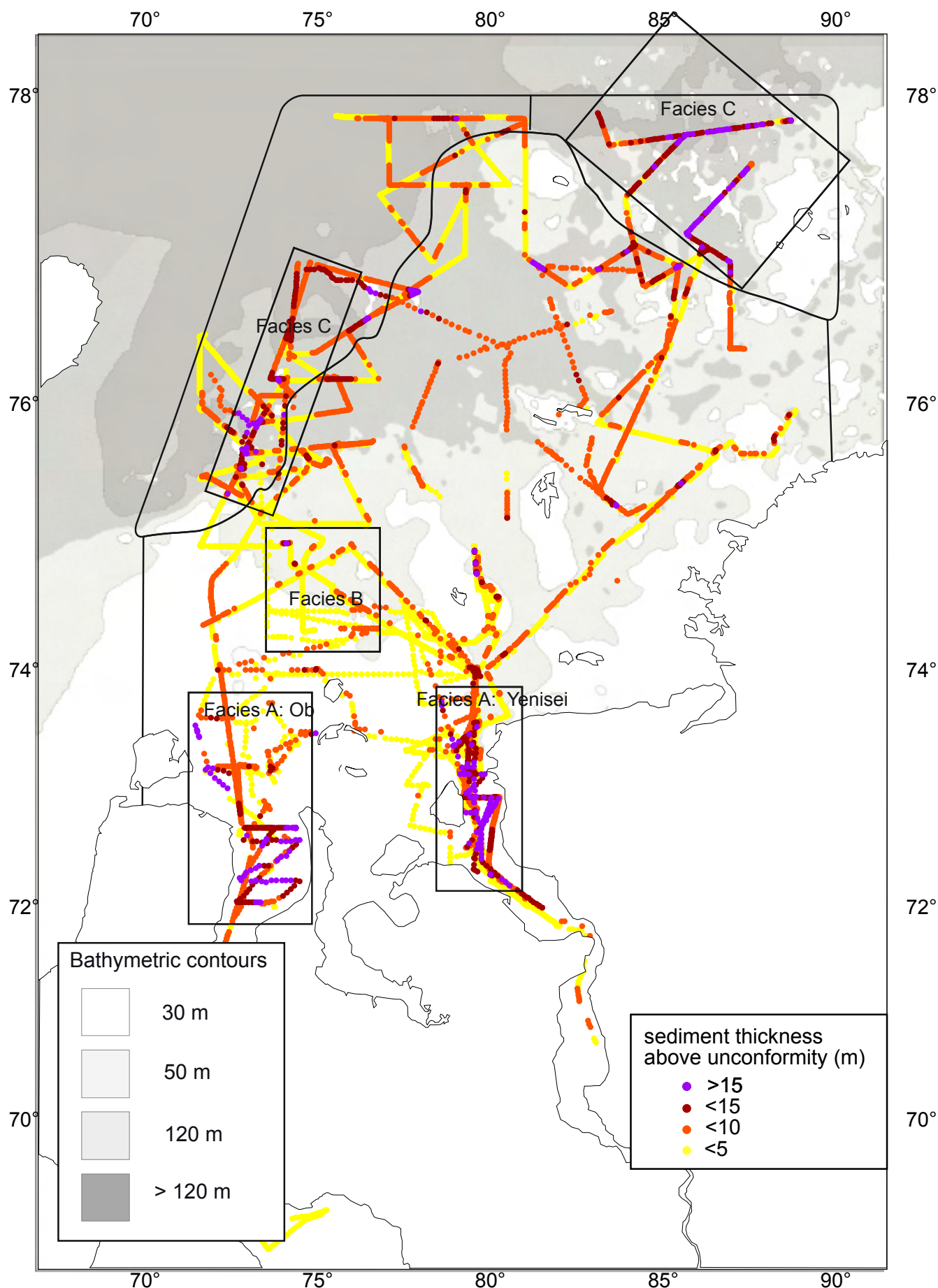
Figure 13. Acoustic sediment penetration above post-glacial unconformity. Boxes indicate areas on the basis of which average thicknesses for each Facies type have been determined.

two areas of Facies C accumulate to nearly the same sediment volume, i.e. for the western facies 266 km^3 and 24.0 x 10^{10} t respectively and 285 km^3 and 25.7 x 10^{10} t (Table 3). In total the sediment mass adds up to 114 x 10^{10} t. These values are in good agreement with the results of Stein and Fahl (2003). They based their estimates mainly on AMS ^{14}C-dated sediment cores and in comparison to our data these estimates rather represent an underestimate. Stein and Fahl (2003) come out with a total of 123 x 10^{10} t averaged for the Holocene, their data base extends as far as 82° N, while in this study we only considered data south of 78° N. Therefore, their values must be reduced by approximately 20 x 10^{10} t.

Our data based on acoustic profiling rather overestimate the sediment mass especially for Facies C for the following reasons.

Sedimentation in Facies C is not interrupted by clear unconformities on acoustic profiles, thus it is not exactly clear which time interval is included by sediments overlying the unconformity. In Facies A and B the unconformity itself is of post-LGM age, but sedimentation in Facies C started earlier than on the adjacent Kara Sea Shelf, and the unconformity grades into a conformal surface, because water depth was sufficiently deep (Coe et al., 2003).

Sediment sources

It is beyond the scope of this work to account for all the factors, often impossible to attribute correctly, controlling the sediment input and output so we rather try to evaluate the sedimentary mass in an evolutionary sense. Besides the ambiguity of an absolute age model it is evident that sedimentation in Facies C occurred during sea level lowstand and possibly during the LGM as summarised in the conceptual model in Figure 14. This would account for the high sediment mass included by this facies type. The sediment making up the northern sections of Facies A (Figs 8b and c), closely resembles the conceptual model of a sequence by Vail et al. (1987) with most of the LST probably missing. These sediments are virtually absent in Facies A and B, where sediments by-passed and accumulated in Facies C. It is possible, though that portions of LST strata accumulated in small sinks and "survived" the sea level lowstand, but these are comparatively small, negligible valuess.

During transgression over the very shallow slope of the Kara Sea Shelf the in-situ sediments were subjected to several erosion processes related to the formation of the transgressional surface, as e.g. intense reworking due to wave-action and subsequent shore face ravinement formation (Thorne and Swift, 1991). Although, owing to the long subaerial exposure, large areas were probably permafrozen with abundant ice complexes, consisting of alluvial plains and river channels (Alekseev, 1997). High erosion
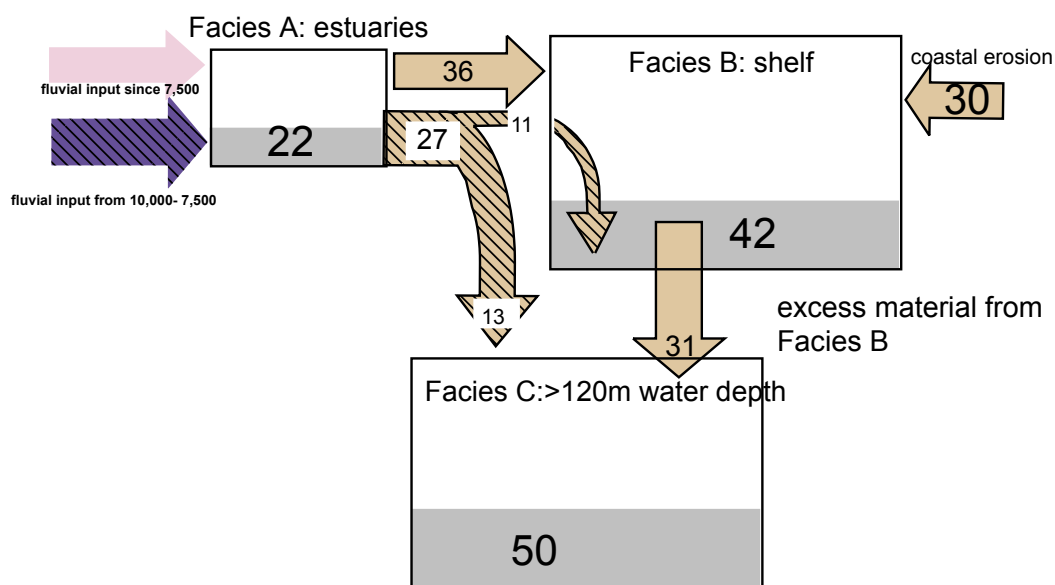
Figure 14. Schematic of sediment masses and bugdet for the three facies types for the Holocene

rates as well as coastal retreat rates increased 5 m per year in permafrozen soils due to thermokarst erosion by the formation of thermocirques (Rekant et al., 2005).

Typically, the upper 5-15 m may be removed during transgression (Walker, 1992), depending on the storm wave base and re-occurrence ratio of storms. Hine and Snyder (1985) found for the North Carolina shelf that (shoreface) erosion stripped off sediments and formed the ravinement surface. As known from the well-studied Eel margin, 50 % of the sediment above the unconformity are older reworked bedrock strata (Burger et al., 2001). We think it reasonable to account at least the same value for the Kara Sea Shelf with its gentle slope, exposing vast shelf areas to the action of waves and storms.

Most parts of the shelf are flooded since 8-9 ka BP(Figs 7b and 9) and since then terrestrial (fluvial) material has been dispersed on the shelf.

Dittmers et al. (2003) established the first parameter-based sediment budget for the region. It emerged that the estuaries effectively acted as "marginal filter" (Lisitzin, 1995) and filtered out about 90 % of the suspended and 30 % of the dissolved material, summing up to 25.5×10^{10} t for the Ob and to 32.4×10^{10} t for the Yenisei for the last 7,500 years, the time they assumed the estuaries to have been active under recent conditions. However the "real" volumes of sediment accumulated in the estuaries are lower, indicating weak material export (Dittmers et al., 2003). This material is thought to

accumulate in Facies B. By subtracting the sediment mass of the Facies A (25.5+32.4) x 10^{10} t – 22.1 x 10^{10} t the net export to Facies B is estimated to = 35.8 x 10^{10} t.

For the Holocene, taking the modern numbers, this would mean that during the first 2500 years another total of 7.4 x 10^{10} t of suspended and 19.2 x 10^{10} t of dissolved fluvial material by-passed Facies A. Assuming an estuarine setting in Facies B at the river ocean boundary, it would filter 6.6 x 10^{10} t of suspended and 5.8 x 10^{10} t of dissolved material while 0.8 x 10^{10} t of suspended and 13.2 x 10^{10} t of dissolved matter would have sedimented in Facies C. However, it is not exactly determinable how much of the material is deposited in Facies B and how much is passed on to Facies C. Furthermore it is difficult to assess how much material was delivered to Facies C during sea level lowstand and how much reworked Facies B material is in incorperated into Facies C.

It is still unclear how much the coastal erosion effects the total sediment balance (e.g. Stein et al., 2004). There are values of Romankevich and Vetrov (2001) of 109 x 10^6 t/y, which are definitely too high, because recent interpretation of satellite images of Rachold and Cherkashov (2004) indicate erosion rates in the order of 30 x 10^6 t/y (Vasiliev et al., 2005).

5. Conclusion:

The Kara Sea can be subdivided into three Facies provinces:

• Facies province A: a high mud accumulation, fluvial to marine succession with laterally consistent reflectors. It is restricted to the modern estuaries up to 74° N.

• Facies province B: covers the shallow and flat central shelf to water depths up to 120 m; sediment thickness is variable and concentrates in depressions. Outside the depressions sediment penetration is minor. It is restricted to the shelf.

• Facies province C: with the highest relief energy associated and little sediment accumulation and high sediment thickness with draping reflectors in channel-levees complexes. It occurs north and westward of Facies B and generally below the 120 m isobath.

• Sediments above the regional unconformity are of Holocene age for Facies A and B, while in Facies C constant deep water conditions prevailed, with no distinct unconformity

• Late Weichselian to Holocene strata consist of a threefold division, according to the concept of sequence stratigraphy. including

• The total post-LGM sediment mass through all three facies areas sums up to 114 x 10^{10} t.

• Constant deposition occurred continuously in Facies C, with higher sedimentation rates

during sea level lowstand when all material by-passed Facies A and B. Sediment accumulation progressively shifted towards the modern coastline and the recent estuary of Ob and Yenisei, making up Facies A.

• There is a significant component of reworked material in Facies B making up at least 50 % of the sediment mass.

Acknowledgements

3.5 Late Weichselian Fluvial Evolution on the Southern Kara Sea Shelf, North Siberia

3.5 Late Weichselian Fluvial Evolution on the Southern Kara Sea Shelf, North Siberia

Dittmers, K.*, Niessen, F. and Stein, R.

Alfred Wegener Institute for Polar and Marine Research, Bremerhaven, Germany

Corresponding Author. kdittmers@awi-bremerhaven .de

Abstract

Glaciations had a profound impact on the global sea level and particularly on the Arctic environments. One of the key questions related to this topic is how the discharge of the Siberian Ob and Yenisei rivers did interact with a proximal ice sheet? In order to answer this question high-resolution (1-12 kHz), shallow-penetration seismic profiles were collected on the passive continental margin of the Kara Sea Shelf to study the paleo-drainage pattern of Ob and Yenisei rivers. Both rivers incised into the recent shelf, leaving filled and unfilled river channels and river canyons/valleys connecting to a complex paleo-drainage network.

These channels have been subaerially formed over a period of regressive phase of the global sea level during the Last Glacial Maximum. Beyond recent shelf depths of 120 m particle transport is manifested in submarine channel-levee complexes acting as conveyor for fluvially-derived fines. In the NE area uniform draping sediments are observed. Major morphology determining factors are a) sea level fluctuations and b) LGM ice sheet influence. Most individual channels show geometries typical for meandering rivers and appear to be an order of magnitude larger than recent channel profiles of gauge stations on land. The Yenisei paleo-channel dimensions are than the Ob examples and could be originated by additional water release during the melt down of LGM Putoran ice masses.

Asymmetrical submarine channel-levee complexes with Channel depths of 60 m and more developed, in some places bordered by glacially dominated morphology. Channels situated on the shelf above 120 m water depth exhibit no phases of ponding and or infill during sea level lowstand.

1. Introduction

The exact spatial ice sheet extent during the late Weichselian = Late Glacial Maximum (LGM) glaciation is still under debate, particularly in the Siberian Arctic. Large scale ice domes as proposed by Grosswald (1980) are not realistic for the Russian sector of the Arctic. Recent outcomes of the QUEEN project ("Quaternary Environments of the European North") summarised in Svendsen et al. (2004) rather give evidence for relative small ice masses in the Siberian sector, with some ambiguity about the exact spatial extent of such an ice cover, especially on the NE mainland (Alexanderson et al., 2001).

Especially for the Kara Sea one of the key questions related to this subject is: how did the discharge of the Ob and Yenisei rivers interact with a proximal ice sheet? Glaciations have sustained impact on the discharge pattern of large streams, in particular in high latitudes, by I) influencing the global water budget and II) by the physical presence of large ice sheets.

I) In the first place the build-up of huge ice bodies/sheets "consumes" water from the ocean, resulting in a world-wide eustatic sea level fall (Fairbanks, 1989; Chappell et al., 1996). This has profound effect on the longitudinal profile of a river. The river has to adjust to a new slope gradient which can locally result in pronounced erosion and deposition and in a total reorganisation of the whole drainage pattern and direction (Allen, 1992; Schumm, 1993; Leopold, 1994).

II) The second mode of action is the physical interaction between ice sheets and adjacent river systems. River systems may either be deflected by ice sheets or get totally dammed. This has also been proposed by several workers for the middle Weichselian glaciation in Siberia, when the Ob and Yenisei rivers were thus re-routed southward into the Caspian Sea via the Aral Sea, instead of a northward drainage into the Kara Sea (Mangerud et al., 2003, 2004).

There were several major pro-glacial lakes in the Arctic realm like the late Weichselian Lake Agassiz (e.g. Clark et al., 2004) in front of the Laurentide ice sheet, the middle Weichselian Lake Komi in central Siberia (e.g. Mangerud et al., 2004) and a White Sea lake (Mangerud et al., 2001a; 2001b). Their degradation is often coupled with cataclysmic dam failures as documented in the Altai Mountains (Baker et al., 1993) possibly resulting in earth's greatest flood.

Glaciation history

The general eastern boundary of the LGM Barents Sea ice sheet extent is now well-studied with the exception of some small uncertainties in the north-eastern area of the Kara Sea Shelf (Fig. 1; Svendsen et al., 1999, 2004; Alexanderson et al., 2001; Mangerud et al., 2002; Polyak et al., 2002; Stein et al., 2002). There is still an enigmatic, isolated record of an ice advance towards the Taimyr peninsula in the late Weichselian (Svendsen et al., 1999; Alexanderson et al., 2001), forming the LGM part of the North Taimyr ice-marginal zone (NTZ, Alexanderson et al., 2001). It is still under debate whether this Taimyr ice sheet was a locally isolated ice cap or whether it was linked to the Barents and Kara Sea-ice sheet. In case this ice sheet covered the northern Kara Sea Shelf, it might have blocked the major Siberian rivers during the Holocene as postulated by Polyak et al. (2002) and as proposed for the early Weichselian (Grosswald, 1980; Arkhipov et al., 1995; Mangerud et al., 2001a, 2001b).
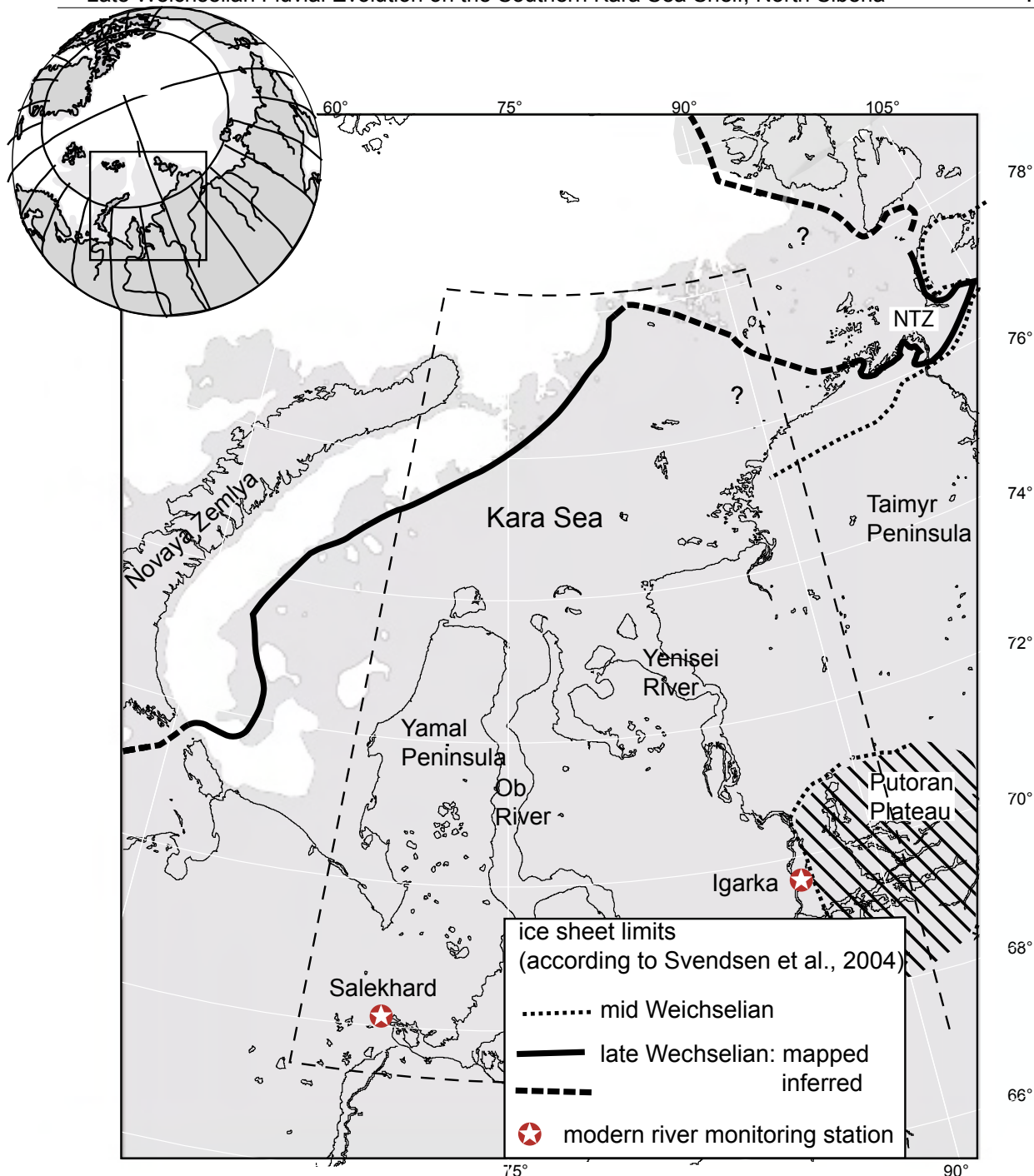
Figure 1. Overview map of working area (trapezium) in the central southern Kara Sea after Svendsen et al. (2003). Limits of early and middle Weichselian glaciations and LGM as figured. Grey shaded area indicates maximum subaerially exposed land extent during LGM according to modern bathymetry at 120 m depth contour.

Study Area

In the Arctic Ocean continental shelves make up more than 50 % of the entire area, a significantly larger proportion compared to other world oceans (Jakobsson, 2002). The Kara Sea Shelf (Fig. 1) occupies 10 % of the whole Arctic area. Being very shallow with an average water depth of about 50 m for the inner Kara Sea, this shelf area is in

particular sensitive to eustatic sea level changes between glacial and interglacial time periods. This probably resulted in a profound impact on the drainage pattern of modern river extensions on the Kara Sea Shelf.

Modern river run-off

Today the Ob and Yenisei rivers supply more than 30 % of the total Arctic freshwater volume and some of the suspended sediment into the Arctic Ocean with a strong inter-annual variation (Gordeev et al., 1996; Holmes et al., 2002; Rachold et al., 2003). The Ob and Yenisei discharge 429 km^3y^{-1} and 620 km^3y^{-1} respectively, through their estuaries into the Kara Sea (Aagaard and Carmack,1994).

Sediment fluxes have been investigated by Stein et al. (2002, 2003b, 2004). For a detailed summary of factors acting on riverine originated sediments and their distribution on the shelf see Stein et al. (2004), Dittmers et al. (2003) and citations therein. Water masses supplied by the two rivers pass the estuaries, whereas the main portion of the suspended and minor dissolved matter flocculates and is deposited here (Lisitzin, 1995; Dittmers et al., 2003). The remaining, by-passing matter accumulates on the Kara Sea Shelf, only a minor amount is transferred into the deep Arctic areas (Stein and Fahl, 2003). Research mainly focussed on sediment fluxes (Stein et al., 2002, 2003b, 2004; Dittmers et al., 2003) but little has been known about paleo-discharge.

Evidence of ancient fluvial activity on the recent shelf

During sea level lowstand fluvial activity rather resulted in widespread channel incision on the shelf, typical for several LGM shelf areas (Schumm, 1993) and as for example the well studied New Jersey continental margin (Evans et al., 2000). This process was probably enhanced during Termination I (Fairbanks, 1989) after the LGM with increasing river run-off.

On the Kara Sea Shelf widespread occurrence of channels documents active fluvial discharge during lowered sea level and subaerial exposure, in contrast to an ice-dammed lake scenario (Stein et al., 2002; Dittmers et al., 2003).

Nansen (1904) was the first to observe incisions on the sea-floor of the Kara Sea Shelf. The first extensive high-frequency sonar investigations of the bottom relief were carried out by Johnson and Milligan (1968) who published results of geomorphologic investigations of the Kara Sea and reported unfilled channels of unknown origin on the shelf. Later Russian workers constructed charts of Quaternary fluvial features including reconstructions of fluvial valleys, drainage networks and watersheds of rivers on the basis of widespread seismic surveys (Lastochkin, 1977; 1978) but did not present the basis of their data sets, leaving a tentative picture of visible fluvial features on the shelf so far. Sediment investigations of the south-western Kara Sea region show

that sediments consist of fluvially-derived material, whereas subsequent Holocene sediments show stronger marine influences (Polyak et al., 2000).

For the Laptev Sea shelf Bauch et al. (2001) report a fluvial-dominated sediment regime during sea level lowstand based on cores documenting sea level related differences in sediment flux. Kleiber and Niessen (1999) describe submarine channels as major distributors of terrestrially-derived sediments.

The main objective of this study is to determine the extent and character of fluvial features visible on the sea-floor on the inner shelf of the Kara Sea concentrating on the morphometric dimensions of identified channels. The fluvial geometries bear important paleo-hydrological implications (Sidorchuk and Borisova, 2000; Sidorchuk et al., 2001). This information can be used to develop a better understanding of the paleo-riverine discharge and, thus, sediment dispersal and dynamics on the southern Kara Sea Shelf in the past. We mainly interpret high-resolution acoustic reflection profiles (2-12 kHz) to identify the morphology of the Kara Sea-bottom between 70° N and 78° N (Fig. 1) and to trace and measure individual channels. Furthermore, the behaviour of Siberian river run-off during the late Quaternary glaciation (MIS 2) and subsequent transgression is reconstructed.

Dittmers et al. (2003) established the first regional seismostratigraphic framework concentrating on the Ob and Yenisei estuaries. The most prominent feature is an erosional boundary, formed during subaerial exposure of the shelf, subsequently conformably overlain by marine sediments dating back into the Holocene (Dittmers et al., 2003, Stein et al., 2003b). This boundary at the base of channel-fill occurred during the transgressive postglacial sea level rise (Chapter 3.4). Channel incision is favoured during phases of extreme relative sea level lowstand as in the middle and late Weichselian. Subsequent channel infilling occurred during sea level rise - the Holocene transgression - see Dittmers et al. (2003) for detailed discussions.

2. Data Base and Methods

2.1 Geophysical data collection/acquisition

Data were collected during four expeditions of RV "Akademik Boris Petrov" in 1999, 2000, 2001 and 2003 (Fig. 2) using several different echosounding systems summarised in Table 1. For echosounding surveys in 1999-2001 we used the hull-mounted ELAC echograph of RV "Akademik Boris Petrov" (ELAC echograph LAZ 72, Honeywell-Nautik, Kiel, Germany) operating at a frequency of 12 kHz. Since 2003, RV "Akademik Boris Petrov" is equipped with a parametric ATLAS PARASOUND system, operated at a frequency of 3.5 kHz (Table 1).

Legend:
- 2003 cruise
- 2001 cruise
- 2000 cruise
- 1999 cruise

Novaya Zemlya

Izvestai Islands

Fig. 15

Fig. 9 b)

Fig. 10 a)
Fig. 4 d) & 9 a)
Fig. 10 b)

Fig. 8 c)
BP00-07
Fig. 4 c) & 8 b)
Fig. 4 b)
Fig. 8 a)
Fig. 4 a)

B

Taimyr Peninsula

Yamal Peninsula

A

Yenisei River

Bathymetric contours
- 30 m
- 50 m
- 120 m
- > 120 m

Ob River

A`   A
50 m
100 m
400 km

B`   B
50 m
100 m
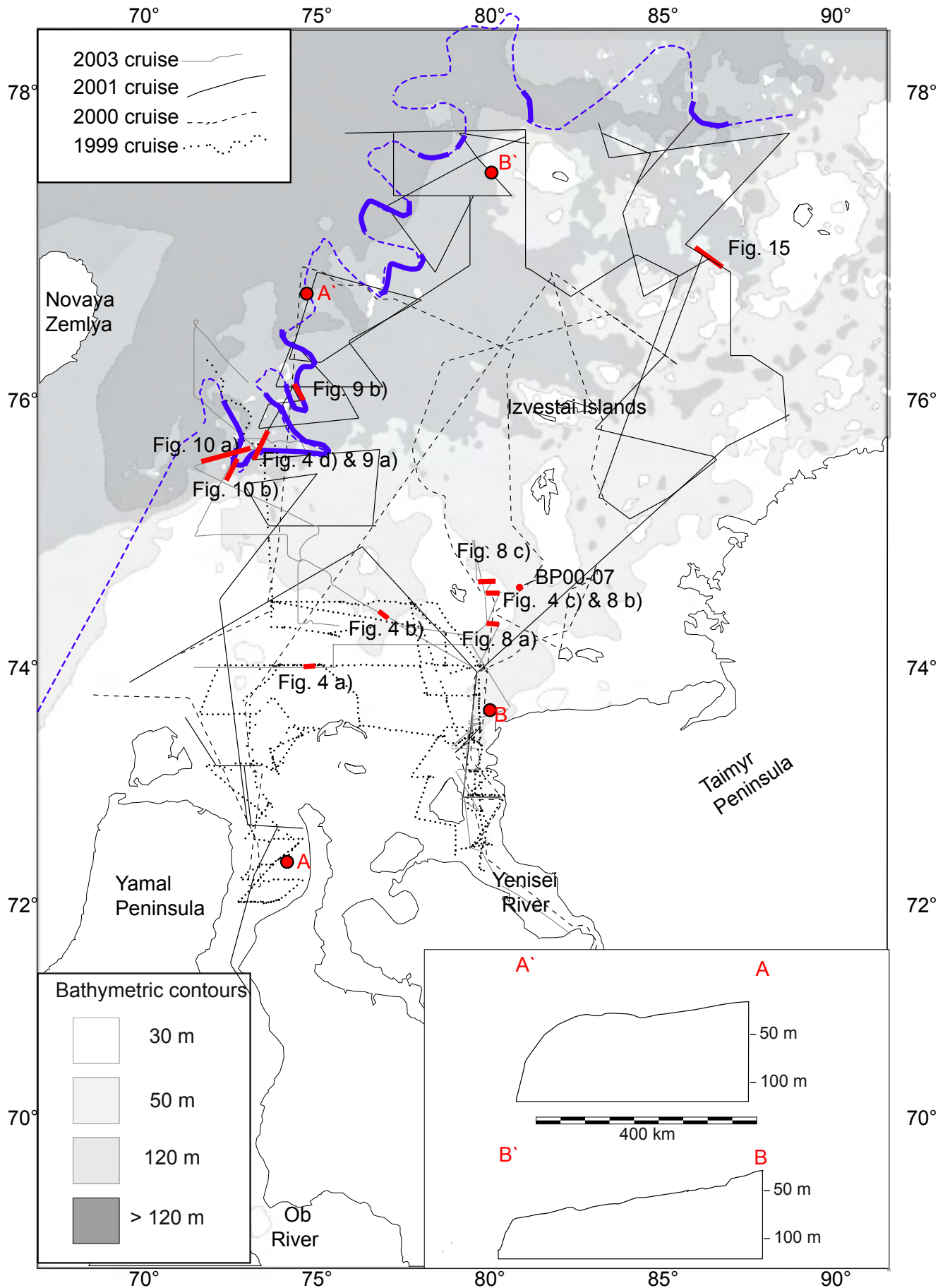
Table 1. Overview of expeditions and sounding systems: summary of sounding systems and references for detailed set up information; * indicates digital data processing (Niessen and Dittmers, 2002; Dittmers and Schoster, 2004)

Expedition	Hull-mounted system	profile (km)	Mobile system	profile (km)	Reference
1999	ELAC 12khz	3000	---		Stein and Stepanets, 2000
2000	ELAC 12kHz	5200	3.5 kHz*	220	Stein and Stepanets, 2001
2001	ELAC 12kHz*	10000	2-8 kHz *	150	Stein and Stepanets, 2002
2003	PARASOUND 3.5 kHz*	2300	---		Schoster and Levitan, 2004

2.2 Morphometric Analysis

Fluvial channels depicted by echo-soundings were morphometrically analysed. Channels were characterised on the basis of their classical geometric features basically described by channels` depth and width e. g. Langbein and Leopold (1966), Leeder (1973) and Schumm (1977) (Fig. 3). The following features were measured: channel width, channel depth (average vertical distance from thalweg bottom to base of levee sediments) and water depth (from sea level to levee crest) (Fig. 3). Channels width and depth were measured below Holocene sediment infill to account for channel formation during incision. Holocene sediment thickness can easily be identified by the basal unconformity underlying the Holocene sediments (Fig. 4), separating Units I and II (Dittmers et al., 2003; Stein et al., 2004). Channel depth and width are synonymously used with bankful stage coinciding with bankful discharge defined by Rosgen (1994).

In our data, most relief energies of channel cross sections are underestimated because track-lines are rarely exactly perpendicular to channel thalwegs and orientation of cruise track to the morphology is random. However, determination of channel depth is reliable in all cases. Nevertheless, these morphological features may still function as a useful qualitative, descriptive parameter. Furthermore, it must be underlined that the majority of all cruise tracks is concentrated in shallower water depths while on the outer shelf data density is lower. Thus, more data on shallow water channels have been collected.

On the basis of echo-soundings, together with additional information from navigational charts, a detailed digital elevation model of the Kara Sea Shelf relief was compiled

Figure 2. Working area with cruise tracks of „Akademik Boris Petrov" expeditions 1999, 2000, 2001 and 2003 (Stein and Stepanets 2000, 2001, 2002). Key acoustic sediment profiles in solid lines and gravity core BP00-07 are indicated by numbers. The position of morphological sections across the Kara Sea Shelf in the northward vicinity of Ob (A-A') and Yenisei (B-B') river mouths, along thalweg of paleo-rivers of both rivers, is given by red solid lines; note the extreme gentle slope and the relatively steeper gradient for the Ob river branch.
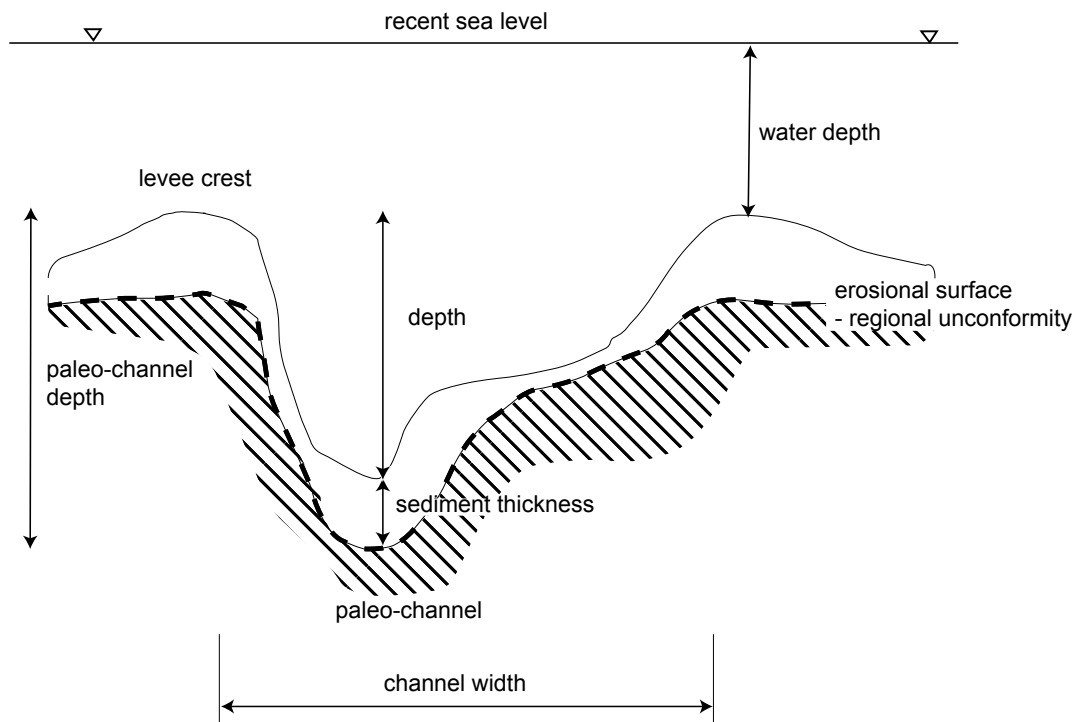
Figure 3. Idealised channel geometry morphological parameters measured in acoustic cross sections

3. Results

3.1 Topography

In general, the Kara Sea Shelf is characterised by a gentle slope gradient ranging from an average of 1:1,351 in a representative section between 73°30 N 73°18 E and 78°00 N 73°18 E north of the recent Ob Bay to 1:4,166 along a more easterly section between 73°30 N 79°40 E and 78°00 N 79°40 E north of the Yenisei Estuary (Fig. 2). The topography remains relatively flat to a depth of the present 50 m contour line where a distinct change in slope gradient from an average of 1:6,000 to more than 1:1,100 is observed, defining a major shelf/slope break. The whole inner shelf has a smooth relief with elongated deeps and troughs aligned in northerly direction in some places. At the shelf/slope break the relief gets very rough with high relief intensity and elevation changes of more than 50 m within lateral distances of a few hundred metres. These features are related to the eastern boundary of the grounded LGM Barents/Kara Sea ice sheet (Stein et al., 2002; Polyak et al., 2002).

3.2 Channel geometry and morphological parameters

Channels have concave-up erosional bases with different levels of sedimentary infill. In the western area, associated with the LGM glaciation margin, there are typical levees which form the channel margins. They are characterised by their typical external wedge shape, with internal sub-parallel layered reflectors, drapes, and thinning away from the channel axis. The analysis of echosounding profiles generally reveals two different types of channels defined by their morphometric and morphogenetic character (Fig. 4):

Type I consists of filled or buried channels, characterised by a deflection of the prominent basal reflector representing the top of Unit II (Dittmers et al., 2003). These channels are filled with younger well-stratified sediments (Figs 4a and b). The majority of these channels is dominated by parallel reflectors of the channel infill (Fig. 4a). In some cases these sediments display asymmetric fill patterns (Fig. 4b). Channel incision depth rarely exceeds 15 m, and reaches an average of 10.4 m (Table 2). In some places the sea-bottom smoothly ponds these incisions by leaving not more than 1 metre of relief. Channel width is 650 m on average (Table 2). The majority of this

Table 2. Morphometric characteristics of sampled channels

	channel type		Water depth (m)	bankful width (m)	bankful depth (m)
type I	Filled channel				
		Min:	22.0	370.0	4.0
	n=49	Max:	50.0	9600.0	35.0
		Mean:	35.5	650.0	10.4
type II	OB				
		Min:	25.0	250.0	12.0
	n=11	Max:	80.0	13500.0	55.0
		Mean:	44.1	2767.8	22.2
	Yenisei				
		Min:	14.4	300.0	4.4
	n=93	Max:	122.0	30000.0	106.4
		Mean:	56.8	5178.7	28.5
	Channel Levee				
		Min:	71.0	1230.0	13.0
	n=9	Max:	120.0	35200.0	100.0
		Mean:	97.3	10344.0	49.7
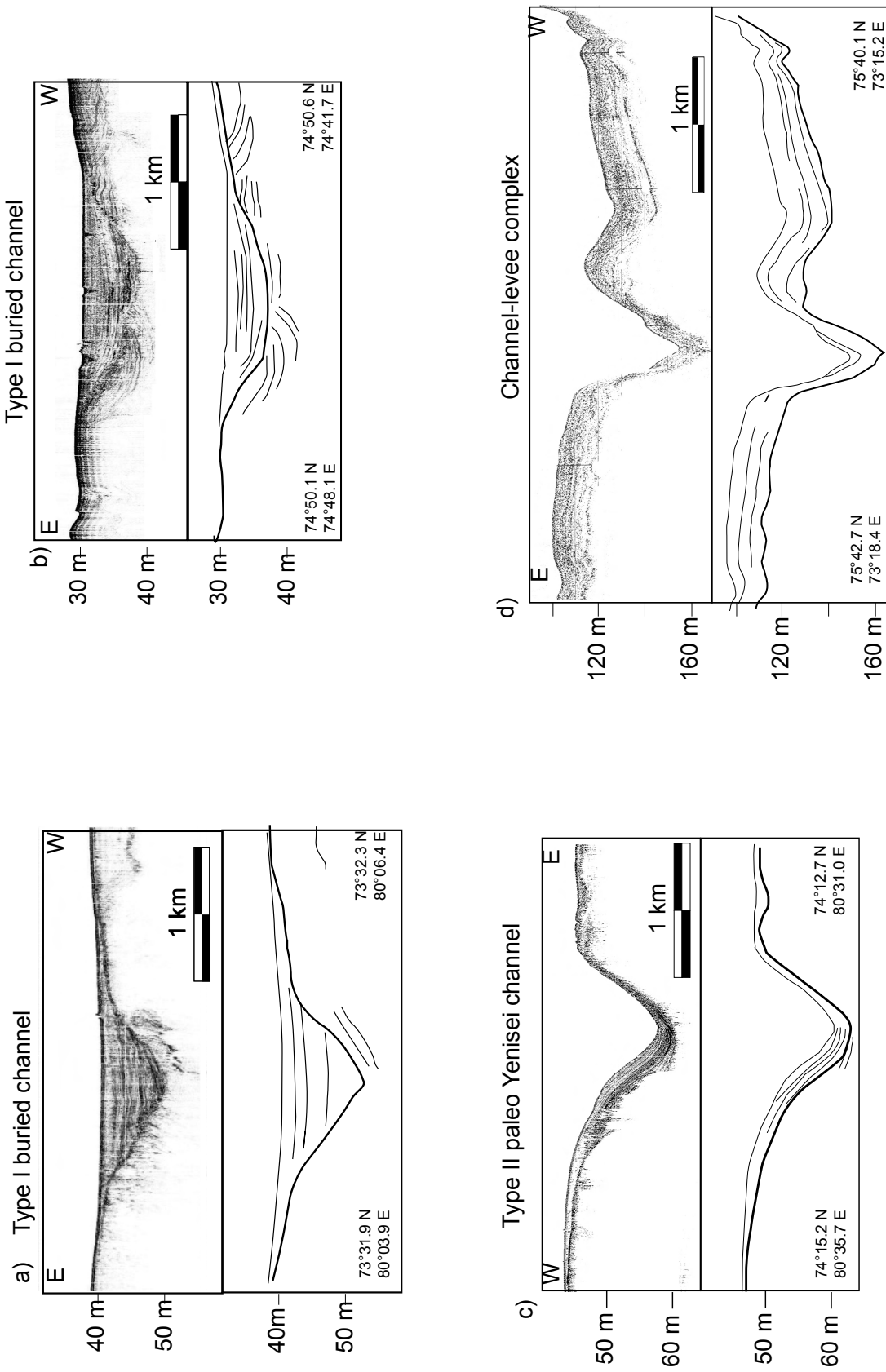
Figure 4. Differentiated channel types; for location see Fig 2. Acoustic profiles of different river channel types; a - d) 3.5 kHz Parasound (Dittmers and Schoster, 2004), e) 12 kHz ELAC (Niessen and Dittmers, 2002) echograms.

channel type clusters predominantly in areas with water depths of 36 m or less.

Type II channels are made up of open, or partly filled, channels (Figs 4 c and d). There is some varying amount of sediment accumulation inside the channel axis. This type of channels has been subdivided on the basis of shelf morphology into a paleo-Ob River branch up towest of 79° E (Fig. 4) and a paleo-Yenisei River branch of channels east of 79° E (Figs 4c). These two types seem to represent and reflect two different morphologies mainly induced by different shelf/slope gradients (Fig. 2). In general, the gradient steepens to the north with increasing water depth, minimising channel width and increasing depth.

The paleo-Ob River channels occur at a mean water depth of 44 m with average bankful-depths of 22.2 m and an average width of almost 2.7 km (Table 2). Compared to the Ob system Yenisei paleo-channels show similar bankful-depths with an average of 28.5 m and distinctively wider developed morphologies averaging to 5.2 km. They cluster around a water depth of nearly 57 m (Table 2).

Nine Channel-levee complexes could be identified in the NW of the working area. In average they are found in 97.3 m water depth, are 10.3 km wide and 50 m deep.

In Figure 5a the relationship between channel-bankful-depth versus water depth is displayed. Type I channels display the lowest depth values. Type II data points scatter widely but show a general decrease in this ratio with increasing water depth, in particular below 50 m water depth. Ob River channels are generally distinguishable from Yenisei River channels by smaller widths. Channel depth in relation to water depth is shown in Figure 5 b. Type I channels are grouped below 50 m of water depth with low scattering and only few individual Channel depths exceeding 15 m. Type II channels show a wider scatter of Channel depth values with the difference that Ob River channels are dominant at higher water depths, displaying higher values than the Yenisei examples and are more scattered. In general, there is a pronounced drop of Channel depth in shallower than 50 m water depth.

The same trend is depicted in Figure 5c), which displays water depth versus channel width/ depth ratio (w/d-ratio). This ratio decreases significantly in more than 50 m of water depth. Type I channels are characterised by highest w/d-ratios, while the Type II channels of the Ob River form the other end-member, with low w/d-ratios. Yenisei River channels lie between both. Again the ratio diminishes distinctly with increasing water depth.

Channel-levee complexes are characterised by high bankful-depth values and relatively small w/d-ratios.

3.3 Spatial distribution of channels on the shelf

Evidence for fluvial incision is visible in the bathymetry especially at the 30 m isobath which is deeply entrenched in the northward extension of the modern river estuaries (North of 74° N; Figure 6). Downstream thalweg slope on the inner shelf, up to 120 m of water depth, gradients of Ob and Yenisei paleo-channels lie in the range of 1:1,351 and 1:4,166, respectively (Fig. 2). There is an apparent difference in the drainage patterns of the Ob and Yenisei rivers paleo-channels on the shelf (Fig. 6). The Yenisei paleo-river pathways display a more dendritic pattern, probably related to channel branch formation around several obstacles such as islands and topographic highs. There are more channel branches in the Yenisei River drainage system, generally trending north-eastward, with smaller tributaries orientated north-westward.

Clusters of paleo-channels have been mapped as river branches which extend across the entire shelf. According to the morphology and abundance of identified channels, paleo-river pathways have been defined (Fig. 6). Branch here describes the general path of channel(s) with incorporation of sea-
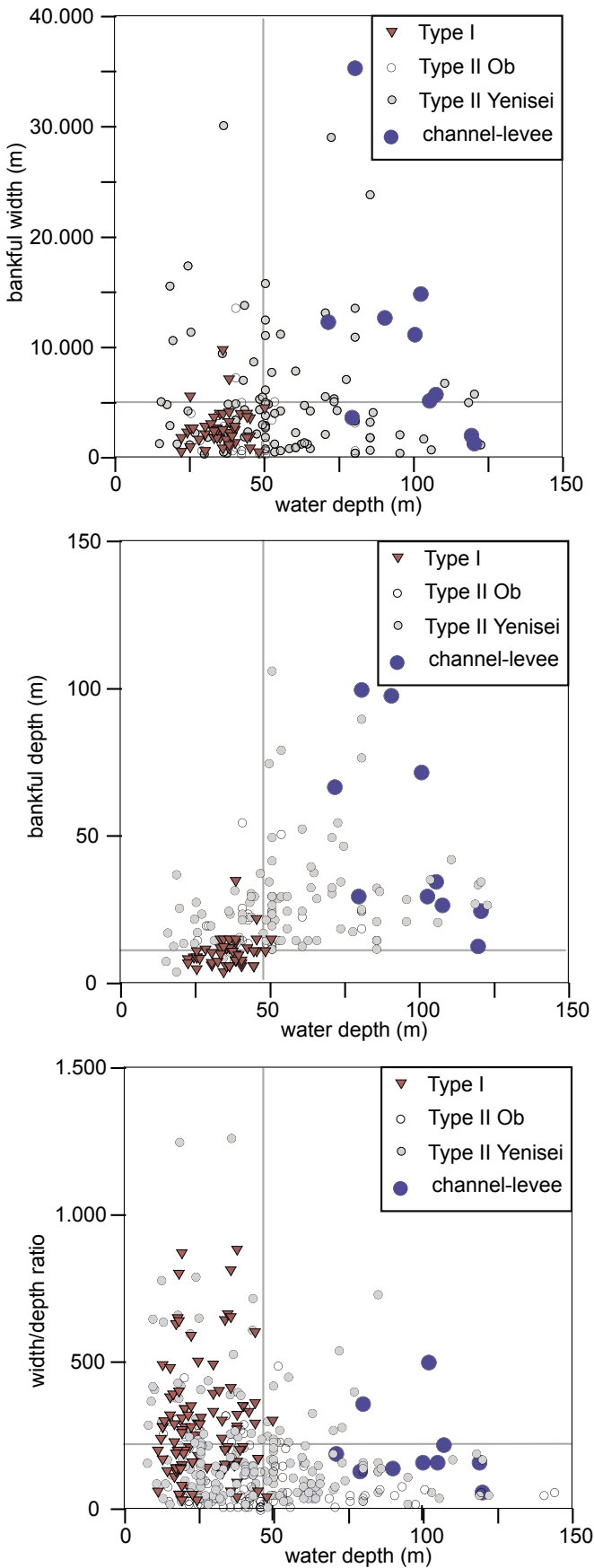
Figure 5. Channel morphometric parameters
a) Relationship of water depth (m) versus channel-bankful width (m)
b) Relationship of water depth (m) versus channel-bankful-depth (m)
c) Relationship of water depth (m) versus channel width/depth ratio
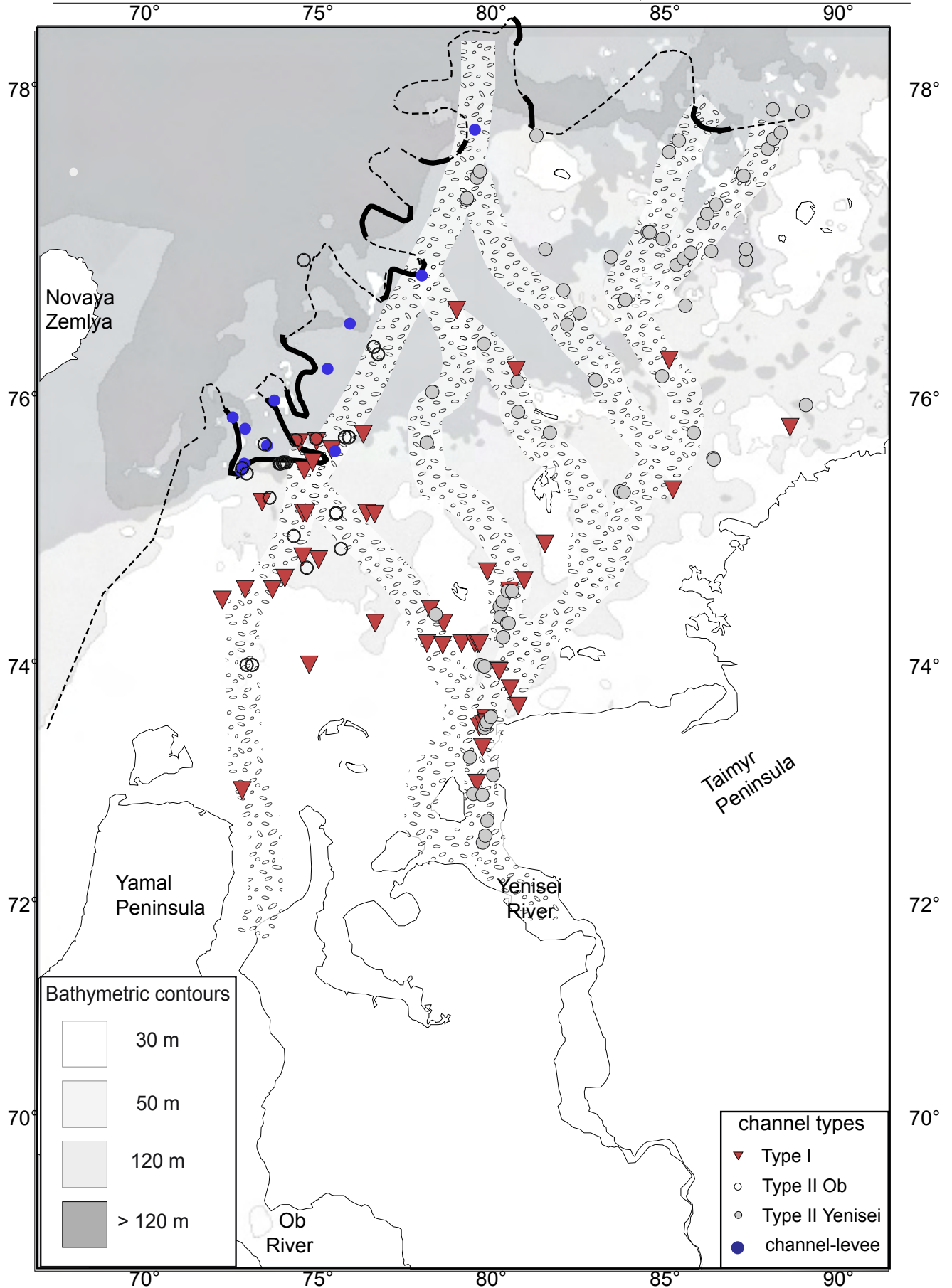
Figure 6. Channel distribution of identified channels, based on channel distribution and sea-floor morphology (Dittmers, 2004). A tentative distribution of major paleo-valleys has been inferred. Type I channel represented by filled triangles, Type II by circles. Paleochannel pathways have been defined by morphology specified by the abundance of mapped channels.

floor morphology (Chapter 3.1). They are large scale depressions with all types of different channels (filled and unfilled), resulting from fluvial incision. Buried and filled (Type I) river channels are concentrated on the inner shelf and are very widespread above 30 m water depth (Fig. 6). Type II river channels show no distinct preferred allocation (Fig. 6) in dependence to water depth. Channel-levee complexes exclusively formed in water depths exceeding 70 m and are associated with the LGM ice margin westward of the Kara Sea Shelf.

4. Discussion

4.1 Isostasy

Little has been known about isostatic movement, the relaxation after crustal down-bending from an ice sheet load, in the inner Kara Sea. In particular, there is still bias about the extent and especially the thickness and loading duration of such an ice sheet. However, these are important factors for the calculation of crustal movements.

Zeeberg et al. (2001) postulate a rebound rate of 1-2 mm/y from an estimated ice load of 1,000 m for Novaya Zemlya resulting in an uplift of 8-16 m for 8 ka but they present no estimates for the Kara Sea. Gataullin et al. (2001) report modest uplift following deglaciation from the south-eastern Pechora Sea, but this area is closer to the proposed centre of the Barents Sea-ice dome. Studies of raised beaches concentrating on Novaya Zemlya reported only moderate uplift of maximally 20 m during the Holocene (Forman et al., 1995, 2004; Zeeberg et al., 2001). This implies that isostatic rebound of the Kara Sea coast is less than eustatic rise and that consequently, the maximum thickness of any ice on the shelf and adjacent coastal plain is unlikely to have exceeded about 400 m (Lambeck et al., 1996; Svendsen et al., 2004). First isostatic rebound modelling results (Chapter 3.4) underline the field evidence.

A radiocarbon dated gravity core BP00-07/5 (632 cm core length) was obtained from the shallow Kara Sea Shelf (43 m water depth) at 80° E, 74° N approximately 150 km south of the islands (Fig. 2). Simstich et al. (2003) argue that linear extrapolation of 5 m uplift at Izvestia Islands for the last 5 ka backwards to 8 ka BP reveals a maximum isostatic depression of 8 m, here. In contrast, Svendsen et al. (2004) resume from the available sea level data that there was no transgression above the present sea level in the Kara Sea region. There is no evidence for raised beach lines on the Siberian mainland in our working area implying neglectable isostatic movement. The same conclusion is ascertained by Dittmers et al. (2003) by comparing dated sediment cores from the Yenisei Estuary with the Fairbanks (1989) sea level curve. Estimates of eustatic sea level during LGM indicate that sea level was approximately 120 m lower than today (Chappell and Shakleton, 1986; Fairbanks, 1989, Chappell et al., 1996).

Neglectable isostatic movement is also supported by first occurence of dinoflagellates in core BP99-04/7 in correlation with Fairbanks´ (1989) sea level curve (Kraus et al., 2003; Stein et al., 2003b, 2004)

4.2 Fluvial style of Ob and Yenisei rivers and paleohydrology

In case the profile of a river does not coincide with the equilibrium profile, the river will re-adjust its gradient in order to reach equilibrium, by either erosion into its substratum, or the river will aggregate by accumulating sediment on the floodplain and the channel (Allen and Posamentier, 1993). When the river has attained its equilibrium profile, it is said to be at grade (Allen, 1992). When relative sea level exposes a shelf with a different slope than the equilibrium gradient of the river (Schumm, 1993), valley incision is commonly thought to occur at the knickpoint that develops at the topographic shoreline and shelf-slope break retreating upriver.

Channel classification

Leeder (1973) and many other researchers (e.g. Osborn and Stypula, 1987; Schumm and Khan, 1972) used w/d-ratio of stream channels as a classical parameter to characterise dimension and shape controlled by the hydraulic regime. Flood and Damuth (1987) were the first to apply fluvial geometries of subaerial formed meandering rivers for submarine channel-levee systems of the Amazon fan successfully.

Fielding and Crane (1987) assembled data from numerous studies to differentiate styles of fluvial geometry. The w/d-ratio is suited here to discriminate between braided, meandering, and straight channels in particular. Although the relationship is not straight forward and there are other "degrees of freedom" (Morisawa, 1985) to be considered, as e. g. initial relief, lithology, climate, and vegetation (Schumm, 1977, 1981), it serves as a good first order discrimination and classification scheme. Our data plotted in this scheme illustrates the different fluvial styles of Type I and II channels and between Ob and Yenisei channels (Fig. 7). Interestingly, size relationships on the shelf represent a straight prolongation of recent channel proportions on land (after Chavlov, 1994), which is a typical feature of stream systems (Leopold and Maddock, 1953), indicating that they are related features. Generally, their morphologies display features an order of magnitude larger than the dimensions of recent fluvial cross sections on land.

Meandering rivers make up the majority of all channels under investigation. All channels on land and the majority of Type I and II channels represent this class (Fig. 7). Except for Type II channels and minor recent channels, most channels representhe "fully developed" meandering streams (Collinson, 1978). There is a slight difference between Type II Ob and Yenisei River channels. The Yenisei River channels cluster

Table 3. Discharge characteristics of several gouge stations in the West Siberian Lowland; data by courtesy of Aleksey Y. Sidorchuk (sidor@yas.geogr.msu.su)

gauge station	mean annual discharge (m³/s)	bankful discharge (m³/s)	width (m)	depth(m)
Kuibyshev	20,4	184	76,8	4,4
Demianka Lymkoevskie	145	953	138	6,8
Konda Chantyria	76,1	102	83,3	2,6
Konda Urai	123	235	123	3,2
Konda with Bolchary	286	551	262	3,3
Konda with Altai	327	424	208	3,4
Amnya with Kazym	61,6	52,7	97,2	1,2
Sev Sosva with Nyaximvol	90,1	369	130	3,2
Sev Sosva Kimkiasui	269	468	169	5,1
Sev Sosva with Sartynia	652	780	679	4
Sev Sosva Igrim	750	3190	497	6,7
Lyapin with Saran Paul	248	1360	520	5,5
Sob Kharp	30,1	150	63	2
Polui with Polui	132	364	133	4,6
Nadym Nadym	446	192	160	1,9
Pur Urengoi	801	4470	1300	4
Pur Samburg	899	4610	1240	4,9
PyakuTarkocakeice	298	2740	5,6	4,4
Basin Sidorovsk	1070	3750	625	8,1
Ob Barnaul	1470	3960	338	9,1
Ob Stone Calculuson	1560	4960	703	6,8
Ob Mogochino	4110	11700	1260	7,7
Ob Kolpashevo	4260	11400	835	9,6
Ob with Belogore	10300	21800	1300	16
Ob Salekhard	12300	25900	2240	13,1
Berd Maslyanino	20,1	132	107	1,6
Berd Iskitim	45,8	300	110	2,3
Tom Mezhdurechensk	168	1660	334	4,2
Mras Ust	67,1	616	103	2,9
Mundybash Mundybash	22,6	281	69,8	1,8
Top Ters Aspen Pleso	47,6	481	80	2,6
Comp Ters Monashka	82,2	587	142	1,9
Taidon Medvezhka	47	454	100	2,4
Chulym with Balakhta	102	599	113	3,9
Chulym with Zyryanskoe	550	1530	467	3,7
Chulym with Sergeevo	737	2760	594	4,6
Chulym Kommunarka	794	2900	508	5,5
Uriup with Izyndaeva	31,9	131	92,7	1,4
Kiyacuecue Kiyacue Mariinsk	148	719	162	3,7
Kiyacuecue Kiyacue Okuneevo	177	781	192	4,5
Ket Maximkin Yar	243	793	208	4,6
Orlovka Druzhnyi	63,5	281	128	2,9
Chuzik Osipovo	30,5	225	240	2,2
Vasiugan	164	557	162	5,6
Vasiugan Naunak	381	1020	244	7
Tym with Vanzhil	74,3	567	128	5
Tym with Napas	182	612	195	3,8
VakhwithLobchinskoe	504	1150	245	7,8
Tromwith Ermakovo	102	362	244	2,1
Agan with Var	127	630	117	5,9
Pim Pim	68,2	217	168	1,8
Lyaminfact Gorshkovo	81,4	423	111	4,4
Bollugan with Ugut	143	402	159	4,4
Tobol with Zverinogolovskoe Zaboloch	26,2	172	126	2,2
Tobol Mound	45	364	124	4,6
Tobol with Lipovskoe	809	3500	411	8,3
Iset Kataisk	23,9	300	249	3,8
Iset with Mekhonskoe	64,8	109	175	2,9
Iset with Isetskoe	68	299	150	4,2
Miass with Newly	7,1	50,1	33,9	1,4
Miass with Sosnovskoe	12,4	105	36,9	2,5
Miass with Karachelskoe	14,7	200	115	2,5
Tura Turinsk	109	500	149	5,2
Tura Tyumen	178	1180	230	5,9
TavdaTavda	462	1580	244	7,8
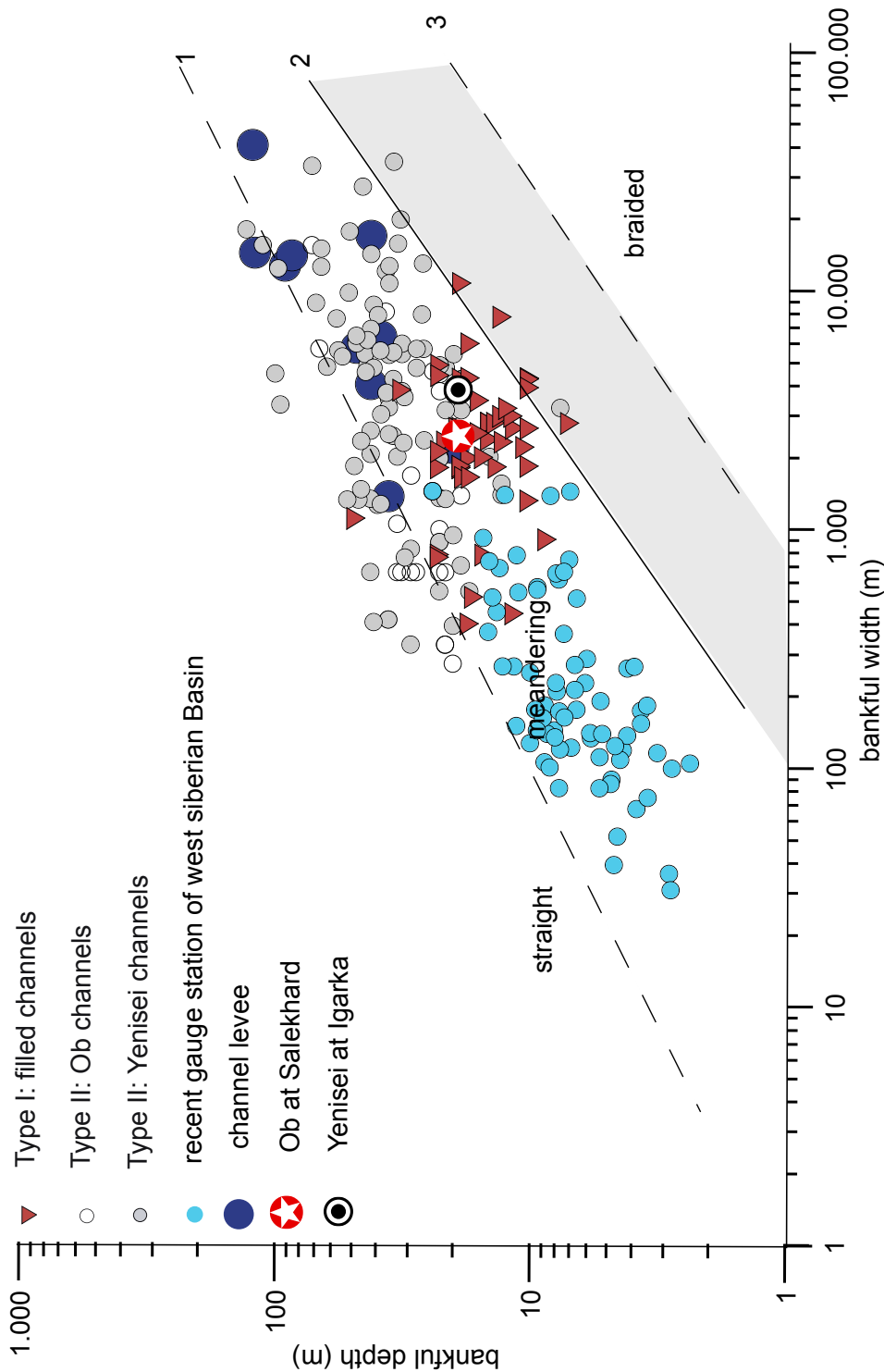
Figure 7. Bankful width and depth of channels under investigation plotted in classification scheme according to Fielding and Crane (1987), recent dimensions of Ob and Yenisei rivers at Salekhard, Igarka, respectively; note double logarithmic scale. 1) refers to upper boundary for meandering rivers; 2) the limit of Collinson's (1978) "fully developed" meandering streams; 3) shows the bounding line for deposits of meandering rivers and represents deposits of laterally unrestricted rivers, such as braided rivers. Small filled circles stand for channel dimensions of recent gauge station of west Siberian lowland (see Table 2).

closely between line 1 and line 2 (Fig. 7), characterised by high w/d ratios and some of them come close to the "braided river field", probably resulting from a lower general slope gradient. In contrast, the Ob River channels exclusively plot to the left of line 2 and closer to line 1 (Fig. 7). The Ob and Yenisei river geometries reflect different

shelf physiography, whereas Type I channels probably represent a different mode of channel genesis. No channels plot in the "braided river field", but the majority of the "fully developed" meandering streams (Collinson, 1978). The Yenisei River channels cluster closely between line 1 and line 2 (Fig. 7), characterised by high w/d-ratios and some of them come close to the "braided river field", probably resulting from a lower general slope gradient. In contrast, the Ob River channels exclusively plot to the left of line 2 and closer to line 1 (Fig. 7). The Ob and Yenisei river geometries reflect different shelf physiography/gradient, whereas Type I channels probably represent a different mode of channel genesis. No channels plot in the "braided river field", but the majority of Type I plot between line 1 and 2 in the true meandering river field (Fig. 7). Channel-levee complexes are characterised by relatively high thalweg depth values and bankful widths, but depict the general trend and rarely fall into the straight channel field. It should be emphasised that they are underwater formations with different physical processes behind especially the density contrast between air and water and sediment-saturated water to sea water is highly different. But interestingly their dimensions, and morphometric behaviour is similar to subaerially formed meandering river systems (Clark and Pickering, 1996; Flood and Damuth, 1987).

The filled channels are consequently interpreted as small tributaries, existing for short distances, quickly feeding into more stable, longer lived channels that are more deeply incised, and self-adjusting to the shelf gradient (Schumm, 1993). This is reflected in higher w/d-ratios. This type could be classified as immature as it is not adapted to the equilibrium profile, because adjustment of base-level to a st eady state has not been achieved. In contrast, meandering channels act as relatively stable sediment transport agents by-passing suspended material after incision (Schumm, 1981). The spatial distribution of the differentiated channel types is shown in Figure 6.

Examples of Yenisei channels are shown in Figure 8 a) to c) as typical meandering channels of the middle Kara Sea Shelf.

Figure 8 Examples of Type II Yenisei channels in the vincinity of recent estuary (Fig. 2 for location).

Submarine channel-levees are concentrated along the LGM ice margin (Figs 9 and 10). They are indicative of underwater formation as described by Flood and Damuth (1987) from the Amazon fan. Water depth of channels exceeds 80 m in all cases.

Paleo-hydrology

By analysing hydraulic geometry of streams, Leopold and Maddock (1953) and Matthes (1956), later refined by Dury (1964, 1965, 1967), found that in both, normal and flood conditions, stream width, depth and velocity increase as simple power functions of discharge. From records of streams and rivers in central and southwest USA, they established that the depth of a channel increases nearly as the square root of discharge, regardless whether it is a small mountainous river or a large stream (Dury, 1967). The same rules for channel width, but with a different local factor.

Rivers often act as recorders of sudden catastrophic events rather than of "normal" discharge conditions prevailing most of the year (Schumm, 1977, 1981). Channel forming stages and incision events, for example, occur during bankful discharge, when stream power increases dramatically (Dury, 1986). In the Arctic realm these events usually coincide with the snow melt originated spring flood. Thus, all geometries might reflect only one event in an extreme situation. In our working area the quantification of pre-Holocene fluvial discharge is hard to determine from the maximum discharge channel (geometry) forming stage, as it rather reflects a momentary annually re-occurring event.

Although difficult to quantify it is evident from Figure 7 that channels on the shelf, thus, represent higher discharge events than their recent analogues on land (Fig. 7). There are several arguments for higher peak discharge that could explain the greater geometries of the channels under examination. These could be possibly related to a hinterland blocking of the Ob and Yenisei rivers as proposed by Yamskikh (1996, 1998). He reports several fluvial terraces, dating into the late Weichselian, in the upstream Ob and Yenisei rivers interpreted as polycyclic short time blocking events, in the order of months, due to ice damming in narrower parts of the river bed, combined with catastrophic release events.

Another explanation are "macro meanders", fluvial features an order of magnitude larger than recent fluvial dimensions, formed during the LGM/postglacial transition until 14 ka BP (Sidorchuk et al., 2001). They relate these features to a very punctuated river run-off during glaciation; although the mean precipitation was lower than today, an increased discharge may have been caused by the existence of permafrost, draining all surface waters immediately towards the river.

Furthermore, river run-off volume is reduced by peat accumulation since 14 ka BP with a distinct peak during 11.5 - 9 ka BP in the West Siberian Lowlands (Kremenetski
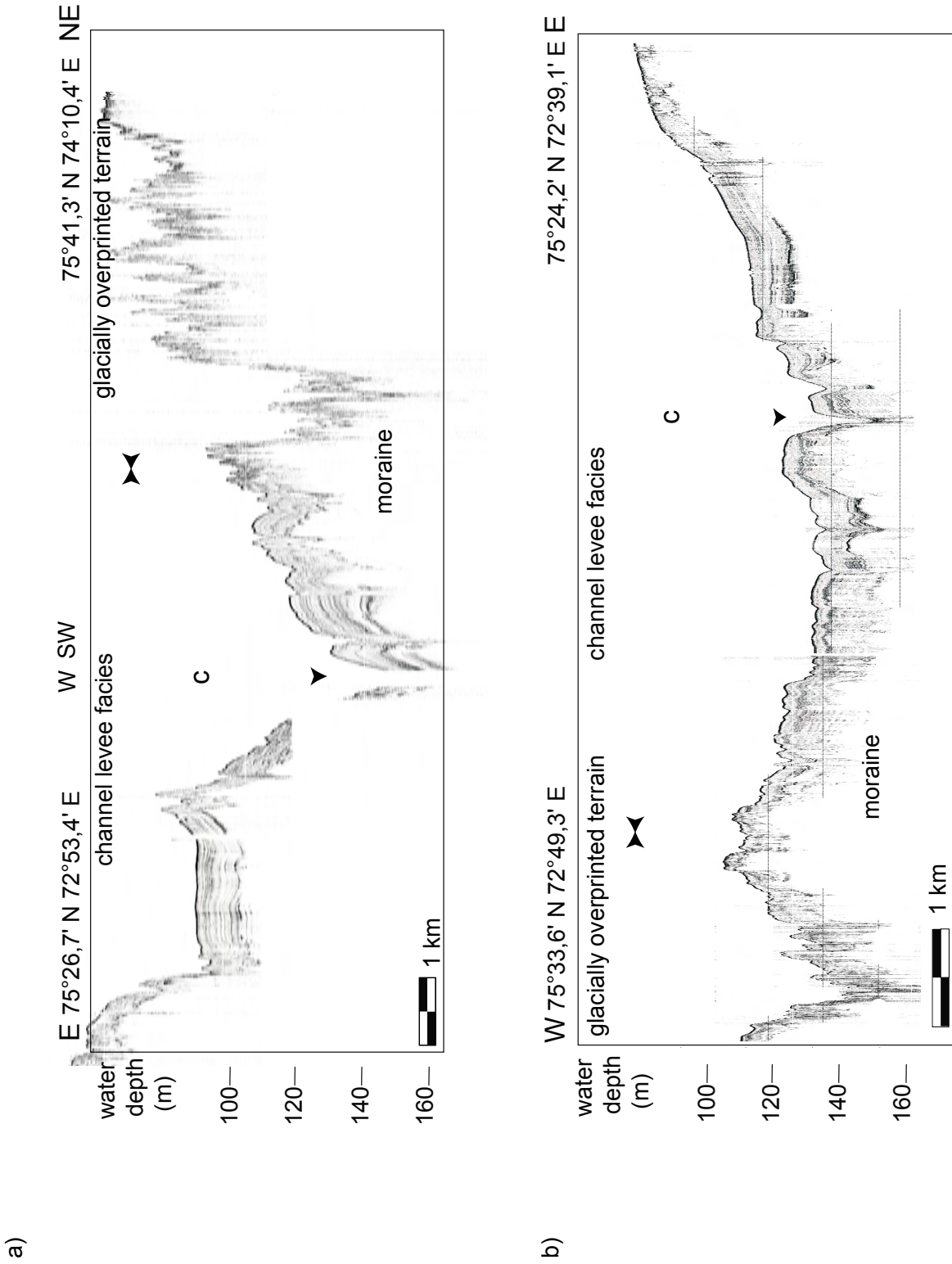
Figure 9. Parasound run at 3.5 kHz Examples of fluvial facies neighbouring to LGM margin (Fig. 2 for location). Profiles were recorded with the 12 kHz ELAC system and Figure10 with ELAC 12 kHz. Glacially overprinted terrain is characterised by typical hummocky relief, related to glacial deformation. Channel-levve facies is characterised by overdeepened channel with wide adjacent floodplains, made up of thick sediments. Note abrupt change in facies; there is no indication for glacial facies underneath fluvial facies. Moraines possibly represent terminal moraines of LGM.
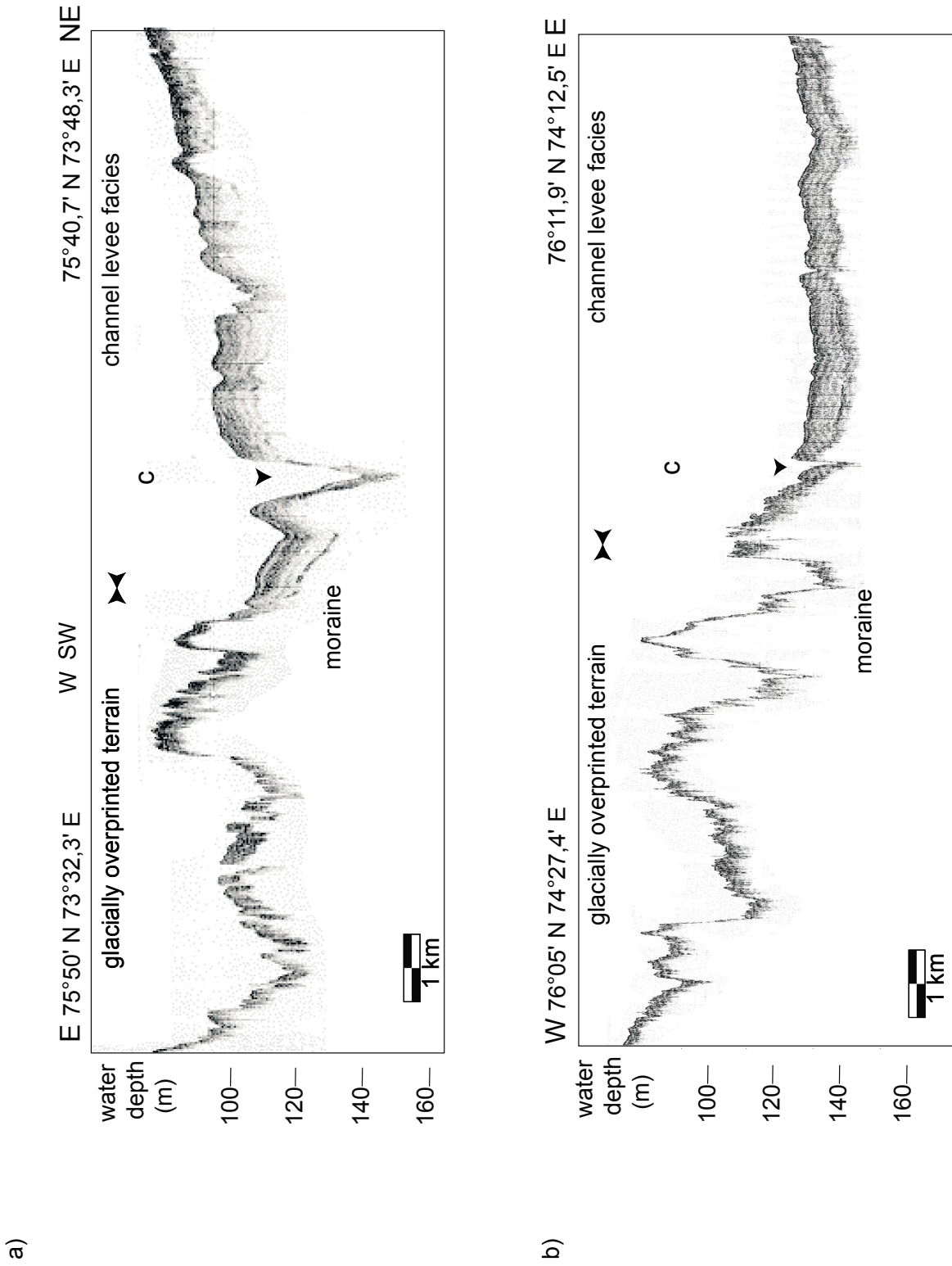
Figure 10. ELAC 12 kHz examples of channel-levee facies neighbouring glaciated area.

et al., 2003; Smith et al., 2004). These accumulations have lead to the formation of the worlds largest peat lands possibly containing 50 % of the total worldwide peat (Smith et al., 2004). Today, this large area acts as a buffer for the whole discharge dynamics and store huge amounts of water. Another important factor for the sudden release of huge water masses is the whole post-glacial termination process, manifested for example in sediment cores by a distinct susceptibility spike after deglaciation (Kleiber et al., 2001; Dittmers et al., 2003). The peak is explained by enhanced decay of continental (Putoran) ice sheets and increased fluvial discharge rates due to climatic warming (Kleiber and Niessen, 2000; Dittmers et al., 2003). This incident does not only mark the melt down of the Circum-Arctic and Putoran ice sheets, but also the degradation of permafrost, enhanced precipitation, and the decay of mountain glaciations in the whole drainage area (Velichko, 2002; Svendsen et al., 2004). All these processes boosted up the amount of water released and drained towards the Arctic Ocean. The above arguments lead to the picture that peak discharge during late Weichselian and Termination I has been even more pronounced and enhanced, compared to today, despite of a smaller total net water discharge during glacial times.

Difference between Ob and Yensiei paleo-channels

To estimate the discharge of both quantitatively, we calculated the relationship of channel depth and discharge volume of recent distributary channels in order to establish a characteristic basin discharge (data provided by Sidorchuk, pers. comm., 2004). As outlined earlier the depth of the paleo-channels is always determined correctly. On the basis of this relationship we took the average depth of Yenisei and Ob paleo-channels (Table 2) and calculated both the annual discharge, 15,089 m^3/s and 8,494 m^3/s, respectively, and the bankful discharge, 20,225 m^3/s and 12,271 m^3/s, respectively (Fig. 11). As expected from Figure 7 the paleo-examples resulted from higher (peak) discharge, but furthermore the Yenisei channels indicate significant higher discharge volumes, almost twice as high as the Ob examples.

Spielhagen et al. (2005) studied sediment core PS 2456 on the Laptev Sea shelf and describe oxygen-isotope fluctuations in foraminifera caused by regional freshwater release from ice masses. Their study reveals a major excursion from 13 ka BP to 12.2 ka BP with the distinct lack of foraminifera in this interval, due to a salinity drop below critical limit. They interpret this finding with the massive partly ice-dammed river-water release of the Lena river. This event lasted for 350-400 years and they postulate a catastrophic water release of 100, 000 km^3 and resulting in a salinity drop of 1.2 ‰. We think this event marks the deglaciation of the Hinterland feeding the drainage area, as documented by the abundant susceptibility spike of Kleiber and Niessen (2000, 2001),
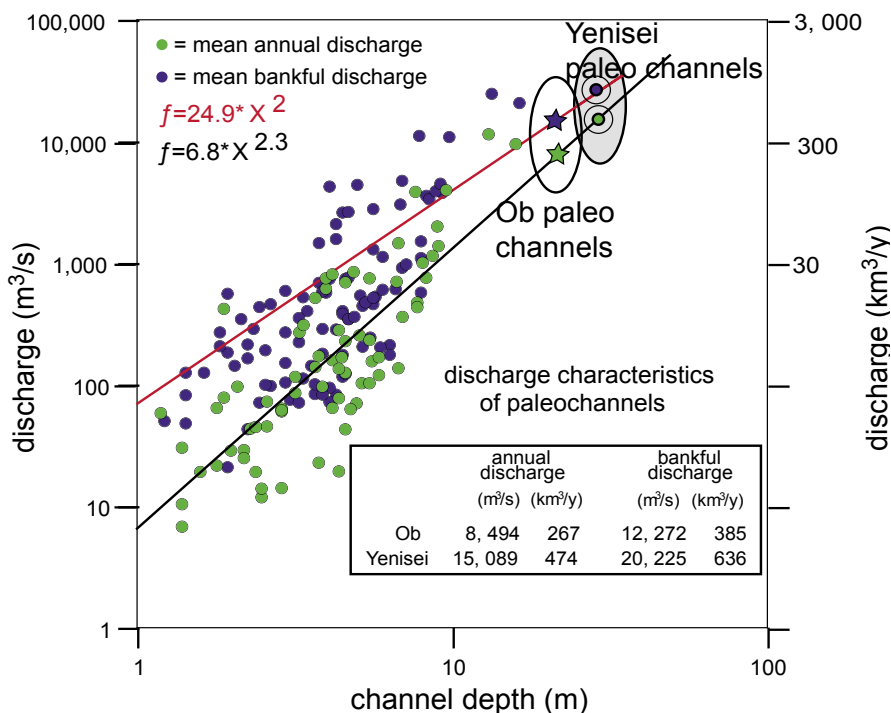
Figure 11. Calculated relationship of Channel depth and discharge volume of recent distributary channels of the Ob and Yenisei catchment (data basis is shown in Table 2, for the Ob and Yenisei paleo-channels the average depth is 22.2 m and 28.5 m, respectively). Note double logarithmic scale. As outlined earlier the depth of the paleo-channels is always determined correctly. On the basis of this relationship we took the average depth of Yenisei and Ob paleo-channels (Table 2) and calculated both the annual discharge, in order to account a characteristic basin discharges.

which is documented in the Kara Sea as well (Chapter 3.3 and 3.4). We would like to consider the possibility that the Putoran Mountains contributed to the paleo-discharge of the Yenisei river and could be responsible for the larger fluvial dimensions of Yenisei channels and larger paleo discharge values.

Today 80 % of the water volume drained from the Putoran Mountains flows into the Yenisei, i.e. 430 km³/y, while approximately 100 km³/y drain into the Kathanga and Anabar (Rachold et al. in Stein and MacDonald, 2004). We determined the portion of the Putoran Mountains that lie above 500 m with the GIS tool Global Mapper based on the IBCAO data set: 285,015 km². Assuming that 300 m of ice accumulated summing up to a volume of 85,205 km³, a number in correspondence with Velichko et al.`s (1997) estimate of 80, 000 km³ (Table 4). We think it plausible to assume that this additional melt-water volume boosted up the Yenisei paleo-discharge and is responsible

Table 4. Discharge estimates based on different ice thicknesses of the LGM Putoran ice cap are shown in the first row (hatched box denotes the most realistic) and annual discharge volumes additionally released into the Yensiei in the last columns for different discharge periods. Today approximately 80 % of the total Putoran water Volume is drained into the Yenisei (Rachold et al. In Stein and MacDonald 2004).
The shaded boxes indicate values that match into the estimated discharge difference of Ob and Yenisei

Ice (m)	Total Ice volume (km³)	Drainage area (km²)	water volume draining into the Yenisei (km³)			average annual discharge during 200 years (km³/y)			average annual discharge during 400 years (km³/y)			average annual discharge during 1000 years (km³/y)		
			60%	70%	80%	60%	70%	80%	60%	70%	80%	60%	70%	80%
100	28502	285015	17101	19951	22802	86	100	114	43	50	57	17	20	23
200	57003	285015	34202	39902	45602	171	200	228	86	100	114	34	40	46
300	85505	285015	51303	59854	68404	257	299	342	128	150	171	51	60	68
400	114006	285015	68404	79804	91205	342	399	456	171	200	228	68	80	91
500	142508	285015	85505	99756	114006	428	499	570	214	249	285	86	100	114

for the larger extensions of Yenisei paleo-channels on the shelf. Table 4 summarises the ice volume in relation to different ice thickness and discharge portions draining into the Yenisei.

It is remarkable that a sudden decay of a relative thin ice cap (300 to 400 m, red box in Table 4), could account for the additional water volume released over a time period of several hundred years. Spielhagen et al. (2005) date their "freshwater event" after 13 ka falling into the younger Dryas. It is known from pollen studies that temperatures in middle Siberia had been higher than today (Hubberten et al., 2004). A change from dry hot to humid climate occurred since 12.5 ka BP, which could mark the triggering of the ice decay. We propose a relatively sudden warming event that led to a rapid (self accelerating) non-linear meltdown of the Putoran/Siberian ice masses. It is obvious that a complete decay of the whole ice mass could not have occurred in this short interval. However, the process could have been enhanced by additional hinterland melting in the upper reaches of the river system in the Altai mountains for example.The same processes could have happened in the Laptev Sea and boosted up the riverine water discharge.

4.3 Development/evolution of channel geometry

Channel depth and width in dependence to water depth (Table 1, Figure 5) increase and decrease, respectively, down slope as observed for natural rivers (Schumm, 1977). This confirms subaerial formation and no underwater setting as for e.g. the well-studied Amazon fan where these attributes behave inversely (Flood and Damuth, 1987). Schumm (1993) reports that channels rather incise into steeper parts of the slope than deposit material. This accounts for the progressive decrease of channel width and vice versa, increasing channel depth (Fig. 5c) with increasing water depth, which yields a steeper gradient in our working area (Fig. 2). Considering the distribution of channels versus water depth (Fig. 5a) in the light of changing sea level (Chappell et al. 1996; Fig. 12) the Kara Sea comprises some information about channel incision.

In Figure 12 channel formation and infill is drafted according to their sequence stratigraphic interpretation introduced by Dittmers et al. (2003). Channel incision ceases as soon as sea level starts to rise giving (accommodation) space for transgressive sediments. Channel-fill pattern is dependent on sediment supply and relative position of the channel on the shelf during transgression. Filled channels concentrate in water depths below 50 m, probably representing an area of most intense reworking during transgression. On the other hand, terrestrial sediment supply might have abated during passage over the shelf, only reaching shallow water depths. As shown by Dittmers et al. (2003) most of the fluvially-derived material is stored in the Ob and Yenisei estu-
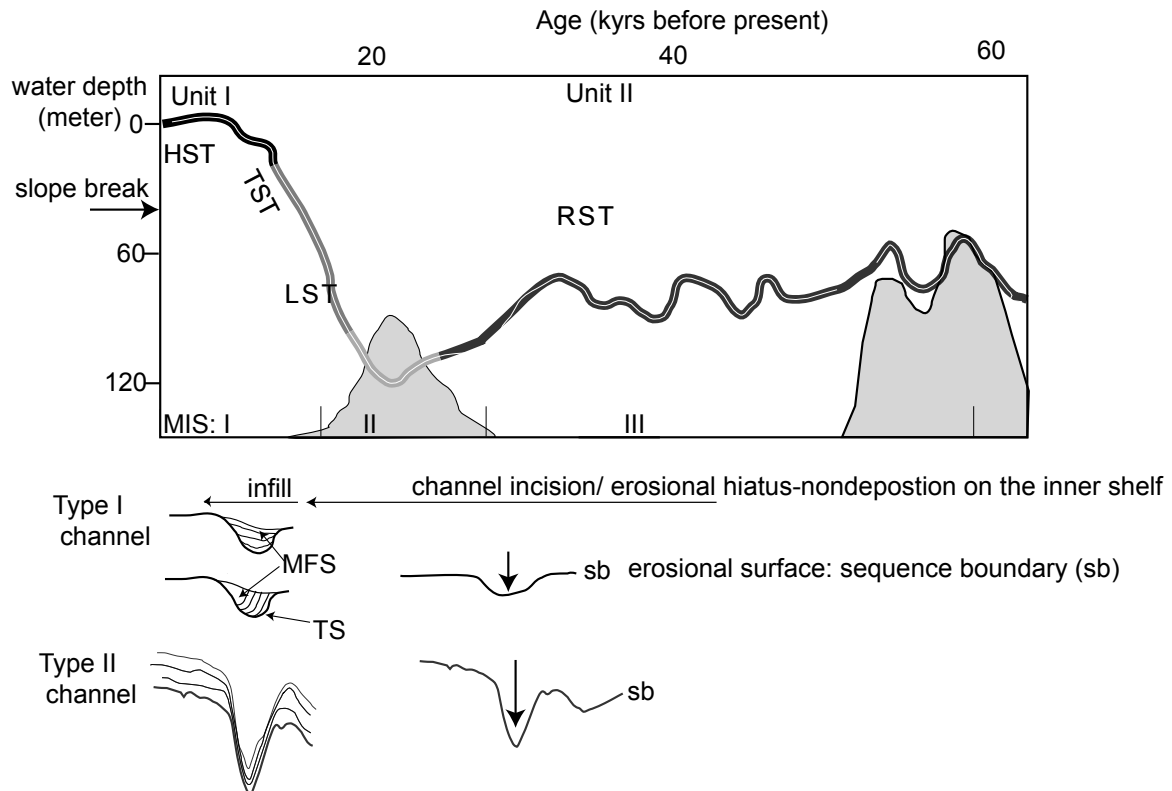
Figure 12. Eustatic sea level curve for the last 120 ka BP (after Chappell et al., 1996). Main marine isotopic stages, according to Mangerud et al. (1996), are given in roman numbers; glaciations of Kara See area are indicated by grey-shaded areas (Mangerud et al., 1999, 2001); sequence stratigraphic system tracts are indicated in capitals: RST = regressive system tract, LST = lowstand system tract, TST = transgressive system tract, HST = highstand system tract; terminology as defined by Mitchum et al. (1977), according to Dittmers et al., 2003. (Chapter 3.4) Enlarged section of curve with identified depositional units and major events of fluvial incision with succeeding infill phase compromising the last 30000 years. Major sequence stratigraphic events are given in abbreviations: TS = transgressive surface, MFS = maximum flooding surface, see Chapter 3.4.

aries during Holocene times.

Figure 13 shows a longitudinal profile of the whole drainage area. The slope increases continuously from south to north and as a consequence channels incised into the shelf in contrast to an "unincised" scenario (Schumm, 1993; Sommerfield et al., 1995) where the shelf gradient is lower than in the Hinterland. As slope increases stream power, it increases the tendency for channels to incise (Schumm, 1993). During subsequent transgression, these areas of increased accommodation space are preferred sedimentation areas.

4.4 Paleo-environmental implications

It is still under debate whether there was a pro-glacial basin in front of the LGM ice sheet resulting from blocked Siberian rivers or not (e.g. Mangerud et al., 2001; Polyak et al., 2002; Stein et al., 2002). From our data there is no evidence for such a lake, a deeper/still-water sedimentation on the shelf such as draping sediments in morphological depths as proposed by Polyak et al. (2002). In contrast underneath the recent
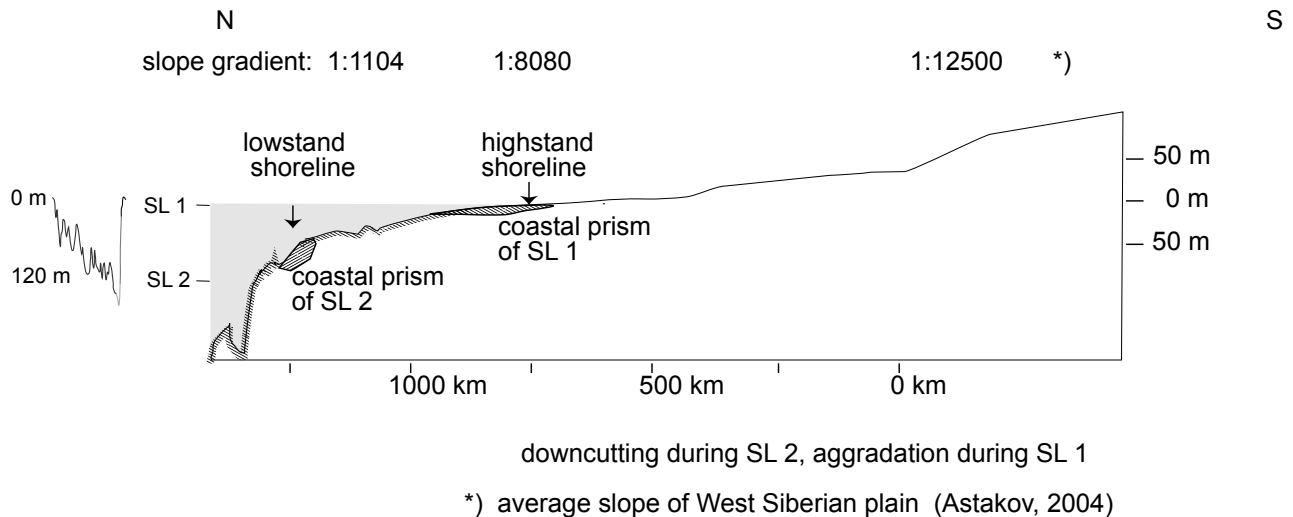
Figure 13. Schematic section through the Kara Sea Shelf and adjacent hinterland of the West Siberian lowland; principle slopes of morphological segments are indicated at the top; amplitude of sea level fluctuations during the Weichselian shown in the left; SL1= recent; SL2= LGM.

water depth of 100 m another facies is encountered at the NW and NE corner of the working area, representing subaqueous formations. Stratigraphically they represent the upper part of a "lowstand fan" (Piper and Normark, 2001) of a "lowstand wedge" which must have been formed during sea level lowstand (Posamentier and Vail, 1988; Posamentier et al., 1992).

Channels on the shelf shallower than 100 m recent water depth

Most of the channels under investigation plot in the fully developed "meandering river" field (Fig. 7), meaning they are quite mature in terms of fluvial development. Although an absolute chronology is missing, the nearly 700 km northward extent of fluvial features on the shelf north of the Ob river, the good conservation of incised channels and their maturity, argue for a long lasting fluvial-dominated history of the Kara Sea Shelf. The findings of Mangerud et al. (1999) and Svendsen et al. (1999) and the widespread occurrence of the "markhida line" on the Siberian mainland indicate a middle Weichselian glaciation having originated in the north at approximately 60 ka BP. This former glaciation would have annihilated the most prominent geomorphological features by overriding the whole southern Kara Sea Shelf, leaving behind a typical rough ground moraine surface as visible in Figure 9 and 10. Into this newly formed topography subaerially exposed rivers started to incise, creating the regional basal unconformity (Dittmers et al., 2003) (Fig. 12), conveying sediments across the shelf towards its edge.

Deeper water (<120 m) facies
NW area

Channel-levees show a delineation of the thalweg route by the LGM ice sheet, and in some places, individual channels directly border to end moraines (Figs 9 and 10) and topographic highs which acted as dams. The marine extensions of the Ob branch clearly postdate the underlying glacial morphology. Thus, here the time of channel formation could not have been initiated before the LGM (approximately 20 ka BP). There are several examples where the areas occupied by LGM ice with its severely deformed topography (Figs 10 a and b) lie deeper than the adjacent channel-overbank complexes. This fact leads us to the conclusion that there still was a certain amount of ice that hindered the channel to enter the lower terrain and channel-levee formation occurred during the physical existence of ice bodies (Chapter 3.4). In classical glaciomarine environments sediment normally accumulates adjacent to the ice in depressions, whereas morainic facies is found in the higher ground (e. g. Dowdeswell et al., 1998; Syvitski et al., 1996; Vorren et al., 1998). According to the Fairbanks (1989) sea level curve and given the fact that isostasy only plays a minor role in our working area, a average water depth of ca. 100 m of the channel-levee complexes would give a maximum age of 14 ka BP (Fig. 14), as they represent underwater formations. Although our evidence bears no absolute chronology, the relative timing implies a synchronous or later formation of channels adjacent to the LGM ice border. It is also possible that large dead ice blocks were separated from the ice sheet during its decay, with the channels flowing around them. The ice blocks could have survived the major part of the postglacial transgression, especially when subjected to sediment entrainment during stranding on the shelf. The water column necessary to elevate an ice package can be estimated by sea-ice = 900 kg m^{-3} water = 1,028 kg m^{-3} densities (Fricker and Padman, 2002) meaning that the water depth needs to exceed ice thickness by approximately 114 %. Channel-levee complexes have been identified at an average water depth of ca. 100 m. Some 120 m of sea water column are necessary to establish a hydrodynamic equilibrium and higher water levels are necessary to elevate an ice body with minimum thickness of 100 m; thus a relatively thin body of ice could have survived the major part of the post-glacial transgression. Probably all processes interacted and submarine channels were deflected by the remnants of the LGM ice sheet, but during its decay, there were some "break-throughs" and the flow pattern reorganised itself, finding new pathways, typical for glacial environment (Elverhoi et al., 1998, 1989). However, an exact (side scan sonar) survey of ice marginal channel-levee complexes with a very high spatial resolution could reveal the exact timing.

The Amazon fan has become a reference example for passive margin channel-levee systems and acts as a good depositional analogue for channel-levee formation

in our working area. Mikkelsen (1997) report sedimentation differing in three orders of magnitude rates of 5 cm/ka during interglacial times with only pelagic background sedimentation and 5,000 cm/ka during glacial times when sediments are channelled to the deep sea. Typical "lifespans" of individual channel-levee systems vary between 1-3 ka (Piper et al., 1997). Once a submarine levee route has been established it is relatively stable, and major adjustments in the self-stabilizing channels pathway are unlikely, ignoring the surrounding morphology. Avulsion and abandonment of channel-levee complexes is triggered by changing sea levels, climatic controlled sediment supply and auto-cyclic processes (Flood et al., 1991): It is likely for our specific environment sea level fluctuations combined with formation and disintegration of (dead) ice caused channel fluctuation and migration.

Interestingly the channel-levee complexes are located at transition from the shelf to basin areas as for example the Novaja Zemelya trough at the shelf/slope breaks with relatively steep gradients. Direct downslope gradient (perpendicular to the ice margin) would have resulted in canyon entrenchment, typical for the upper fan (Bouma, 2000). In contrast sediment transport was oriented parallel to the shelf morphology, resulting in a shallower thalweg gradient enabling the upward growing channel-levee complexes. According to Nelson and Kulm (1973) channel-levee systems occur preferentially between slop gradients of 1:1,000 and 1:4,000. For the Kara Sea these values are found at the shelf/slope break where all of the identified channel-levee systems are located. Average sediment thickness at thalweg is 15 m, which is in good agreement to the average life span of 2 ka Documented channel-levee complexes are not likely to have been connected or formed at the same time, although channel thalweg depths could indicate a progressive northward deepening (Fig. 14). For the Kara Sea channel-levee complexes, we favour an analogon to the Amazon fan model where the documented channels on the shelf act as feeder for the channel-levee complexes formed as under water extensions of the river mouth estuarine point sources, characterised by locally high sedimentation rates. With progressive transgression these point sources migrated southward towards shallower water depths. According to this hypothesis the northernmost channel-levee system is the oldest and to the south, with shallower water depths, channels are younging.

Deeper water (<120 m) facies
NE area

The sediment accumulation in the NE corner of the working area characterised by ponded muds (Fig. 14), with high sediment thicknesses (Fig. 15). No LGM ice or glaciation traces are visible for the LGM, no major undercurrent sub aqueous channel-
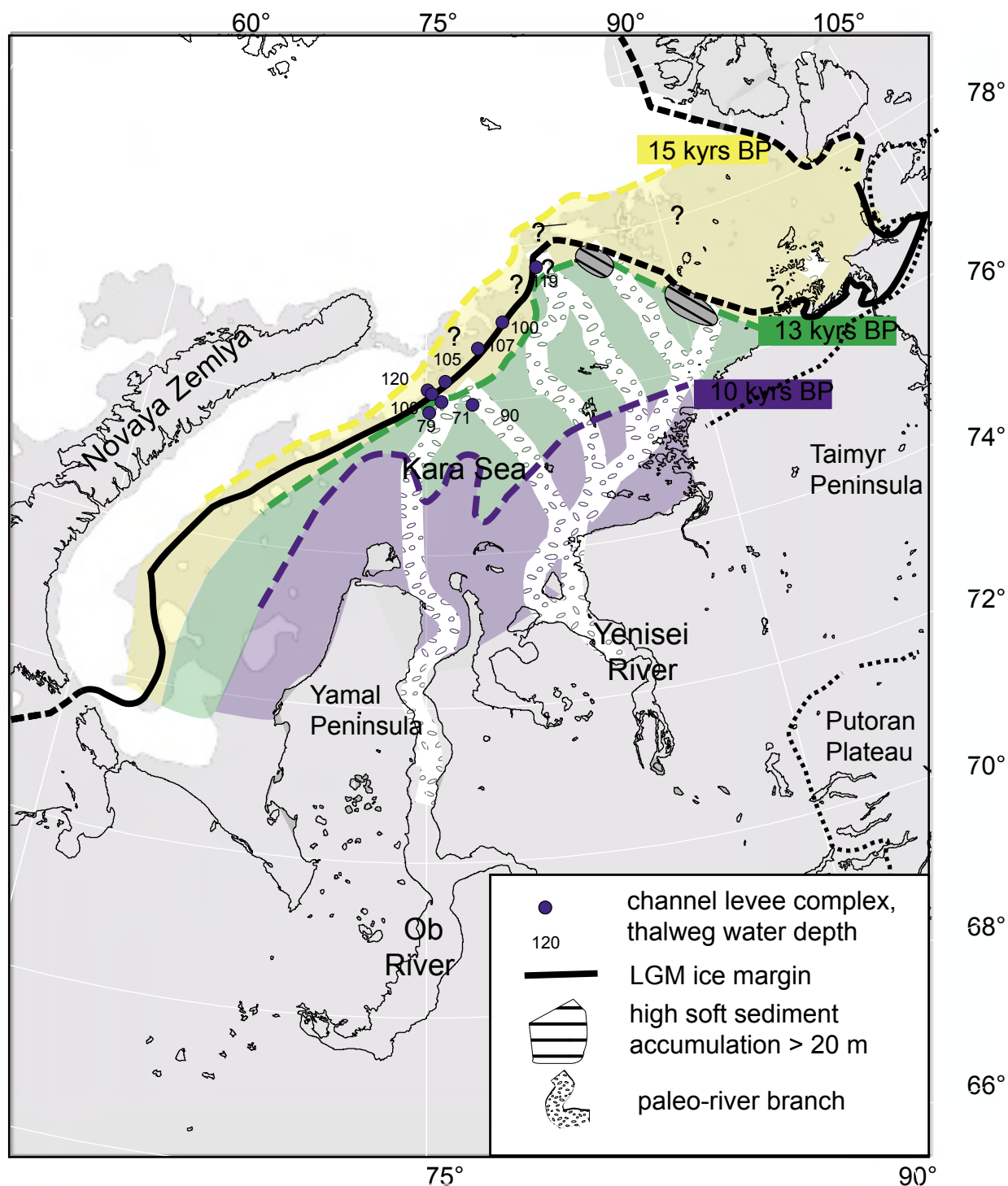
Figure 14. Paleo-geographic map of Kara Sea area and fluvial run-off routes. Grey shaded area corresponds to recent 120 m isobath, and proposed sea level during LGM (Fairbanks 1989). Dashed lines indicate time transgressive position of the paleo-shoreline during the Holocene transgression according to modern bathymetry. Filled dots indicate major channel-levee systems, numbers represent recent water depth.
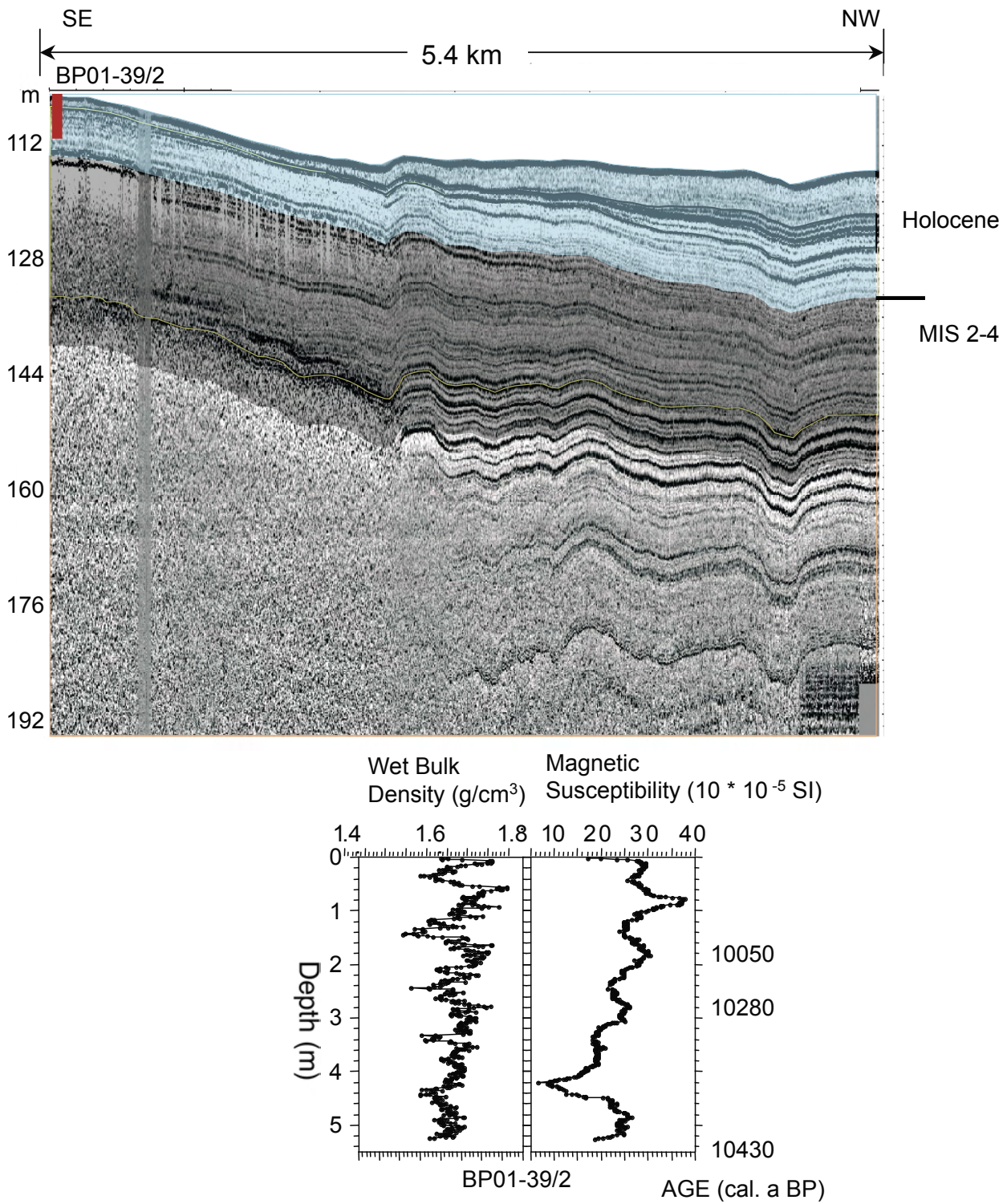
Figure 15. Example of high-resolution CHIRP profile of 2001 cruise (Stein et al., 2002; Niessen and Dittmers, 2002) and physical properties (Dittmers and Niessen, 2002) of dated sediment core BP01-39/2 (Stein et al., 2004).

levee complex, no ice margin setting, smooth relief. The sediment core BP01-39 (106 m water depth) shows continuous marine conditions (Stein et al., 2004) with high accumulation rates up to 10,000 BP in a core at a water depth from approximately 110 m. This indicates forced sedimentation during sea level lowstand and enhanced delivery proximal to the source, while (sea level) highstand sedimentation is much more diminished, manifested in metres of sediment deposited during 10, 000 years. To our understanding, this facies is a still-water deposit formed in depressions, possibly adjacent to the ice sheet, rather than relicts of a reservoir lake expanding over the whole shelf.

Alternatively, these accumulations could be normal pro-deltaic marine sediments that accumulated during a period of low sea level stand as reported by Kleiber et al. (2001) from the eastern Vilkitsky Strait, interpreted as a delta which was possibly fed by fluvial input through the Kara Sea and no local point source. We think that the examples at the edge of the shallow shelf, the channel-levee facies in the NW area and the draping sediment accumulation facies in the NE area document the same in two different primarily morphology-controlled areas. The NW area is characterised by channelled sediment flow, while the NE is characterised by lower slope gradients and suspended sediment spread out into a wide area.

Evidence of Spielhagen et al. (2004) who reviewed the sediment composition of the central Arctic Ocean in the light of ice sheet records, supports our idea of a constant (channelised) northward sediment flux. Major deglaciation events are normally represented by ice-rafted debris (IRD) rich layers associated with elevated smectite concentrations indicative of a source in the eastern Kara Sea and western Laptev Sea area (Nuernberg et al., 1994; Stein and Korolev, 1994; Wahsner et al., 1999). In contrast, indications of melt-water events in the central Arctic Ocean during the last glacial Termination I are much smaller than those during Terminations II and III at 130 and 50 ka, respectively (Knies and Vogt, 2003; Spielhagen et al. 2004 and references therein). This excludes a large LGM ice-dammed lake scenario with its typical self accelerating fresh water out-burst, as reported for Lake Agassi (Magny and Bégeot, 2004). Constant fluvial run-off, therefore, seems reasonable for the Kara Sea at that time.

5. Conclusions

There is evidence that there was a long lasting fluvial activity on the Kara Sea Shelf. The analysis of numerous channels on the Kara Sea Shelf led to the conclusion that they were formed during the last global sea level regression phase, having its peak during the LGM. There is a distinct difference between the Ob and Yenisei branch/system resulting from the different slope gradient of their paleo-drainage paths. Both systems display filled channels, preferable found in shallow water depths, and open,

or partly filled channels. We think, that our data support only a brief glacial surge across the northern Kara Sea during the LGM (Alexanderson et al., 2002) with no evidence of a large territory occupied by an ice-dammed lake for the LGM and subsequent times. Morphometric analysis of channel dimensions showed that they predominantly belong to the meandering river regime. These findings argue for a time interval of subaerial exposure and channel formation sufficiently long enough for rivers to incise and to adjust under equilibrium conditions. The channels dimensions are larger than the modern dimensions of gauge stations of Ob and Yenisei rivers, probably formed under colder climate conditions during LGM resulting in a distinct peakedness of river run-off.

Acknowledgements

Part C

Synthesis

Conclusions
Key results

• How is the fluvially-derived material dispersed on the (recent) shelf: pathways of sediment? (CHAPTER 3.2, partly CHAPTER 3.3)

Silt size surface sediments exhibit a widespread bimodal grain-size distribution, indicative of at least two transport processes acting on grain-size populations in the mud fraction. We favour seasonality with different conditions affecting the sediment distribution. In the summer the whole system is controlled by strong riverine water and sediment influx. Terrestrially-derived sediment settles out of the river plume, being influenced by the prevailing surface currents, mainly induced by winds. After the particles made their way through the water column they flow density-induced along the bottom relief.

The winter situation is characterised by little direct riverine sediment and freshwater input but due to the high current energy, ice transport, and ice erosion, rather marks a period of intense sediment resuspension and redistribution. Coastal, nearshore, and estuarine areas are effectively sheltered by the fast-ice from vigour wave induced currents and finer grain-size populations are dominant.

Terrestrially-derived material is transported along the Kara Sea Shelf bottom relief. Magnetic susceptibility enlightens the pathways of signal and dispersion following the morphology predetermined by ancient incised channels with the established paleo-river "drainage network", probably related to morphology-controlled density-driven sediment distribution for example by a bottom nepheloid layer. The exact transport processes could not be identified. The majority of sediment is trapped in the estuaries of Ob and Yenisei as visible on acoustic profiles.

• The establishment of a Holocene Sediment budget
Estuaries

The total post LGM sediment mass through all three facies areas sums up to 114×10^{10} t. These numbers are in good agreement with results of Stein and Fahl (2003) averaging to 123×10^{10} t for the Holocene. Our calculations for Facies A, the Ob and Yenisei estuaries, 8.0×10^{10} t and 14.1×10^{10} t, respectively, lie in the same range as described by Dittmers et al. (2003) with slightly lower values for the Yenisei Estuary.

Shelf

For Facies B, covering the largest area with least sediment sediment mass of 42.2×10^{10} t is estimated. Facies C accumulates a sediment volume of 49.7×10^{10} t.

Deposition occurred constantly in Facies C, with higher sedimentation rates during

sea level lowstand when all material by-passed Facies A and B. Sediment accumulation progressively shifted towards the recent estuaries of Ob and Yenisei (Facies A) with elevating sea level. There is a significant component of reworked material in Facies B making up at least 50 % of the sediment mass reducing the net sediment mass to some 24.85 x 10^{10} t. It appears as if the estuaries effectively hindered Holocene sediments from entering the Kara Sea. The shelf has been supplied by sediments that "escaped" the estuaries and mostly by coastal erosion, besides the major reworked component. Facies C was built up during sea level lowstand.

• What was the late Weichselian to Holocene evolution of the inner Kara Sea Shelf (CHAPTER 3.3, 3.4 and 3.5)

The sediments in the Ob and Yenisei estuaries can be divided into two major acoustic and lithological Units (I and II). Unit II forms the pre-Holocene basement with little acoustic penetration. During the last sea level lowstand, the erosional surface was formed on top of this unit including several incised river channels. The younger Unit I can be divided into three Subunits, Ia to Ic. The lowermost Subunits Ic and Ib show fluvial seismic features comparable to typical subaerial formed channel-levee complexes representing a fine-grained meandering river depositional environment overlain by a transgressive system tract.

We correlated these units with strata on the shelf, establishing a regional chronostratigraphic frame work:

Regressional and lowstand system tracts (RST and LST) before 15 ka BP: During the sea level lowstand the present shelf areas were transformed into alluvial plains and valleys due to fluvial incision and erosion acting mostly as non-deposition sediment bypassing zones with sediment accumulation beyond the shelf edge. Formation of sequence bounding unconformity on top of Unit II.

Transgressive system tract (TST) 15 ka BP- 5 ka BP: Most sediments on the shelf (< 120 m water depth) comprising this time interval are of fluvial origin. Shortly after the LGM, shoreline transgressed over the shelf area involving a sea level rise of more than 80 m. Accommodation space was rapidly increased resulting in a deepening upward sequence. The transgression formed a shore face ravinement surface defining the boundary between subunit Ic to subunit Ib, dated to 8.5 ka BP in the Yenisei area. In Facies B Holocene sediments contain a reworked component and a recent one above the transgressive surface and maximum flooding surface at ca. 8 ka BP marking the highest rate of available accommodation space between sea and sediment surface and relatively deepest water conditions during sea level rise

Highstand system tract (HST) since 5 ka BP: Since approximately 6 ka BP sea level has approached a relatively stable position. The deposition of draping HST started at

least 5 ka BP, implying weak currents in relatively deep water conditions comparable to the recent estuarine environment.

• What was the fate of the large west Siberian rivers (Ob and Yenisei) during last glacial maximum sea level lowstand, and how far did they extend onto the shelf? (CHAPTER 3.4 and 3.5)

The analysis of numerous channels on the Kara Sea Shelf led to the conclusion that they where formed during the last global sea level regression phase. Morphometric analyses of channel dimensions showed that they predominantly belong the meandering river regime. Dimensions of channels on the shelf are larger than recent analogues of Ob and Yenisei rivers. These findings argue for a time interval of subaerial exposure and channel formation sufficiently long enough for rivers to incise and to adjust under equilibrium conditions. Furhermore river run-off pattern was different than today with minor total run-off but more spiked main flooding events, producing larger geometries.

The interface between LGM morainic morphology with under water extensions of the channels implies a deflection of channel-levee systems by the ice sheet and furthermore a constant drainage to the north. This finding invalidates the proposed link between the Barents Sea-Novaya Zemlya ice sheet and the Taimyr Peninsula glaciation: with the caveat that an exact dating is missing.

There is no geomorphic or sedimentological expression of a large reservoir storage. Our data support only a brief glacial surge across the northern Kara Sea during the LGM (Alexanderson et al., 2002) with no evidence of a large territory occupied by an ice-dammed lake for the LGM and subsequent times. Therefore, we conclude that the lake could only have endured a couple of hundred years - a time span not sufficient enough traceable in the geological record on our data basis.

5. Synthesis

This chapter discusses the results of the thesis relating the main topics to unsolved problems in this particular working area. The discussion of the critical facts specifies the focus of future research. An open question and controversely discussed subject is the question whether there was an LGM ice-dammed lake or not (see Mangerud et al., 2004 and Svendsen et al., 2004, for comprehensive summaries). Another open question is: how was the drainage of Ob and Yenisei rivers influenced by the proximal ice sheet? This issue has been addressed previously in this thesis Chapters 3.4 and 3.5 and to an minor extent in Chapter 3.3, but here we want to tackle the topic in a more speculative way and show where the future work has to focus on.

Landforms and features diagnostic for an ice-dammed lake after Clarke et al. (2004) and references therein are:

1. incised outlet channels, showing fluvial erosion, often characterised by rapid water release due to catastrophic (cataclystic) dam failure (Jökulhaups; Björnsson, 2003)
2. cliffs eroded along the paleo-beach line by lake waves; these should be visible in topography and be documented in the sedimentary record as beach gravel and sand deposits
3. deltaic deposits at the places where rivers enter the lake basin
4. fine-grained lacustrine sedimentation in the central lake, rich in ice rafted debris (IRD)
5. intensive ice gouging on the lake bottom in the relatively shallow waters (Dyke, 2003; Josenhans and Zevenhuizen, 1990)

Possible traces that such a lake could have left behind and evidence from our data:

1. Although we report the widespread abundance of channels on the shelf (Chapter 3.5), no particular lake outlet channel could be found in our working area. It should be characterised by deep incision due to upper flow regime during cataclysm with progressive incision during water release (e.g. Baker et al., 1973, 1993). These channels occur not only at the lake outlets, but are also found in the central lake basin, as reported by Josenhans and Zevenhuizen (1990). Deeper water (<100 m) channels found in the working area, are growth structures, typical for channel-levee complexes (Flood and Damuth, 1989), rather than incised outlet channels.
2. In our soundings and the related elevation model no pronounced beach cliff or paleo-shoreline is visible on the shelf that could have been formed by a lake. Possibly this large scale depression could be revealed by future research including high-resolution side scan sonar surveys.
3. The predecessors of Ob and Yenisei rivers should have had their expression in an ice-dammed lake, where they would have dumped their sediment load. These deltas must have been massive because the sedimentation regime shifts rapidly from moving water to still water and the rivers release a large amount of their (suspension) load, although their net suspended freight volume would be smaller
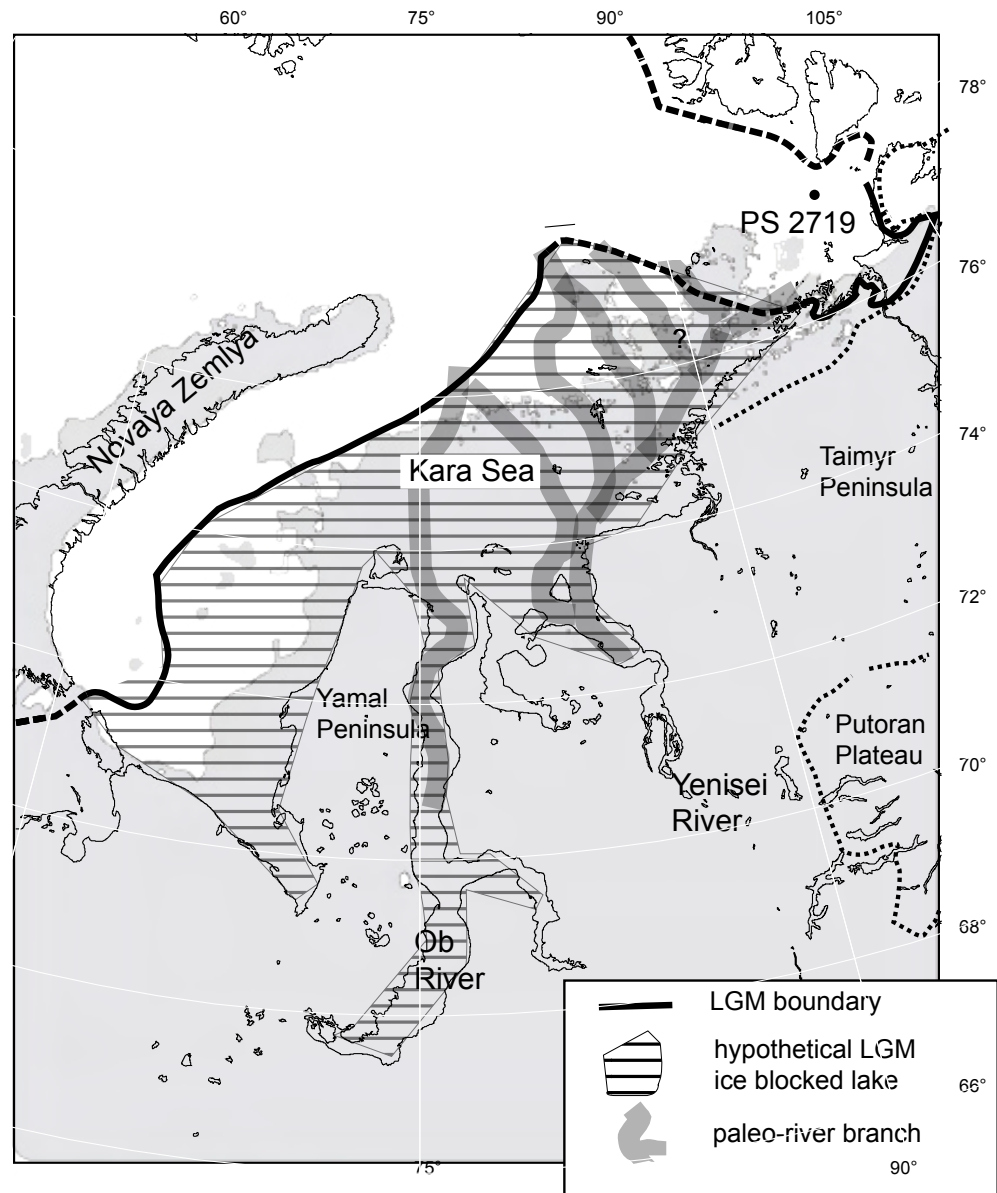
Figure. 5.1. Dimensions of a possible LGM ice-dammed lake (hatched) in the Kara Sea assuming a link between the Taimyr Peninsula and Novaya Zemlya ice sheets

than today because of the dryer climate. Their typical external form makes it difficult to oversee these features, and it seems not very likely that they have been completely removed by erosion during transgression, but no evidence for deltaic features could be found within our working area.

4. It is difficult to differentiate between typical marine muds encountered in our working area and sediments originated in a still water-lake environment. But these sediments should be expressed as draping units in acoustic data, because their sedimentation is not current-controlled. There are no widespread draping sediments

of greater lateral extent visible in our working area.

5. Chapter 3.4 describes a preferred occurrence of ice gouges at approximately 50 m water depth. It is theoretically possible that they were formed in a pro-glacial lake setting, but it remains questionable whether they survived the subsequent reworking processes accompanied with the transgression. Given the fact that they are not covered by sediments of significant thickness and their good state of preservation, it is more likely that they are of recent origin, or have been formed during the transgression.

We conclude that there is little morphological/sedimentological evidence for the existence of an ice-dammed lake in the Kara Sea. However it is still possible that this lake existed and that all its "whitenesses" has been erased by the subsequent transgression, as proposed by Polyak et al. (2002). Nevertheless, even a short lived lake should have been resulted in a catastrophic freshwater release during disintegration of the ice dam.

For further discussion we first estimate the volume of such a lake (Table 5.1; Figure, 5.1), assuming that the river run-off was only the half of the recent value during glacial times due to the glacial climatic conditions, we come to an annual run-off for the Ob and Yenisei rivers of 220 km^3 and 310 km^3, respectively (after Gordeev et al., 1996; Rachold et al., 2003), summing up to 530 km^3. It would take only some 60 years to fill up the estimated pro-glacial lake volume of 27,313 km$^{3.}$; Lake Agassiz measured 9,500 km^3 (Clarke et al., 2004).

The water would have been rapidly banked up in front of the ice sheet, therefore it would have been very likely that drainage occurred during a sudden catastrophic event with typical channel base incision during flood release (Baker et al., 1993; Clarke et al., 2004).

Outburst floods, or islandic "Jökulhaups", as described by (Björnsson, 2003), are documented by the presence of kilometre wide, deeply excavated channels (Josenhans

Table 5.1. measured water volume based on our elevation model (Chapter 3.2 and area deterinations made by global mapper

Depth	area within ice limit (km^2)	volume (km^3)
120 m	457, 123	11036.9
100 m	365, 149	3321
80 m	331, 939	2323.1
60 m	302, 900	473.4
50 m	295, 010	5920.3
40 m	176, 605	1414.5
20 m	141, 243	2824.9
		27314,1

and Zevenhuizen, 1990). The outburst event of lake Agassiz was triggered by northward drainage of the lake (Clarke et al., 2004); catastrophic floodings have a profound impact on global climate as the example of lake Agassiz, that probably stopped the north Atlantic current during the 8.2 ka BP cooling event (Clark et al., 2001).

In the Siberian analogy, these water masses should have been at least recorded in the central Arctic Ocean by IRD peaks or isotopic excursions related to the massive freshwater signal, if not in a deterioration in global climate. Furthermore, Mangerud et al. (2004) report that modern modelling of thermohaline circulation (Stoecker and Wright, 1991) indicate that freshwater discharge of 0.1 Sv (1 x 10^6 m^3/s) influences the oceanic circulation. The meltwater flux of the lake Agassiz outburst is estimated to 4-5 Sv (Clarke et al., 2004) which is the same range as the LGM Kara See lake would have
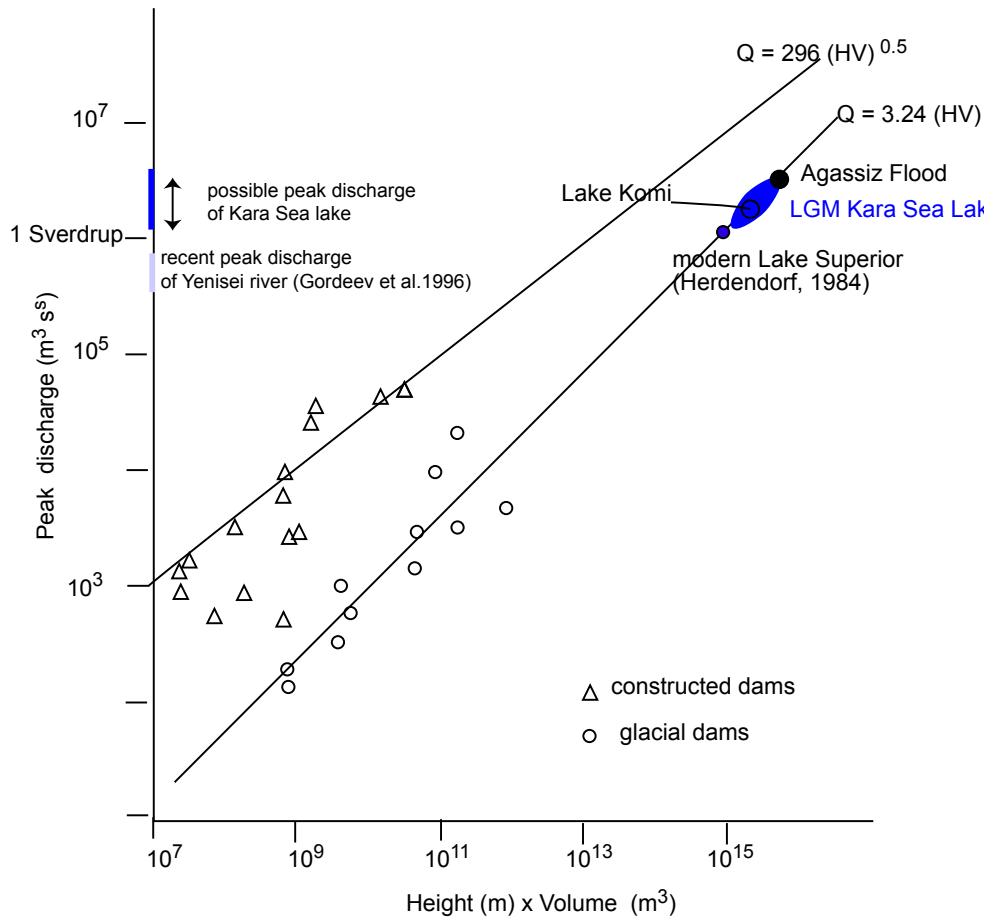

Figure.5.2. Relation of peak discharge to the product of dam height (m) and times lake volume (m^3) after Baker et al. (1993). Data for lake Komi after Mangerud et al. (2004); Lake Agassiz` volume taken from Clarke et al. (2004).

reached utilising Baker´s et al. (1993) equations (Fig. 5.2).

However, data from the central Arctic Ocean show no traces of major freshwater signals (Norgard Petersen et al., 2004; Spielhagen et al., 2004). Norgard Petersen et al. (1998, 2003) report low O^{18} values during LGM highest value in MIS2, IRD maxima before LGM 23-28 ka and only restricted ice proximal meltwater input. Central Arctic ocean shows very low IRD with a peak at 17 ka BP and few icebergs in the central Arctic (Darby et al., 2002).

Therefore, we conclude that the lake only could have endured a couple of hundred years - a time span not sufficient to be handed down in the geological record on our data basis.

Future research perspective

Based on the aforementioned discussion the following topics are of special interest. An exact survey of ice marginal channel-levee complexes by means of geo-accoustics with a very high spatial resolution; combined with sedimentological studies emphasising on the discrimination of marine-fluvial environments: isotopic investigations, palynological and pollen analysis.

there a two areas of high interest:

1. examination of the continental margin north of the Kara Sea Shelf as proposed by Stein et al. in VERITAS in order to investigate sediment by-passing the shelf during sea level lowstand, accumulating in a lowstand wedge/fan

2. close the gap between the Vilkitzky straight and the inner Kara Sea.

In both areas, sediment budget determinations and depositional history reconstructions based on high-resolution acoustic stratigraphy would shed new light on the reconstruction of the LGM paleoenvironment. It would be important to close the gap in data coverage between the Vilkitzky straight (Weiel, 1998; Kleiber and Niessen, 2000) as well as to investigate the continental margin to the North of the Kara Sea Shelf, to trace sediments/fluxes during sea level lowstand and to evaluate sediment masses. These investigations could also lift the last secrets concerning the last glacial maximum and the controversy about a pro-glacial lake.

The employment of a Vibro corer in areas of little Holocene depositions, as well in glacially overprinted terrain would be another important step to improve the regional stratigraphic framework.

In the light of present global change it is of major interest of course to predict future trends. Having established and characterised most processes relevant for the recent

system, the frame has been established, especially for high-resolution studies in the future. The fluvial dominated Siberian part of the Arctic will be strongly influenced by global change. Labat et al. (2004) propose a change in the global hydrological cycle with 4 % higher run off for every 1°C of warming. Furthermore, Manabe et al. (2004) propose that climate change will have 15 % stronger effect in higher latitudes. Peterson et al. (2002) predict the average annual discharge of freshwater from the six largest Eurasian rivers to the Arctic to increase by nearly 10 % during this century. The increase of discharge is coupled to the NAO (North Atlantic Oscillation) and increased surface temperatures (Peterson et al., 2002). The Intergovernmental Panel on Climate Change (IPCC, 2001) estimates a winter warming of more than 40 % greater than the global mean, for high latitude regions by the end of this century.

High-resolution studies of the sedimentary history will play a key role in the prediction of these enormous changes. A proposal (DI 119/2-1) for funding has been submitted to the DFG in order to investigate the Holocene in high resolution(Deutsche Froschungs Gemeinschaft; "Rekonstruktion holozäner Umweltbedingungen in der KaraSee" RUKS).

Part D

**Acknowledgements
Literature**

Acknowledgements

First of all I want to thank Prof. Dieter Fütterer for his enthusiastic leadership in the "SIRRO" project, continuing after his retirement.

I would like to thank my supervisors Prof. Ruediger Stein, who initiated this project including this thesis and gave steady impulse to its forthcoming. He supported me whenever possible and enabled me several attendances on conferences. He always had an open ear for questions. For the scientific support I thank Frank Niessen and his intelligent witty advices. Despite his busy schedule he was able to meet with me and always had a good idea how to solve problems. Both gave me fair amount of freedom, while still stopping me from running into dead ends. I thank Prof. R. Henrich for his agreement on overtaking the second review of this thesis.

Working with my fellows at the Alfred Wegener Institute for Polar and Marine Research in Bremerhaven was both profit and pleasure. First of all I want to thank for their excellent technical help: Rita Fröhlking, Beate Hollmann, Walter Luttmer and Michael Seebeck. Among those I would especially thank is the fabulous "Arctic container" crew: Daniel Birgel, Claudia Didié, Kirsten Fahl, Christian Hass, Jens Hefter, Matthias Kraus, Kristoph Kierdorf, Uwe Langrock, Jens Matthiessen, Michael Pirrung, Christopf Schäfer, Frank Schoster, Tatjana Steinke, Petra Weller and Daniel Winkelmann. Dominik Weiel being no active member anymore is thanked for many fruitful discussion. Christoph Vogt, as former member is also thanked for discussions and advices. Michael Pirrung is thanked for the excellent introduction and sharing of knowledge of the measurement of physical properties and especially magnetic susceptibility. Christain Hass gave me valuable advices in the Silt analysis and insight into heavy metal of the 80`s. A very, very special thank you is dedicated to Jens Mathiessen, who was never tired to read, advice and motivate. Thanks to all crew members of Boris Petrov and cruise participants for their excellent cooperation during three expeditions.

I enjoyed cooperating with the german members of SIRRO in particular Ingo Fetzer, Johannes Simstich, Ingo Harms and Catalina Gebhardt.

I want to thank all my friends in and outside Bremerhaven for all the good times we have been wasted. Frank Schoster for being much more than my flatmate during the expeditions but also for friendship and sharing his music taste. The member of "Erosion" who kept me rocking even at bad times. Christian Müller for many hours not only at the Weser dyke, for good advices not only technically!!!!

Thanks to my sisters and parents for everything and support in any situation. Last but not least I am very grateful for Inken and her endurance, understanding, and support and to make me and my manuscripts digestible LUH.

Aagaard, K. and Carmack, E.C., 1989. The role of sea ice and other fresh water in the Arctic circulation. Journal of Geophysical Research, 94: 14485-14498.

Aagaard, K. and Carmack, E.C., 1994. Contamination of the Arctic. Ocean Processes. Arctic Research of the U.S., 8: 21-33.

Alekseev, M.N., 1997. Paleogeography and geochronology in the Russian eastern Arctic during the second half of the Quaternary, Quaternary of northern Eurasia; late Pleistocene and Holocene landscapes, stratigraphy and environments. Pergamon, Oxford, United Kingdom, pp. 11-15.

Alexanderson, H., Hjort, C., Moller, P., Antonov, O. and Pavlov, M., 2001. The North Taymyr ice-marginal zone, Arctic Siberia; a preliminary overview and dating. Global and Planetary Change, 31(1-4): 427-445.

Alexanderson, H., Adrielsson, L., Hjort, C., Moeller, P.A., O., Eriksson, S. and Pavlov, M., 2002. Depositional history of the North Taymyr ice-marginal zone, Siberia; a landsystem approach. Journal of Quaternary Science, 17(4): 361-382.

Allen, G., 1992. Sequence Stratigraphic Seminar: Analysis in Clastic Sediments. TOTAL: 37.

Allen, G.P. and Posamentier, H.W., 1993. Sequence stratigraphy and facies model of an incised valley fill; the Gironde Estuary, France. Journal of Sedimentary Petrology, 63(3): 378-391.

Allen, J.R.L., 1965. A review of the origin and characteristics of recent alluvial sediments. Sedimentology, 5: 89 –191.

AMAP, 2002. AMAP assessment report: Arctic pollution issues. Arctic Monitoring and Assessment Programme, Oslo, Norway, 859 pp.

Antonov, V.S., 1970. Siberian rivers and Arctic seas. Probl Arktiki Antarktiki, 36/37: 142-152.

Are, F.E., 1996. Dynamics of the littoral zone of Arctic Seas (State of the art and goals). Polarforschung, 64(3): 123-131.

Arkhipov, S.A., Ehlers, J., Johnson, R.G. and Wright, H.E., Jr., 1995. Glacial drainage towards the Mediterranean during the middle and late Pleistocene. Boreas, 24(3): 196-206.

Ashley, G.M. and Sheridan, R.E., 1994. Depositional model for valley fills on a passive continental margin. In: R.W. Dalrymple, R. Boyd and B.A. Zaitlin (Editors), Incised-valley systems; origin and sedimentary sequences, pp. 285-301.

Astakhov, V., 2004. Middle Pleistocene glaciations of the Russian North. Quaternary Science Reviews, 23: 1285-1311.

Bagnold, R.A., 1968. Deposition in the process of hydraulic transport. Sedimentology, 10(1): 45-56.

Baker, V.R., 1973. Paleohydrology and sedimentology of Lake Missoula flooding in Eastern Washington. The Geological Society of America, Special Paper, 144.

Baker, V.R., Benito, G. and Rudoy, A.N., 1993. Paleohydrology of Late Pleistocene superflooding, Altay Mountains, Siberia. Science, 259(5093): 348-350.

Barnes, P.W. and Lien, R., 1987. Icebergs rework sediments on Antarctic shelf. Antarctic Journal of the United States, 22(5): 130-131.

Bauch, H.A., Kassens, H., Naidina, O.D., Kunz-Pirrung, M. and Thiede, J., 2000. Composition and Flux of Holocene Sediments on the Eastern Laptev Sea Shelf Arctic Siberia. Quaternary Research, 55(3): 344-351.

Bauch, H.A., Mueller-Lupp, T., Taldenkova, E., Spielhagen, R.F., Kassens, H., Grootes, P.M., Thiede, J., Heinemeier, J. and Petryashov, V.V., 2001. Chronology of the Holocene transgression at the North Siberian margin. Global and Planetary Change, 31(1-4): 125-139.

Beeskow, B. and Rachold, V., 2003. Geochemical processes in the Yenisei River and estuary. In: R. Stein, K. Fahl, D.K. Fütterer, E.M. Galimov and O.V. Stepanets (Editors), Siberian River Run-Off in the Kara Sea: Characterisation, Quantification, Variability, and Environmental Significance. Proceedings in Marine Science, pp. 125-148.

Bentley, M.J., 1999. Volume of Antarctic Ice at the Last Glacial Maximum, and its impact on global sea level change. Quaternary Science Reviews, 18(14): 1569-1595.

Best, A.I. and Gunn, D.E., 1999. Calibration of marine sediment core loggers for quantitative acoustic impedance studies. Marine Geology, 160(1-2): 137-146.

Bianchi, G.G. and McCave, I.N., 2000. Hydrography and sedimentation under the deep western boundary current on Bjorn and Gardar Drifts, Iceland Basin. Marine Geology, 165(1-4): 137-169.

Bianchi, G.G., Hall, I.R., Mccave, I.N. and Joseph, L., 1999. Measurement of the sortable silt current speed proxy using the Sedigraph 5100 and Coulter Multisizer IIe: precision and accuracy. Sedimentology, 46(6): 1001-1014.

Bianchi, G.G., Vautravers, M. and Shackleton, N.J., 2001. Deep flow variability under apparently stable North Atlantic deep water production during the last interglacial of the subtropical NW Atlantic. Paleoceanography, 16(3): 306-316.

Björnsson, H., Palsson, F., Sigurdsson, O., Flowers, G.E. and Raymond, 2003. Surges of glaciers in Iceland. Annals of Glaciology, 36: 82-90.

Blanchet, D., Bhat, S.U. and Wilkman, G., 1995. Ice conditions in the Ob Bay in western Siberia. In: H.T. Shen (Editor), International Symposium on Ice, 14th, Potsdam, NY, Rotterdam, pp. 259-267.

Bouma, A.H., 2000. Coarse-grained and fine-grained turbidite systems as end member models: Applicability and dangers. Marine and Petroleum Geology, 17(2): 137-143.

Brierley, G.J., Ferguson, R.J. and Woolfe, K.J., 1997. What is a fluvial levee? Sedimentary Geology, 114: 1-9.

Brown, T.M., and Kraus, M.J., 1987. Integration channel and floodplain suites. 1.developmental sequence and lateral relations of alluvial paleosols. Journal of Sedimentary Petrology, 57(4): 587-601.

Burger, R.L., Fulthorpe, C.S. and Austin, J.A., Jr, 2001. Late Pleistocene channel incisions in the southern Eel River basin, Northern California; implications for tectonic vs. eustatic influences on shelf sedimentation patterns. Marine Geology, .177(.3-4): 317-330.

CAPS, 1998. Circumpolar Active-Layer Permafrost System. In: D.a.I.W.G. International Permafrost Association (Editor). National Snow and Ice Data Center/World Data Center for Glaciology, Boulder.

Carmack, E.C., 2000. The Arctic Ocean's freshwater budget: sources, storage and export. In: E.L. Lewis and e. al. (Editors), The Freshwater Budget of the Arctic Ocean. Kluwer Academic Publishers, pp. 91-126.

Chang, S.-B.R. and Kirschvink, J.L., 1989. Magnetofossils, the magnetization of sediments, and the evolution of magnetite biomineralization. Annual Review of Earth and Planetary Sciences, 17: 169-195.

Chappell, J. and Shackleton, N.J., 1986. Oxygen isotopes and sea level. Nature, 324: 137–140.

Chappell, J., Omura, A., Esat, T., McCulloch, M., Pandolfi, J., Ota, Y. and Pillans, B., 1996. Reconciliation of Late Quaternary sea levels derived from coral terraces at Huon Peninsula with deep sea oxygen isotope records. Earth and Planetary Science Letters, 141(1-4): 227-236.

Chavlov, 1994. The Fluvial Processes on the Northern Eurasia Rivers, Moscow, 189 pp.

Clark, J.D. and Pickering, K.T., 1996. Architectural elements and growth patterns of submarine channels; application to hydrocarbon exploration. AAPG Bulletin, 80(2): 194-221.

Clark, P.U., Marshall, S.J., Clarke, G.K.C., Hostetler, S.W., Licciardi, J.M. and Teller, J.T., 2001. Freshwater forcing of abrupt climate change during the last glaciation. Science, 293: 283-287.

Clark, P.U., McCabe, A.M., Mix, A.C. and Weaver, A.J., 2004. Rapid Rise of Sea level 19,000 Years Ago and Its Global Implications. Science, 304: 1141-1144.

Clarke, G., Leverington, D., Teller, J. and Dyke, A., 2003. Superlakes, megafloods, and abrupt climate change. Science, 301: 922-923.

Coe, A.L., Bosence, D.W.J., Church, K.D., Flint, S.S., Howell, J.A. and Wilson, R.C.L., 2003. The sedimentary record of sea level change. Cambridge University Press, Cambridge, 288 pp.

Collinson, J.D., 1978. Vertical sequence and sand body shape in alluvial sequences. Memoir - Canadian Society of Petroleum Geologists, 5: 577-586.

Damuth, J.E., 1975. Echo character of the western equatorial Atlantic floor and its relationship to the dispersal and distribution of terrigeneous sediments. Marine Geology, 18: 17-45.

Damuth, J.E., 1978. Echo character of the Norwegian-Greenland Sea: relationship to Quaternary sedimentation. Marine Geology, 28: 1-36.

Darby, D.A., Naidu, A.S., Mowatt, T.C. and Jones, G., 1989. Sediment composition and sedimentary processes in the Arctic Ocean, The Arctic seas; climatology, oceanography, geology, and biology. Van Nostrand Reinhold Co., New York, NY, United States, pp. 657-720.

Darby, D.A., Bischof, J.F., Spielhagen, R.F., Marshall, S.A. and Herman, S.W., 2002. Arctic ice export events and their potential impact on global climate during the late Pleistocene. Paleoceanography, 17 (2): 15.1-15.17.

Dearing, J., 1994. Environmental magnetic susceptibility - using the Bartington MS2 system. Chi Publishing, Kenilworth, UK, 273 pp.

Degens, E.T., Kempe, S. and Richey, J.E., 1991. Summary; Biogeochemistry of major world rivers, Biogeochemistry of major world rivers. Wiley & Sons, Chichester, United Kingdom, pp. 323-346.

Dethleff, D., 1994. Dynamics of the Laptev Sea flaw lead. Berichte zur Polarforschung - Reports on Polar Research, 144, 49-54 pp.

Dethleff, D., Nies, H., Harms, I.H. and Karcher, M.J., 2000. Transport of radionuclides by sea-ice and dense-water formed in western Kara Sea flaw leads. Journal of Marine Systems, 24(3-4): 233-248.

Dittmers, K., 2001. Bathymetry of the Kara Sea in PanMap layer format, PANGAEA, doi:10.1594/PANGAEA.57961. Dittmers, K; Grobe, Hannes; Stein, Ruediger (2001): Bathymetry of the Kara Sea south of 77° N; compilation for the projects QUEEN and SIRRO from Russian navigational charts and echo soundings of cruises BP99 and BP00.

Dittmers, K. and Niessen, F., 2002. Physical properties of sediment cores. Berichte zur Polarforschung - Reports on polar research, 419: 74-80.

Dittmers, K. and Schoster, F., 2004. Acoustic Facies in the southern Kara Sea: new results by PARASOUND echosounding. Reports on Polar and Marine Research, 479: 55-71.

Dittmers, K. and Stein, R., 2001. 3.5 kHz and ELAC sediment echograph profiling. Berichte zur Polarforschung - Reports on polar research, 393: 83-88.

Dittmers, K., Niessen, F. and Stein, R., 2003. Holocene sediment budget and sedimentary history for the Ob and Yenisei estuaries. In: R. Stein, K. Fahl, D.K. Fütterer, E.M. Galimov and O.V. Stepanets (Editors), Siberian River Run-off in the Kara Sea: Characterisation, Quantification, Variability and Environmental Significance. Proceedings in Marine Sciences. Elsevier, Amsterdam, pp. 457-470.

Divine, D., Korsnes, R. and Makshtas, A., 2003. Variability and climate sensitivity of fast ice extent in the north-eastern Kara Sea. Polar Research, 22(1): 27-34.

Divine, D.V., Korsnes, R. and Makshtas, A.P., 2004. Temporal and spatial variations of shore-fast ice in the Kara Sea. Continental Shelf Research, 24: 1717-1736.

Dowdeswell, J.A., Elverhoi, A. and Spielhagen, R., 1998. Glacimarine sedimentary processes and facies on the polar North Atlantic margins. Quaternary Science Reviews, 17(1-3): 243-272.

Drake, D.E., 1976. Suspended sediment transport and mud deposition on continental shelves, Marine sediment transport and environmental management. John Wiley & Sons, New York, N.Y., United States, pp. 127-158.

Dury, G.H., 1964. Principles of underfit streams, U. S. Geological Survey.

Dury, G.H., 1965. Theoretical implications of undefit streams, US Geological Survey, Washington.

Dury, G.H., 1967. Some channel characteristics of the Hawkesbury river, New South Wales. Australian Geographical Studies, 5(2): 135-149.

Dury, G.H., 1986. Osage-type underfitness on the River Severn near Shrewsbury, Shropshire, England. Background to Palaeohydrology. Wiley, Chichester, 399 pp.

Dyer, K.R., Christie, M.C. and Manning, A.J., 2004. The effects of suspended sediment on turbulence within an estuarine turbidity maximum. Estuarine, Coastal and Shelf Science, 59: 237-248.

Dyke, A.S. and Evans, D.J.A., 2003. Ice-marginal terrestrial landsystems; northern Laurentide and Innuitian ice sheet margins, Glacial landsystems. Arnold, London, United Kingdom, pp. 143-165.

Eicken, H., Reimnitz, E., Alexandrov, V., Martin, T., Kassens, H. and Viehoff, T., 1997. Sea-ice processes in the Laptev Sea and their importance for sediment export. Continental Shelf Research, 17(2): 205-233.

Eicken, H., Kolatschek, J., Lindemann, F., Dmitrenko, I., Freitag, J. and Kassens, H., 2000. A key source area and constraints on entrainment for basin scale sediment transport by Arctic sea ice. Geophysical Research Letters, 27(13): 1919-1922.

Eisma, D., 1982. Supply and dispersal of suspended matter from the Zaire River, Transport of carbon and minerals in major world rivers; Proceedings of a workshop;Part 1. Geologisches Staatsinstitut, Hamburg, Federal Republic of Germany, pp. 419-428.

Eisma, D., 1986. Flocculation and de-flocculation of suspended matter in estuaries. Netherlands Journal of Sea Research, 20(2-3): 183-199.

Elverhoi, A., Pfirman, S.L. Solheim, A. and Larssen, B.B., 1989. Glaciomarine sedimentation on epicontinental seas exemplified by the northern Barents Sea. Marine Geology, 85: 225-250.

Elverhoi, A., Dowdeswell, J.A., Funder, S., Mangerud, J. and Stein, R., 1998. Glacial and oceanic history of the polar North Atlantic margins: an overview. Quaternary Science Reviews, 17(1): 1-10.

Evans, R.L., Law, L.K., St Louis, B. and Cheesman, S., 2000. Buried paleo-channels on the New Jersey continental margin; channel porosity structures from electromagnetic surveying. Marine Geology, 170(3-4): 381-394.

Fader, G.B.J., 1997. The Effects of shallow Gas on Seismic Reflection Profiles. In: T.A. Davies (Editor), Glaciated continental margins: an atlas of acoustic images. Chapman and Hall, London, pp. 315.

Fairbanks, R.G., 1989. 17.000-year glacio-eustatic sea level record: influence of glacial melting rates on the Younger Dryas event and deep ocean circulation. Nature, 342: 637-642.

Fairbanks, R.G., Charles, C.D. and Wright, J.D., 1992. Origin of global meltwater pulses. In: R.E. Taylor, A. Long and R.S. Kra (Editors), Radiocarbon after four decades; an interdisciplinary perspective. Springer-Verlag, New York, NY, United States (USA), pp. 473-500.

Fetzer, I., 2003. Distribution of meroplankton in the southern Kara Sea in relation to local hydrographic pattern. Proceedings in Marine Sciences, 6: 195-212.

Fielding, C.R. and Crane, R.C., 1987. An application of statistical modelling to the prediction of

hydrocarbon recovery factors in fluvial reservoir sequences. In: F.G. Ethridge, R.M. Flores, M.D. Harvey and J.N. Weaver (Editors), Recent developments in fluvial sedimentology: Special Publication - Society of Economic Paleontologists and Mineralogists, pp. 321-327.

Flood, R.D. and Damuth, J.E., 1987. Quantitative characteristics of sinuous distributary channels on the Amazon deep-sea fan. Geological Society of America Bulletin, 98(6): 728-738.

Flood, R.D., Manley, P.L., Kowsmann, R.O., Appi, C.J. and Pirmez, C., 1991. Seismic facies and late Quaternary growth of Amazon submarine fan, Seismic facies and sedimentary processes of submarine fans and turbidite systems. Springer-Verlag, New York, NY, United States.

Forman, S.L., Lubinski, D., Miller, G.H., Snyder, J., Matishov, G., Korsun, S. and Myslivets, V., 1995. Postglacial emergence and distribution of late Weichselian ice-sheet loads in the northern Barents and Kara seas, Russia. Geology, 23(2): 113-116.

Forman, S.L., Lubinski, D.J., Ingólfsson, Ó., Zeeberg, J.J., Siegert, M.J., Snyder, J.A. and Matishov, G.G., 2004. A review of postglacial emergence on Svalbard, Franz Josef Land and Novaya Zemlya, northern Eurasia. Quaternary Science Reviews, 23(11-13): 1391-1434.

Frenz, M., 2003. Grain size composition of Quaternary South Atlantic Heinzes and its paleooceanographic significance. No. 213 Thesis, Berichte, Fachbereich Geowissenschaften, Universität Bremen, 123 pp.

Fricker, H.A. and Padman, L., 2002. Tides on Filchner-Ronne ice shelf from ERS radar altimetry. Geophysical Research Letters, 29(12): 50-1 - 50-4.

Galloway, W.E. and Hobday, D.K., 1996. Terrigeneous clastic depositional systems. Springer: 489.

Gataullin, V., Mangerud, J. and Svendsen, J.-I., 2001. The extent of the late Weichselian ice sheet in the southeastern Barents Sea. Global and Planetary Change, 31(1-4): 453-474.

Gaye-Haake, B., Unger, D., Nöthig, E.-M., Okolodkov, Y., Fahl, K. and Ittekkot, V., 2003. Particle fluxes from short-term sediment trap deployments in late summer in the southern Kara Sea. In: R. Stein, K. Fahl, D.K. Fütterer, E.M. Galimov and O.V. Stepanets (Editors), Siberian River Run-off in the Kara Sea: Characterisation, Quantification, Variability, and Environmental Significance. Proceedings in Marine Sciences, 6. Elsevier, Amsterdam, pp. 309-328.

GEBCO, 1984. General Bathymetric Chart of the Oceans, Canadian Hydrographic Service, Ottawa.

Gebhardt, A.C., Gaye, H.B., Unger, D., Lahajnar, N. and Ittekkot, V., 2004. Recent particulate organic carbon and total suspended matter fluxes from the Ob and Yenisei Rivers into the Kara Sea (Siberia). Marine Geology, 207(1-4): 225-245.

Gibbs, R.J., Matthews, M.D. and Link, D.A., 1971. The relationship between sphere size and settling velocity. Journal of Sedimentary Petrology, 41(1): 7-18.

Global Mapper, 2004. Global mapper. Global Mapper Software, LLC Olathe, KS in the United States.

Gordeev, V.V., 2000. River input of water, sediment, major ions, nutrients, and trace metals from Russian territory to the Arctic Ocean. In: E.L. Lewis (Editor), The freshwater budget of the Arctic Ocean. NATO Sciences Series. Kluwer Academic Press, Dordrecht, pp. 297-322.

Gordeev, V.V., Martin, J.M., Sidorov, I.S. and Sidorova, M.V., 1996. A reassessment of the Eurasian river input of water, sediment, major elements, and nutrients to the Arctic Ocean. American Journal of Science, 296: 664-691.

Grant, J.A. and Schreiber, R., 1990. Modern swathe sounding and sub-bottom profiling technology for research applications; the Atlas Hydrosweep and Parasound systems, Marine geological surveying and sampling. Kluwer Academic Publishers, Dordrecht, Netherlands, pp. 9-19.

Grebmeier, J.M., 1995. Biological processes on Arctic continental shelves, Ice-ocean-biotic interactions. In: W.O. Smith, Grebmeier, J.M., (Editor), Arctic oceanography: Marginal ices zones and continental shelves: Coastal and Estuarine studies, pp. 231-261.

Grobe, H., 1987. A simple method for the determination of ice-rafted debris in sediment cores. Polarforschung, 57(3): 123-126.

Grosswald, M.G., 1980. Late Weichselian ice sheet of northern Eurasia. Quaternary Research, 13(1): 1-32.

Grosswald, M.G. and Hughes, T.J., 1999. The case for an ice shelf in the Pleistocene Arctic Ocean. Polar Geography (1995), 23(1): 23-54.

Hall, A.M., Mellor, A. and Wilson, M.J., 1989. The clay mineralogy and age of deeply weathered rock in North-east Scotland, Weathered mantles (saprolites) over basement rocks of high latitudes. Gebrueder Borntraeger, Berlin-Stuttgart, Federal Republic of Germany, pp. 97-108.

Hamilton, E.L., 1972. Compressional-wave attenuation in marine sediments. Geophysics, 37(4): 620-646.

Hanebuth, T., Stattegger, K. and Grootes, P.M., 2000. Rapid flooding of the Sunda Shelf: A late-glacial sea level record. Science, 288: 1033-1035.

Hanebuth, T.I., Stattegger, K. and Saito, Y., 2002. The stratigraphic architecture of the central Sunda Shelf (SE Asia) recorded by shallow-seismic surveying. Geo-Marine Letters, 22(2): 86-94.

Hanebuth, T.J., Stattegger, K., Schimanski, A., Ludmann, T. and Wong, H.K., 2003. Late Pleistocene forced-regressive deposits on the Sunda Shelf (Southeast Asia). Marine Geology . 199(1-2): 139-157.

Harms, I.H. and Karcher, M.J., 1999. Modelling the seasonal variability of hydrography and circulation in the Kara Sea. Journal of Geophysical Research, 104: 13431-13448.

Harms, I.H., Karcher, M.J. and Dethleff, D., 2000. Modelling Siberian river runoff - implications for contaminant transport in the Arctic Ocean. Journal of Marine Systems, 27: 95-115.

Harms, I.H., Backhaus, J.O. and Huebner, U., 2002. Numerical modeling of shelf and estuary hydrodynamics in the Kara Sea, Arctic coastal dynamics; report of an International workshop. Kamloth, Bremerhaven, Federal Republic of Germany, pp. 18-19.

Harms, I.H., Huebner, U., Backhaus, J.O., Kulakov, M., Stanovoy, V., Stepanets, O.V., Kodina, L.A. and Schlitzer, R., 2003. Salt intrusions in Siberian river estuaries; observations and model experiments in Ob and Yenisei, Siberian river run-off in the Kara Sea; characterisation, quantification, variability and environmental significance. Elsevier, Amsterdam, Netherlands, pp. 27-46.

Hass, H.C., 1996. Northern Europe climate variations during late Holocene; evidence from marine Skagerrak. Palaeogeography, Palaeoclimatology, Palaeoecology, 123(1-4): 121-145.

Hass, H.C., 2002. A method to reduce the influence of ice-rafted debris on a grain size record from northern Fram Strait, Arctic Ocean. Polar Research, 21(2): 299-306.

Herdendorf, C.E., 1984. Inventory of the morphometric and limnologic characteristics of the large lakes of the world. Inventory of the morphometric and limnologic characteristics of the large lakes of the world, 17. State University technical bulletin, Ohio, 78 pp.

Hill, P.S., Milligan, T.G. and Geyer, W.R., 2000. Controls on effective settling velocity in the Eel River flood plume. Continental Shelf Research, 20(16): 2095-2111.

Hill, P.S., Voulgaris, G. and Trowbridge, J.H., 2001. Controls on floc size in a continental shelf bottom boundary layer. Journal of Geophysical Research, 106: 9543-9549.

Hine, A.C. and Snyder, S.W., 1985. Coastal lithosome preservation: Evidence from the shoreface and inner continental shelf off Bogue Banks, North Carolina. Marine Geology, 63(1-4): 307-330.

Holmes, R.M., McClelland, J.W., Peterson, B.J., Shiklomanov, I.A., Shiklomanov, A.I., Zhulidov, A.V., Gordeev, V.V. and Bobrovitskaya, N.N., 2002. A circumpolar perspective on fluvial sediment flux to the Arctic Ocean. Global Biogeochemical Cycles, 16(4): 45/1-45/13.

Holz, C., 2005. Climate-induced variability of fluvial and aeolian sediment supply and gravity-driven sediment transport off Northwest Africa, Bremen.

Jakobsson, M., 2002. Hypsometry and volume of the Arctic Ocean and its constituent seas. Geochemistry, Geophysics, Geosystems, 3(5): 1-18.

Jakobsson, M., Cherkis, N., Woodward, J., Macnab, R. and Coakley, B., 2000. New grid of Arctic bathymetry aids scientists and mapmakers. Eos, Transactions, American Geophysical Union, 81(9): 89-96.

Jakobsson, M., Lovlie, R., Arnold, E.M., Backman, J., Polyak, L., Knutsen, J.O. and Musatov, E., 2001. Pleistocene stratigraphy and paleoenvironmental variation from Lomonosov Ridge sediments, central Arctic Ocean. Global and Planetary Change, 31(1-4): 1-22.

Johnson, G.L. and Milligan, D.B., 1968. Some geomorphological observations in the Kara sea. Deep-Sea Research and Oceanographic Abstracts, 14(1): 19-28.

Josenhans, H. and Zevenhuizen, J., 1990. Dynamics of the Laurentide Ice Sheet in Hudson Bay Canada. Marine Geology, 92(1-2): 1-26.

Kleiber, H.P. and Niessen, F., 1999. Late Pleistocene paleoriver channels on the Laptev Sea shelf - implications from sub-bottom profiling, In: Kassens, H., Bauch, H. A., Dmitrenko, I., Eicken, H., Hubberten, H.-W., Melles, M., Thiede, J., Timokhov, L. (Eds.), Land-Ocean Systems in the Siberian Arctic: Dynamics and History. Springer, Berlin, pp. 657-665.

Kleiber, H.-P. and Niessen, F., 2000. Variations of continental discharge pattern in space and time: Implications from the Laptev Sea continental margin Arctic Siberia. International Journal of Earth Sciences, 89: 605-616.

Kleiber, H.P., Niessen, F. and Weiel, D., 2001. The Late Quaternary evolution of the western Laptev Sea continental margin, Artic Siberia - implications from sub-bottom profiling. Global and Planetary Change, 31: 105-124.

Knies, J. and Vogt, C., 2003. Freshwater pulses in the eastern Arctic Ocean during Saalian and Early Weichselian ice-sheet collapse. Quaternary Research, 60(3): 243-251.

Knox, J.C., 1993. Large increases in flood magnitude in response to modest changes in climate. Nature, 361: 430-432.

Kodina, L.A., Tokarev, V.G., Vlasova, L.N. and Korobeinik, G.S., 2003. Contribution of biogenic methane to ikaite formation in the Kara Sea; evidence from the stable carbon isotope geochemistry.

Proceedings in Marine Science, 6: 349-374.

Kranck, K., 1984. The role of flocculation in the filtering of particulate matter in estuaries, The estuary as a filter. Academic Press, Orlando, FL, United States, pp. 159-175.

Kraus, M., Matthiessen, J., Stein, R., 2003. A Holocene marine pollen record from the northern Yenisei Estuary (southeastern Kara Sea, Siberia). Proceedings in Marine Science; Elsevier, 6: 435-457.

Kremenetski, K.V., Velichko, A.A., Borisova, O.K., MacDonald, G.M., Smith, L.C., Frey, K.E. and Orlova, L.A., 2003. Peatlands of the western Siberian lowlands; current knowledge on zonation, carbon content and late Quaternary history. Quaternary Science Reviews., 22(5-7): 703-723.

Krumbein, W.C., 1936. Application of logarithmic moments to size-frequency distributions of sediments. Journal of Sedimentary Petrology, 6(1): 35-47.

Kulikov, N.N. and Martynov, V.T., 1961. O drevnikh beregovykh liniyakh na dne Karskogo morya. Eesti NSV Teaduste Akadeemia Toimetised, Geoloogia = Izvestiya Akademii Nauk Estonskoy SSR, Geologiya.

Labat, D., Godderis, Y., Probst, J.L. and Guyot, J.L., 2004. Evidence for global runoff increase related to climate warming. Advances in Water Resources, 27(6): 631-642.

Lambeck, K., 1996. Limits on the areal extent of the Barents Sea ice sheet in late Weichselian time, Impact of glaciations on basin evolution; data and models from the Norwegian margin and adjacent areas. Elsevier, Amsterdam, Netherlands, pp. 41-51.

Lambeck, K. and Chappell, J., 2001. Sea level change through the last glacial cycle. Science, 292(5517): 679-686.

Lambeck, K., Smither, C. and Johnston, P., 1998. Sea level change, glacial rebound and mantle viscosity for northern Europe. Geophysical Journal International, 134(1): 102-144.

Lambeck, K., Yokoyama, Y. and Purcell, A., 2002. Into and out of the last glacial maximum; sea level change during oxygen isotope stages 3 and 2, Ice sheets and sea level of the last glacial maximum. Pergamon, Oxford, United Kingdom, pp. 343-360.

Langbein, W.B. and Leopold, L.B., 1966. River meanders - Theory of minimum variance. River meanders - Theory of minimum variance, No. 422-H: 15.

Lastochkin, A.N., 1977. Kompleks geologo-geomorfologicheskikh issledovaniy neftegazonosnykh oblastey na sushe i shel'fe. Complex geological-geomorphological research in oil- and gas-bearing regions on dry land and shelves. Trudy Vsesoyuznogo Neftyanogo Nauchno-Issledovatel'skogo Geologorazvedochnogo Instituta, 393: 7-39.

Lastochkin, A.N., 1978. Submarine valleys on the northern continental shelf of Eurasia. Polar Geography, 2(4): 240-250.

Leeder, M.R., 1973. Fluviatile fining-upwards cycles and the magnitude of palaeochannels. Geological Magazine., 110(3): 265-276.

Leopold, L.B., 1994. River morphology as an analog to Darwin's theory of natural selection. Proceedings of the American Philosophical Society, 138(1): 31-47.

Leopold, L.B. and Maddock, T., 1953. The hydraulic geometry of stream channels and some physiographic implications. U.S. Geological Survey Professional Paper, 252. U.S. Government Printing Office, Washington, DC, 57 pp.

Lindstrom, D.R. and MacAyeal, D.R., 1993. Death of an ice sheet. Nature, 365(6443): 214-215.

Lisitsyn, A.P., 1995. The marginal filter of the ocean. Oceanology (engl. transl.), 34(5): 671-682.

Lisitsyn, A.P., Shevchenko, V.P., Vinogradov, M.E., Severina, O.V., Vavilova, V.V. and Mitskevich, I.N., 1995. Particle fluxes in the Kara Sea and Ob and Yenisey estuaries. Oceanology (engl. transl.), 34(5): 683-693.

Løset, S., Shkhinek, K., Gudmestad, O.T., Strass, P., Michalenko, E., Frederking, R. and Kaernae, T., 1999. Comparison of the physical environment of some Arctic seas. Cold Regions Science and Technology, 29(3): 201-214.

Magny, M. and Begeot, C., 2004. Hydrological changes in the European midlatitudes associated with freshwater outbursts from Lake Agassiz during the Younger Dryas event and the early Holocene. Quaternary Research, 61(2): 181-192.

Manabe, S., Wetherald, R.T., Milly, P.C., Delworth, T.L. and Stouffer, R.J., 1984. Century-Scale Change in Water Availability: CO sub(2)-Quadrupling Experiment. Climatic Change, 64(1-2): 59-76.

Mangerud, J., Jansen, E. and Landvik, J.Y., 1996. Late Cenozoic history of the Scandinavian and Barents Sea ice sheets. Global and Planetary Change, 12(1-4): 11-26.

Mangerud, J., Svendsen, J.-I., Astakhov, V.I., Andreicheva, L., Funder, S., Henriksen, M., Hufthammer, A.K., Indrelid, S., Matiouchkov, A., Murray, A.S., Paus, A., Pavlov, P., Tveranger, J. and Ulvedal, P., 1999. Age and extent of the Barents and Kara ice sheets in northern Russia. Boreas, 28(1): 46-80.

Mangerud, J., Astakhov, V., Jakobsson, M. and Svendsen, J.-I., 2001a. Huge ice-age lakes in Russia.

Journal of Quaternary Science, 16(8): 773-777.

Mangerud, J., Astakhov, V.I., Murray, A. and Svendsen, J.-I., 2001b. The chronology of a large ice-dammed lake and the Barents-Kara ice sheet advances, northern Russia. Global and Planetary Change, 31(1-4): 321-336.

Mangerud, J., Astakhov, V. and Svendsen, J.-I., 2002. The extent of the Barents-Kara ice sheet during the last glacial maximum. Quaternary Science Reviews, 21(1-3): 111-119.

Mangerud, J., Lovlie, R., Gulliksen, S., Hufthammer, A.-K., Larsen, E. and Valen, V., 2003. Paleomagnetic correlations between Scandinavian ice-sheet fluctuations and Greenland Dansgaard-Oeschger events, 45,000-25,000 yr B.P. Quaternary Research, 59(2): 213-222.

Mangerud, J., Jakobsson, M., Alexanderson, H., Astakhov, V., Clarke, G.K.C., Henriksen, M., Hjort, C., Krinner, G., Lunkka, J.P., Möller, P., Murray, A., Nikolskaya, O., Saarnisto, M. and Svendsen, J.I., 2004. Ice-dammed lakes and rerouting of the drainage of northern Eurasia during the Last Glaciation. Quaternary Science Reviews, 23(11-13): 1313-1332.

Matthes, G., 1956. River engineering. American Civil Engineering Practice, 214 pp.

Matthiessen, J. and Stepanets, O.V., 1999. The expedition to the Kara Sea in summer 1997: Summary of the shipboard scientific results. The Kara Sea Expedition of RV "Akademik Boris Petrov" 1997: First results of a joint Russian-German pilot study. J. Matthiessen, O. V. Stepanets, R. Stein, D. K. Fütterer and E. M. Galimov. Bremerhaven., 300: 5-16.

McCave, I.N., 1972. Transport and Escape of Fine-Grained Sediment from Shelf Areas, Shelf Sediment Transport; Process and Pattern, pp. 225-248.

McCave, I.N. and Carter, L., 1997. Recent sedimentation beneath the Deep Western Boundary Current off northern New Zealand. Deep-Sea Research. Part I: Oceanographic Research Papers, 44(7): 1203-1237.

McCave, I.N., Manighetti, B. and Robinson, S.G., 1995. Sortable silt and fine sediment size/composition slicing: Parameters for palaeocurrent speed and palaeoceanography. Paleoceanography, 10(3): 593-610.

McClimans, T.A., Johnson, D.R., Krosshavn, M., King, S.E., Carroll, J. and Grennes, Ø. 2000. Transport processes in the Kara Sea. Journal of Geophysical Research, 105(C6): 14121-14139.

Menard, H.W. and Smith, S.M., 1966. Hypsometry of ocean basin provinces. Journal of Geophysical Research, 71(18): 4305-4325.

Miall, A.D., 1993. The architecture of fluvial-deltaic sequences in the upper Mesaverde Group (Upper Cretaceous), Book Cliffs, Utah, Braided rivers. Geological Society of London, London, United Kingdom, pp. 305-332.

Miall, A.D., 1996. The geology of fluvial deposits: sedimentary facies, basin analysis, and petroleum geology. Springer, 583 pp.

Middleton, G.V., 1973. Johannes Walther's Law of the Correlation of Facies. Geological Society of America Bulletin, 84: 979-988.

Mikkelsen, N., 1997. Upper Quaternary diatoms in the Amazon Fan of the Western Atlantic, Proceedings of the Ocean Drilling Program; scientific results, Amazon Fan; covering Leg 155 of the cruises of the drilling vessel JOIDES Resolution, Bridgetown, Barbados, to Bridgetown, Barbados, sites 930-946, 25 March-24 May 1994. Texas A & M University Ocean Drilling Program, College Station, TX, United States, pp. 367-373.

Milliman, J.D. and Syvitski, J.P.M., 1992. Geomorphic/tectonic control of sediment discharge to the ocean: The importance of small mountainous rivers. Journal of Geology, 100(5): 525-544.

Mitchum, R.M.J. and Van Wagoner, J.C., 1991. High-frequency sequences and their stacking patterns; sequence-stratigraphic evidence of high-frequency eustatic cycles. Sedimentary Geology, 70(2-4): 131-160.

Mitchum, R.M., Vail, P.R. and Thompson, S., 1977. Seismic stratigraphy and global changes of sea level; Part 2, The depositional sequence as a basic unit for stratigraphic analysis. Memoir - American Association of Petroleum Geologists, 26: 53-62.

Morisawa, M., 1985. Development of quantitative geomorphology, Geologists and ideas; a history of North American geology. Geological Society, pp. 79-107.

Nakada, M. and Lambeck, K., 1988. The melting history of the late Pleistocene Antarctic ice sheet. Nature (London), 333(6168): 36-40.

Nansen, F., 1904. The bathymetrical features of the North Polar Seas, with a discussion of the continental shelves and previous oscillations of the shore-line. The Norwegian North Polar Expedition 1893-1896. Scientific Results, IV: 1-232.

Nelson, C.H. and Kulm, L.D., 1973. Submarine fans and deep-sea channels. In: G.V. Middleton and A.H. Bouma (Editors), Turbidites and Deep-Water Sedimentation. Society of Economic Paleontologists and Mineralogists,, pp. 39-78.

Niessen, F. and Dittmers, K., 2002. Geochirp and Elac sediment echograph profiling. Reports on Polar

and Marine Research, 419: 64-73.

Niessen, F. and Jarrard, R.D., 1998. Velocity and porosity of sediments from CRP-1 Drillhole, Ross Sea, Antarctica, Studies from the Cape Roberts Project; Ross Sea, Antarctica; scientific report of CRP-1. Universita di Siena Dipartimento di Scienze della Terra, Siena, Italy, pp. 311-318.

Niessen, F. and Weiel, D., 1996. Distribution of magnetic susceptibility on the Eurasian shelf and continental slope - implications for source areas of magnetic minerals. In: R. Stein, Ivanov GI, Levitan MA, Fahl K (Editor), Surface-sediment composition and sedimentary processes in the central Arctic Ocean and along the Eurasian Continental Margin. Reports on Polar Research, pp. 81-88.

Nittrouer, C.A. and Wright, L.D., 1994. Transport of particles across continental shelves. Reviews of Geophysics, 32(1): 85-113.

Nørgaard-Pedersen, N., Spielhagen, R.F., Thiede, J. and Kassens, H., 1998. Central Arctic surface ocean environment during the past 80 000 years. Paleoceanography, 13(2): 193-204.

Nørgaard-Pedersen, N., Spielhagen, R.F., Erlenkeuser, H., Grootes, P.M., Heinemeier, J. and Knies, J., 2003. Arctic Ocean during the Last Glacial Maximum: Atlantic and polar domains of surface water mass distribution and ice cover. Palaeogeography, 18(3): 1063.

Nuernberg, D., Wollenburg, I., Dethleff, D., Eicken, H., Kassens, H., Letzig, T., Reimnitz, E. and Thiede, J., 1994. Sediments in Arctic sea ice: Implications for entrainment, transport and release. Marine Geology, 119(3-4): 185-214.

Osborn, J.F. and Stypula, J.M., 1987. New models of hydrological and stream channel relationships. IAHS-AISH Publication, 165: 375-384.

Pak, H., Codispoti, L.A. and Zaneveld, J.R.V., 1980. On the intermediate particle maxima associated with oxygen-poor water off western South America. Deep-Sea Research, Part A: Oceanographic Research Papers. 27(10A): 783-797.

Pavlov, V.K. and Pfirman, S.L., 1995. Hydrographic structure and variability of the Kara Sea: Implications for pollutant distribution. Deep-Sea Research II, 42(6): 1369-1390.

Peterson, B.J., Holmes, R.M., McClelland, J.W., Vörösmarty, C.J., Lammers, R.B., Shiklomanov, A.I., Shiklomanov, I.A. and Rahmstorf, S., 2002. Increasing river discharge to the Arctic Ocean. Science, 298: 2171-2173.

Pettijohn, F.J., 1975. Sedimentary rocks. Harper & Row, New York, 80 pp.

Pfirman, S.L., Koegeler, J. and Anselme, B., 1995. Coastal environments of the western Kara and eastern Barents Seas. Deep Sea Research Part II: Topical Studies in Oceanography, 42(6): 1391-1412.

Piper, D.J.W. and Normark, W.R., 2001. Sandy fans; from Amazon to Hueneme and beyond. AAPG Bulletin, 85(8): 1407-1438.

Piper, D.J.W., Flood, R.D., Cisowski, S.M., Hall, F.R., Manley, P.L., Maslin, M.A., Mikkelsen, N. and Showers, W.J., 1997. Synthesis of stratigraphic correlations of the Amazon Fan, Proceedings of the Ocean Drilling Program; scientific results, Amazon Fan; covering Leg 155 of the cruises of the drilling vessel JOIDES Resolution, Bridgetown, Barbados, to Bridgetown, Barbados, sites 930-946, 25 March-24 May 1994. Texas A & M University Ocean Drilling Program, College Station, TX, United States, pp. 595-609.

Pirrung, M., Fuetterer, D., Grobe, H., Matthiessen, J. and Niessen, F., 2002. Magnetic susceptibility and ice-rafted debris in surface sediments of the Nordic seas: implications for Isotope Stage 3 oscillations. Geo-Marine Letters, 22(1): 1-11.

Polyak, L., Forman, S.L., Herlihy, F.A., Ivanov, G. and Krinitsky, P., 1997. Late Weichselian deglacial history of the Svyataya (Saint) Anna Trough, northern Kara Sea, Arctic Russia. Marine Geology, 143: 169-188.

Polyak, L., Levitan, M., Gataullin, V., Khusid, T., Mikhailov, V. and Mukhina, V., 2000. The impact of glaciation, river-discharge and sea level change on Late Quaternary environments in the south-western Kara Sea. International Journal of Earth Sciences, 89(3): 550-562.

Polyak, L., Levitan, M., Khusid, T., Merklin, L. and Mukhina, V., 2002. Variations in the influence of riverine discharge on the Kara Sea during the last deglaciation and the Holocene. Global and Planetary Change, 32(4): 291-309.

Polyakov, I.V. and Johnson, M.A., 2000. Arctic decadal and interdecadal variability, Geophysical Research Letter, pp. 4097-4100.

Polyakov, I.V. and Timokhov, L.A., 1994. Mean fields of temperature and salinity of the Arctic Ocean. Russian Meteorology and Hydrology, New York, NY, 7.

Posamentier, H.W. and Vail, P.R., 1988. Eustatic controls on clastic deposition; II, Sequence and systems tract models, Society of Economic Paleontologists and Mineralogists. Special Publication, pp. 124-154.

Posamentier, H.W., Jervey, M.T. and Vail, P.R., 1988. Eustatic controls on clastic deposition; I,

Conceptual framework, Sea level changes; an integrated approach. SEPM (Society for Sedimentary Geology), Tulsa, OK, United States, pp. 109-124.

Posamentier, H.W., Allen, G.P. and James, D.P., 1992. High resolution sequence stratigraphy; the East Coulee Delta, Alberta. Journal of Sedimentary Petrology, 62(2): 310-317.

Postma, G., 1990. An analysis of the variation in delta architecture. Terra Nova, 2(2): 124-130.

Rachold, V. and Cherkashov, G., 2004. Arctic Coastal Dynamics - Report of the 4th International Workshop, NII Okeangeologia, St. Petersburg (Russia), 10-13 November 2003. Reports on Polar and Marine Research-Berichte zur Polarforschung, 482, Bremerhaven, 187 pp.

Rachold, V., Grigoriev, M.N., Are, F.E., Solomon, S., Reimnitz, E., Kassens, H. and Antonow, M., 2000. Coastal erosion vs riverine sediment discharge in the Arctic Shelf seas. International Journal of Earth Sciences, 89: 450-460.

Rachold, V., Grigoriev, M.N., Hubberten, H.W. and Schirrmeister, L., 2003. Modern coastal organic carbon input to the Arctic Ocean. In: V. Rachold, J. Brown, S.M. Solomon and J.L. Sollid (Editors), Berichte zur Polar- und Meeresforschung-Reports on Polar and Marine Research, pp. 97.

Reimnitz, E., Barnes, P., Forgatsch, T. and Rodeick, C., 1972. Influence of grounding ice on the Arctic Shelf of Alaska. Marine Geology, 13: 323-334.

Reimnitz, E., Toimil, L. and Barnes, P., 1978. Arctic continental shelf Morphology related to sea ice-zonation, Beaufort Sea, Alaska. Marine Geology, 28: 179-210.

Reimnitz, E., Marincovich, L., McCormick, M. and Briggs, W.M., 1992. Suspension freezing of bottom sediment and biota in the Northwest Passage and implications for Arctic Ocean sedimentation. Canadian Journal of Earth Sciences, 29: 693-703.

Reimnitz, E., McCormick, M., McDougall, K. and Brouwers, E., 1993. Sediment export by ice rafting from a coastal polynya, Arctic Alaska, USA. Arctic and Alpine Research, 25(2): 83-98.

Reimnitz, E., Dethleff, D. and Nürnberg, D., 1994. Contrasts in Arctic shelf sea-ice regimes and some implications: Beaufort Sea versus Laptev Sea. Marine Geology, 119: 215-225.

Rekant, P., Cherkashev, G., Vanstein, B. and Krinitsky, P., 2005. Submarine permafrost in the nearshore zone of the southwestern Kara Sea. Geo-Marine Letters, 25(2-3): 183 - 189.

Robinson, S.G., 1993. Lithostratigraphic applications for magnetic susceptibility logging of deep-sea sediment cores; examples from ODP Leg 115. Geological Society Special Publications, 70: 65-98.

Romankevich, E.A. and Artemyev, V.E., 1985. Input of organic carbon into seas and oceans bordering the territory of the Soviet Union, Mitteilungen des Geologosch-Paläontologischen Institutes. Universität Hamburg, Hamburg, pp. 459-469.

Romankevich, E.A. and Vetrov, A.A., 2001. Cycle of Carbon in the Russian Arctic Seas (in Russian). Nauka, Moscow, 302 pp.

Rosgen, D.L., 1994. A classification of natural rivers. Catena, 22: 169-199.

Rostek, F., Spiess, V. and Bleil, U., 1991. Parasound echosounding; comparison of analogue and digital echosounder records and physical properties of sediments from the equatorial South Atlantic. Marine Geology, 99(1-2): 1-18.

Rudels, B., Muench, R.D., Gunn, J., Schauer, U. and Friedrich, H.J., 2000. Evolution of the Arctic Ocean boundary current north of the Siberian shelves. Journal of Marine Systems, 25: 77-99.

Schirrmeister, L., Siegert, C., Kunitzky, V.V., Grootes, P.M. and Erlenkeuser, H., 2002. Late Quaternary ice-rich permafrost sequences as a paleoenvironmental archive for the Laptev Sea region in northern Siberia. International Journal of Earth Sciences, 191(1): 154-167.

Schoster, F. and Levitan, M., 2003. Scientific Cruise Report of the joint Russian-German Kara Sea Expedition in 2002 with RV "Akademik Boris Petrov". Berichte zur Polar- und Meeresforschung-Reports on Polar and Marine Research, 450: 109.

Schoster, F. and Levitan, M.A., 2004. Scientific Cruise Report of the Kara Sea Expedition with RV Akademik Boris Petrov in 2003 within the frames of the Russian - German project SIRRO and the Russian - Norwegian project MAREAS. Berichte zur Polar- und Meeresforschung-Reports on Polar and Marine Research, 479, 147 pp.

Schoster, F., Behrends, M., Muller, C., Stein, R. and Wahsner, M., 2000. Modern river discharge and pathways of supplied material in the Eurasian Arctic Ocean: evidence from mineral assemblages and major and minor element distribution. International Journal of Earth Sciences, 89(3): 486-495.

Schultheiss, P.J. and McPhail, S.D., 1989. An automated p-wave logger for recording fine scale compressional wave velocity in sediments. In: M.S. Ruddiman (Editor), Proc. ODP Init. Rep, pp. 407-413.

Schultheiss, P.J. and Mienert, J., 1987. Whole-core p-wave velocity and gamma-ray attenuation logs from Leg 108 (sites 657 through 668). In: M.S. Ruddiman (Editor), Proceedings ODP Initial Reports, pp. 1015-1017.

Schumm, S.A., 1977. The fluvial system. Wiley, New York, 338 pp.

Schumm, S.A., 1981. Evolution and response of the fluvial system, sedimentologic implications. Special Publication - Society of Economic Paleontologists and Mineralogists, 31: 19-29.

Schumm, S.A., 1993. River response to baselevel change: Implications for sequence stratigraphy. Journal of Geology, 101(2): 279-294.

Schumm, S.A., 1994. Erroneous perceptions of fluvial hazards. In: M. Morisawa (Editor), Geomorphology and Natural Hazards, pp. 129-138;.

Schumm, S.A. and Khan, H.R., 1972. Experimental study of channel patterns. Geological Society of America Bulletin, 83: 1755–1770.

Seibold, E., 2001. Early maps of the Arctic coast of Russia. Polarforschung, 71(3): 121-148.

Shanley, K.W. and McCabe, P.J., 1993. Perspectives on sequence stratigraphy of continental strata. American Association of Petroleum Geologists Bulletin, 78: 544-568.

Sharkov, Y.V., 1980. Crystallization of tholeiitic and alkali basalts in the systems Ol-Cpx-Pl-Qu, Ol-Cpx-Pl-Ne, and Cpx-Pl-Ne-Or and the origin of alkali magmas. Geochemistry International, 17(1): 11-22.

Shepard, F.P., 1954. Nomenclature based on sand-silt-clay ratios. Journal of Sedimentary Petrology, 24(3): 151-158.

Shevchenko, V., Lisitzin, A., Vinogradova, A. and Stein, R., 2003. Heavy metals in aerosols over the seas of the Russian Arctic. Science of the total environment, 306: 11-25.

Shiklomanov, I.A. and Skakalsky, B.G., 1994. Studying water, sediment and contaminant runoff of Siberian rivers; modern status and prospects, Interagency Arctic Research Policy Committee; Workshop on Arctic contamination. National Science Foundation, Washington, DC, United States, pp. 295-306.

Sidorchuk, A. and Borisova, O., 2000. Method of paleogeographical analogues in paleohydrological reconstructions. Quaternary International, 72: 95– 106.

Sidorchuk, A., Borisova, O. and Panin, A., 2001. Fluvial response to the Late Valdai/Holocene environmental change on the East European Plain. Global and Planetary Change, 28(1-4): 303-318.

Simstich, J., Stanovoy, V., Novikhin, A., Erlenkeuser, H. and Spielhagen, R.F., 2003. Stable isotope ratios in bivalve shells; suitable recorders for salinity and nutrient variability in the Kara Sea?, Siberian river run-off in the Kara Sea; characterisation, quantification, variability and environmental significance. Elsevier, Amsterdam, Netherlands, pp. 111-123.

Smith, L.C., MacDonald, G.M., Velichko, A.A., Beilman, D.W., Borisova, O.K., Frey, K.E., Kremenetski, K.V. and Sheng, Y., 2004. Siberian peatlands a net carbon sink and global methane source since the early Holocene. Science, 303(5656): 353-356.

Solheim, A. and Kristoffersen, Y., 1984. Sediments above the upper regional unconformity; thickness, seismic stratigraphy and outline of the glacial history, 179B. Skrifter - Norsk Polarinstitutt, 26 pp.

Sommerfield, C.K., Nittrouer, C.A. and Figueiredo, A.G., 1995. Stratigraphic evidence of changes in Amazon shelf sedimentation during the Late Holocene. Marine Geology, 125(3-4): 351-371.

Spielhagen, R.F., Baumann, K.H., Erlenkeuser, H., Frederichs, T., Nowaczyk, N.R., Nørgaard-Pedersen, N., Thiede, J., Vogt, C. and Weiel, D., 2004. Arctic Ocean deep-sea record of Northern Eurasian ice sheet history. Quaternary Science Reviews, 23(11-13): 1455-1483.

Spielhagen, R.F., Erlenkeuser, H. and Siegert, H., 2005. History of freshwater runoff across the Laptev Sea (Arctic) during the last deglaciation. Global and Planetary Change, In Press, Corrected Proof, Available online; (http://www.sciencedirect.com/science/article/B6VF0-4FY9MC7-1/2/bf5ffad757df3f8778311686d6e2099d).

Spieß, V., 1993. Digitale Sedimentechographie-Neue Wege zu einer hochauflösenden Akustostratigraphie. Berichte, Fachbereich Geowissenschaften, 35. Universität Bremen, Bremen, 199 pp.

Stein, R., 1985. Rapid grain-size analyses of clay and silt fraction by SediGraph 5000D; comparison with Coulter counter and Atterberg methods. Journal of Sedimentary Petrology, 55(4): 590-593.

Stein, R., 1991. Accumulation of Organic Carbon in marine sediments. Lecture Notes in Earth Sciences, 34. Springer, Heidelberg, 217 pp.

Stein, R., 1996. Organic-carbon and carbonate distribution in surface sediments from the eastern central Arctic Ocean and the Eurasian continental margin; sources and pathways, Surface-sediment composition and sedimentary processes in the central Arctic Ocean and along the Eurasian continental margin. Kamloth, Bremerhaven, Federal Republic of Germany, pp. 243-267.

Stein, R. and Fahl, K., 2003 . The Kara Sea: Distribution, sources, variability and burial of organic carbon. In: R. Stein and R.W. Macdonald (Editors), The Arctic Ocean Organic Carbon Cycle. Springer Verlag, Berlin, Heidelberg, pp. 237-266.

Stein, R. and Korolev, S., 1994. Shelf-to-basin sediment transport in the eastern Arctic Ocean. Reports

on Polar Research-Berichte zur Polarforschung, 144: 87-100.

Stein, R. and Nürnberg, D., 1995. Productivity proxies: Organic carbon and biogenic opal in surface sediments from the Laptev Sea and the adjacent continental slope. Reports on Polar Research, Alfred Wegener Institut for Polar and Marine Research, 176: 286-298.

Stein, R. and Stepanets, O., 2000. Scientific Cruise Report of the Joint Russian-German Kara-Sea Expedition of RV "Akademik Boris Petrov" in 1999. Reports on Polar Research-Berichte zur Polarforschung, 360, 141 pp.

Stein, R. and Stepanets, O., 2001. The German-Russian Project on Siberian River Run-off (SIRRO): Scientific Cruise Report of the Kara-Sea Expedition "SIRRO 2000" of RV "Akademik Boris Petrov" and first results. Reports on Polar Research-Berichte zur Polarforschung, 393, 287 pp.

Stein, R. and Stepanets, O., 2002. Scientific Cruise Report of the Kara-Sea Expedition 2001 of RV "Akademik Boris Petrov": The German-Russian Project on Siberian River Run-off (SIRRO) and the EU Project "ESTABLISH". Reports on Polar Research-Berichte zur Polarforschung, 419, 278 pp.

Stein, R., Niessen, F., Dittmers, K., Levitan, M., Schoster, F., Simstich, J., Steinke, T. and Stepanets, O.V., 2002. Siberian river run-off and Late Quaternary glaciation in the southern Kara Sea, Arctic Ocean: preliminary results. Polar Research, 21(2): 315-322.

Stein, R., Fahl, K., Fütterer, D.K. and Galimov, E.M., 2003a. Siberian River Run-off in the Kara Sea: Characterisation, Quantification, Variability, and Environmental Significance, vol. 6, Amsterdam, 488 pp.

Stein, R., Fahl, K., Dittmers, K., Niessen, F. and Stepanets, O., 2003b. Holocene siliciclastic and organic carbon fluxes in the Ob and Yenisei estuaries and the adjacent inner Kara Sea: Quantification, variability, and paleoenvironmental implications. In: R. Stein, K. Fahl, D.K. Fütterer, E.M. Galimov and O. Stepanets (Editors), Siberian River Run-Off in the Kara Sea: Characterisation, Quantification, Variability, and Environmental Significance. Proceedings in Marine Sciences vol. 6, Elsevier, Amsterdam, pp. 401-434.

Stein, R., Dittmers, K., Fahl, K., Kraus, M., Matthiessen, J., Niessen, F., Pirrung, M., Polyakova, Y., Schoster, F., Steinke, T. and Futterer, D.K., 2004. Arctic (palaeo) river discharge and environmental change: evidence from the Holocene Kara Sea sedimentary record. Quaternary Science Reviews, 23(11-13): 1485-1511.

Steinke, T., 2002. Rekonstruktion spätquartärer Paläo-Umweltbedingungen in der Karasee anhand sedimentologischer und mineralogischer Untersuchungen, Bremen University, 98 pp.

Stoecker, T.F. and Wright, D.G., 1991. Rapid transitions of the ocean's deep circulation induced by changes in surface water fluxes. Nature, 351: 729-732.

Subba Rao, D.V. and Platt, T., 1984. Primary production of Arctic waters. Polar Biology(3): 191– 201.

Suter, J.R. and Berryhill, H.L., 1985. Late Quaternary shelf-margin deltas, Northwest Gulf of Mexico. American Association of Petroleum Geologists Bulletin, 69(1): 77-91.

Svendsen, J.-I., Astakhov, V.I., Bolshiyanov, D.Y., Demidov, I., Dowdeswell, J.A., Gataullin, V., Hjort, C., Hubberten, H.-W., Larsen, E., Mangerud, J., Melles, M., Moeller, P., Saarnisto, M. and Siegert, M.J., 1999. Maximum extent of the Eurasian ice sheets in the Barents and Kara Sea region during the Weichselian. Boreas, 28(1): 234-242.

Svendsen, J.I., Gataullin, V., Mangerud, J. and Polyak, L., 2003. The glacial history of the Barents and Kara Sea region. In: J. Ehlers and P. Gibbard (Editors), Quaternary Glaciations - Extent and Chronology. Elsevier, Amsterdam.

Svendsen, J.I., Alexanderson, H., Astakhov, V.I., Demidov, I., Dowdeswell, J.A., Funder, S., Gataullin, V., Henriksen, M., Hjort, C., Houmark-Nielsen, M., Hubbertenk, H.W., Ingólfsson, Ó., Jakobsson, M., Kjaer, K.H., Larsen, E., Lokrantz, H., Lunkka, J.P., Lysa, A., Mangerud, J., Matiouchkov, A., Murray, A., Möller, P., Niessen, F., Nikolskaya, O., Polyak, L., Saarnisto, M., Siegert, C., Siegert, M.J., Spielhagen, R.F. and Stein, R., 2004. Late Quaternary ice sheet history of northern Eurasia. Quaternary Science Reviews, 23(11-13): 1229-1271.

Swift, D.J.P., 1968. Coastal erosion and transgressive stratigraphy. Journal of Geology, 76(4): 444-456.

Swift, D.J.P. and Thorne, J.A., 1991. Sedimentation on continental margins; I, A general model for shelf sedimentation. Special Publication of the International Association of Sedimentologists, 14: 3-31.

Syvitski, J.P.M., Andrews, J.T. and Dowdeswell, J.A., 1996. Sediment deposition in an iceberg-dominated glacimarine environment, East Greenland; basin fill implications, Impact of glaciations on basin evolution; data and models from the Norwegian margin and adjacent areas. Elsevier, Amsterdam, Netherlands, pp. 251-270.

Telang, A., S., Pocklington, R., Naidu, A.S., Romankevich, E.A., Gitelson, I.I. and Gladyshev, M.I., 1991. Carbon and mineral transport in major North American, Russian Arctic, and Siberian rivers: the

St. Lawrence, the Mackenzie, the Yukon, the Arctic Alaskan, the Arctic Basin rivers in the Soviet Union and the Yenisei. In: E.T. Degens, S. Kempe and J. Rickey (Editors), Biogeochemistry of Major World Rivers. SCOPE, pp. 75-104.

Thompson, R. and Oldfield, F., 1986. Environmental Magnetism, Allen and Unwin, London.

Thorne, J.A. and Swift, D.J.P., 1991. Sedimentation on continental margins, VI: a regime model for depositional sequences, their component system tracts, and bounding surfaces. In: D.J.P. Swift, G.F. Oertel, R.W. Tillman and J.A. Thorne (Editors), Shelf Sand and Sandstone Bodies. Geometry Facies and Sequence Stratigraphy, pp. 189-255.

Treshnikov, V., 1985. Atlas of the Arctic (Atlas Arktiki). Glavnoye Upravleniye Geodezii i Kartografii pri Sovete Ministrov SSSR, Moscow.

Tushingham, A.M. and Peltier, W.R., 1992. Validation of the ICE-3G model of Wurm-Wisconsin deglaciation using a global data base of relative sea level histories. Journal of Geophysical Research, 97(B3): 3285-3304.

Vail, P.R., 1987. Seismic stratigraphy interpretation using sequence stratigraphy; Part 1, Seismic stratigraphy interpretation procedure, Atlas of seismic stratigraphy. American Association of Petroleum Geologists, Tulsa, OK, United States, pp. 1-10.

Vail, P.R. and Posamentier, H.W., 1988. Principles of sequence stratigraphy. Memoir - Canadian Society of Petroleum Geologists, 15: 572.

Vail, P.R., Mitchum, R.M., Todd, R.G., Widmier, J.M., Thompson, S., Sangree, J.B., Bubb, J.N. and Hatelid, W.G., 1977. Seismic stratigraphy and global changes of sea level. In: Seismic stratigraphy; applications to hydrocarbon exploration Payton-C-E (editor). Memoir-American Association Petroleum Geologists, 26: 49-212.

Vail, P.R., Audemard, F., Bowman, S.A., Eisner, P.N. and Perez-Cruz, C., 1991. The stratigraphic signatures of tectonics, eustasy and sedimentology - an overview. In: W. Einsele, A. Ricken and Seilacher (Editors), Cycles and events in stratigraphy. Springer-Verlag, pp. 617-659.

Van Wagoner, J.C., 1998. Sequence stratigraphy and marine to nonmarine facies architecture of foreland basin strata, Book Cliffs, Utah, U.S.A.; reply. AAPG Bulletin, 82(8): 1607-1618.

Van Wagoner, J.C., Mitchum, R.M., Jr., Posamentier, H.W. and Vail, P.R., 1987. Seismic stratigraphy interpretation using sequence stratigraphy; Part 2, Key definitions of sequence stratigraphy, Atlas of seismic stratigraphy. American Association of Petroleum Geologists, Tulsa, OK, United States, pp. 11-14.

Van Wagoner, J.C., Posamentier, H.W., Mitchum, R.M., Jr, Vail, P.R., Sarg, J.F., Loutit, T.S. and Hardenbol, J., 1988. An overview of the fundamentals of sequence stratigraphy and key definitions. Special Publication - Society of Economic Paleontologists and Mineralogists, 42: 39-45.

Vasiliev, A., Kanevskiy, M. and Cherkashov, G., 2005. Coastal dynamics at the Barents and Kara Sea key sites. Geo-Marine Letters, 25(2-3): 110 - 120.

Velichko, A.A., 2002. Long-term climate variations; paleoclimates with global warming similar to that expected in the 21st century. Izvestiya, Atmospheric and Oceanic Physics, 38(Suppl. 1): 40-58.

Velichko, A.A., Kononov, Y.M. and Faustova, M.A., 1997. The last glaciation of Earth; size and volume of ice-sheets, Quaternary of northern Eurasia; late Pleistocene and Holocene landscapes, stratigraphy and environments. Pergamon, Oxford, United Kingdom, pp. 43-51.

Volkov, V.A., Johannessen, O.M., Borodachev, V.E., Voinov, G.N., Pettersson, L.H., Bobylev, L.P. and Kouraev, A.V., 2002. Polar seas oceanography - An integrated case study of the Kara Sea. Springer Verlag, Berlin, 450 pp.

Vorren, T.O., Laberg, J.S., Blaume, F., Dowdeswell, J.A., Kenyon, N.H., Mienert, J., Rumohr, J. and Werner, F., 1998. The Norwegian-Greenland Sea continental margins; morphology and late Quaternary sedimentary processs and environment, Glacial and oceanic history of the polar North Atlantic margins. Pergamon, Oxford, United Kingdom, pp. 273-302.

Wahsner, M., Mueller, C., Stein, R., Ivanov, G., Levitan, M., Shelekhova, E. and Tarasov, G., 1999. Clay-mineral distribution in surface sediments of the Eurasian Arctic Ocean and continental margin as indicator for source areas and transport pathways - a synthesis. Boreas, 28(1): 215-233.

Walker, H.J., 1992. Sea level change: Environmental and socio-economic impacts. Geo Journal, 26(4): 511-520.

Weaver, C.E., 1989. Clays, muds, and shales. SOURCE: (Elsevier; Developments in Sedimentology, 44), 1989, 819 pp, indexes.

Weaver, P.P.E. and Schultheiss, P.J., 1990. Current methods for obtaining, logging and splitting marine sediment cores. Marine and Geophysical Research, 12: 85-100.

Weber, M.E., Niessen, F., Kuhn, G. and Wiedicke, M., 1997. Calibration and application of marine

sedimentary physical properties using a multi-sensor core logger. Marine Geology, 136: 151-172.

Weiel, D., 1997. Paleozeanographische Untersuchungen in der Vilkitzy -Straße und östlich von Severnaja Zemlya mit sedimentologischen und geophysikalischen Methoden, Geologische Institut der Universität zu Koeln/ Alfred Wegener Institut Polar und Meeresforschung Bremerhaven, Koeln/ Bremerhaven, 138 pp.

Wells, J.T. and Shanks, A.L., 1987. Observations and geologic significance of marine snow in a shallow-water, partially enclosed marine embayment. Journal of Geophysical Research, C, Oceans, 92(12): 13,185-13,190.

Weltje, G.J., 1997. End-member modeling of compositional data; numerical-statistical algorithms for solving the explicit mixing problem. Mathematical Geology, 29(4): 503-549.

Wessel, P. and Smith, W.H.F., 1991. Free software helps map and display data. Eos, Transactions, American Geophysical Union, 72(41): 441, 445-446.

Westervelt, P., 1963. Parametric acoustic array. Journal of the Acoustic Society of America, 35: 535-537.

Wetzel, A. and Allia, V., 2000. The significance of hiatus beds in shallow-water mudstones: An example from the Middle Jurassic of Switzerland. Journal of Sedimentary Research, 70,(1): 170-180.

Wheeler, H.E., 1958. Time-stratigraphy. Bulletin of the American Association of Petroleum Geologists, 42(5): 1047-1063.

Windom, H.L. and Gross, T.F., 1989. Flux of particulate aluminium across the Southeastern U.S. continental shelf. Estuarine, Coastal and Shelf Science, 28(3): 327-338.

Wright, L.D., Wiseman, W.J., Jr., Yang, Z.S., Bornhold, B.D., Keller, G.H., Prior, D.B. and Suhayda, J.N., 1990. Processes of marine dispersal and deposition of suspended silts off the modern mouth of the Huanghe (Yellow River). Continental Shelf Research, 10(1): 1-40.

Yamskikh, A.F., 1996. Late Quaternary intra-continental river palaeohydrology and polycyclic terrace formation; the example of South Siberian river valleys. Geological Society Special Publications, 115: 181-190.

Yamskikh, A.F., 1998. Late Pleistocene and Holocene Siberian River Valley Geomorphogenesis as a Result of Palaeogeographical Cyclic Changes. In: G. Benito, V.R. Baker and K.J. Gregory (Editors), Palaeohydrology and environmental change. Wiley, Chichester ; New York, pp. 353.

Yokoyama, Y., Esat, T.M., Lambeck, K. and Fifield, L.K., 2000. Last ice age millennial scale climate changes recorded in Huon Peninsula corals. Radiocarbon, 42(3): 383-401.

Zanke, U., 1982. Grundlagen der sedimentbewegung. principles of sediment transport. Springer, Berlin.

Zeeberg, J., Lubinski, D.J. and Forman, S.L., 2001. Holocene Relative Sea level History of Novaya Zemlya, Russia, and Implications for Late Weichselian Ice-Sheet Loading. Quaternary Research, 56(2): 218-230.